UTS UNIVERSITY OF TECHNOLOGY SYDNEY

A COMPOSITE REACTIVE FILTER MEDIA FOR HEAVY METALS REMOVAL FROM SOIL BY ELECTROKINETIC PROCESS

by Faris Mohammed Y Hamdi

Thesis submitted in fulfilment of the requirements for the degree of

Doctor of Philosophy

under the supervision of Dr Ali Altaee and Prof John Zhou

University of Technology Sydney
Faculty of Engineering and Information Technology

July 2025

CERTIFICATE OF ORIGINAL AUTHORSHIP

I, Faris Mohammed Y Hamdi declare that this thesis is submitted in fulfillment of the requirements for the award of Doctor of Philosophy in the School of Civil and Environmental Engineering/ Faculty of Engineering and Information Technology at the University of Technology, Sydney.

This thesis is wholly my own work unless otherwise referenced or acknowledged. In addition, I certify that all information sources and literature used are indicated in the thesis.

This document has not been submitted to any other academic institution for qualification.

This research is supported by the Australian Government Research Training Program.

Signature

Production Note:
Signature removed prior to publication.

Date: 07/07/2025

ACKNOWLEDGEMENT

I would like to express my sincere and profound gratitude to my principal supervisor, Dr. Ali Altaee, for his invaluable guidance, continuous support, and constructive supervision throughout the duration of my research. His extensive knowledge, critical insights, and unwavering patience have been fundamental to the successful completion of this thesis and my overall academic development.

I am also indebted to my co-supervisor, Dr. John Zhou, whose expert advice, meticulous feedback, and sustained encouragement have significantly contributed to the rigor and scholarly quality of this research.

I would also like to acknowledge the University of Technology Sydney for offering a stimulating academic environment and providing the necessary resources and facilities that supported the progression and completion of this study. Additionally, I extend my gratitude to the Kingdom of Saudi Arabia and the Ministry of Education at Jazan University for their support.

Finally, I extend my heartfelt appreciation to my family and friends for their unwavering support, understanding, and encouragement during the entirety of this academic endeavor.

Table of Contents

CERTIFICATE OF ORIGINAL AUTHORSHIP i
ACKNOWLEDGEMENT ii
LIST OF FIGURES vi
LIST OF TABLES ix
PUBLICATIONS x
ABSTRACT xi
CHAPTER ONE: INTRODUCTION 1
1.1. Background 1
1.2. Research gap and significance 4
1.3. Research Objectives 7
1.4. Thesis Outline 8
CHAPTER TWO: LITERATURE REVIEW 11
2.1. Principles of electrokinetic soil remediation 11
2.2. Type of contaminants treated by the EK 15
2.3. Factors Affecting Electrokinetic 16
2.3.1. Type of soils 17
2.3.2. Type of Electrode 19
2.3.3. Applied voltage. 22
2.4. Techniques for enhancement and integration with EK 26
2.4.1. EK using enhancement agents 27
2.4.2. EK coupled with Bioremediation 31
2.4.3. EK coupled with phytoremediation 33
2.4.4. EK coupled with RFM 37
2.5. EK coupling with solar power 43
2.6. Comparison of combined-EK with conventional processes 46
2.7. System selection and recommendation 57
2.8. Conclusion and research gaps 58
CHAPTER THREE: MATERIALS AND METHODS 61
3.1. Materials 61
3.2. Methods 63
3.2.1. Properties of kaolinite clay soil and natural soil 63
3.2.2. Preparation of reactive filter media (RFM) 64

3.2.3. Electrokinetic cell set-up 64
3.2.4. Adsorption/desorption testing using RFM 66
3.2.5. Removal efficiency 68
3.2.6. Power consumption 68
3.2.7. Analytical methods 69
CHAPTER FOUR: IRON SLAG/ACTIVATED CARBON-ELECTROKINETIC SYSTEM WITH ANOLYTE RECYCLING FOR SINGLE AND MIXTURE HEAVY METALS REMEDIATION **71**
4.1. Introduction 71
4.2. Materials and methods 76
4.2.1. Materials and soil sample preparation 76
4.2.2. Electrokinetic cell and test design 77
4.3. Results and discussion 79
4.3.1. Electric current 79
4.3.2. Soil pH and Electric conductivity 83
4.3.3. Removal Rate 86
4.3.4. Characteristics of RFM 92
4.3.5. RFM adsorption/desorption 97
4.3.6. Specific Energy Consumption 101
4.4. Conclusion 103
CHAPTER FIVE: BLACK TEA WASTE/IRON SLAG REACTIVE FILTER MEDIA-ELECTROKINETIC FOR MIXED HEAVY METALS TREATMENT FROM CONTAMINATED SITE **105**
5.1. Introduction 105
5.2. Materials and methods 109
5.2.1. Preparation of samples and methods for analysis 109
5.2.2. EK cell experimental setup 111
5.2.3. Test design 112
5.3. Results and discussion 114
5.3.1. Electric current 114
5.3.2. pH and electrical conductivity of soil 118
5.3.3. Heavy metal removal rate 122
5.3.4. Characteristics of RFM 129
5.3.5. RFM adsorption/desorption 138
5.3.6. Specific energy consumption 141
5.4. Conclusion 143

CHAPTER SIX: DECONTAMINATION OF HEAVY METALS FROM SOIL BY ELECTROKINETIC COMBINED WITH REACTIVE FILTER MEDIA FROM INDUSTRIAL WASTES **143**

6.1. Introduction 143

6.2. Materials 147

6.2.1. Sample Preparation 147

6.2.2. EK cell experimental setup and design 148

6.3. Results and Discussion 151

6.3.1. The Electric Current 151

6.3.2. Electric conductivity and pH 156

6.3.3. Removal of contaminant 161

6.3.4. Specific Energy Consumption 168

6.3.5. Characteristics of RFM 170

6.3.6. RFM adsorption/desorption 179

6.4. Implications 182

6.5. Conclusion 184

CHAPTER SEVEN: CONCLUSIONS AND FUTURE RESEARCH RECOMMENDATIONS **186**

7.1. Conclusions 186

7.2. The importance of the research and its impact on the field 188

7.3. future studies 190

References **191**

LIST OF FIGURES

Figure 2.1: The main principles and mechanisms that occur during EK processing. 12

Figure 2.2: EK coupled with Bioremediation. Anions and cations transport to the respective electrode of opposite charge while microorganisms transport towards the cathode via electroosmosis flow. 32

Figure 2.3: EK pollutants removal coupled with phytoremediation. 34

Figure 2.4: EK coupled with RFM (Location and thickness of the RFM media depends on the size of the cell and the type of contamination in the soil). 39

Figure 2.5: EK coupled with solar power. 45

Figure 3.1: Schematic representation of heavy metal removal in an EK-RFM reactor (a) EK+RFM test design (b) EK+RFM with anolyte recycling test design. 66

Figure 4.1: (a) Change in Current (mA) in the electrokinetic experiments and (b) Change in Voltage (V). Experiments were conducted at 20 mA direct current. 83

Figure 4.2: Soil pH and electric conductivity (EC) at the end of the EK experiments (a) soil pH and (b) electric conductivity. 86

Figure 4.3: Cu in all experiments and Ni and Zn removal in experiment 6 at the end of the EK process 91

Figure 4.4: (a) the XRD spectrum of iron slag; (b) FTIR bands of iron slag, iron slag/AC before and after EK treatment; (c to l) iron slag, iron slag/AC SEM images with EDS before and after EK treatment. 97

Figure 4.5: Copper and mixed solution adsorption experiments, a) impact of iron slag/AC adsorption of $CuSO_4$ with time, b) The impact of contact time on the adsorption of metal ion (Cu), c) impact of iron slag/AC adsorption of mixed solution (Cu, Ni, Zn) with time, d) The effect of contact time on the adsorption of metal ion (Cu, Ni, Zn), e) Adsorption and desorption of Cu, Ni, and Zn across three successive cycles. 99

Figure 4.6: Total Cu, Ni, and Zn removal and specific energy consumption during EK. 102

Figure 5.1: (a) The electrokinetic tests' current change (mA) and (b) the voltage change (V). A direct current of 25 mA was used for the experiments. 118

Figure 5.2: Soil pH and electrical conductivity were assessed after the electrokinetic tests. 121

Figure 5.3: Shows (a) to (f) the removal of single and mixed elements from kaolin soil, (g) the removal of mixed elements from natural soil, and (h) the total metal removal for all experiments. 128

Figure 5.4: FTIR spectra of (a & b) PIS/BTW and GIS/BTW before and after EK, and SEM and EDS of (c to n) PIS, GIS, PIS/BTW, and GIS/BTW before EK, and SEM and EDS of (o to z) PIS/BTW and GIS/BTW after EK. 138

Figure 5.5: (a) Influence of PIS/BTW and GIS/BTW on copper adsorption over time, (b) Effect of contact duration on copper ion adsorption efficiency. (c) Adsorption of meatl from mixed solutions by PIS/BTW over time. (d) Influence of contact duration on the adsorption of metal ions, and (e&f) Adsorption/desorption behavior of metal across three consecutive cycles. 141

Figure 5.6: Total metal removal rate and specific energy consumption during EK experiments. 143

Figure 6.1: Schematic illustration of metal treatment by EK-RFM hybrid system. 150

Figure 6.2: (a) Electric current variation during EK tests at 20, 25, and 30 mA. (b) Corresponding voltage changes, showing the influence of current and soil interactions on EK efficiency. 155

Figure 6.3: pH and EC of the soil post-remediation across the sections from the anode to the cathode (a) Exp1 (control) (b) Exp2 (c) Exp3 (d) Exp4 (e) Exp5 (f) Exp6 (g) Exp7 (h) Exp8. 161

Figure 6.4: (a&b) Residual metal concentration in soil sections/RFM after EK, and (c) Total metal removal/Specific Energy Consumption at the end of the EK. 167

Figure 6.5: (a) the XRD spectrum of iron slag, (b) FTIR bands of iron slag, SD/iron slag, TSD/iron slag, and SD/iron slag mix with 2% GA before and after EK treatment, and (c to x) iron slag, SD/iron slag, TSD/iron slag, and SD/iron slag mix with 2% GA SEM images with EDS before and at the end of the EK treatment. 179

Figure 6.6: Cu^{2+} adsorption tests, (a) The Cu^{2+} adsorption on sawdust/slag, (b) The influence of the duration on the Cu^{2+}adsorption, (c) Adsorption, and desorption of Cu^{2+} across three successive cycles, sawdust (SD), treated sawdust (TSD) with slag, and sawdust/iron slag with 2% GA RFM. 182

LIST OF TABLES

Table 2.1: Prerequisites for electrodynamic treatment of soil. 15

Table 2.2: Summary of the types of electrodes coupled to the EK process 20

Table 2.3: Heavy metal removal by the impact of different soil and voltage/current of the EK efficiency..... 24

Table 2.4: Evaluation of electrokinetic treatment performance for different soil contaminants. 30

Table 2.5: Evaluation of EK-bioremediation performance for different soil contaminants. 33

Table 2.6: Evaluation of EK-phytoremediation performance for different soil contaminants. .. 36

Table 2.7: Optimal operating circumstances for combining EK and RFM in removing heavy metals from soil..... 42

Table 2.8: The summary of the results of the thermal, physical, chemical, and biological technology used to remove heavy metals from the soil. 52

Table 3.1: Shows the chemical and physical parameters of kaolinite clay soil. 62

Table 3.2: Natural soil properties and heavy metal content. 62

Table 4.1: Different physicochemical characteristics of RFM. 77

Table 4.2: The type of EK tests and heavy metals concentration is 1000 mg/kg. 78

Table 4.3: EK experimental conditions for copper removal and its mass balances. The concentration of metal ions is 1 g/kg, and tests were conducted at 22 ^{o}C..... 91

Table 5.1: Various physicochemical properties of RFM. 110

Table 5.2: Shows the conditions under which the different EK tests. 113

Table 5.3: Removal efficiency and Mass Balance of EK tests. 128

Table 6.1: Characteristics of RFM, Kaolin, and Natural soil..... 148

Table 6.2: Description of the EK-RFM system. 151

Table 6.3: Removal efficiency and Mass Balance of EK experiments. 168

PUBLICATIONS

I have three peer-reviewed articles based on this thesis that advance scientific discourse by offering unique insights and experimental data on the electrokinetic remediation of heavy metals in kaolinite and natural soils.

- **Hamdi, F.M**., et al. (2024) "Iron slag/activated carbon-electrokinetic system with anolyte recycling for single and mixture heavy metals remediation," ***Science of the Total Environment***, 172516.

- **Hamdi, F.M**., et al. (2025) "Hybrid and enhanced electrokinetic system for soil remediation from heavy metals and organic matter," ***Journal of Environmental Sciences***, 147, pp.424-450.

- **Hamdi, F.M**., et al. (2025) "Black tea waste/iron slag reactive filter media-electrokinetic for mixed heavy metals treatment from contaminated site," ***Journal of Contaminant Hydrology***, pp.104517–104517.

- **Hamdi, F.M**., et al. (2025) "Decontamination of heavy metals from soil by electrokinetic combined with reactive filter media from industrial wastes," ***Water, Air, & Soil Pollution,*** 236(9).

Throughout my PhD study, I co-authored peer-reviewed publications and participated in scholarly forums.

- Ganbat, N., Altaee, A., Zhou, J.L., Lockwood, T., Al-Juboori, R.A., **Hamdi, F.M.,** Karbassiyazdi, E., Samal, A.K., Hawari, A. and Khabbaz, H., 2022. Investigation of the effect of surfactant on the electrokinetic treatment of PFOA contaminated soil. ***Environmental Technology & Innovation***, 28, p.102938.

- Ganbat, N., **Hamdi, F.M.,** Ibrar, I., Altaee, A., Alsaka, L., Samal, A.K., Zhou, J. and Hawari, A.H., 2023. Iron slag permeable reactive barrier for PFOA removal by the electrokinetic process. ***Journal of Hazardous Materials***, 460, p.132360.

- Namuun Ganbat, Altaee, A., **Hamdi, F.M.,** Zhou, J., Chowdhury, M.H., Zaidi, S.J., Samal, A.K., Raed Almalki and Tapas, M.J. **(2024)**. PFOA remediation from kaolinite soil by electrokinetic process coupled with activated carbon/iron coated activated carbon - permeable reactive barrier. ***Journal of Contaminant Hydrology***, 267, pp.104425–104425.

ABSTRACT

Electrokinetic (EK) is an effective technique for electrochemical remediation of low-permeability soils. It involves applying a low-intensity direct current to mobilize soluble chemical species and soil pore solution. EK has been proposed for in-situ soil remediation to reduce excavation and hazardous exposure. However, the precipitation of heavy metals near the cathode in alkaline conditions remains a challenge. To enhance heavy metal removal, reactive filter media (RFM) and enhancement agents are employed, facilitating adsorption and resource recovery.

This study explored combining industrial iron slag waste with organic waste materials (activated carbon, tea waste, and sawdust) as RFMs to improve the performance of the EK process. Iron slag offers high heavy metal adsorption but struggles to control alkaline pH near the cathode. Blending iron slag with organic materials improved metal ions adsorption and pH control while recycling the anolyte solution eliminated the need for acids to neutralize the cathode's alkaline front.

Experiments conducted at 20 mA for 2-3 weeks demonstrated that coupling iron slag-activated carbon RFMs with EK increased copper removal from 3.11% to 23%, reaching 93.45% with anolyte recirculation and longer treatment. Testing a mixture of heavy metals showed 81.1% copper, 89.04% nickel, and 92.31% zinc removal after 3 weeks. Enhanced nickel and zinc removal was attributed to higher solubility compared to copper.

Recyclable RFMs composed of powder iron slag/black tea waste (PIS/BTW) and granular iron slag/black tea waste (GIS/BTW) were tested. PIS/BTW outperformed GIS/BTW, achieving 98.75% copper removal versus 90.06%. For a heavy metals mixture in kaolinite soil, copper, nickel, and zinc removal reached 97.15%, 98.30%, and 96.68% after 4 weeks, while natural soil results were lower due to environmental complexity.

Additionally, incorporating sawdust crosslinked with glutaraldehyde and iron slag into RFMs improved copper removal, achieving 97.92% in kaolinite soil at 0.18 kWh/kg specific energy. In natural soil, copper, nickel, and zinc removal reached 26.72%, 54.36%, and 56.44% after 5 weeks. The variability between kaolinite and natural soils highlights the challenges of applying laboratory findings to field conditions. This dissertation demonstrates that eco-friendly, recyclable RFMs can significantly optimize EK remediation, offering a sustainable solution for heavy metal contamination in soils.

CHAPTER ONE:

INTRODUCTION

CHAPTER ONE: INTRODUCTION

1.1. Background

Soils that are problematic present significant challenges for cultivation and require unique management strategies. Physical constraints such as texture, colour, structure, density, dryness, porosity, temperature, and chemical regulations like acidity, alkalinity, and fertility are typical (Parameswarappa Jayalakshmamma et al., 2021; Rehman et al., 2023). Due to industrial and urban development, there has been a significant increase in waste generation from various industries, including institutional, commercial, residential, agricultural, and chemical industries (Liu et al., 2021). Most infractions have metal contamination levels that exceed safe levels, mainly because metals are commonly incorporated into sediments and persist in the ecosystem. Heavy metals such as copper, mercury, and lead were used in mining and smelting by ancient civilizations like the Romans and Phoenicians, resulting in one of the earliest international contamination incidents. Heavy metals are associated with human diseases, and they can poison humans. Copper and aluminium have been found in groundwater in several countries, including India, Bangladesh, Inner Mongolia, Taiwan, and the United States, and they are linked to skin, lung, and bladder cancer. They can increase naturally occurring heavy metal concentrations in groundwater (Kim et al., 2000). The leading causes of soil pollution are agricultural activities, chemical industries, bad waste management policies, and other anthropogenic activities. Health and environmental risks are imposed by soil pollution (Brillas, 2021). Metallic substances with a relatively higher density than water are called heavy metals.

A class of metals and metalloids known as "heavy metals" are relatively dense and poisonous even at ppb levels. Metalloids, such as arsenic, antimony, and tin, are poisonous at low exposure levels (Mao et al., 2018). According to reports, sources of heavy metals are atmospheric, geogenic, industrial, agricultural, medicinal, and home effluent sources in the environment. Point source industries, including mining, foundries, oil refineries, paper and pulp, metal-produced industries, etc., are primary environmental pollution sources (Usman et al., 2022). The following powerful ingredients can penetrate cells and tissues due to their physicochemical characteristics, like ionic charge (Ait Ahmed et al., 2016). The latter group, thought to pose the greatest threat to life as we know it, requires special attention. It serves no vital purpose in living things and is too poisonous even at fewer exposure conditions and levels (Li et al., 2022a). According to the Environmental Protection Agency (EPA), the most harmful metals present in the environment are cadmium, lead, arsenic, and mercury (Isidro et al., 2022).

Additionally, environmental pollution is caused by heavy metal leaching, corrosion of heavy metals, soil erosion, and leachate transport to soil and groundwater through landfills, leading to soil and groundwater pollution (Chu et al., 2022). Industrial sources include plants that process metal in refineries, coal from thermal power plants, oil from oil refineries, nuclear power plants, textile industries, plastic manufacturing industries, electronic goods industries, and paper and pulp industries. Most studies mentioned that soil and groundwater get contaminated by the leachate produced by landfills (Vidal et al., 2021). This leachate has toxic elements depending on the waste it was generated. In most developing nations, leachate collection and treatment facilities are frequently not incorporated into dump site designs. Surface and groundwater contamination by leachate is one of the adverse effects of disposing of solid waste in landfills (Yang et al., 2020). The landfill's leachate quality determines the level of this pollution. The waste in landfills

is made up of different materials depending on the location. Some of them include the site's geographic location, the socioeconomic status of the community the landfill serves, the technology used in the landfill, the age of the waste generated, and current environmental factors like the local climate, all of which affect the leachate's composition (Zhou et al., 2019). Leachate transport has become a serious issue, mostly near landfill locations. Contaminant Flume demonstrates the concentration levels of contaminants like heavy metals, agricultural waste, and domestic waste.

In recent years, there has been a significant focus on using soil to remove pollutants that threaten the environment. While several methods are already available, most are expensive and do not provide optimal results. The primary reason is the high cost associated with generating soil using chemical technologies. Chemical and thermal methods for remediating heavy metal-contaminated soils are difficult to implement and can potentially damage the most valuable components of the soil (Gholizadeh and Hu, 2021a). The conventional methods for managing on-site contamination or excavation and subsequent disposal in a landfill are not sustainable. This practice merely shifts the problem of contamination to another location. Soil washing is an option for eliminating contaminated soil after excavation and disposal in a landfill. Still, it is prohibitively expensive and leaves behind a residue containing significant heavy metals. Relevant technologies have been developed to assess the presence of metals in soil and groundwater to address environmental concerns.

Saichek and Reddy conducted a study in 2004 on the use of surfactants/cosolvents for in situ flushing of soils contaminated with PAH. The study found that this method was effective in treating uniform and highly permeable soils but was not very efficient in dealing with heterogeneous and low-permeability soils. To address such challenging scenarios, electrokinetically enhanced in situ flushing emerged as a viable alternative,

depending on the choice of purging agent. The study also revealed that phenanthrene had a stronger binding affinity to the soil with higher organic content. Surfactants with a higher hydrophile-lipophile balance (HLB) demonstrated more significant potential for PAH desorption and solubilization. Also, the surfactant solutions showed improved performance at higher concentrations. When used independently, the surfactant solution surpassed the combined mixture of the cosolvent and surfactant solutions in the desorption and solubilization of the contaminants. However, for more challenging cases involving heterogeneous and low permeability soils, electrokinetically enhanced in situ flushing offers promising results, mainly when surfactants with appropriate HLB values are employed at higher concentrations. In 2017, Da Silva et al. conducted a study to investigate the effectiveness of electrokinetic remediation (EK) in eliminating petroleum contaminants from carbonaceous soils. They used graphite electrodes and Na2SO4 as electrolytes in their process. The study showed that the EK technique effectively removed the petroleum contaminants from the soil. This research provides valuable insights into the optimal operating conditions for achieving successful soil remediation through EK. A recent study conducted by Parameswarappa Jayalakshmamma et al. in 2021 has shown that combining Electrokinetic (EK) and a nonionic surfactant can effectively remove hydrocarbon contaminants from soils with high clay content. The study found that EK achieved an impressive removal rate of 80%, surpassing the efficiency of hydraulic flushing, which only managed to remove 52% under the same surfactant concentration. This research highlights the potential of EK as an effective remediation technique for addressing hydrocarbon pollution in soils with high clay content.

1.2. Research gap and significance

Electrokinetic soil remediation has been rigorously evaluated through experimental studies at both laboratory and field scales, highlighting its effectiveness and suitability

for soil remediation applications (Aboughalma et al., 2008; Chen et al., 2011; Ghobadi et al., 2021a; Hawal et al., 2023; Kim et al., 2012, 2002; Lee and Kim, 2010; Mohamadi et al., 2019; Parameswarappa Jayalakshmamma et al., 2021; Wang et al., 2021). The electrokinetic (EK) technique enjoys several distinct advantages compared to conventional soil remediation methods (Ghobadi et al., 2020; Kim et al., 2011). This method can be effectively employed for both in-situ and ex-situ treatment of polluted soils, demonstrating promise in addressing contamination concerns in saturated and unsaturated soils. It shines particularly in soils of low permeability, typically challenging to remediate using alternative techniques. Notably, EK offers the unique ability to treat soils contaminated with organic and inorganic substances simultaneously (Mohamadi et al., 2019; Zheng et al., 2024). EK is known for being easy to set up and operate in practical field applications. It can work seamlessly without disrupting site activities, making it a potentially cost-effective solution with relatively short treatment durations (Acar and Alshawabkeh, 1993). However, using electrokinetic remediation as the sole remediation technique can present some challenges. Applying a direct current across the treated soil can trigger the development of an alkaline pH front near the cathode zone. This phenomenon leads to the precipitation of contaminants, which can hinder their further transport and removal (Ghobadi et al., 2021b, 2020). Moreover, contaminants that precipitate within the soil adjacent to the cathode necessitate further treatment to inhibit their re-emergence and subsequent soil recontamination.

Currently, efforts are concentrated on increasing electrokinetic (EK) processing's range of applications and efficiency through several strategies, including careful control of electrolyte (pH), using enhancement agents like surfactants, chelating agents, or high molecular polymers, and applying combined systems (Zhao et al., 2016a). However, because it influences the length of treatment, cost, and environmental impact, choosing

the right enhancement approach is essential in the EK system. For instance, the introduction of an enhancement agent may have an impact on the soil matrix, which calls for the use of environmentally safe reagents in the EK system. Additionally, it is crucial to recover the electrolyte at the end of the EK system. Among the various techniques used for enhancement, RFM stands out due to its ability to quickly enrich or detoxify contaminants, thereby reducing treatment time and preventing contamination of the catholyte solution. Additionally, certain RFM materials can be regenerated through acid leaching, making them even more attractive. However, the effectiveness of EK treatment in conjunction with RFM depends heavily on the choice of RFM materials, as different materials have different degrees of effectiveness in this context (Ghobadi et al., 2021a, 2021b, 2020).

Previous studies have utilized high-permeability organic and inorganic RFM, such as activated carbon, biochar, and nanoscale zero-valent iron (nZVI), to capture metal ions. However, these approaches have demonstrated only moderate metal accumulation in the RFM, with significant precipitation of heavy metals remaining in the soil. This precipitation complicates both the EK efficiency and subsequent heavy metal extraction. Additionally, biochar and nZVI are not economically viable materials for widespread application. Research should prioritize the development of cost-effective, high-permeability RFM with strong affinities for heavy metals, including exploring organic and inorganic waste materials with excellent metal-binding properties. It becomes crucial to design recyclable RFMs that can be regenerated and reused to enhance sustainability. Using enhancement agents, such as acids, to neutralize the alkaline front generated at the cathode will increase the remediation cost and human risks. Therefore, research should focus on developing low-cost and innovative techniques in the RFM and EK process that enhance heavy metals removal and recovery.

The significance of this work is to develop an environmentally friendly, recyclable, high-permeability, and cost-effective RFM with a high affinity for heavy metals, leveraging organic and inorganic waste materials. Such an approach seeks to capture heavy metal contaminants while facilitating their recovery effectively. Iron slag byproduct was selected as a base inorganic material in all RFMs due to its availability in Australia, high adsorption capacity to heavy metals, and high permeability, while sawdust, activated carbon, and tea waste were the organic waste materials in the RFMs. The composite RFMs were evaluated for single and multi-heavy metals remediation from kaolinite and naturally contaminated soils. Finally, the experimental work evaluated, for the first time, anolyte recycling to the cathode to suppress alkaline front advancement in the soil instead of using chemical enhancement agents.

1.3. Research Objectives

Mainly, this study investigates the use of custom-designed RFM as an inexpensive material, and environmentally friendly to remove selected inorganic impurities from the soil. As a part of this investigation, we are trying to figure out the best operating conditions and possible applications for the most resistant material in removing hazardous metals from soil.

i) To investigate the adsorption and desorption capacity of various composite organic-inorganic RFMs. The adsorption capacity of iron slag mixed with sawdust, activated carbon, or tea waste was tested in multiple cycles to evaluate its efficiency in capturing heavy metals and reusability after desorption. The desorption tests evaluated the feasbility and effectiveness of heavy metals recovery at the end of the EK process. FTIR and EDX analyses were conducted to understand the mechanism of metal ions adsorption and desorption by the RFMs.

ii) To evaluate the feasibility of a hybrid organic and inorganic RFM for heavy metals treatment by the EK process. Iron slag waste was combined with organic waste adsorbent such as activated carbon to serve as the RFM in the EK process. The impact of the electric current, the process duration, and the RFM composition were evaluated for the removal of heavy metals by the EK process.

iii) To investigate the efficiency of the RFM-EK system for heavy metals removal from kaolinite model soil and naturally contaminated soil. The effect of soil compositions, including the concentration of organic and inorganic matter and soil pH, on the metal removal was studied in the EK process tested under different conditions, including the process duration, electric current, and EK combined with recycled RFM.

iv) To investigate the feasibility of recirculating the anolyte for the neutralization of the alkaline front, preventing its advancement in the soil. For the first time, the anolyte solution was recirculated to the cathode to neutralize the pH of the catholyte instead of using traditional enhancement agents, such as acids. Experiments also tested the effect of the EK duration and the multi-heavy ions contamination on the performance of the RFM-EK system.

This study offers valuable insights into the feasibility of removing contaminants from kaolin using EK and EK-RFM systems. Additional experiments were conducted to assess the treatment of multiple metals in natural soil using EK-RFM, along with the post-treatment processes for the recycling and reuse of EK-RFM. To ensure quality assurance, tests were repeated to verify the reproducibility of the results.

1.4. Thesis Outline

This thesis is organized into seven chapters, outlined below:

Chapter 1 introduces this PhD work by defining the research problem, heavy metal removal technology, research gap, significance and objectives. It highlights the key tasks required to achieve these goals and defines the scope of the research. This chapter also provides an overview of the background and importance of the study.

Chapter 2 provides a comprehensive review of remediation technologies for heavy metal-contaminated soils, with a particular focus on electrokinetic remediation. It offers an in-depth analysis of the scientific literature on the application of this technology, discussing key factors that influence its effectiveness, such as types of pollutants, soil characteristics, and electrical materials. The chapter also explores enhancement techniques and their integration with EK processes for metal removal, comparing combined EK approaches with conventional methods. Finally, Chapter 2 reviews the main insights from the literature and outlines the most suitable research direction for this study.

Chapter 3, Materials and Methodologies, outlines the materials and methods employed in this PhD study.

Chapter 4, titled "Iron slag/activated carbon-electrokinetic system with anolyte recycling for single and mixture heavy metals remediation," investigates the use of iron slag and activated carbon RFMs in the EK system for the removal of single and mixture heavy metals remediation.

Chapter 5 explores “black tea waste/iron slag reactive filter media-electrokinetic for mixed heavy metals treatment from contaminated site.” This chapter discussed the application of comparing powder iron slag with granular iron slag coupled with black tea waste as a novel and recyclable RFM. Also, in this study, an innovative strategy is being

developed to optimize the EK process for removing one element or mixing elements from kaolinite soil and heavy metal pollutants from natural soil.

Chapter 6 explores “Decontamination of heavy metals from the soil by electrokinetic combined with reactive filter media from industrial wastes.” The study's novelty lies in introducing an environmentally sustainable method of soil treatment by coupling the EK process with a hybrid organic-inorganic sawdust/iron slag RFM. Also, to develop an innovative technique to optimize the EK system for the removal of copper from kaolinite soil and heavy metal contaminants from natural soil.

Chapter 7 summarizes the main conclusions of this study on heavy metal removal from soil using the EK system, along with suggestions for additional research.

CHAPTER TWO:

LITERATURE REVIEW

CHAPTER TWO: LITERATURE REVIEW

This chapter offers a concise literature review on Electrokinetic Systems for Soil Remediation targeting Heavy Metals and Organic Matter. It delves into the drawn solutions employed in Electrokinetic soil treatment applications, alongside discussions on RFM (Reactive Filter Media), fouling, and methods for fouling mitigation. The content of this chapter the publication details below:

Hamdi, F.M., et al. (2025) "Hybrid and enhanced electrokinetic system for soil remediation from heavy metals and organic matter," Journal of Environmental Sciences, 147, pp.424-450.

2.1. Principles of electrokinetic soil remediation

Electrokinetic techniques have provided a considerable practical strategy for removing heavy metals from the soil. Electrokinetic methods are based on low-intensity electricity for soil remedy, through which heavy metal ions are transported and precipitate at the reverse electrode by electroosmosis (Xie et al., 2021). A low electrical current is transferred between the cathode and anode electrodes inserted into the contaminated soil, resulting in heavy metal dissolution and removal. A guiding pore liquid in the soil mass that needs to be treated is crucial for this treatment method (Guo et al., 2022; Kumar et al., 2022; Wei et al., 2022; Zhang et al., 2022). The main transport mechanisms of pollutants in the EK process are electroosmosis, electromigration, and electrophoresis (Hassan and Mohamedelhassan, 2012). Electroosmosis is the motion of liquid generated in soils under an electric current. Water movement can work for charged and uncharged organic contaminants in response to an electrical gradient since the dissolved molecules will carry the moving water.

In contrast, electromigration is the transport mechanism of charged ionic molecules under an electric field where ions migrate towards the electrode of opposite charge. Finally,

electrophoresis is the transport of charged species towards anode under the influence of the electric field. The transport mechanism of contaminants is bound to a charged particle.

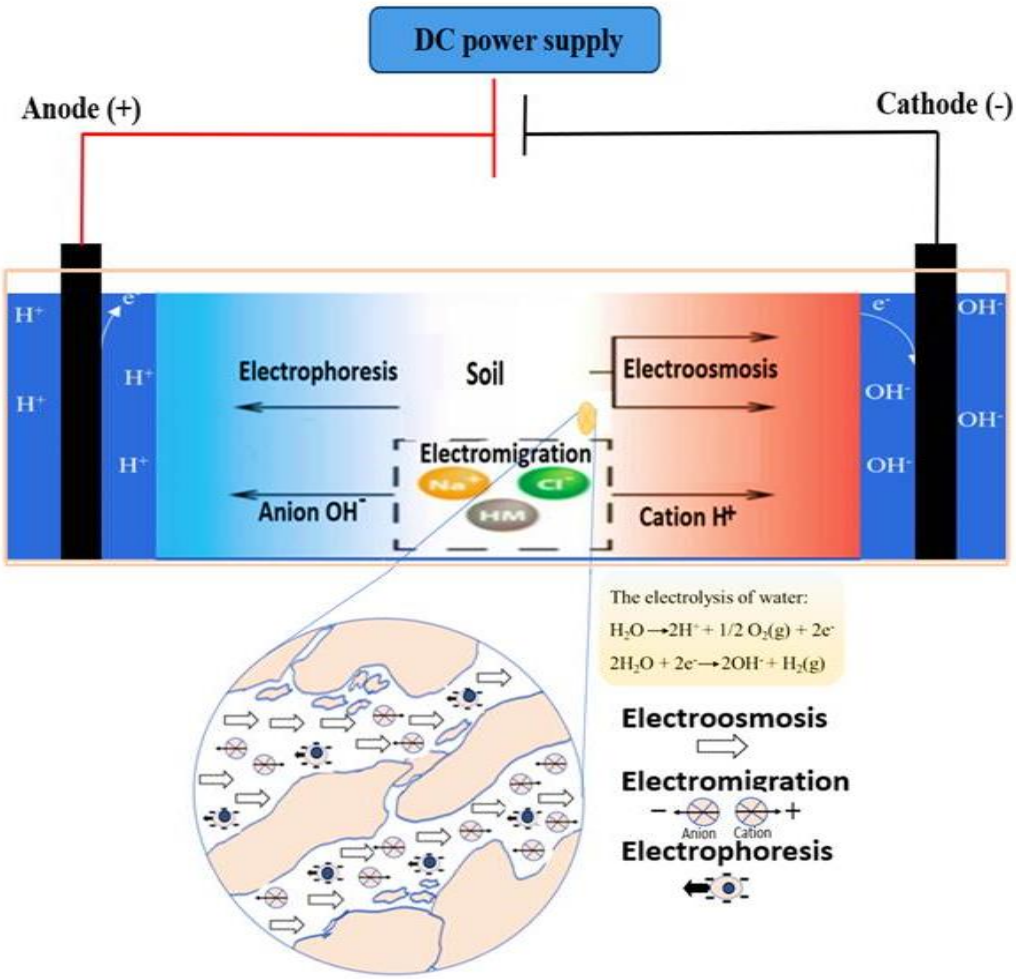

Figure 2.1: The main principles and mechanisms that occur during EK processing.

Additionally, the toxic species must be solubilized during the treatment process by adding acids or other superior synthetic compounds for this remediation approach to be effective (Ahmed et al., 2022; Azhar et al., 2022). The electrical flow causes electro-assimilation and particle displacement, transferring pollutants in the subsurface in the watery stage from one cathode to the next. Depending on their charge, impurities in the aqueous phase or pollutants desorbed from the dirt surface are sent in different directions towards

different anodes (Gnanasundar and Akshai Raj, 2021; Yusni and Tanaka, 2015). The pollutants could then be saved at the terminal or transferred to a recovery structure. Reagents could be introduced at the cathodes to increase the removal rate of heavy metal pollutants (Brillas, 2021; Chu et al., 2022; Isidro et al., 2022; Usman et al., 2022).

The technique of electrokinetic remediation relies on the gradient electric field theory, as shown in **Figure 2.1**. Electrolytes, such as distilled water or organic acids, are crucial for maintaining soil pH and increasing the effectiveness of electrokinetic treatment. This technology works under different conditions and places, such as wells, to contain low-permeability solids. This technique is reasonably practical and straightforward compared to other methods for removing contaminants from soil. Direct electrokinetic treatment is limited by the variability in soil pH (Rebello et al., 2021).

Recently, electrokinetic studies have shown an effective method of separating inorganic pollutants from the soil using reactive filter media (RFM) (Ghobadi et al., 2021a). It works by electromigration or reverses osmosis, which separates inorganic minerals from the soil. One of the earlier investigations by Kim et al. (2021) on electrokinetics to separate contaminants such as Cd, Cu, Pb, Ni, and Zn from the soil. By using the effect of the seven electrodes on the removal and deposition of pollutants (Gholizadeh and Hu, 2021a; Kim et al., 2021). The results showed the high efficiency of removing heavy metals from the soil. However, using seven electrodes may not be cost-effective, and the cost must be considered in the treatment conditions.

Furthermore, an experiment was performed by Ghobadi et al. (2021b) to remove heavy metals under different EK operating conditions, using compost RFM (reactive filter media) for heavy metal collection and extraction from the soil. The observed results agree with Kim et al.'s previous experience (2021). Electric current is a prominent factor in displacing organic and inorganic minerals. The amount of electric charge flowing through

the soil pore solution during a given time was positively related to the electric current density in the sample. During the EK technique, pH change performance reactions occur, creating a pH gradient from lower pH at the anode to higher pH at the cathode due to the electrolysis of water. In principle, developing a low pH front at the anode will dissolve heavy metal ions in the soil and electromigrate them toward the cathode region. However, acid front movement in the soil results in soil acidification, which is one of the EK process drawbacks.

Hence, the pH changes dynamically, resulting in the migration of heavy metal ions in the soil when hydronium ions move toward the cathode. It has been observed that when the pH is low, it contributes significantly to transporting pollutants such as cadmium and zinc. In contrast, it does not contribute considerably to transporting copper and lead from the soil, and perhaps this is due to its complex organic composition. Copper and lead migration have improved significantly when the soil contains organic matter. Also, it was observed that there is an electrostatic attraction between the negatively charged ions in the compost with RFM and the metal cations, which can improve the adsorption of Heavy metals (Ghobadi et al., 2021a).

In addition, most researchers are currently focusing on the experimental work associated with several feasibility studies to demonstrate the efficiency of EK technology. Research on developing it to enhance the removal of target pollutants, consume less energy and reduce side impacts on remedied porous media and runtime (Ghobadi et al., 2021a; Gholizadeh and Hu, 2021a).

The characteristics of soil pollution vary significantly based on the specific industry or activities that cause contamination. When considering electrodynamic treatment of soil pollutants, there are particular prerequisites to ensure effective remediation. Some prerequisites for electrodynamic treatment are listed in **Table 2.1.**

Table 2.1: Prerequisites for electrodynamic treatment of soil.

Requirements	Experimental parameter	Comment
Understanding Pollutant Characteristics	Heavy metals, organic compounds, or contaminants with different chemical properties.	It is necessary to conduct a comprehensive analysis of the soil and its pollutants. Each industry may introduce specific contaminants, and understanding these contaminants is vital to determining appropriate electrodynamic treatment methods.
Soil Composition Analysis	Porosity, pH, moisture content, and texture	A comprehensive understanding of soil properties helps in devising a suitable electrodynamic approach.
Electrokinetic Remediation Suitability	Type of contamination and type of soils.	Assess if the contaminants and soil type are suitable for electrokinetic remediation. Not all pollutants or soil types are ideal for this method. For instance, fine-grained soils are generally more amenable to electrokinetic remediation.
Electrode Placement and Configuration	Locations of electrodes, types of electrodes, and types of contamination	Determining the optimal electrode placement and configuration is crucial. The design and placement of electrodes should consider the soil's characteristics and the distribution of contaminants to ensure efficient treatment.
Current and Voltage Control	Type of electrodes, type of soils, and types of contamination	The appropriate current and voltage applied during electrodynamic treatment must be controlled and optimized. Excessive or inadequate application might affect the treatment efficiency and soil structure.
pH and Ionic Strength Adjustment	Type of soils and types of contamination	Sometimes, adjusting the pH or ionic strength of the soil might be necessary to enhance the efficiency of electrodynamic treatment. This adjustment can facilitate the mobility of certain pollutants within the soil.
Complementary Remediation Techniques	Phytoremediation, bioremediation, or the use of reactive filter media.	Consider integrating electrodynamic treatment with other technologies to treat specific contaminants or enhance the overall treatment process.

2.2. Type of contaminants treated by the EK

The efficiency of the electrokinetic removal process depends not only on the physical and chemical effects of the soil. And also on the type of pollutants deposited, their distribution, and their concentration in the soil (Lim et al., 2016a). Therefore, in recent

years, the EK process has shown its high efficiency in removing contaminants, but the effectiveness depends mainly on the type of target pollutant. The target pollutants must be soluble or transportable to be transported by electroosmosis or electromigration (Ghobadi et al., 2021b). Insoluble metal hydroxides may precipitate near the cathode region, which makes the EK technique less efficient in removing contaminants (Vocciante et al., 2017). The pollutants the EK process may contribute to their treatment are i) Heavy metals mixed with organic/inorganic contaminants, ii) Anions (sulfates, nitrates), iii) Radioactive species (Sr90, Cs137, Co60, U), iv) Cyanides, v) Petroleum hydrocarbons (diesel fuel, gasoline, lubricating oils, and kerosene), vi) Dense non-aqueous phase liquids (DNAPLs), vii) Polycyclic aromatic hydrocarbons (PAH), viii) Explosives, ix) Halogenated hydrocarbons (TCE), and x) Nonhalogenated organic contaminants (BTEX) (Ghobadi et al., 2020; Lim et al., 2016b).

Overall, heavy metals removal efficiency depends on their solubility; the more soluble heavy metal is, the higher the removal efficiency by the EK process. Metal ions of high concentration, low solubility, and uncharged organic substances are challenging pollutants for the EK treatment. For example, low solubility and uncharged organic pollutants, such as phenanthrene and metal sulphide precipitates, are difficult to remove by the EK process.

2.3. Factors Affecting Electrokinetic

The effectiveness of the electrokinetic process will depend on various factors like soil type, the topography of the contaminated area, the physical and chemical properties of soil, electrode type, spacing, electrode configuration, and the voltage employed during the treatment process, according to earlier studies. Steel tubes are used as cathodes, and iron or aluminium bars are used as anodes in most practical electrokinetic applications (WANG et al., 2021). Graphite terminals are occasionally used for both the anode and

the cathode. It is more affordable than other electrodes. When the current thickness was raised from 4.36 - 13.1 $mA.cm^{-2}$, the efficiency of nickel removal increased from 49.3 - 57.2% (Rahman et al., 2021). **Table 2.2** shows the impact of soil type, current, and voltage on the removal efficiency of the EK.

2.3.1. Type of soils

Natural soil is a mixture of organic and inorganic materials distributed across the soil matrix. The physicochemical characteristics of contaminated soil will significantly affect the performance of the EK process and the remediation process efficiency. Organic matter negatively affects the EK performance, slowing the acid-front advancement across the soil through reaction with the hydronium ions (Ghobadi et al., 2021a). The buffering effect of soil's organic matter can bind and release hydronium ions, maintaining a relatively stable pH in the soil. Also, organic matter contributes to the soil's cation exchange capacity (CEC), which allows it to retain and release various cations, including hydronium ions. Metal ions, including alkaline earth metals, could negatively affect contaminant transport by competing for the exchange sites, forming precipitants with contaminants, or fouling the electrode surfaces, leading to a less efficient EK process. Therefore, soil analysis and characterization are essential before commencing the EK process. Determining soil pH, permeability, particle size analysis, CEC, and moisture content is essential before field tests.

Soil resistivity depends on several factors in EK, including soil properties, initial moisture, content type, and ion concentration present in the soil. For example, soil type, pore water pH, soil pH, storage capacity, sorption capacity, and electrical conductivity influence the effectiveness of electrokinesis in removing organic, inorganic, and radioactive materials (Ghobadi et al., 2021a). Soil's desorption and absorption capacity are related to the contaminant types and their concentration in the soil. At the same time,

highly active soils containing clay minerals like impure kaolinite, montmorillonite, and Illite have a higher ion exchange capacity. Therefore, various enhancement agents are needed to make the pollutants soluble before they proceed through the subsurface soil pores. Kaolinite was employed as a model soil to investigate the influence of experimental variables on the EK performance. Nonetheless, it should be noted that kaolinite does not comprehensively reflect the EK efficiency in actual soils, which are characterized by greater complexity. Clayey soils usually carry a negatively charged and can firmly retain positive species resulting from ionic interactions such as inorganic (Ghobadi et al., 2021b).

In addition, the high sorption capacity of clay soils of positive species will exacerbate the problem by impeding the movement of pollutants. Kim and colleagues (2002) found that pore water and soil pH significantly influence pollutant ion valence, sorption, and solubility. It is crucial to comprehend the electrical conductivity of the soil, as it can significantly influence the performance of the electrokinetic process. Electrical conductivity, typically in milli-siemens per meter, is defined as a material's capacity to convey an electric current (Kim et al., 2002). The soil's moisture content and ion concentration also affect its electrical conductivity. For uncontaminated clay soils, the electrical conductivity of soil usually ranges from 10 to 500 mS per m, and for sandy soils, it ranges from 0.1 to 5 mS per m (Ghobadi et al., 2020). As a result of these factors, the variation in the soil’s electrical conductivity leads to fluctuations in the applied electric field during electrokinetic experiments.

Furthermore, soil physicochemical characteristics significantly influence pollutant removal by the EK process. The cation exchange capacity of kaolinite, illite, montmorillonite, vermiculite, and organic matter is up to 15, 40, 100, 160, and 400 meq/100 g, respectively. Technically, soils of high cation exchange capacity, such as

montmorillonite, exhibit strong affinity high and adsorption capacity to heavy metals. In contrast, kaolinite soil, because of its low cation exchange capacity and metal ions adsorption, was used as a model soil to facilitate investigating the impact of various experimental parameters on the process performance. For example, compost RFM-EK tests achieved 74% copper removal from kaolinite soil and decreased to 16% in natural Sydney soil (Ghobadi et al., 2021b). Besides, organic matter in soil binds metal ions, forming complexes by ion exchange, adsorption, and chelation. Since most natural soils contain organic matter, the latter effect on the EK remediation of heavy metals should not be ignored when scaling up to field tests. Generally, the efficiency of the EK process decreases in soils of high cation exchange capacity or when they contain organic matter at high concentrations. In addition, soil acidification, as a drawback, often occurs at the end of the EK process.

2.3.2. Type of Electrode

Electrodes, critical to the EK process, are electrical conductors that transmit electrical current from one side to the other. The electrodes' materials, shapes, and configurations significantly affect process efficiency, installation cost, and operating time (Ghobadi et al., 2021a). In the EK process, electrodes are used from various materials and may be made of metal or non-metallic materials such as steel, tubes, rods, plates, or wires. These materials are the most desirable electrokinetic applications because they are inert, corrosion resistant, inexpensive, and low in voltage, which is of high importance because of their resistance to rust, high electrical conductivity, and ease of implementation and installation, such as graphite, steel, and titanium (Ghobadi et al., 2021a; Suzuki et al., 2014b). **Table 2.2** shows a few examples of the electrode types coupled to the EK process, including these electrodes' advantages and disadvantages.

Table 2.2: Summary of the types of electrodes coupled to the EK process (Chatterjee and Schiewer, 2014; Ghobadi et al., 2020; Suzuki et al., 2014b; Yuan and Weng, 2006).

Type of Electrode	**(Pt/Ti)**	**(IrO2/Ti)**	**Graphite**	**Iron**	**(BDD)**
Type of contaminants	Heavy metals	Heavy metals	Heavy metals	salt extraction	organic contaminants
Advantages	• Electrochemical inertness and mechanical strength • Good operability and electrical conductivity • It is characterized by durability and high protection from corrosion. • Low consumption and environment friendly	• The current density is maintained over time with considerable continuity over its initial range. • It is characterized by durability and high protection from corrosion.	• Low-cost and somewhat effective • Rich in raw materials • Good electrical conductivity	• More economical than other electrodes • Good operability and electrical conductivity	• High conductivity and wide potential window. • High resist corrosion • Provides longer EK process lifetime. • Chemical inactivity • Low resistance and good thermal conductivity • Reduced contaminants
Disadvantages	• High cost • The conductivity depends on the type of titanium anode with platinum coated.	• High cost • The conductivity depends on the type of titanium anode with platinum coated.	• Significant decrease in current over time • Accumulation of gases on porous graphite electrodes • low current density • - low oxidation temperature	• Low electrical conductivity • It has a short life • Soluble, produces iron oxides, easily seeps into the soil, and may change its colour	• Can raise electrochemical oxidation of contaminants. • Unsuitable because its insulator behaviour makes it less interesting for electrochemical applications

[Pt/Ti – Platinum-coated titanium; IrO2/Ti – Iridium dioxide-coated titanium; BDD – Boron-doped diamond]

To overcome the accumulation of the electric double layer during the EK process, periodically reversing the polarity of the electrodes can disrupt the accumulated electric double layer. This intermitted operation can reduce energy consumption. Selection of an appropriate electrolyte solution will maintain the soil's ionic conductivity, reducing the risk of electromigration passivation and maintaining the efficiency of the process. Surfactants can help reduce energy consumption by improving the wetting and mobilization of contaminants, making the process efficient. Rinsing the electrodes with DI water dissolves and carries away contaminants on the electrode surface (Yeung and Gu, 2011). Also, adjusting the voltage and current density can help manage the formation of these layers (Ganbat et al., 2022). In terms of affordability, iron electrodes are available and inexpensive but not recommended for use in the EK process as they corrode over time (Reinout Lageman, 2011). Graphite electrodes are suitable for alkaline conditions in the cathode, while a particular type of steel is used at the anode. Coated titanium is not recommended since generated hydrogen will remove the coating, leading to titanium corrosion.

In one study by Suzuki et al. in 2014, they investigated Pb ions removal from polluted kaolin soil under the influence of three different electrodes for each electrode material established on the current density change over time. The study showed that the electrode material type significantly affects the EK process's efficiency in removing lead. It contributes better to lead removal with platinum-coated titanium than iridium-coated titanium, followed by graphite. Graphite electrodes demonstrated a substantial decrease in current density overtime during the removal process, as observed in experiments and comparisons with other electrodes. This reduction can be attributed to the release of oxygen or hydrogen gases due to water electrolysis on the electrode surfaces, along with the accumulation of these gases within the porous graphite electrodes.

In contrast, the other two types of electrodes used in the experiment did not show any reduction in current density over the period. They kept their initial range to a considerable extent (Suzuki et al., 2014b). Due to the electrolysis reaction constantly generating hydroxide ions at the cathode and hydronium ions at the anode, a pH gradient is inevitable during the EK process. Depending on the electrode in use, corrosion at the anode may occur because of the continuous release of H^- however, heavy metal removal is pH-dependent. Lower pH favors transporting heavy metals towards the cathode region (Ghobadi et al., 2021a). Hydronium ion's ionic mobility is 1.8 times higher than hydroxide ion. Therefore, hydronium ions can sweep across the soil at a higher rate; however, integrating the EK process with surfactants or applying RFM can mitigate the issue.

2.3.3. Applied voltage.

One of the critical factors in the EK process is the voltage gradient across the soil specimen. A low voltage gradient is usually applied during laboratory experiments at the beginning of the EK. The voltage is gradually increased to a maximum throughout the treatment process, or a specified constant voltage is applied from start to finish on the EK system (Huweg, 2013). When applying a higher voltage gradient, soils may lose their physical and chemical properties. It was recommended by Ghobadi et al. (2021a) that the voltage should not exceed 50 V/m on the soil to avoid loss of soil properties, which may affect electrical permeability due to soil heating, and prevent energy loss, which limits the effectiveness of the EK process. Increased electric resistance may be related to reduced electric current through the EK (Ghobadi et al., 2021a; Suzuki et al., 2014b). Removing ions and precipitation near the cathode region, which is the source of the formation of a high electric resistivity zone, decreases the current flow over time under constant voltage application across the soil in the EK system (Huweg, 2013). Various

factors led to the present decline. Accordingly, the soil ions were moved by electromigration towards the electrode compartments, and metal ions precipitated because of elevated soil pH close to the cathode, lowering the EC (Ghobadi et al., 2020).

Table 2.3: Heavy metal removal by the impact of different soil and voltage/current of the EK efficiency.

Type of Soil	Target contaminant/Duration	Electrode material	Anolyte/ Catholyte	Voltages	Current	Removal efficiency (%)	Ref.
Red soil	Cu and Zn for 24 days	Graphite	No mentioned/ Lactic acid	1 V/cm	100 mA	63.0% & 65.0%	(Zhou et al., 2005)
Kaolin	Cd for 6 days	Titanium iridium - ruthenium oxide coating	Potassium nitrate/ Nitric acid	1.0±0.1 V/cm	100 mA	98.0%	(Almeira O. et al., 2012)
Paddy and dry soil	As for 56 days	Stainless-steel	Sodium hydroxide/ EDTA	1 V/cm	-	78.8% & 78.6%	(Kim et al., 2012)
Kaolin	Cu for 7 days	Graphite	Deionized water on both sides	-	20 mA	84.09 %	(Ghobadi et al., 2021b)
Natural soil	Cu, Pb, Cd, Mn and Zn	Graphite	Deionized water on both sides	-	30 mA	Cu and Pb were removed from 28.2% to 29.1%, Cd, Mn and Zn from 51% to 71%	(Ghobadi et al., 2021a)
Kaolin	Cr for 7 days	Graphite	Citric acid on both sides	1 V/cm	-	13.07%	(Wu et al., 2016)
Kaolin	Cu for 8 days	Graphite	Ammonium acetate/ Deionized water	-	10 mA	35.9%	(Chen et al., 2011)

Industrial wastewater	Pb for 10 days	Platinum-coated titanium	Sodium hydroxide/ EDTA	1 V/cm	10 mA	36.3%	(Amrate et al., 2005)
Industrial wastewater sludge	Cu^{2+}, Cr^{2+}, Ni^{2+}, Fe^{2+}, and Zn^{2+} for 5 days	Graphite	-Tap water on both sides -Sodium dodecyl sulfate on both sides -Citric Acid on both sides	1.25V/cm	24 mA	11.2% to 60% 37.2% to76.5% 43.4% to 78%	(Yuan and Weng, 2006)
Clay soil	Pb for 1 to 2 days	Graphite	Tri ammonium citrate on both sides	1 V/cm	-	10% to 25%	(Utchimuthu et al., 2012)
Kaolin	Cd and Pb for 4 days	Platinum/ Titanium	KNO_3 (0.01M) on both sides	-	100mA	42.64% and 26.74 %	(Kim et al., 2005)

2.4. Techniques for enhancement and integration with EK

During the research, it was found that many techniques contribute to treating inorganic compounds in soil. It is possible to say that we can apply no specific technique to all inorganic contaminants. The reason is due to these heavy metals' physical and chemical compositions, and each metal has its unique composition. Before treatment, the type, concentration, and physical and chemical properties of these minerals must be known at the site to ensure the quality of treatment and the removal of these pollutants (Ghobadi et al., 2021a; Rebello et al., 2021; Xu et al., 2021). The techniques created over time to improve the efficacy of EK remediation in contaminated soils have been extensively reviewed. They have categorized these techniques into three methods:

1) Techniques involving complexing agents, surfactants, oxidizing/reducing agents, chelators, and cation solutions are employed to solubilize pollutants and keep them in a chemically mobile state.

2) Techniques like electrolyte conditioning and ion exchange membranes maintain soil pH within a range favourable to the EK application.

3) The EK may use remediation techniques such as oxidation/reduction, bioremediation, phytoremediation, Nanoremediation, reactive filter media, and permeable reactive barriers to simultaneously break down or transfer the pollutants.

However, the first and second methods are connected because they maintain pollutants soluble throughout the EK procedure. Most of these techniques differ in their efficiency in removing heavy metals, and different methods and strategies have been applied to treat soil polluted with inorganic compounds. These methods have been used both on-site and off-site. In contrast, more studies have shown that when two or more soil remediation methods are combined, they are more effective in removing pollutants (Rebello et al., 2021). Factors influencing contaminant removal methods and the selection of an

appropriate treatment are the technology cost, the method's efficacy, general acceptability, commercial availability, applicability to different metal concentrations, mobility, and contaminant toxicity and size reduction (Ghobadi et al., 2021a).

2.4.1. EK using enhancement agents

Researchers incorporated specific extraction agents to interact with the target pollutant to manage pH fluctuations during the EK process and to enhance the solubility of inorganic contaminants. This enhanced method dramatically increases the process's efficiency, allows for the selective extraction of the target contaminants, and prevents adverse effects on soil remediation (Ghobadi et al., 2021b). Adding an enhancement agent to the treated soil will improve its ionic conductivity, increasing the electric current flowing through the soil sample in an EK system. As a result, an enhanced EK method would require more time to treat patients than the unenhanced EK method (Altaee et al., 2008). Examples of substances that solubilize pollutants and preserve their chemical mobility include complexing agents, chelators, surfactants, oxidizing/reducing agents, and cation solutions (Ghobadi et al., 2020). However, choosing an agent is essential for the EK method; thus, various criteria should be evaluated when selecting a suitable enhancement agent (Ghobadi et al., 2020). During the EK process, the agents must not produce insoluble salts in different pH values with the pollutant. Thus, applying a direct-current electric field makes transporting pollutants effectively by generating soluble compounds possible. Therefore, they should also not produce hazardous remains in the soil after treatment (Paramkusam et al., 2015). Paramkusam et al. (2015) researched the impact of several desorption agents on the sorption/desorption behaviour of copper and cadmium in clayey soil during the EK technique. The results showed that the EK process removed Cu and Cd at higher rates when ammonium citrate (1 M) was a desorption agent. Due to several unsatisfactory laboratory tests, enhancing agents in the EK technique is not always

encouraged. Tian et al. (2017) assessed an EK method's ability to use environmentally friendly enhancing agents (citric acid, saponin, and rhamnolipids) to simultaneously remove heavy metals, including Cu, Pb, Cd, Cr, and PAH/PCB from harbour sediment. According to the findings of their experiments, the combination of the agents was unable to entirely remove the high concentrations of metals (4.4% and 15.8%), and it did a marginally better job at removing PAH (29.2%) and PCB (38.2%). The harbour sediment exhibited strong resistance to the mobilization and movement of heavy metals due to old pollution, higher storage capacity, very low hydraulic permeability, a reduced environment, and a large quantity of organic matter. As a result, the technique's effectiveness did not improve much (Ghobadi et al., 2021a; Tian et al., 2017).

According to Adrion et al. (2016), “surfactants are agents that assist in remediation processes by enhancing the efficiency of contaminant removal.” Surfactants are typically categorized as anionic, cationic, or nonionic, but the first and last types are more commonly used in remediation. Their effectiveness lies in their ability to attach to pollutants, allowing easier movement and removal, particularly for stubborn organic contaminants (Adrion et al., 2016; Luthy et al., 1997). The low solubility and limited bioavailability of hydrophobic organic compounds hinder their removal using conventional remediation methods. Therefore, surfactants are employed to enhance the removal efficiency of these organic contaminants. Surfactants in the environment can lower water's surface and interfacial tension, thus improving the solubility of organic pollutants. Surfactants typically have a molecular structure with a hydrophobic chain at one end and a hydrophilic, water-soluble group at the other. The different behaviors of surfactants and co-solvents in desorbing organic pollutants from soil stem from their distinct chemical properties and interactions. Surfactants enhance desorption by improving accessibility and solubilizing pollutants, while co-solvents, while helpful in

increasing solubility, might have limited effectiveness in displacing pollutants from soil particles due to competitive interactions and limited affinity for soil surfaces.

The interaction between the water-soluble group and the soil's interstitial fluid facilitates solubility, while the hydrophobic group interacts with organic pollutants to solubilize them. This process leads to the formation of a micelle, which occurs at a specific minimum concentration known as the critical micelle concentration (CMC) (Alcántara et al., 2008). Surfactants diminish surface and interfacial tension, making persistent hydrophobic substances more water-soluble and biodegradable. They consist of a water-soluble group and an insoluble group. Through interaction with hydrophobic organic compounds, surfactants form spherical-shaped molecules, significantly increasing organic contaminant solubility when the concentration exceeds the critical micelle concentration (CMC). In environmental applications, surface-active agents modify the solution's surface properties, thereby improving the solubility of hydrophobic contaminants (Adrion et al., 2016; Yao et al., 2017). Surfactants have hydrophobic and hydrophilic properties; therefore, surfactants reduce the surface tension of the water in the soil pores when added to the soil. This reduction in surface tension allows water to wet the soil and contact the organic contaminants more effectively. As water infiltrates the soil, it helps mobilize the organic contaminants by surrounding and solubilizing them. Organic contaminants in soil are often bound to soil particles and may not be readily available for removal. Surfactants can disrupt these bonds by adsorbing onto soil particles, creating micelles, and facilitating the desorption of organic contaminants. Micelles are small, water-enclosed structures formed by surfactant molecules that can trap and solubilize hydrophobic organic compounds. The addition of surfactants in the EK process can enhance electroosmotic flow by reducing the friction between the soil particles and the infiltrating water, which mobilizes and transports solubilized organic

contaminants toward the electrode with an opposite charge, facilitating their removal. The HOC solubilized with surfactants is transported to the electrode of the opposite charge, and it can be captured, treated, or immobilized and managed for appropriate disposal (Ganbat et al., 2022). **Table 2.4** presents several examples of using surfactants or other remediation techniques to remove heavy metals and persistent organic pollutants from contaminated soils, thereby improving contaminant removal efficiency. Notably, using enhancement agents will increase the cost of the EK treatment and could introduce new chemical pollutants to the environment.

Table 2.4: Evaluation of electrokinetic treatment performance for different soil contaminants.

EK treatment **Target pollutant**	**Enhancement**	**Removal rate**	**Ref.**
Chromium	Citric acid pre-acidification enhancement	77.66%	(Meng et al., 2018)
Chromium, Copper and Nickel	EDTA-enhanced EK in combination with cation exchange membranes	Reduction from 80% to 20%	(Song et al., 2020)
Organochlorine pesticide	Triton-X advanced oxidation Surfactant enhanced.	88.05% (1,2,4-TCB) 56.36% (4,4-DDE)	(Suanon et al., 2020)
Organochlorine pesticide D.D.T. and chlordane	TX-100; S.D.B.S., ethanol as solubilizing agents	TX-100 on chlordane and DDDs 80%; on DDT 70.4%; SDBS inefficient.	(ZHANG et al., 2019)
Cadmium and Lead	Acid enhanced EK	The kaolin-Pb/Cd model demonstrated effective removal performance, making it a reliable predictive tool.	(Rezaee et al., 2019)
Phenanthrene	SDS; Brij 30; Hydrogen peroxide	SDS 9.97%; Brij 6.31% Hydrogen Peroxide 54.7% At 10mA(7 Days) 84.2%	(Park et al., 2002)
Phenanthrene	Hydroxypropyl-β-cyclodextrin	56% removal rate with 6.85mM HPCD	(Ko et al., 2000)
Phenanthrene	Brij30; APG, SDS Surfactant enhanced EK	APG-75.1% removal rate after 4 weeks; Brij30 56.5% after 4 weeks.	(Park et al., 2007)

Mixed contamination Heavy metals and organic pollutants	Co-solvent (n-butylamine) extraction coupled with EK	Phenanthrene migrated toward the cathode proportional to the co-solvent concentration, while nickel ions were immobilized rather than extracted.	(Maturi and Reddy, 2008)
PFAS	Ion-exchange membrane	26%-56%	(Sörengård et al., 2019)

2.4.2. EK coupled with Bioremediation

Bioremediation is one of the most cost-effective methods for cleaning contaminated soils. Various remediation strategies have been used with varying levels of effectiveness to minimize soil pollution. The research establishment believes no single remediation technique will be appropriate for all pollutants and soils. Due to soil heterogeneity and the variety of contaminants, a helpful solutions plan may involve the collective execution of two or more methods. Individual bioremediation applications in fine-grained soil are expensive and generally inefficient (Ghobadi et al., 2021b). Because this soil type has low permeability, it is challenging to supply pollutants with microorganisms and the required electron acceptors or nutrients (Gill et al., 2014). Also, the fundamental obstacle in putting in-situ conventional bioremediation approaches is getting nutrients to local bacteria effectively and precisely, especially in soils with limited hydraulic conductivity (Jamshidi-Zanjani and Khodadadi, 2016). EK-enhanced bioremediation (EK-BIO) was developed to get over these limitations. It uses microorganisms to integrate bioremediation into the EK process or EK flow mechanisms to transfer toxins to the organisms (**Figure 2.2**). EK is a cutting-edge technology that can significantly improve native bacteria's access to nutrients, opening up a wide range of contaminated soils, comprising fine-grained soils, which are typically challenging to clean up using traditional techniques. In practice, electromigration transports nutrients in low-porosity materials, while electroosmosis or electrophoresis mechanisms mobilize microorganisms

(Yeung and Gu, 2011). Electrokinetic-bioremediation hybrid systems remove heavy metals and persistent organic pollutants from polluted soils, as shown in **Table 2.5.**

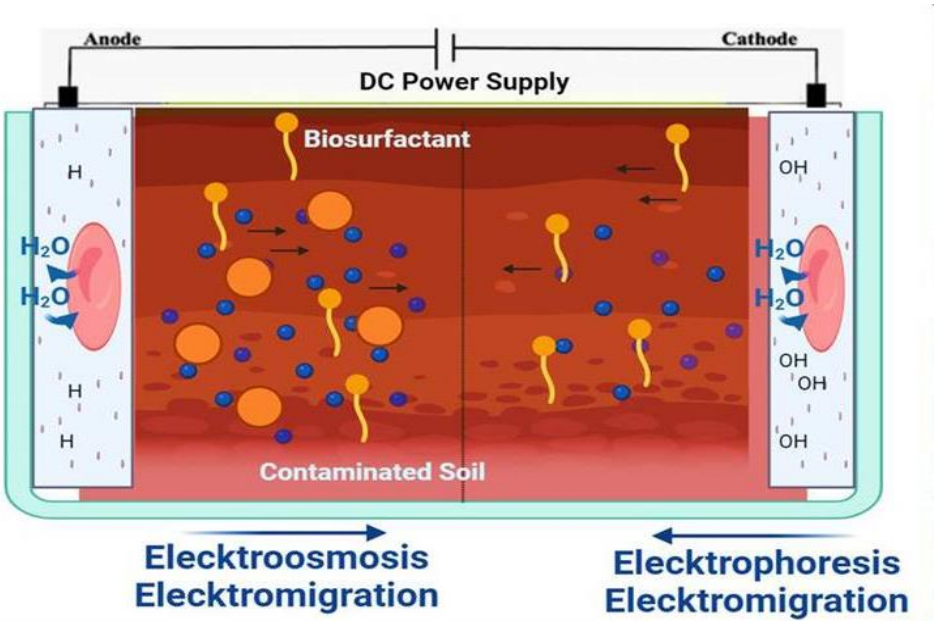

Figure 2.2: EK coupled with Bioremediation. Anions and cations transport to the respective electrode of opposite charge while microorganisms transport towards the cathode via electroosmosis flow.

Lee & Kim (2010) used the EK-enhanced bioremediation technique by injecting sulfur-oxidizing bacteria into shooting range soil polluted with metals like Zn, Cu, and Pb under the influence of an electric field. The bioleaching procedure improved the removal rates of Zn and Cu. EDTA was added to solve the problem of $PbSO_4$ precipitated as a byproduct of sulfur-oxidizing. This method showed enhanced removal efficiency for Pb (92.7%), superior to an abiotic process. Sarankumar et al. (2020) investigated using Alkalophilic bio-analytes to treat Cr-contaminated soil by the EK and EK-bioremediation system. According to the results, EK and EK-bioremediation removed 40.12% and 90.4% of the chromium within 7 days of treatment, respectively.

Table 2.5: Evaluation of EK-bioremediation performance for different soil contaminants.

Type of soil	Target pollutant	Enhancement	Functional nature of Enhancement chemical	Duration	Voltages/ Currents	Removal efficiency	Ref.
Natural Soil	POPs, Cu, Pb and Ni	Citrate Sodium-$NaNO_3$	Complexing agents help in the mobilization	30 days	2 V/cm	90% of POPs and More than 60% of metals	(Chen et al., 2021)
Clay Soil	Phenanthrene	NH_4NO_3	Enhances bioremediation/microbial activity	30 days	20 V	More than 80% of metals	(Xu et al., 2010)
Sediment soil was collected from North India	Cr	Alkalophilic Bio-anolyte	Enhances microbial growth	7 days	1.44 mA/cm^2	90.4 %	(Sarankumar et al., 2020)
Natural Soil	Pb, Cu and Zn	HNO_3	Acidification helps in heavy metal precipitation	20 days	2 mA/cm^2	7.6%,71.3 % and 52.6%	(Lee and Kim, 2010)
Natural Soil	Pb, Cu and Zn	Na_2CO_3 + EDTA	Solubility and chelation of heavy metals	20 days	2 mA/cm^2	92.7%, 64.3% and 45.9%	(Lee and Kim, 2010)
Clay Soil	Chlorinated ethene	Sodium lactate	Enhances microbial activity	60 days	38 mA	Complete removal	(Mao et al., 2012)
Contaminated soil	Cr	200g Humic substances	Aids in the degradation of various contaminants	8 days	1 V/cm	98.33 %	(He et al., 2018)

[POPs-persistent organic pollutants; EDTA-ethylene-diamine-tetraacetic acid]

2.4.3. EK coupled with phytoremediation

Phytoremediation removes or reduces pollutants using living plants and their related microbes, which can extract and concentrate elements from the soil environment (Wang et al., 2021). Heavy metals and organic contaminants are usually accumulated in plant

tissues or degraded by plant enzymes. However, phytoremediation is time-consuming and inefficient due to plants' slow growth rate and poor biomass production. When EK with phytoremediation are used together, pollutants can be moved around and redistributed in situ, improving their ability to reach plant roots and promoting tree development by moving nutrients to the root region (**Figure 2.3**) (Siyar et al., 2020). In the EK-Phytoremediation technique, electromigration aids in moving ions and pollutants to the root region, and the charged electrical field can offer the plant the optimum circumstances for uptake (Yeung and Gu, 2011).

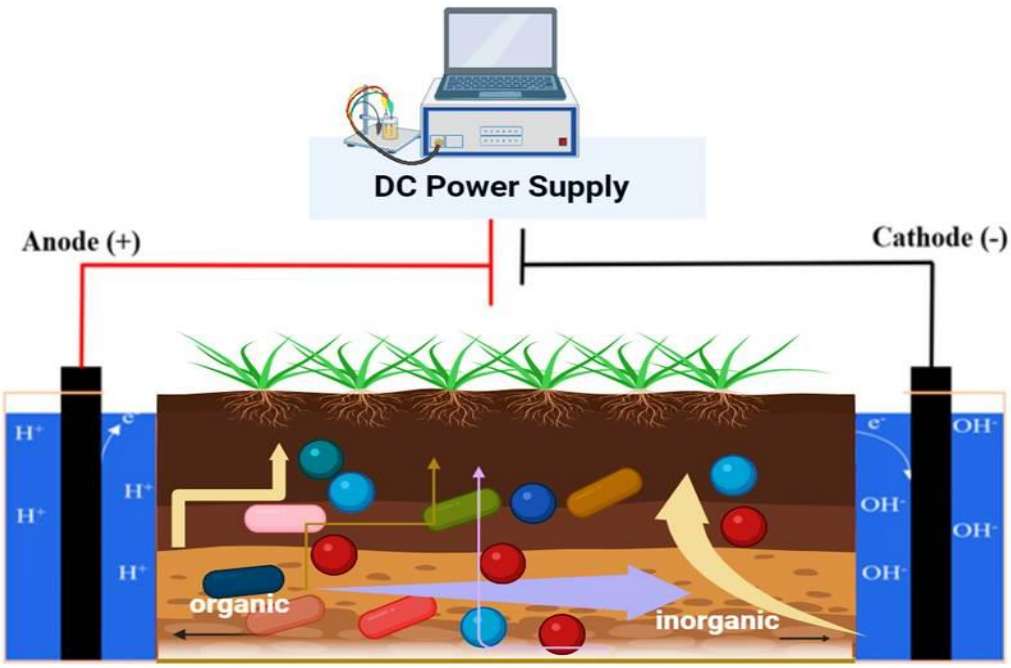

Figure 2.3: EK pollutants removal coupled with phytoremediation.

One study by Cang et al. (2011) used a lower-intensity direct current for 35 days to observe the treatment of soil contaminated with several metals in Indian mustard (Brassica juncea). According to their experimental findings, combining EK with phytoremediation improved the effectiveness of plant uptake of metals. Also, the electric

gradient was one of the most important factors affecting plant growth, soil properties, and soil mineral concentrations (Cang et al., 2011). According to Lim et al. (2004), an experiment integrated EK with phytoremediation to remove lead from the soil. They investigated the efficacy of Indian mustard grown in polluted soils in higher concentrations of information in tissues while applying an electric field and incorporating EDTA into the soil. The results of their pilot study provided the best results with the performance of an electric field in the phytoremediation technique. **Table 2.6** summarizes some cases of heavy metal and persistent organic pollutant removal from contaminated soils using the electrokinetic-phytoremediation hybrid system.

Table 2.6: Evaluation of EK-phytoremediation performance for different soil contaminants.

Type of soil	Target pollutant	Plants type	Enhancement	Duration	Voltages/ Currents	Removal efficiency	Ref.
Natural soil	TPH	Sunflower	Tap water at the anode and 50 mM SDS at the cathode	20 days	1 V/cm	84 %	(Rocha et al., 2019)
The soil was taken from mine tailings located in southern Spain	Cu, Pb, Cd and Zn	Ryegrass	Tap water	58 days	1 V/cm	32%, 41%, 34% and 17%	(Medina-Díaz et al., 2023)
Natural soil	Cu, Cd and Zn	Ryegrass	-	89 days	30 V	-	(O'Connor et al., 2003)
Natural soil	Pb and As	Indian mustard	EDTA	84 days	30-40 V	-	(Lim et al., 2004)
The soil was taken from the Jiuhua mining area, which is located east of Nanjing city	Cu and Zn	Ryegrass	EDTA at the anode and EDDS at the cathode	50 days	10 A/m^2	-	(Zhou et al., 2007)
Natural soil	Heavy metals	Potato	-	90 days	500 mA	-	(Aboughalma et al., 2008)
Sand soil	Pb	Kentucky Bluegrass	Urea	30 days	500 mA	-	(Putra et al., 2013)

[TPH- Total Petroleum Hydrocarbon; SDS-sodium dodecyl Sulfate; EDTA-ethylene-diamine-tetraacetic acid; EDDS- ethylenediaminedisuccinic acid]

2.4.4. EK coupled with RFM

Over the past ten years, contaminated sites have become a significant environmental issue. Technologies suited for removing environmental toxins from soil have drawn much interest recently. Due to their compatibility with the environment, adaptability, practicability, scale-up potential, and cost-effectiveness, RFM and electrokinetic remediation must be significant. Many techniques are available to deal with groundwater and soil contamination caused by oil, petroleum mining, chemical industries, and agricultural activities. RFM and electrokinetic methods are two of these remediation methods (Ahmed et al., 2022). Based on the characteristics of the reactive material and the target pollutants, adsorption, precipitation, and degradation occur in the RFM system. Different adsorbent materials, like activated carbon, atomizing slag, and zero-valent iron, may be used as the treatment media in RFM with EK. The most used reactive substance among all RFM is zero-valent iron because of its low price (Sweetman et al., 2017). In contrast, the build-up of contamination on the ZVI particles' surfaces may prevent flow through the barrier and limit the lifetime of ZVI (Ren et al., 2014). The direction of heavy metal migration can be controlled by manipulating the placement and polarity of the electrodes. Typically, heavy metals will move toward the electrode of the opposite charge, which is often the cathode. A layer of RFM is strategically placed within the soil, either in direct contact with the contaminated area, along the migration pathway of the heavy metal ions, or near the cathode. The RFM is chosen for its high affinity for heavy metals and its ability to capture or immobilize them. The heavy metals that encounter the RFM are effectively removed from the mobile phase (soil pore water) and trapped within the RFM. This leads to reduced heavy metal concentrations in the soil and a gradual cleanup of the contaminated area. Over time, RFM may require a replacement (Ghobadi et al., 2021a).

Cang et al. (2009) investigated using ZVI as an RFM to treat Cr-contaminated soil by EK. According to the findings, a ZVI-RFM and electrochemical remediation may remove Cr with a maximum effectiveness of 72%. When EK and ZVI were combined, the concentration of Cr in both the anolyte and catholyte decreased (Cang et al., 2009a). Yuan and Chiang (2007) investigated the viability of combining EK with RFM on As removal from the soil. In their investigation, RFM was made up of FeOOH and ZVI. The elimination efficiency of As was enhanced by 60–120% by using RFM in the EK system (Yuan and Chiang, 2007a). Yuan et al. (2009) also investigated how the EK-RFM system removed As from contaminated soil using a cobalt-coated carbon nanotube (CNT-Co) reactive barrier. According to the experimental findings, the RFM constructed of CNT-Co and the EK remediation achieved only 35% to 62% As removal (C. Yuan et al., 2009). Growingly a global issue, soil contamination has adverse effects on human health. Electrokinetic (EK) remediation is a relatively new technology for treating organic and inorganic toxins in the soil, among several soil decontamination methods. Compost has recently been added to the EK process as an adsorbent for the complete remediation of heavy metals, increasing its efficiency. Compost is an environmentally friendly, recyclable reactive filter medium (EK-RFM). These studies show that compost is more effective in buffering soil pH than other RFMs like biochar, activated carbon, and compost and biochar combined. Due to the wide range of organic compounds in compost, many different mechanisms may play when compost RFM adsorbs metal ions. Research has investigated the transmission and discharge of other heavy metals through EK remediation in virgin soil. Up to this point, most EK research has been done for kaolinite soil with heavy metals. Model soils, such as kaolin, with spiked contaminants, are sometimes used to investigate the principles of the technique. However, the behaviour of the pollutants in these soils differs from that in natural soils. Since spiked kaolinite might

be remedied more quickly than complex soils, research with natural soils is necessary. Due to organic matter in natural soils, heavy metals are trapped and retained, which makes their solubilization and mobility quite challenging. Many studies concentrated mainly on the heavy metals and their transport behaviour in the soil (such as Zn, Cu, Pb, and As) and the results of electrolyte familiarization in the EK combined with RFM (Ghobadi et al., 2021a).

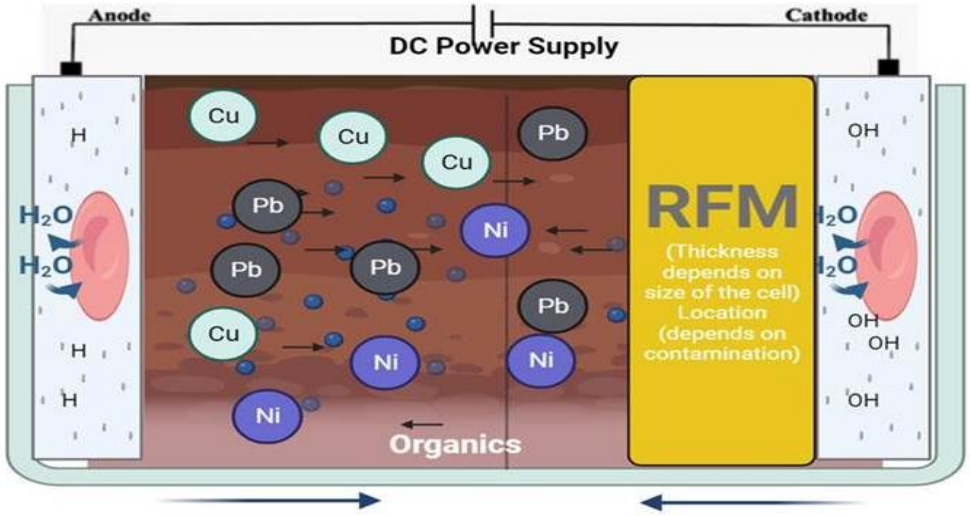

Figure 2.4: EK coupled with RFM (Location and thickness of the RFM media depends on the size of the cell and the type of contamination in the soil).

Ghobadi et al. (2021b) investigated a compost or biochar mixture as RFM combined with an EK for treating copper-polluted kaolin. The laboratory results showed the EK-RFM process under the application of a constant electric current when using EK with 100% compost treatment improved the removal of copper to 84.09%. Results showed the compost's capability to buffer the pH near the cathode area, where most copper accumulated. On the other hand, the removal of Cu ions was not improved when mixed with different grades of biochar with compost in the soil during the process of EK-RFM.

In addition, compost was renewed and used again during the EK process even though the overall Cu removal dropped from 84.09% to 74.11%. The results demonstrate compost as a viable green RFM that improves heavy metal removal in the EK process, particularly when an electric current is applied continuously by lowering the soil pH. Since compost contains various organic compounds, several mechanisms may be involved in metal ions adsorption (Vidal et al., 2022). There are multiple ways metal ions can be adsorbed to compost via van der Waals forces; they can be complexed with various functional groups within the compost and exchanged between metal ions and cations in compost (co-precipitation). In the EK-RFM system, improved electromigration and RFM adsorption are essential for heavy metal extraction. The potential application of EK integrating compost RFM is to encourage cleaning the soil contaminated with heavy metals (Zhang et al., 2022).

Contaminated soils have received wide attention, and many studies have been conducted. One study combined the EK process with AC and CA. The soil samples were taken from the surface by a depth of 30 cm of forest land in Penglai City, Shandong Province, China. The soil was pulverized to 2 mm after being allowed to air dry for 48 hours. Then, soil samples were mixed entirely with Pb (NO3)2 solution to create Pb-polluted soil, and the contaminated soil was loaded onto the EK cell (Xie et al., 2021). Xie et al. (2021) removed heavy metal pollutants in soil by electrokinetic. It is a new process for treating contaminants of complex components such as lead and copper, using EK technology combined with AC with CA. In one of the tests with citric acid only on the EK technique, a high pH was observed near the cathode, which reached around 13, which caused the accumulation of several pollutants from metal ions next to the cathode, causing clogging the soil pores, which hinders the treatment process. As a result, lead removal did not improve with this process, and the removal rate was only about 15%.

On the other hand, the curing process is greatly improved when active carbon is added to EK with CA. Lead removal efficiency improved from 15% to 58% within 20 days. In addition, the pH decreased from 13 to 10, both during the activated carbon treatment process and after the introduction of alternating current to the cathode region. Through the results of this study, it is clear that activated carbon effectively contributed to removing lead from contaminated soil and the possibility of improving the treatment of soils polluted with complex minerals (Xie et al., 2021).

In addition, the RFM approach and the EK method have been used to improve the efficacy of toxin removal from low-permeability soil, as shown in **Figure 2.4.** Pollutants may migrate from the anode to the cathode, moving both organic and inorganic materials to either the anode or the cathode under the impact of an external electric field. Here, tainted groundwater flows perpendicular to a reactive medium. RFM has been utilized to meet groundwater criteria to different degrees of success (Chu et al., 2022). Aquifer treatment is shown to have high potential with passive, in situ technologies. In comparison to traditional pump-and-treat techniques, RFM has the following advantages: i) absence of the necessity for disposal, storage, or other means of conveyance; ii) lack of need for a constant input of energy; iii) Phase transition and contaminant degradation are both accomplished; iv) lack of need for effluent discharge, and iv) reasonably inexpensive, but its cost-effectiveness has not been established because of lack of low-cost alternatives.

This system is susceptible; thus, fundamental and applied research (done in the lab) frequently concentrates on a particular organic or inorganic contaminant. The procedures and operational variables are more straightforward to understand, allowing for the creation of intricate contaminated site treatment systems. Most soil remediation research has focused too far on heavy metal and metalloid-contaminated soils (Li et al., 2022b). The EK-RFM technology has several uses, is highly economically advantageous, and

generates few secondary pollutants. The ability to apply to soil with less permeability and the ability for soil treatment in the field are critical advantages above other conventional approaches (Chu et al., 2022). Due to the complexity of soil, additional experimental data are required to replicate contaminated soil in real-world settings. EK-RFM research has primarily been conducted in laboratories. Low RFM media material prices are necessary for EK-RFM, and the location of the reaction barrier is critical for contaminant removal. Examining the electrolyte composition and the use of surfactants is crucial when there are numerous interactions on the reactive barrier (Ahmed et al., 2022). **Table 2.7** highlights the efficacy and removal rates of various soil pollutants utilizing EK with RFM treatment in prior research.

Table 2.7: Optimal operating circumstances for combining EK and RFM in removing heavy metals from soil.

Type of soil	contaminant / Duration	Anolyte/ Catholyte	RFM type/location	Voltages/ Currents	Removal efficiency	Ref.
kaolin	Cu/4 days	$NaNO_3$/ Citric acid	Activated carbon/cathode	1 V/cm	96.60 %	(Zhao et al., 2016a)
kaolin	Cr/5 days	$NaNO_3$, on both sides	Iron Oxide (fe3o4)/ anode	1 V/cm	65 %	(Suzuki et al., 2014a)
Natural Soil near e-waste	Pb/17 days	Citric acid/ Fe $(NO_3)_3$	Activated carbon fibre/ cathode	0.9 V/cm	80.53 %	(Zhang et al., 2021)
Mixing kaolin, illite and quartz soil	Cr/12 days	Deionized water on both sides	Transformed Red Mud (30 g) + Kaolin/ anode	1 V/cm	93.2 %	(De Gioannis et al., 2008)
Industrial Park	Cr/8 days	KCI / DL-tartaric acid	Mixed modified zeolite Fe (0) and (CTMAB-Z)/ cathode	2.5 V/cm	80.92 %	(Yu et al., 2019a)

Contaminated soil from a mine site in Mexico	Hg/3 days	EDTA, on both sides	Fe (0)/ separated from EK systems	0.55 V/cm	76.30 %	(Robles et al., 2015)
Kaolin	Cu/7 days	Deionized water on both sides	Organic Compost/ cathode	10 V	45.65 %	(Ghobadi et al., 2021b)
Kaolin	Cu/7 days	Deionized water on both sides	Organic Compost/ cathode	20mA	84.09%	(Ghobadi et al., 2021b)
Kaolin	Cu/7 days	Deionized water on both sides	Activated carbon/ cathode	10 V	10 %	(Ghobadi et al., 2020)
Kaolin	Cu/7 days	Deionized water on both sides	Biochar/ cathode	10 V	27 %	(Ghobadi et al., 2020)
Natural Soil	Zn, Cd, Mn, Cu and Pb/14 days	Deionized water on both sides	Organic Compost/ cathode	20 - 30mA	Zn, Cd and Mn were removed 51.1 – 71.1%, Cu and Pb 28.2 - 29.1 %	(Ghobadi et al., 2021a)

2.5. EK coupling with solar power

Electrokinetic remediation technology uses a direct current (DC) electric field to remove inorganic and organic contaminants from low permeability contaminated soils, including heavy metals and hydrocarbons (Souza et al., 2016). This method involves sending a low-level DC between a row of electrodes implanted into the soil, one of which is positively charged (anode) and another negatively charged (cathode), to mobilize the pollutants or remove them (Hassan and Mohamedelhassan, 2012). Page (2002) states that low current is used in electrokinetic remediation techniques for safety and to reduce potential heating effects. The energy required during an electrokinetic remediation procedure might become a significant issue, limiting the technology's wide-ranging applicability (Page and Page, 2002; S. Yuan et al., 2009). A source of low-cost electric power should be available to reduce the electrokinetic treatment cost. Solar cell power is one of the alternatives.

Because electrokinetics requires a direct electric field, electric transformers convert (AC) alternating current to (DC) direct current before using it in an EK process. Solar cells generate a direct rather than an alternating current, making them a good alternative for generating the electrical energy needed for EK (**Figure 2.5**). Solar power may be the most effective solution for EK of polluted sites with no or insufficient power supply lines in distant places. Finally, solar energy is environmentally friendly, making it an attractive option for processing (Hassan and Mohamedelhassan, 2012). According to an investigation by Yuan et al. (2009), the cost of EK with solar cell panels in the Chain was around 40% of that borne by an electric power supply from the grid. However, the climate and location affect the electricity generated by solar cells, resulting in fluctuations in the power supply throughout the day and power outages at night. As a result, the system is fueled by a variable energy source. Furthermore, because the period of remediation treatment is often highly long, a connection of a noncontinuous supply may affect the efficiency of removing pollutants from the soil.

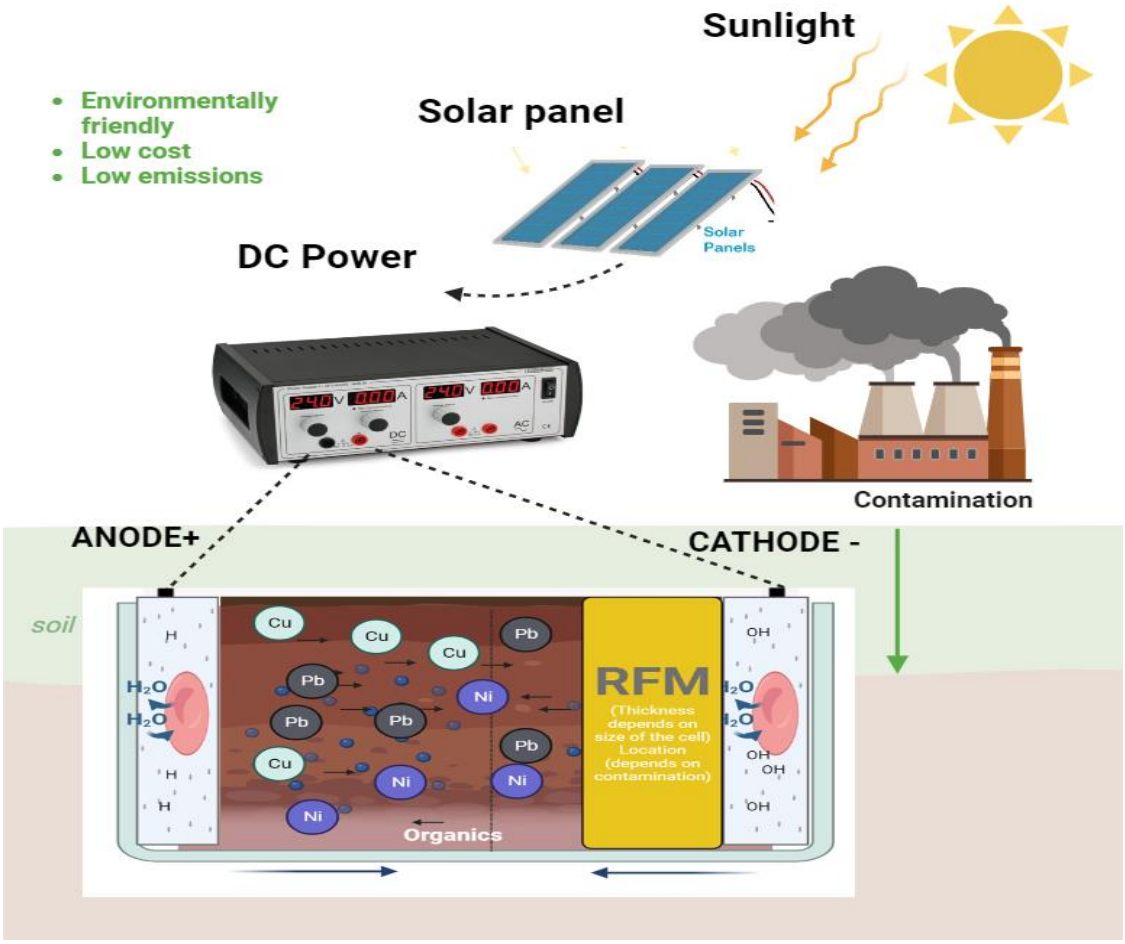

Figure 2.5: EK coupled with solar power.

Zhou et al. (2018) investigated the influence of EK technology on the chromium removal rate from the soil by using a solar power supply. The results revealed that the procedure was practical and feasible for chromium-polluted soil remedy. Jeon, Ryu, and Baek 2015 used a power supply (DC) and a solar power supply to conduct EK studies on arsenic-contaminated soil. After five weeks of treatment, the removal rate of As by the solar-driven system was comparable to that of the conventional direct current system as a result of 27% and 32% for As, while the energy consumption of the solar system was only half that of the direct current system.

Recent research has studied the influence of electrode arrangement, electrode material, and the inclusion of fluids to promote contaminants' mobility to improve EK's efficacy.

However, despite EK's high adaptability, the electrical power consumption (about 10-15% of the overall cost) is a significant hurdle to its application (Souza et al., 2016). In addition, several studies (Hansen et al., 2007; Kim et al., 2013) have found that a pulsed EK technique can improve soil pollutant removal while lowering electrical energy consumption and reducing operation difficulties caused by electrode corrosion. Similarly, recent investigations (Jeon et al., 2015) reveal that solar-powered EK drives metal-polluted soil treatment with removal efficiency comparable to power supply DC. However, much research on solar-powered EK was confined to short treatment periods, making it impossible to accurately assess the benefits of using this energy source (Souza et al., 2016; Zhou et al., 2018).

2.6. Comparison of combined-EK with conventional processes

There is a wide range of treatment methods for contaminants removal from soil. The standard methods for removing organic and inorganic materials from the soil include physical and chemical treatment of the contaminated soil. Some of these methods are insufficient to remove all pollutants, especially in fine-grained soil, or economically unfeasible. Besides, they could effectively remove some types of pollutants, e.g., biological processes require a long processing time or high energy required for thermal treatment (Gholizadeh and Hu, 2021a). Table 8 shows the most popular soil remediation technology, including these processes' advantages and disadvantages.

Thermal processes are some of the standard physical methods for soil remediation. Thermal technology primarily involves heating the soil, vaporizing the pollutants, and collecting them for safe disposal. Thermal remediation is an effective technique for decontaminating hydrocarbons when chemical oxidation and bioremediation are not working. Different thermal techniques can be used, such as steam, electric resistance heating, and desorption (Millán et al., 2020; O'Brien et al., 2018). When the

concentrations of hydrocarbons are high, a smouldering method can degrade the molecules. Steam-enhanced extraction uses hydraulic conductivity (O'Brien et al., 2018). The basic mechanism for effective contaminant removal involves direct steam injection, where contaminants are collected in extraction wells. Steam injection enables the breakdown of certain organic compounds, reduces contaminant viscosity, and enhances volatility. This method is particularly suitable for removing volatile and semi-volatile hydrocarbons from highly permeable and semi-permeable soils. However, since it relies on direct steam injection, its effectiveness is limited in low-permeable soils and by the boiling point of water. Studies indicate that factors such as time, temperature, and soil texture significantly affect treatment efficiency. It requires high energy to provide adequate heat to remove some pollutants, which makes the technology unsuitable due to the increased cost. Thermal processes are primarily designed for organic matter removal and are ineffective for heavy metals treatment. Instead, the EK hybrid system could tackle this problem. For example, EK coupling with surfactants could tackle organic pollutants and address the elevated cost of thermal processes. Besides, the EK-enhancement agent system is suitable for organic and inorganic treatment (**Table 2.8**).

Physical and chemical processes are popular for soil remediation from organic and inorganic pollutants, such as soil washing, Soil replacement, chemical leaching, chemical oxidation/reduction, electrokinetic, vapour extraction, and air sparging. Several models have been conducted to separate pollutants in soil by washing technique, most notably in (2015) by Yi & Sung at the beginning of the experiment. The water was used to wash the lead from the soil, efficiently removing most lead, 90.5%, and reducing lead concentration from 650 mg/kg to 62 mg/kg. Also, the zinc-polluted soil has been washed with dilute hydrochloric at a ratio of 10 l/kg - 20 l/kg of soil. This method appeared to have a high efficiency of zinc removal in extracting about 61.2% of the amount of zinc

in soil from 413.45 to 160.37 mg/kg. Their results showed that washing contaminated soil with water and solution effectively removes copper and zinc, but it was not satisfactory in terms of cost. In addition, this method has observed that it affects soil properties, fine-grained soils, and soil bioactivities. This property has a vital role in removing and passing pollutants. Overall, soil washing could remove organic and inorganic materials, but the soil's physical, chemical, and biological specifications can be significantly affected (Yi and Sung, 2015). A combined EK-enhancement agent system can address the shortcomings of soil washing using acid for conditioning the alkaline front at the cathode for better metal ions removal. Also, an EK with a compost RFM system was applied to remove heavy metals from different soils (Ghobadi et al., 2021a). For organic pollutants, EK can be integrated with surfactant for in-situ soil remediation and avoid the excavation work required for soil washing.

An electrokinetic remediation technique mainly involves supplying voltage to the soil's two sides and creating an electric field gradient (Miller de Melo Henrique et al., 2021). It can restore the ecosystem and protect the original ecotope because it is suitable for low-permeability soil, is simple to set up and maintain, is cheap, and does not hurt the environment (Guo et al., 2022). However, the direct electrokinetic remediation's performance was fundamentally low and could not control the soil system's pH level. The primary methods have been enhanced, including adding buffer solution to the anode and cathode to control pH, using an ion exchange membrane to maintain pH, adding complexant to facilitate migration, etc. It is still under improvement in the soil process of removing inorganic pollutants.

Biological methods effectively eliminate heavy metals from the environment (Kumar et al., 2022). These techniques include phytoremediation, bioremediation, attenuation, and bioventing, which use vegetation and microorganisms to remove pollutants from soil.

Microbial remediation lowers the expense of organic pollutants treatment. Simultaneously, it is practical, economical, and ecologically friendly (Tang et al., 2016). Phytoremediation is cost-effective for treating soil polluted with organic and inorganic contaminants. Using plants to clean up soil, sediment, and water contamination is called phytoremediation (Siyar et al., 2020). Environmentally friendly and potentially cost-effective. The efficiency of pollutant treatment by phytoremediation could be improved by coupling with the EK process to redistribute pollutants in the soil to reach the root region (Yeung and Gu, 2011).

Bioremediation technology uses living things and their enzymes to break down, remove, or immobilise hazardous substances. Ex-situ soil bioremediation refers to physically removing contaminated soil from its original location, while in-situ soil bioremediation refers to treating the soil without excavation. Due to the required transportation, ex-situ bioremediation is typically more expensive and energy-intensive than in-situ Bioremediation (Fardin et al., 2021; Fernández-Marchante et al., 2022; Usman et al., 2022; Xu et al., 2021). In many cases, Bioremediation is a suitable and affordable replacement for conventional physicochemical remediation methods. Although bioremediation is widely used for contaminated site treatment, it experiences drawbacks such as being time-consuming and unsuitable for low-permeability soil or heavy metals treatment (**Table 2.8**). However, the EK-bioremediation system can address the shortcomings of bioremediation technology for treating organic and inorganic pollutants. Besides, electroosmosis flow will facilitate the microorganisms' transport across the contaminated soil.

Over the past three decades, many bench and field experiments have shown that enhanced and hybrid EK processes successfully and cost-effectively remove a wide range of heavy metals. Moreover, it has high scalability and can be efficiently combined with many other

technologies. Chemically enhanced EK processes exhibited excellent efficiency in removing contaminants by controlling the soil pH or the chemical reaction of contaminants. EK hybrid systems were tested to overcome environmental hurdles or technical drawbacks of decontamination technologies. Hybridization of the EK process with phytoremediation, bioremediation, or reactive filter media (RFM) improved the remediation process performance by capturing contaminants or facilitating biological agents' movement in the soil. Also, EK process coupling with solar energy was proposed to treat off-grid contaminated soils or reduce the EK energy requirements. Hybrid technology may be a dependable choice for improving remediation ratios.

The main challenges of scaling up the EK process from a laboratory to a pilot scale are the soil chemistry, pollutant concentration, and interferences of organic and inorganic substances with target pollutant/s. Several laboratory EK tests evaluated organic or inorganic pollutant removal from a model kaolinite soil, which does not resemble naturally contaminated soil where a mixture of heavy metals or heavy metals and organic matter exists. Soil contamination is often due to a pollutants mixture rather than a single pollutant; hence, the EK efficiency should be tested in actual soil samples before scaling up to field tests. Contaminated sites with extremely high concentrations could be irrelevant for the EK treatment; hence, a hybrid EK system should be considered an alternative option. Besides, omnipresent organic and inorganic substances interferences with the target pollutants are highly likely in real contaminated sites. Soil contamination by organic and inorganic pollutants mixture will compromise the EK effectiveness due to metal ions-organic matter complexation or metal ions precipitation at different pHs, increasing the soil resistivity to current. Soil contamination by organic and inorganic pollutants will compromise the EK effectiveness due to uncontrolled reactions between metal ions and soil organic matter or metal ions precipitation at different pHs. Metal ions

precipitation will increase the soil resistivity to electric current, resulting in a sharp drop in the electric potential and compromising EK efficiency. Thus, the removal efficiency compared to laboratory tests on model soils. Heavy metals should be solubilized before being transported and removed from the soil; hence, soil pH should be low enough to solubilize heavy metals. Soil pH is a function of the electrolysis reaction at the anode and soil chemistry. Soils with extensive organic contents are more complex and time-consuming for remediation due to reactions between natural organic matter and heavy metals and soil resistance to acid front advancement (Mohamadi et al., 2019).

The EK process is also affected by the soil ion exchange capacity; the higher the ion exchange capacity, the more challenging the remediation process (Xu et al., 2020). Organic pollutant removal depends on its charge and water solubility. On the one hand, nonionic organic pollutants, such as phenanthrene, are affected by the electroosmosis transport mechanism when soluble. On the other hand, ionic organic pollutants, such as PFAS compounds, are affected by electroosmosis and electromigration mechanisms, making them more difficult for the EK treatment (Ganbat et al., 2022). Based on field tests, an optimal EK design is site- and contaminant-specific (Reinout Lageman, 2011; USAEC, 2000). Therefore, a small pilot test should be conducted to optimize the operating condition of the EK process. Nevertheless, some recommendations from field tests suggested a 1.5 to 2 m distance between the electrodes of opposite charge, a minimum soil moisture of 15 to 20%, and 0.2 mA/cm^2 current density, depending on the site. Graphite electrodes are recommended for the cathode, while graphite is for the anode since inexpensive iron electrodes will corrode over time.

Table 2.8: The summary of the results of the thermal, physical, chemical, and biological technology used to remove heavy metals from the soil.

Remediation technology	Treatment site	Advantages	Technical and environmental concerns	References
		Physical remediation		
Thermal	In situ/Ex situ	- Suitable for treating a wide variety of soils - Appropriate for sedimentary bedrock - Suitable for fractured zones - High removal efficiency	- Unsuitable for heavy metal pollutants - Small-scale heat loss - Interference from co-contaminants - High energy expenditure	(Bonnard et al., 2010; Gholizadeh and Hu, 2021a)
Soil thermal desorption	In situ/Ex situ	- A shorter duration of treatment - High efficiency - Applicable to the cleanup of diverse places - Absence of secondary contamination - Soil and heavy metals recycling	- Expensive devices - Possibility of pollutant migration to unaffected areas - Treatment challenges when close to occupied sites - Impacts of post-treatment on soil characteristics - Side reactions may occur due to the heating temperature and the oxygen concentration of the atmosphere.	(Song et al., 2022; Zhao et al., 2019)
Soil washing	Ex situ	- Suitable for soils with clay content or low silt - The ability of recovered fluids to be reused - Ease of operation and design - High removal efficiency - Short remediation period - Suitable for small areas of contaminated soil	- Expensive above-ground treatments - Hydraulic control is required - Problems with contaminant mobility - Unsuitable for the treatment of hazardous substance mixtures. - inevitable soil environment disturbance - Soil loses its properties	(Kuppusamy et al., 2016)
Soil replacement	In situ/Ex situ	- High removal efficiency - Short remediation period - Suitable for small areas of contaminated soil	- The depth of the soil to be removed and replaced must be considered - Remediation may be expensive - Further action may be required for the removal and disposal of polluted soil	(Gong et al., 2018)
Soil vapor extraction	In situ/Ex situ	- Cost is very effective in situ	- Ex-situ processing is more complex and cost.	(Kuppusamy et al., 2016)

		- It can be used to remediate large sites in a short period - Soil disturbance is kept to a minimum - Installation is simple - Compatibility with other methods	- Removal rates are reduced to soils with higher organic content and moisture - Treatment of residuals before disposal - Unsuitable for saturated zones, with heterogeneous soil, or low permeability - Only volatiles are limited in how they can be used - Not suitable for mixture chemical remediation	
Chemical remediation				
Chemical leaching	In situ	- Suitable for heavily polluted soil - High removal efficiency - Short remediation period - Suitable for small areas of contaminated soil	- High-cost and effective - This technique may result in secondary pollution during the treatment process - Unsuitable for the treatment of hazardous substance mixtures - Soil loses its properties	(Azhar et al., 2022; Song et al., 2022)
Chemical oxidation/reduction	In situ	- Suitable for heavily polluted soil - It produces heat by which reaction rates, bacterial activity, and, thus, efficiency increase.	- Higher cost because they need to use a lot of chemicals - Unsuitable for complete heavy metal removal - This technique may result in secondary pollution during the treatment process	(Song et al., 2022)
Electrokinetic	In situ/Ex situ	- In situ / ex-situ technology - Need to use less energy than ex-situ methods - Cost and remedial efficiency are competitive with other methods - Compatible with most remediation technologies - Strict control of water flow/direction and concentration of dissolved pollutants - Retention of pollutants within a confined space	- Depends on the pH of the removal - The necessity of applying an enhancing technique - Unsuited to treat non-polar pollutants - Unsuited for pollutants mixtures of varying concentrations - Post-treatment waste disposal requirements - The efficiency of the process reduces when greater voltages are applied to the soil because of the rising temperature	(Kuppusamy et al., 2016; Usman et al., 2022; Xie et al., 2021)
Biological remediation				
Bioremediation	In situ/Ex situ	- Natural process - Cost is very effective	- Process is slow	(Kuppusamy et al., 2016)

		- Need less energy - Reduced exposure to the general public or site personnel - Toxic chemicals are eliminated - Reduced need for human oversight	- Possibility of toxicity from incomplete decomposition - Process is sensitive to toxicity levels & environmental conditions - Unsuitable for complete heavy metal removal - Unsuitable for soils with low permeability	
Phytoremediation	In situ/Ex situ	- Low-cost and effective - Technique that is friendly to the environment - Possibilities for wildlife to thrive after vegetation is established - Simple to monitor - Maintains the environment in a more natural state - Suitable for both pollutants (organic/inorganic) and field applications - Reduces the quantity of waste that must be landfilled (by up to 95%) and can be used as a bio-ore of heavy metals - In situ, applications reduce contaminant dispersal through air and water	- Transfer of pollution from the soil to the air - Limited to shallow sites that have low contamination levels - Treatment is limited to deeply rooted contaminated sites - Unsuitable for complete heavy metal removal - Post-treatment of used plants is required - Slow approach - Need for a lot of space - It could take several years to treat a contaminated location - Climate is a limiting factor	(Ghosh and Singh, 2005; Kuppusamy et al., 2016)
Attenuation	In situ/Ex situ	- Natural process - Cost is very effective - Reducing risks in the long term - Minimal surface disruption	- It is impossible to predict the reliability - Slow approach - Cost is affected by the duration of treatment - Regular and long-term monitoring is required.	(Kuppusamy et al., 2016)
Bioventing	In situ	- Treatment of unsaturated soils is effective - Economic - It produces biologically active soils - Low and simple maintenance	- Unsuitable for clayey soils with low permeability - Unsuitable for treating highly polluted sites - Inefficiency in saturated zones and shallow contaminated sites	(Kuppusamy et al., 2016)

Combined remediation				
EK combined with enhancement agents	In situ/Ex situ	- Treatment of organic and inorganic contamination simultaneously in porous media - Using the pH change caused by the electrolysis of water to absorb pollutant ions effectively - Improved removal efficiency compared to EK - Better control of operating parameters, such as soil pH and conductivity, than EK - Reduce the liquid's surface tension - Enhanced solubility of pollutants than EK	- The addition of surfactants depends on the pollutants and other environmental factors - Redox reaction produces undesirable products in soil - Interference from metals in the soil - Changing the physicochemical characteristics of the soil - Removal efficiency is greatly reduced when the soil contains carbonates, hematite, and big rocks - The necessity of applying an enhancing technique - Increasing the EK remediation cost	(Rezaee et al., 2019; Song et al., 2020)
EK combined with RFM	In situ/Ex situ	- In situ / ex-situ technology - High removal efficiency - Need to use less energy than ex-situ methods - Depending on the RFM, the cost and treatment efficiency is competitive with other methods - Early response to treatment - Facilitate contaminnats extraction and recovery from the soil	- Treatment efficiency decreases as soil moisture increases and unfavourable site circumstances, such as cation exchange capacity, salinity, organic content, etc., persist - Precipitation of species near the electrode is a barrier to the technique - Transfer of pollution from the soil to the air	(Ghobadi et al., 2021a; ZHANG et al., 2019)
EK combined with bioremediation	In situ/Ex situ	- Improving the removal efficiency of bioremediation process - Reducing bioremediation process treatment time - Better control of microorganism transport in the soil when combined with biological processes - Need to use less energy than ex-situ methods	- Unsuited for pollutants mixtures of varying concentrations - The efficiency of the process reduces when greater voltages are applied to the soil because of the rising temperature - The electric field negatively affects the viability of microorganisms	(Sarankumar et al., 2020; Wang et al., 2021)

EK combined with Phytoremediation	In situ/Ex situ	- Increases the bioavailability of contaminants when combined with phytoremediation - Need to use less energy than ex-situ methods - Faster treatment than phytoremediation - Possibilities for wildlife to thrive after vegetation is established	- Unsuited for pollutants mixtures of varying concentrations - In situ remediation may be complicated by acidic environments and anode corrosion - Transfer of pollution from the soil to the air - Removal efficiency is greatly reduced when the soil contains carbonates and hematite, as well as big rocks	(Wang et al., 2021)
EK combined with solar power.	Ex situ	- Reduces the operating cost significantly, environmental friendly - Reduce potential heating effects - It may be the most effective solution for off-grid polluted sites with no or insufficient power supply lines in remote locations	- Climate and location affect the electricity generated by solar cells - Discontinuous supply connection may affect the removal efficiency	(Hassan and Mohamedelhassan, 2012)

2.7. System selection and recommendation

Furthermore, EK-hybrid systems were proposed to improve pollutant removal efficiency from the soil. For example, enhancement agents facilitate the removal of organic and inorganic contaminants by increasing their solubilities. Yet, using enhancement agents increases the cost of the remediation process and changes the soil's physicochemical characteristics (Rezaee et al., 2019; Song et al., 2020). Combining the EK with phytoremediation and bioremediation processes would be an alternative to coupling the EK with enhancement agents for organic and inorganic contaminants treatment. The drawbacks of the bio and phytoremediation processes are that they are not suitable for treating waste mixtures or high concentrations and are time-consuming. As shown in **Table 2.7**, the EK-bioremediation efficiency decreases at high voltages due to soil heating, whereas EK-phytoremediation is affected by the acid environment developed during the remediation process (Wang et al., 2021). More innovative approaches were recently developed to enhance the EK's contaminant removal with a suitable RFM. The EK-RFM system is competitive with other systems, suitable for organic and inorganic contaminants, cost-effective, and facilitates contaminants extraction. Recyclable waste materials, such as compost and biochar, are candidates for RFMs, offering significant cost reduction (Ghobadi et al., 2021a). An EK-solar hybrid system offers tremendous energy savings and an environmentally friendly approach that could be coupled with all EK hybrid systems (Hassan and Mohamedelhassan, 2012). The preference for the EK hybrid system depends on several factors, such as type and concentration of contaminant, technology development level, technology availability, and cost. Therefore, a pre-remediation contaminated soil analysis is recommended to decide on the best fit EK hybrid system for the soil remediation.

Despite the advantages of the standalone and hybrid EK systems, there are several issues in translating the laboratory results into the field application. For example, many laboratory experiments were conducted on kaolinite model soil rather than natural soils that vary in physical and chemical characteristics. Also, contaminated soils are usually by a mixture of heavy metals, organic matter, or both rather than a single contaminant in most laboratory tests, affecting the EK efficiency when transferred to the field application. The lack of pilot tests of standalone and hybrid EK systems negatively affected the commercialization of the EK process since there is no data about the field performance and cost. Pilot plant tests are essential for evaluating the scaled-up process efficiency and conducting techno-economic studies. The EK has the advantage of combining with other hybris system technologies, such as solar, phytoremediation, bioremediation, enhancement agents, and RFMs. This advantage should be stressed in literature when the EK is compared with other remediation processes. Laboratory and fieldwork of soil remediation should not also underestimate the EK advantage presented in its low-energy requirements and feasibility to operate by solar energy, reducing greenhouse gas emissions and excluding the excavation work.

2.8. Conclusion and research gaps

The study reviewed the advancement in remediation technologies to remove heavy metals and organic matter from contaminated soils. Despite their relative maturity, various soil remediation techniques are subject to restrictions in heavy metal-contaminated sites. For instance, phytoremediation needs treating or stacking the recovered soils since soil leaching will not eliminate contaminants like heavy metals, and this process takes a long time. Thus, by utilizing several technologies, it is possible to maximize the benefits and minimize the drawbacks. A large-scale application of integrated remediation technologies

should also be developed. Regional remediation strategies and scientific approaches are also necessary to reduce the harmful consequences of soil pollution accumulation.

Among the many treatment methods, EK technology provides the possible mechanism to reduce heavy metal ions and separate inorganic elements from nutrients based on the reducing potential. Previous studies involving the use of the EK technique to remove soil contaminated with heavy metals have noted a significant challenge arising from the EK technique, which was brought on by the precipitation of heavy metals in areas with higher pH. The EK technique for removing inorganic metals from soil has become constrained by this pH, and the EK process was paired with complex agents to get over this restriction. Previous research showed that powerful acids, like electrical conductivity and pH, could alter soil properties and contribute to increased treatment costs due to electrolyte recovery after EK. In addition, many complicating agents for inorganic mineral extraction are not recommended because of their poor applications in a large-scale process of EK. EK was combined with bioremediation treatment. Although the method is a viable environmentally friendly treatment option for removing heavy pollutants from the soil, it is comparatively inexpensive. The treatment process can take an extended time to remove inorganic material. RFMs were used to avoid these limits and improve the EK process's processing states. There was better heavy metal processing performance than the improved conventional EK.

Generally, hybrid remediation systems have advantages over a single treatment method, such as physical, chemical, or biological, that hardly achieves the desired removal effect. As a result, combined EK remediation technologies receive much attention for maximizing the benefits of a single process and improving removal efficiency. Future studies should include pilot tests of EK coupled with chemical, physical, phyto, and bioremediations for organic and heavy metals removal to evaluate their efficiency for soil

remediation compared to standalone remediation technologies. Coupling EK with other remediation technologies will also assist in speeding up the EK process commercialization. The EK cost is case-specific, i.e., it depends on the site and contaminants characteristics. Although essential, models to predict the EK costs fail to provide accurate data without significant field/pilot tests. The EK cost depends on several technical and environmental factors that cannot be easily approximated in laboratory tests, such as electrode cost, energy cost, type of power source, labour cost, and site importance.

CHAPTER THREE:

MATERIALS AND METHODS

CHAPTER THREE: MATERIALS AND METHODS

3.1. Materials

Copper sulfate ($CuSO_4$) with a purity greater than 99%, along with zinc sulfate ($ZnSO_4$) and nickel chloride ($NiCl_2$) of 98–99% purity, were procured from Sigma Aldrich, Australia. This study utilized commercial kaolinite and natural soil to enhance electrokinetic (EK) remediation for heavy metal removal. Commercial kaolinite, a fine white clay mineral powder obtained from Keane Ceramic Pty, Australia, served as the model soil. Its properties are detailed in **Table 3.1**. Although heavy metal-spiked model soils like kaolinite are useful for understanding the fundamental principles of the technology, their behavior significantly differs from that of real soils. Consequently, natural soil samples from the sub-surface at a depth of 15 to 20 cm were obtained from a contaminated site in Northwest Sydney (Australia). Upon the removal of debris, roots, and stones, the soil was initially air-dried and subsequently sifted through a 600 μm sieve (Ghobadi et al., 2021a; Yuan et al., 2017). **Table 3.2** outlines the characteristics of the natural soil before preparation.

Iron slag sourced from the environmental engineering laboratory was used as an adsorbent for copper removal during the EK process. Powdered activated carbon, with a particle size of 100 mesh, was procured from Sigma-Aldrich, Australia. Additionally, a reactive filter material (RFM) consisting of iron slag alone or a mixture of iron slag and powdered activated carbon was investigated within the EK system. Another RFM variant included a combination of granular or powdered iron slag and black tea waste. In the last chapter, sawdust sourced from a construction project by the Labour Revolution Company, Australia, was combined with iron slag to form an RFM. For this chapter, glutaraldehyde solution, also purchased from Sigma-Aldrich (Australia), was used to crosslink sawdust

within the RFM. A 2% glutaraldehyde solution was blended with sawdust and iron slag to ensure uniformity in the RFM for the EK process.

A steady electrical current was employed to uphold experimental integrity, facilitated by a direct current power supply, model EA-PS 3015-11B. Hourly measurements and recording of electric current and voltage were carried out by a multimeter (Keithley 175). The reactor's electrode compartments flanking the reactor were equipped with 15 cm x 1 cm (graphite rod electrodes) obtained from Graphite Australia Pty Ltd. Electrical leads for connecting the power supplies and electrodes were purchased from Jay Cars Australia Pty. To prevent soil particles from entering the electrode chambers, cellulose filter papers with a pore size of 5–13 μm (LLG labware) were used in every test.

Table 3.1: Shows the chemical and physical parameters of kaolinite clay soil.

Soil characteristics	**Range of values**
Particles size analysis	
Clay	45.80
Silt	50.16
Sand	2.12
Permeability (m/sec)	3.95×10^{-10}
Density (g/cm^3)	1.35
Porosity (kg/m^3)	599
Organic matter	0.01
TDS (ppm)	129
pH	4.24 ± 0.04
Electrical conductivity (mS/cm)	0.39 ± 0.010
Initial copper concentration (mg /kg)	990

Table 3.2: Natural soil properties and heavy metal content.

Characteristics	**Range of values**
Particle size analysis (%)	
Clay	13.8
Silt	65.7
Sand	20.5
Permeability (m/sec)	1.0×10^{-6}
Density (g/cm^3)	1.42
Porosity (kg/m^3)	985
Organic matter (%)	1.2

TDS (mg/L)	303.6
pH	4.29± 0.2
Electrical conductivity (mS/cm)	0.692± 0.2
Elemental composition (%)	
C	5.85
O	91.29
Fe	2.36
Others	Negligible
Initial metal concentration (mg/kg)	
Cu	430
Ni	325
Zn	652
Others	Negligible

3.2. Methods

3.2.1. Properties of kaolinite clay soil and natural soil

Copper was chosen as the primary heavy metal contaminant for this study due to the prevalence of soil contamination by copper ions and the need for effective remediation (Ghobadi et al., 2021a, 2020; Hawal et al., 2023; Zheng et al., 2024). To prepare the contaminated kaolinite soil, 1 liter of distilled water was mixed with 1 kilogram of kaolinite soil and stirred for 30 minutes. During agitation, 2.21 grams of nickel chloride ($NiCl_2$), 2.52 grams of copper sulfate ($CuSO_4$), and 2.51 grams of zinc sulfate ($ZnSO_4$) were added as individual or combined pollutants. The resulting solution was then added to the kaolinite and mixed thoroughly using a stainless steel spatula. The contaminated soil was stored for 72 hours to allow copper adsorption and achieve equilibrium (Altaee et al., 2008). Once saturated, the soil was packed into the EK cell in layers and compacted uniformly using a hand compactor.

In addition, natural soil was used in the study. After collection, debris, visible roots, and stones were carefully removed. The soil was initially air-dried and subsequently sifted through a 600 μm sieve. A total of 1.4 kg of contaminated soil was combined with a measured amount of deionized water to reach the desired water content of 34%. The

prepared soil was then placed into the experimental apparatus and uniformly compacted using a tamper.

3.2.2. Preparation of reactive filter media (RFM)

This study explored the integration of the EK process with industrial iron slag waste and its combinations with activated carbon, sawdust as a cellulose source, and black tea waste. These materials, when mixed with granular and powdered iron slag of alkaline pH, were utilized to create a superabsorbent material capable of sequestering heavy metals during the EK process. This hybrid RFM was designed for the removal of single or mixed contaminants from kaolinite and natural soils. Iron slag was chosen due to its availability as an industrial byproduct and its exceptional adsorption capacity for metal ions. The study aims to develop an environmentally friendly and recyclable composite RFM to enhance the removal of heavy metals from contaminated soils.

Although sawdust has low electrical conductivity, the high conductivity of iron slag renders the RFM suitable for EK applications. A novel RFM was created by blending organic and inorganic components to enhance adsorption capacity while maintaining a total weight of 100 g (1:1 ratio). This composite material underwent a series of EK-RFM experiments to evaluate its efficiency in extracting Cu^{2+}, Ni^{2+}, and Zn^{2+} from kaolinite soil. For the remediation of heavy metal-contaminated natural soils, the RFM quantity was increased to 130 g and placed in the EK system's RFM section for performance assessment.

3.2.3. Electrokinetic cell set-up

The experimental setup involved constructing a reactor made of plexiglass with dimensions of (23L x 8W x 11H) cm, designed for optical monitoring and featuring compartments for electrodes at both ends, along with a central compartment for the contaminated soil. An EAPS-3015-11B power supply was utilized to deliver electric

current via graphite rod electrodes (15 cm x 1 cm) positioned at both ends of the reactor. Cellulose filter sheets (pore size 5-13 µm, LLG Labware) were placed between the electrode compartments and the soil to prevent soil particles from entering the electrolyte. The moisture content of the soil was 100% in all experiments. A perforated plexiglass plate was used to provide support for the filter sheets. The Reactive Filter Media (RFM) was positioned near the cathode compartment within the soil. Throughout the experiment, (Milli-Q water) was periodically introduced into the anolyte compartment to counterbalance water depletion caused by electrolysis and electroosmotic flow. Continuous monitoring was conducted with hourly current measurements using a Keithley 175 auto-ranging multimeter. **Figure 3.1** illustrates a detailed schematic of the experimental setup for electrokinetic (EK) experiments conducted in this study.

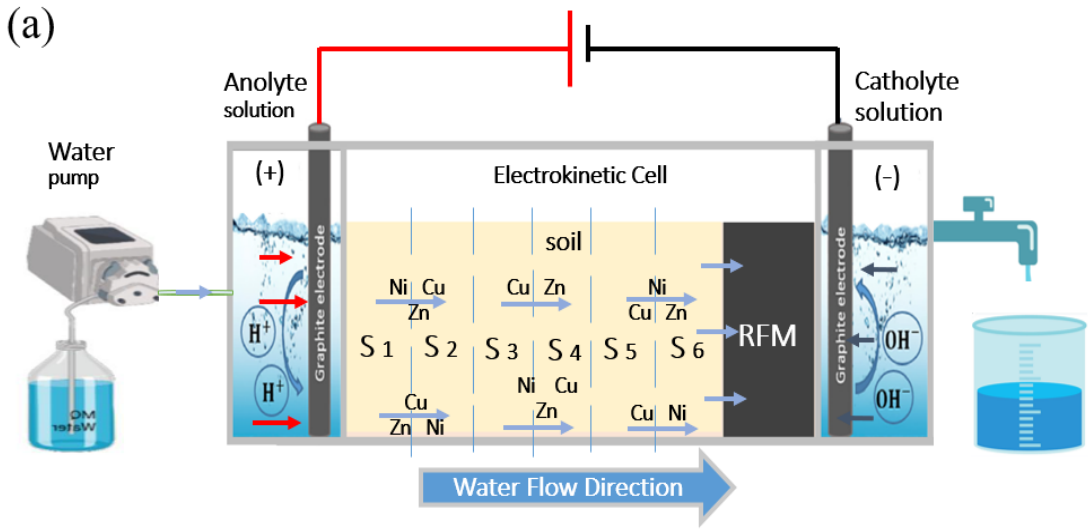

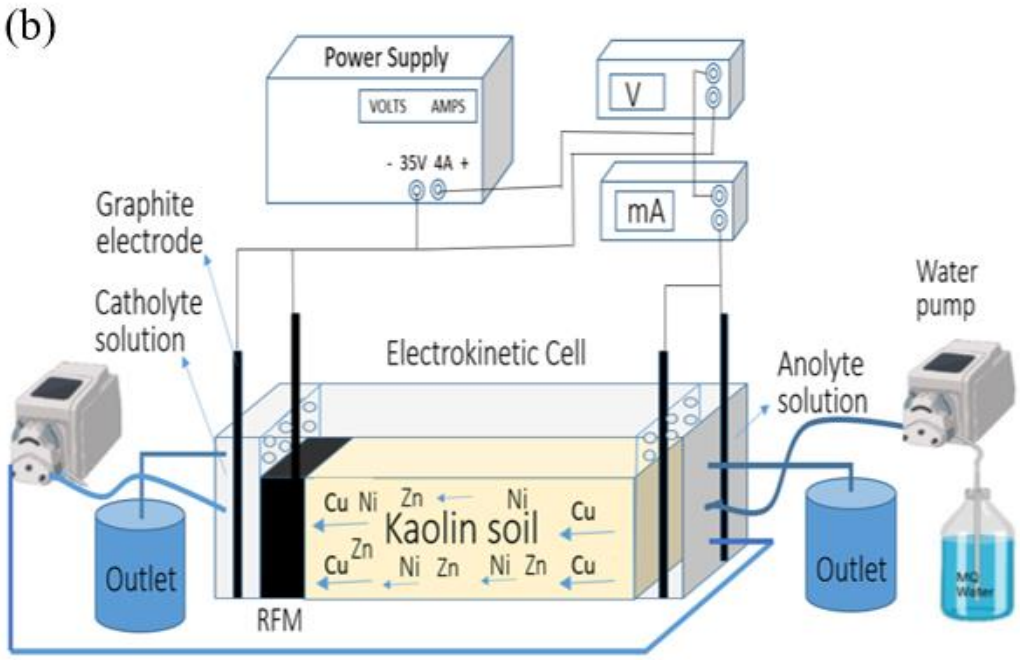

Figure 3.1: Schematic representation of heavy metal removal in an EK-RFM reactor (a) EK+RFM test design (b) EK+RFM with anolyte recycling test design.

3.2.4. Adsorption/desorption testing using RFM

The adsorption capacity of RFM was evaluated using a thermostatic shaker maintained at controlled conditions of 20 ± 1°C with a rota shaking rate of 150 rpm for 3.5 to 24 hours. Both the copper solution and the composite solution had concentrations of 2.52 g/ L. For the combined solution, the solid-to-liquid ratios were 2.21 g/ L for nickel, 2.52 g/ L for copper, and 2.51 g/ L for zinc. Equal proportions of RFMs were used as adsorbents to assess heavy metal adsorption. Following the adsorption process, the mixture was separated by centrifuging at 10,000 rpm for a quarter of an hour. The concentrations of Cu^{2+}, Ni^{2+}, and Zn^{2+} were measured using Inductively Coupled Plasma Mass Spectrometry (ICP-MS), and the adsorption capacity (mg/g) was calculated from Equation (1). Breakthrough curves were constructed by plotting the (C_f/C_i) ratio, where

C_i represents the initial concentration of the pollutant and C_f is the concentration at a given time.

Breakthrough curve tests are executed to establish the breakthrough point, indicating the time when the outflow concentration attains a designated fraction of the inflow concentration. Following the adsorption test, we conducted desorption experiments to examine the reversibility and measure the amount of heavy metals released. A 50 mL solution of 0.1 M hydrochloric acid (HCl) was added to the vials containing the RFMs. The desorption process was conducted on a thermostatic shaker maintained at 24 ± 1°C and a speed of 150 rpm for 24 hours. Subsequently, the RFM was isolated from the solution using centrifugation at a speed of 10,000 revolutions per minute for a quarter of an hour. The samples were analyzed using the Inductively Coupled Plasma (ICP) technique to determine the concentrations of copper, nickel, and zinc. The desorption capacity, measured in milligrams per gram, was determined using Equation (2). The financial benefits of recycling adsorbents in numerous cycles are apparent in decreasing the costs of the adsorption process, which is especially important for large-scale industrial applications. Adsorption-desorption tests were undertaken in a single cycle to evaluate the recyclability of the adsorbents. The desorption experiments were carried out in an acidic environment characterized by a pH (1.4±0.01). The desorption was determined by applying Equation (3.3) (Jain et al., 2018; Meez et al., 2021; Rahchamani et al., 2011).

$$\text{Adsorption capacity } q_e \left(\frac{mg}{g}\right) = \frac{(C_{initial} - C_{residual}) * V}{W} \tag{3.1}$$

$$\text{Desorption } \left(\frac{mg}{g}\right) = \frac{(C_{residual}) * V}{W} \tag{3.2}$$

$$\text{D } (\%) = \left(\frac{C_{desorbed}}{C_{adsorbed}}\right) * 100 \tag{3.3}$$

The adsorption capacity equation includes $C_{initial}$, representing the initial concentration of metals (in mg/L); $C_{residual}$, indicating the equilibrium concentration of metals (in mg/L); *V,* the solution volume (in L); and *W,* the weight of the RFM (in g), $C_{desorbed}$ refers to the concentration of desorbed metal ions, while $C_{adsorbed}$ refers to the concentration of adsorbed metal ions.

3.2.5. Removal efficiency

The efficiency of the EK treatments was assessed by calculating the heavy metal removal efficiency for each soil section using the specified Equation (3.4) (Ganbat et al., 2023; Ghobadi et al., 2021b, 2020).

$$\text{Removal efficiency}_i = ((m_{i,initial} - m_{i,final})/m_{i,initial}) * 100\% \quad (3.4)$$

where $m_{i,initial}$ is the initial metal concentration (mg/kg) in section i before treatment, and $m_{i,final}$ is the residual metal (mg/kg) in section i after EK treatment. A negative value for removal efficiency shows that metal ions have accumulated in that area. Total heavy metal removal from the soil sample is a significant measure that indicates the overall EK treatment performance, which is calculated using Equation (3.4).

$$\text{Total heavy metal removal} = ((m_{initial} - m_{final})/m_{initial}) * 100\% \quad (3.5)$$

where $m_{initial}$ is the initial heavy metal mass (mg) before treatment and m_{final} is the final residual heavy metal mass (mg) after treatment in the whole soil sample.

3.2.6. Power consumption

Power consumption is one of the most critical factors in evaluating the overall cost of EK remediation. In the EK process, energy consumption plays a key role, as the electric current drives the transport of contaminants and facilitates the dissolution of compounds under the applied electric field. Therefore, assessing power consumption is essential for

determining both the efficiency and cost-effectiveness of the remediation process (Ganbat et al., 2022; Ghobadi et al., 2021a; Yuan et al., 2017).

In this investigation, the specific energy consumption was determined using the equation (3.6):

$$E_u = \frac{10^{-3}}{V_s} \int V\ I\ dt \qquad (3.6)$$

In this context, "Eu" stands for the specific energy consumption (kWh/kg), "I" represents the electric current (A), "V" denotes the applied voltage (V), "t" indicates the experimental time (h), and "Vs" signifies the total volume of treated soil (kg).

3.2.7. Analytical methods

At the end of the EK trials, the soil was divided into six equal segments labeled S1 through S6, ranging from the anode to the cathode. After homogenizing each segment, it was dried in the oven at 100°C for 12 hours. Next, the dried soil samples were prepared for measuring the amounts of Cu^{2+}, Ni^{2+}, and Zn^{2+} for experiments, as well as pH and conductivity for all experiments. Dry soil was combined with distilled water in a 1:5 (w/v) ratio to generate a soil suspension, which was then agitated for at least 5 minutes using a magnetic mixer. A multimeter (HACH HQ40d model) was employed to assess the pH levels and electrical conductivity (EC) of the kaolinite and natural soils. Two samples were taken from each soil portion after drying and homogenized. Ten milliliters of 2M HNO_3 were added to one gram of dry soil for each sample to undergo digestion. After that, the soil-acid mixture was shaken for four hours. After stirring, the soil suspension was subjected to centrifugation for three minutes at 3,000 rpm in order to extract the solution from the soil particles (Groenenberg et al., 2017). ICP-MS was used to determine the amounts of metals. The RFM was extracted using the same procedure as the soil

samples, and the concentrations of heavy metals were analyzed. Moreover, RFM was retrieved through an acid solvent extraction method and utilised again in the EK-RC.

All analyses were conducted in triplicate, with results reported as averages. A variety of analytical methods were used to investigate the physical and chemical characteristics of the soil and RFM comprehensively. Data was collected using Energy Dispersive X-ray Spectroscopy (EDX), Zeiss Evo-SEM, and Scanning Electron Microscopy (SEM) techniques. This combination allowed for comprehensive microchemical analysis. Shimadzu Miracle-10 instrument was employed for Fourier Transform Infrared Spectroscopy (FTIR) to examine the RFMs surface functional groups in pre and post-electrokinetic (EK) experiments. The analyses were conducted using a Micrometrics 3Flex surface characterization analyzer operating at 77K.

CHAPTER FOUR:

IRON SLAG/ACTIVATED CARBON-ELECTROKINETIC SYSTEM WITH ANOLYTE RECYCLING FOR SINGLE AND MIXTURE HEAVY METALS REMEDIATION

CHAPTER FOUR: IRON SLAG/ACTIVATED CARBON-ELECTROKINETIC SYSTEM WITH ANOLYTE RECYCLING FOR SINGLE AND MIXTURE HEAVY METALS REMEDIATION

The content of this chapter is based on the following publication:

Hamdi, F.M., et al. (2024) "Iron slag/activated carbon-electrokinetic system with anolyte recycling for single and mixture heavy metals remediation", Science of the Total Environment, 172516.

4.1. Introduction

The presence of heavy metal contaminants in soils has become a matter of global significance, primarily because of their toxic nature, long-lasting effects, and the potential risk they pose to food safety (Wen et al., 2021). Numerous strategies and techniques have been proposed to address soil contamination problems (Song et al., 2017). In addition to traditional decontamination methods, electrokinetic has been suggested for low permeability soil treatment at a low cost (Agnew et al., 2011) by placing electrodes strategically in polluted soil to induce heavy metal transport under the effect the electric field across the soil (Peppicelli et al., 2018). The precipitation of heavy metals near the cathode adversely affects the EK process, increasing the soil resistivity to electric current and complicating contaminants extraction (Yeung, 2011). As a result, there is an increasing demand to improve the EK method to stop the advancement of the alkaline front and maintain the soil pH low enough for heavy metals removal (Ghobadi et al., 2021a; Wen et al., 2021; Yuan et al., 2016a).

Researchers have focused on improving the EK process and making it more practical by incorporating enhancement agents like chelating and surfactants to boost contaminant

mobility. Acidic or basic solutions were also used to regulate the pH of the electrolyte (Ganbat et al., 2022; Ghobadi et al., 2020; Li et al., 2020). While there has been a considerable amount of research on the electrokinetic (EK) process in soil remediation, only a limited number of studies have focused explicitly on remediating soil contaminated with a mixture of heavy metals (Bahemmat et al., 2016; Yuan et al., 2016a). Yuan et al. (2016b) investigated the use of an assisting agent, citric acid combined with calcium chloride (CA+$CaCl_2$), for the simultaneous removal of five heavy metals (namely Zn, Cd, Ni, Cu, and Pb) from contaminated kaolin. This example closely resembles real-world scenarios where polluted soil is frequently affected by a mixture of various heavy metals rather than being polluted by a single metal ion alone. The study reported varying removal efficiencies ranging from 86.2% to 99.0% for Zn, Ni, Cd, Cu, and Pb. Also, in a study conducted by (Yuan et al., 2016b), the researchers investigated the impact of carbon nanotube-covered polyethylene terephthalate yarns (PET-CNT) when used as a cathode electrode in the simultaneous electrokinetic remediation of multi-heavy metals (Zn, Ni, Cd, Cu, and Pb) contaminated kaolin. Introducing PET-CNT as the cathode electrode significantly increased the electric current and electroosmotic flow while reducing the soil pH, leading to enhanced extraction efficiencies of the heavy metals. The study's findings revealed that the order of heavy metal removal efficiency decreased in the following sequence: Ni > Cd > Zn > Cu > Pb, indicating that Ni, Cd, and Zn were relatively easier to extract from the contaminated soil compared to Cu and Pb, which posed greater challenges for removal. However, selecting the proper enhancement technique is essential in the EK process concerning treatment duration, cost, and environmental impact. For instance, it is possible to affect the soil matrix when applying the enhancement agent. Consequently, it becomes necessary to recover the electrolyte after the EK treatment (Ghobadi et al., 2020; Lim et al., 2016a). Indeed, despite the

widespread use of enhancing agents in the EK process, laboratory-scale studies have revealed the adverse effects of strong acids on specific soil characteristics, such as electrical conductivity and pH, post-treatment. Moreover, applying these agents increased remediation costs due to the need for electrolyte recovery after the EK treatment (Gong et al., 2018; Mao et al., 2015). Certain enhancement agents are not recommended for extracting heavy metals because of their unsuccessful applications in full-scale EK operations (Bahemmat et al., 2016; Gong et al., 2018). Tian et al. (2017) explored the use of eco-friendly enhancing agents like rhamnolipids, saponin, and citric acid in the EK remediation process to address soil contamination with Cd, Cr, Cu, Pb, Zn, and PAH/PCB in harbour sediments. Results revealed that the combination of these agents only managed to remove small amounts of metals (4.4% to 15.8%) and achieved a slightly better removal rate for PAH (29.2%) and PCB (38.2%) (Tian et al., 2017).

Bio-EK remediation, considered one of the most environmentally friendly options for extracting heavy metals from the soil, may require a longer remediation time, albeit relatively inexpensive (Gong et al., 2018). The simultaneous extraction of heavy metals has also been investigated by implementing EK remediation coupled with reactive filter media (RFM), another technique to enhance metal ion removal by the EK process. Researchers suggested several types of RFMs for soil remediation by the EK process, including activated carbon (AC), zerovalent iron (ZVI), and charcoal made from the activation of bamboo (Cang et al., 2009a; Gholizadeh and Hu, 2021a; Ren et al., 2014; Yuan and Chiang, 2007b; Zhao et al., 2016b). The factors that should be considered in selecting the RFM media are cost, efficiency, availability, ease of use and recycling, and lifetime of the RFM (Ghobadi et al., 2021b, 2020). Ghobadi et al. (2021b) investigated the utilization of a compost or biochar mixture as a reactive filter material (RFM) combined with an electrokinetic remediation (EKR) process to treat copper-polluted

kaolin. According to their laboratory findings, the EK-RFM process, with the application of a constant electric current and the use of EK with 100% compost treatment, significantly enhanced the removal of copper from 1.03% to an impressive 84.09%. However, it's worth noting that this improvement in removal efficiency was accompanied by increased energy consumption. Contrarily, adding different grades of biochar to the compost in the soil during the EK-RFM process did not improve the removal of Cu ions. In addition, the overall Cu removal dropped from 84.09% to 74.11% when the compost was renewed and reused during the EK process. The study's results highlight compost as a promising and environmentally friendly reactive filter material (RFM) that enhances heavy metal removal in the EK process, especially when a continuous electric current is applied to lower the soil's pH due to its diverse organic compounds. In a consecutive study, Ghobadi et al. (2021a) investigated the removal of a mixture of heavy metals from natural soil using compost as an RFM. The study achieved a significant removal of Zn, Cd, and Mn, ranging from 51.6% to 72.1%, while Pb and Cu, resulting in smaller extractions of 28.2% and 29.1%, in conjunction with an electric current of 30.00 mA for a treatment duration of 14 days. The presence of soil organic matter had an adverse effect on the mobilization and migration of heavy metals, including Cu and Pb.

In 2021, Xie et al. conducted a study that combined the EK process with AC and Citric Acid (CA) to treat natural lead-contaminated soil by mixing the lead-contaminated soil with $Pb(NO_3)2$ solution to create the lead-contaminated soil. A concern arose during one test using only CA with the EK technique, as a high pH of approximately 13 was observed near the cathode. This high pH led to the accumulation of metal ions adjacent to the cathode, clogging the soil pores and significantly hindering the treatment process. However, a remarkable improvement was observed when RFM added AC to the EK process with CA. The lead removal efficiency increased dramatically from 15% to 58%

within 20 days. Because of its excellent efficacy in removing various heavy metal contaminants, AC is extensively employed in soil and water treatment as an adsorbent. Due to its extensive surface area, AC efficiently eliminates metal pollutants from the soil through surface adsorption. Despite its advantages, insufficient quantities of acceptable AC and the high production cost pose disadvantages to using AC RFM (Ahmed et al., 2015; Alhashimi and Aktas, 2017; Xie et al., 2021).

Yu et al. (2019) explored the application of EK combined with RFM to treat Cr(VI)-contaminated soil. Two types of RFM were employed: CTMAB-Z, a modified zeolite prepared with cetyltrimethyl ammonium bromide, acting as RFM-1, and a combination of CTMAB-Z and Fe(0) serving as RFM-2. Additionally, the study investigated the impact of chemical enhancers/additives, specifically DL-tartaric acid and Tween 80, on the EK of Cr(VI) in a series of contrasting experiments. Furthermore, the multifactor orthogonal investigation revealed that the highest Cr(VI) removal rate (80.92%) and leaching efficiency (85.25%) were obtained when the samples were treated with a voltage gradient of 2.5 V cm^{-1} for eight days. The study effectively demonstrated that the EKR process for Cr(VI) remediation could be significantly enhanced by incorporating RFM and additives. Another RFM commonly used due to its high adsorption and low cost is zerovalent iron (ZVI) (Cang et al., 2009a; Ren et al., 2014; Yu et al., 2019a; Zhao et al., 2016b). According to Cang et al. (2009), combining EK remediation with a ZVI RFM resulted in 72% Cr removal from the soil. However, the precipitation of contaminants on the ZVI surface controls its lifespan. Moreover, exposure to silica or natural organic materials can decrease the reactivity of the ZVI (Cang et al., 2009a; Ren et al., 2014). To address the limitations of using chemical agents in the EK process, researchers constructed RFM with activated carbon (AC), activated bamboo charcoal, and zerovalent iron (Ren et al., 2014; Xue et al., 2017). Despite their benefits, the widespread application

of these RFMs is hindered by cost, availability, and life cycle concerns. Additionally, RFMs alone may not be sufficient to halt the advancement of the alkaline front, necessitating the use of additional chemical reagents, thereby reducing the overall cost-effectiveness of the EK treatment (Cang et al., 2009a; Ren et al., 2014; Zhao et al., 2016b).

This study investigated coupling the EK process with industrial iron slag waste and iron slag/AC RFM for a single or mixture of contaminants removal from kaolinite soil. Iron slag was selected because it is an industrial waste with excellent adsorption to metal ions and is available. The kaolinite soil spiked with Cu, Ni, and Zn ions are common contaminants and were tested for EK decontamination as a standalone or mixture of contaminants. The iron slag alkalinity pH 11 is suitable for metal ions precipitation when captured by the RFM. The study also implemented a new technique of anolyte recycling to neutralize alkaline pH at the cathode and promote acid front transport across the soil. The method replaces using chemical agents for alkaline front neutralization to reduce chemical use. The research questions are: i) what is the efficiency of metal ions removal from kaolinite with and without iron slag RFM, ii) what is the effect of anolyte recycling to the cathode zone on metal ions removal during the EK process, and iii) what is the effect of multiple contaminants in the kaolinite soil on the efficiency of the electrokinetic remediation process? The study also investigated the impact of the RFM, EK duration, iron slag to AC ratio, and metal ion types on the EK remediation efficiency.

4.2. Materials and methods

4.2.1. Materials and soil sample preparation

Chapter 3 provides a detailed account of the materials, soil preparation methods, and apparatus used in the EK experiments. This study also incorporated iron slag sourced from the local steel manufacturing industry in Australia (InfraBuild, Rooty Hill, NSW

2766). The RFM was either iron slag alone or a mixture of iron slag and AC (Sigma-Aldrich, Australia). The chemical and physical properties of RFM are listed in **Table 4.1**, while **Table 3.1 in** (**Chapter 3**) provides a comprehensive overview of the characteristics of the kaolin soil used in the EK tests.

The morphological and chemical characteristics of the RFMs (Reactive Filter Media) were assessed through Energy Dispersive X-ray (EDX). Fourier Transform Infrared Spectroscopy (FTIR) using the Miracle-10 instrument (Shimadzu) was employed to analyze the surface functional groups of the RFMs before and after the EK tests. To determine the RFM's specific surface area, the Brunauer-Emmett-Teller (BET) nitrogen adsorption-desorption isotherms tests were conducted pre- and post-EK treatment. The Barrett-Joyner-Halenda (BJH) method was also utilized for a post-EK treatment analysis. These measurements were performed using a Micrometrics 3-FlexTM surface characterization analyzer at 77K.

Table 4.1: Different physicochemical characteristics of RFM.

Parameter	**Iron slag**	**Iron slag/AC (50/50)**
Particle size analysis (%)		
Greater than 2 mm	2.61	2.48
In between 1-2 mm	-	-
Less than 1mm	-	-
Permeability of soil (m s^{-1})	1.67×10^{-3}	2.54×10^{-2}
Specific Surface area (m^2g^{-1})	0.037	146.57
pH	11.38	10.63
Electrical conductivity (mS/cm)	0.643	0.551

4.2.2. Electrokinetic cell and test design

Figure 3.1 in (**Chapter 3**) displays a schematic diagram of the EK experimental apparatus and the EK cell employed in this study. Six electrokinetic experiments were conducted to evaluate the removal of single and mixed heavy metals from the

contaminated soil. The first five experiments investigated the removal of copper with and without iron slag/AC RFM, while the sixth experiment aimed at removing mixtures of copper, nickel, and zinc contaminants, as described in **Table 4.2**. The electrodes were subjected to a constant 20mA current in all tests. The experiments were terminated after 14 days, except for Exp5 and 6, which terminated after 21 to study the impact of the EK duration on heavy metals removal. The experiments were conducted at 1000 mg/kg Cu, Ni, and Zn concentration, RFM weight of 100 g near the cathode area, and 20 mA electric current.

Exp1 was a typical EK experiment with kaolinite, for which 1000 mg/kg Cu was added. Exp2 and 3 were performed to study the effect of the slag or slag/AC RFM on removing Cu from kaolinite soils by the EJ process. Exp4 and Exp5 were conducted to study the effect of slag/AC RFM with anolyte recycling on Cu removal from the kaolin soils in 14 days in Exp4 and 21 days in Exp5. Low-pH anolyte recycling to the cathode is used to control the alkaline front movement in the soil. Finally, with an anolyte recycling test, the Exp6 slag/AC RFM-EK system was performed for 21 days to evaluate the efficiency of removing Cu, Ni, and Zn from the kaolin.

Once the experiments were completed, the aqueous solutions were collected from the anode, cathode, and electrode assemblies. The kaolin soil was divided into six equal sections and kept separately in the designated plastic bag. Then, each section was homogenized before taking samples for metal ion measurement. Each soil sample's pH, conductivity, and Cu, Ni, and Zn concentrations were measured in triplicates.

Table 4.2: The type of EK tests and heavy metals concentration is 1000 mg/kg.

No of Exp	Experiment type	Heavy metal	Metal concent. (mg/kg)	Anolyte recycling	RFM	Current (mA)	Time (day)

Exp1	EK only	Cu	1000	NA	NA	20	14
Exp2	EK-Iron slag	Cu	1000	NA	100% Iron slag	20	14
Exp3	EK- Iron slag /AC	Cu	1000	NA	50% Iron slag+50%AC	20	14
Exp4	EK- Iron slag /AC	Cu	1000	Anolyte	50% Iron slag+50%AC	20	14
Exp5	EK- Iron slag /AC	Cu	1000	Anolyte	50% Iron slag+50%AC	20	21
Exp6	EK- Iron slag /AC	Cu, Ni, Zn	1000	Anolyte	50% Iron slag+50%AC	20	21

4.3. Results and discussion

4.3.1. Electric current

Contaminant transport across the soil during the electrokinetic treatment is significantly influenced by the applied electrical current, which strongly correlates with free ion concentration (Ghobadi et al., 2020). Therefore, the electrical current is a crucial factor that directly impacts the effectiveness of contaminants' movement in the soil (Ghobadi et al., 2021a). Initially, the electric current in the EK experiment was kept at 20 mA. **Figure 4.1a** illustrates the variation of electric current during the ED experiments Exp1 to (Ghobadi et al., 2021a, 2021b)Exp6. Water electrolysis produces H^+ and OH^- ions at the anode and cathode, respectively, and the electric current increases due to the ions' migration towards the electrode of an opposite charge (Ganbat et al., 2022). Metal ions dissolution occurs due to the advancement of acid front towards the cathode, increasing the ionic strength of pore fluid. Still, the influx of ionic species decreases over time due to the neutralization of acid and base front when they meet in the soil and the precipitation of metal ions (Ghobadi et al., 2020).

The EK electric current decreases over time due to the metal ions precipitating near the cathode region at alkaline soil pH (Ganbat et al., 2022). The dropdown in the electric current could be due to metal hydroxide precipitation, fouling of the electrodes, or acid and hydroxide fronts meeting near the cathode. After 72 to 96 hours, a decline was observed in the electric current of Exp1 to Exp6. The sharpest drop in electric current was in Exp1, conducted without RFM or anolyte recycling to the cathode, allowing the advancement of the alkaline front in the soil. A similar observation was recorded in Exp2, conducted with 100% iron slag RFM, in which the electric current decreased from 20 mA to 17 mA after 72 h and reached 3 mA after 240 h before it jumped to 4.5 mA after 264 h and reached 5.6 mA at the end of the experiment. The erratic change in the Exp2 electric current could be due to the solubilization of ionic species caused by acid front movement at a later stage of the EK test. Experiment Exp3 was conducted using 50% iron slag mixed with 50% activated carbon (AC) to buffer alkaline front advancement in the soil. The maximum electric current in experiment Exp3, 19 mA, was slightly lower than in experiment Exp2 because of the lower electric conductivity of the RFM in experiment Exp3 (**Table 4.1**). There was a sharp drop in the electric current from 19 mA to 12.5 mA after 120 h due to metal hydroxide precipitation and acid and alkaline front meeting in the soil. At the end of experiment Exp3, the electric current reached 10 mA, which is 78% greater than the current in experiment Exp2. Incorporating AC in the RFM of experiment Exp3 probably slowed down the advancement of the alkaline front, hence meeting with the acid front, resulting in a higher electric in experiment Exp3.

Experiment Exp4 operating conditions were similar to experiment Exp3, with the anolyte being recycled to the cathode well to neutralize the alkaline front, allowing the acid front to sweep across the soil. The electric current of experiment Exp4 was 20 mA for about 24 h, declined to 14.2 mA after 72 h and progressively decreased to 6 mA at the end of a

2-week test. When the EK duration increased to three weeks in experiment Exp5, the electric current was 20 mA for 48 h, slightly decreased to 16.3 mA after 72 h, and gradually decreased to 5.5 mA after 504 h. The decrease in experiment Exp5 electric current indicates a steady state operating condition where alkaline front neutralization by the anolyte circulation facilitated the steady advancement of the acid front in the soil and solubilization and precipitation of metal ions near the cathode. Experiment Exp6 was conducted for 3 weeks with multiple heavy metal pollutants, i.e., Cu^{2+}, Ni^{2+}, and Zn^{2+}, to evaluate the EK efficiency for treating soil contaminated with a heavy metals mixture. The electric current of 19.5 mA lasted for 96 h due to the higher ionic strength in experiment Exp6 than in experiment Exp5. After 120 h, the electric current in experiment Exp6 dropped to 15.2 mA, gradually decreasing, and reached 3.8 mA at the end of the 3-week experiment. The lower recorded electric current at the end of experiment Exp6 compared to experiment Exp5 was attributed to the precipitation of metal ions as they approached the cathode compartment. The precipitation of Cu^{2+}, Ni^{2+}, and Zn^{2+} at different pHs increased the soil resistivity, causing a further decline in the electric current of experiment Exp6 compared to experiment Exp5.

As depicted in **Figure 4.1b,** a negative correlation exists between the electric current and the alteration in voltage. Metal ions precipitation diminished the electric current, increasing the voltage due to the increased soil resistivity. In all EK experiments, the voltage decreased during the first 24 h due to the solubilization of metal ions and increased ionic strength of pore fluid. The initial voltage was between 18 and 28 V, then decreased to about 11 V after 24 hours. The voltage increased to about 35 V in experiments Exp1, Exp2, Exp4, and Exp5 after 72 h and in experiments Exp3 and Exp6 after 120 h due to the high soil conductivity and ionic strength in experiments Exp3 and

Exp6. Compared to a conventional EK process, EK experiments incorporated the RFM with or without anolyte recycling, which exhibited a higher electric current.

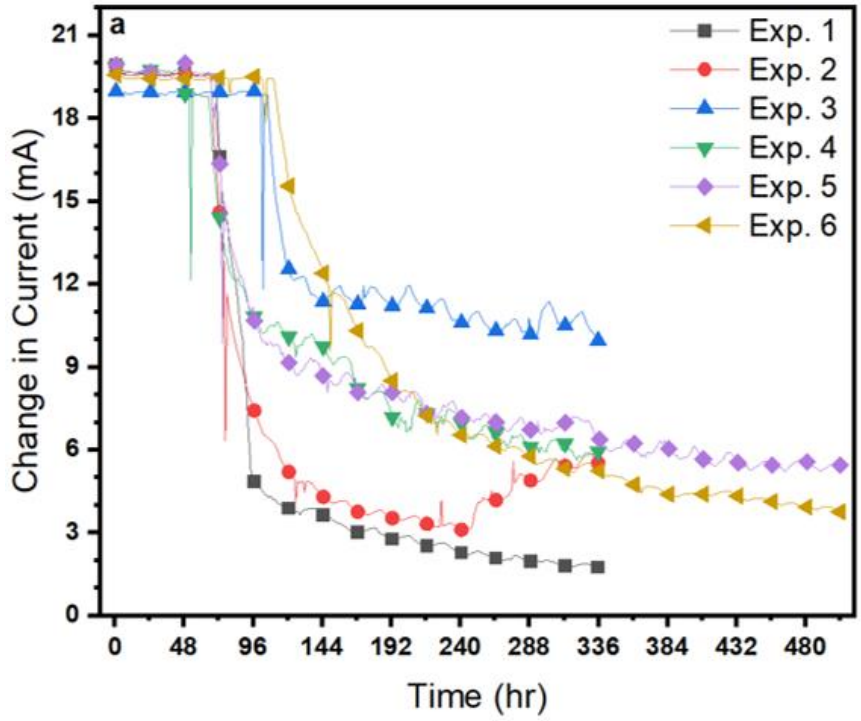

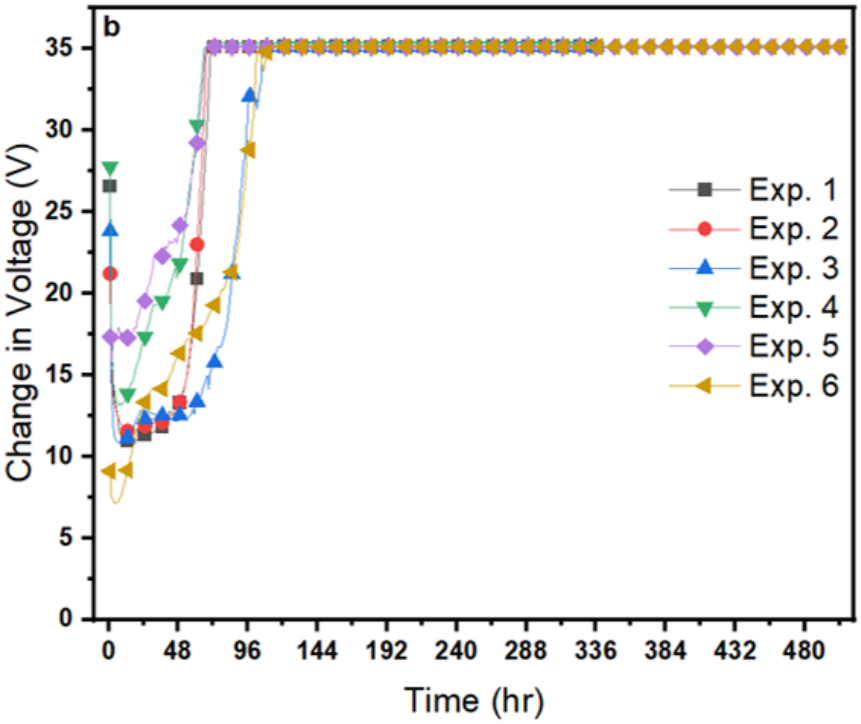

Figure 4.1: (a) Change in Current (mA) in the electrokinetic experiments and (b) Change in Voltage (V). Experiments were conducted at 20 mA direct current.

4.3.2. Soil pH and Electric conductivity

Figure 4.2a shows the pH of soil sections S1 to S6 and the RFM for the EK experiments Exp1 to Exp6. The main electrode reactions at the cathode and anode generate OH^- and H^+ ions according to the reactions below:

$$2H_2O - 4e^- \Rightarrow O_2 + 4H^+ \text{ (anode)} \quad (4.1)$$

$$4H_2O + 4e^- \Rightarrow 2H_2 + 4OH^- \text{ (cathode)} \quad (4.2)$$

According to Equation (4.1), the electrolytic reaction at the anode generates H^+, which migrates towards the cathode, reducing the soil pH. The alkaline soil pH at the cathode is due to the generation and migration of OH^- towards the anode region (Equation 4.2). The H^+ ions' effective ionic mobility is about 1.8 times larger than the OH^- ions, signifying that H^+ ions exhibit greater mobility and displacement in the soil than the OH^- ions (Acar and Alshawabkeh, 1993).

The initial soil pH was about pH 4.24 (**Table 3.1**). The soil pH decreased to less than the initial soil pH for sections S1 to S5 and was higher than in section S6 for experiments Exp1 to Exp3, whereas it was close to or slightly lower than soil pH in section S6 for experiments Exp4 to Exp6 (**Figure 4.2a**). For experiments Exp1 to Exp3, the soil pH was about pH 3 in section S1, increased slightly in the soil sections S2 and S3, and reached pH 4 in section S4. The soil pH of section S6 jumped to about 6.5 in experiment Exp1, pH 7 in experiment Exp2, and pH 5.2 in experiment Exp3. Compared to experiment Exp1, the higher soil pH in section S6 of experiment Exp2 was attributed to the 100% iron slag RFM (pH 11.38), which promoted alkaline front movement in the soil. However, mixing

50% AC in the iron slag RFM buffered alkaline pH movement towards the anode, and hence, the acid front advanced towards the cathode faster than in experiment Exp2.

For experiments Exp3 to Exp6, 50% iron slag-50% AC RFM was placed next to the cathode with the anolyte circulated to the cathode to control alkaline front transport in the soil. Experiment Exp4 was conducted for 2 weeks, and experiments Exp5 and Exp56 for 3 weeks. In experiments Exp4 and Exp5, the soil pH increased gradually from pH 3 in section S1 to about pH 3.7 in section S5 (**Figure 4.2a**). Compared to the latter experiments, the soil pH in experiment Exp6 remained constant at about pH 3 in sections S1 to S5 due to the rapid advancement of the acid front in the soil. The soil pH of section S6 increased and reached close to the soil pH (pH 4.24) in experiments Exp4 and Exp5 and pH 4 in experiment Exp6. The RFM pH was alkaline in all experiments but was slightly higher in experiment Exp2 (pH 11.4) with 100% iron slag RFM due to its higher initial pH (**Table 4.1**). In all experiments, lowering the soil pH to less than the initial soil pH will impart a positive charge onto the soil surface, decreasing the adsorption of metal ions.

Figure 4.2b shows the electric conductivity (EC) of the EK experiments. In experiments, Exp1 to Exp3, the soil EC in sections S1 to S3 was more significant than the initial soil EC due to the high ionic strength of pore fluid caused by metal ions solubilization by the acid front. However, the soil EC decreased gradually in sections S4 to S6 due to the precipitation of metal ions or ions moving toward the cathode region in these experiments. In contrast, the soil EC in experiments Exp4 and Exp5 was greater than the initial soil EC in sections S1 to S4 due to the high ionic strength of pore fluid, then decreased to lower than the initial soil EC in sections S5 and S6 as a result of metal ions precipitation and transport toward the cathode. In experiment Exp6, the soil EC remained less than the initial soil EC because of ions migration towards the cathode and precipitation in the

RFM, as discussed in section 3.4. Finally, the RFM EC in experiments Exp2 to Exp6 was greater than the initial soil EC because of the higher EC of initial iron slag and iron slag-AC than the initial soil EC (**Table 4.1**).

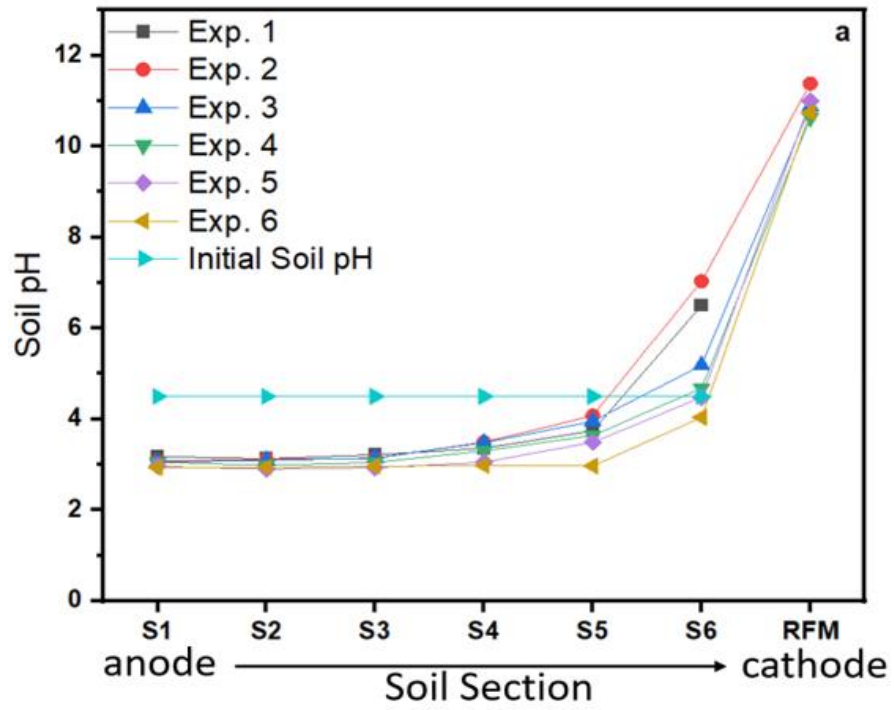

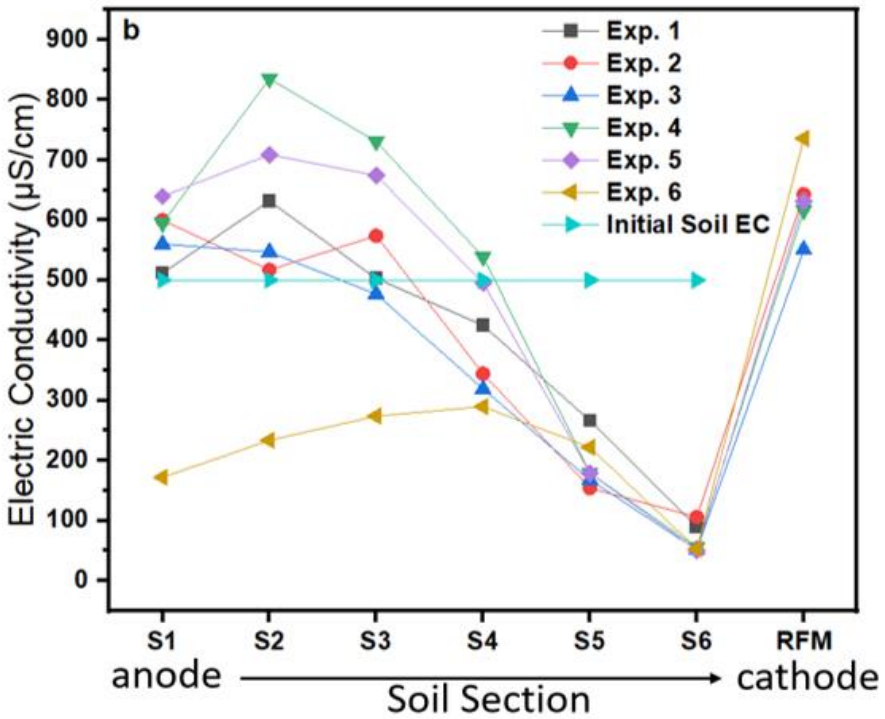

Figure 4.2: Soil pH and electric conductivity (EC) at the end of the EK experiments (a) soil pH and (b) electric conductivity.

4.3.3. Removal Rate

Six EK experiments were carried out to remove a single metal ion and a mixture of heavy metals from a contaminated kaolinite soil (**Table 4.2**). Experiments Exp1 to Exp3 were conducted without the anolyte recycling, whereas experiments Exp4 to Exp6 with the anolyte recycling to the cathode compartment. Experiments Exp1 to Exp4 lasted for 2 weeks whilst Exp5 and Exp6 lasted for 3 weeks, and the latter tested to remove a mixture of heavy metals.

Heavy metal ions moved across the soil from the anode to accumulate in the soil sections near the cathode after being solubilized by the acid front developed from the electrolysis reaction at the cathode. In the experiment, Exp1, copper ions (Cu^{2+}) were solubilized by the low pH front and transported across the soil from section S1 to S6. Generally, when pH drops below the point of zero charges (pzc), the soil surface charge will be positive, reducing the adsorption of metal ions. Therefore, the copper concentration was removed almost entirely from section S1, increased progressively in sections S2 to S5, and increased dramatically to 3486 mg/L in section S6 (**Figure 4.2a**). However, the amount of copper removed from the soil was about 3.11% (**Figure 4.3g**). Applying iron slag RFM near the cathode in experiment Exp2 increased copper removal from the soil section S1 to S5 (**Figure 4.3b**), and most of the copper was precipitated in section S6 as the soil pH became alkaline (**Figure 4.2a**). The copper concentration was 44 mg/L in section S1 and increased to 4242 mg/L in section S6. Only 81 mg/L copper concentration was found in the iron slag RFM, and 23.36% copper removal was achieved in the experiment Exp2 (**Figure 4.3g**). Iron oxide, the primary component of iron slag, has a strong adsorption

capacity to heavy metals, e.g., copper, nickel, and zinc (Yeongkyoo, 2018). The mechanisms of retaining heavy metals by iron oxide include surface complexation, precipitation, and electrostatic interactions (Hu et al., 2018). Despite copper removal in experiment Exp2 being 7 times greater than in experiment Exp1, the removal rate is still low, with only 21.6% of the copper captured by the RFM (**Table 4.3**). The alkaline conditions in section S6 favoured copper precipitation. Using iron slag-AC (50%-50%) RFM in the experiment Exp3 improved the copper removal from most soil sections, and 62.5% of the copper was accumulated in the RFM (**Table 4.3**). The copper concentration increased from 71 mg/L in the soil section S1 to 613 mg/L in section S6, reaching 4400 mg/L in the RFM (**Figure 4.3c**). The prevalent acid condition in most soil sections in experiment Exp3 enhanced the copper removal greater than in experiment Exp2. Also, incorporating AC in the RFM hampered the rapid advancement of the alkaline front.

To further improve the removal of heavy metal ions from the soil, the anolyte was recycled to the cathode compartment to neutralize the alkaline pH in experiments Exp4 to Exp6. As shown in **Figure 4.3d**, copper was removed from soil sections S1 to S6 and accumulated in the RFM of experiment Exp4. The concentration of copper in section S1 was 33 mg/L and increased to 261 mg/L in section S6, whilst it reached 6549 mg/L in the RFM. Almost 81.8% of the copper was accumulated in the RFM (**Table 4.3**), and the total copper removal in experiment Exp6 was 89.21% (**Figure 4.3g**). The greater copper removal in experiment Exp4 compared to experiment Exp3 was attributed to the anolyte recirculation to the cathode compartment, neutralizing alkaline pH. As a result, the acid front swept across the soil, solubilized, and carried the copper ions towards the RFM. Experiment Exp5 evaluated the impact of the EK duration on the copper ion removal by extending the EK process to 21 days (**Table 4.2**). **Figure 4.3e** shows that copper concentration in the soil sections S1 to S5 remained less than 50 mg/L and moderately

increased to 198 mg/L in section S6. Copper removal in the soil sections S1 to S5 was about 99% and decreased slightly to 96% in section S6. Anolyte recirculation to the cathode compartment neutralized the alkaline front and promoted the acid front advancement in the soil, carrying the copper ions to the RFM section in experiment Exp5. The total copper removal at the end of the 3 weeks EK process was 93.45% (**Table 4.3**), about 5% greater than in the experiment Exp4. Experiment Exp6 evaluated the efficiency of the EK process coupled with iron slag-AC RFM, and anolyte was recycled to the cathode compartment. In addition to, copper, nickel, and zinc were spiked into the kaolinite soil at 1 g/L to simulate the EK process treating a mixture of contaminants. The acid front swept across the soil in experiment Exp6, dissolved, and transported heavy metals to the RFM near the cathode region (**Figure 4.3f**). Copper, nickel, and zinc concentrations decreased gradually from the soil section S1 to S6 and accumulated in the RFM near the cathode. Furthermore, 71.7% of the copper, 83.9% of nickel, and 89.2% of zinc were captured by the RFM (**Table 4.3**). Copper, nickel, and zinc concentrations in the RFM are 5133 mg/L, 7302 mg/L, and 8191 mg/L, respectively. The corresponding removal of these heavy metals at the end of the EK process is 81.1% for copper, 89.09% for nickel, and 92.31% for zinc. The higher removal of nickel and zinc than copper is attributed to the pH of metal hydroxide precipitation, pH 6.9 for copper, pH 8.5 for zinc, and 8.8 for nickel (Kabdaşlı et al., 2012). Therefore, nickel and zinc removal was greater than copper at the end of experiment Exp6.

Copper removal increased from 3.11% (Exp1) to 23.36% (Exp2) when using iron slag RFM. Further increase in copper removal was achieved by mixing iron slag with AC in Exp3 due to the affinity of AC to alkaline pH. Anolyte recirculation to the cathode compartment in experiment Exp4 further improved copper removal in experiment Exp4 due to alkaline pH neutralization. Copper removal was 93.45 in experiment Exp5 when

the EK processing was extended to 3 weeks. The EK efficiency was slightly affected in experiment Exp6 with a mixture of heavy metals. The total metals removal was between 81.1% and 92.31%, depending on their solubility. In such a case, the duration of the EK process must be extended to achieve the desired removal rate.

Placing the RFM near the cathode, where inorganic pollutants are expected to accumulate in the EK process, aims to adsorb heavy metals and facilitate their extraction at the end of the EK experiment. In experiment Exp1, the alkaline front swept across the soil section S6, where most of the copper precipitated as metal hydroxide. Incorporating iron slag RFM in experiment exp2 slightly improved copper removal from 3.11% in Exp2 to 23.36% in Exp3. Although iron slag improved copper adsorption to some extent, it was ineffective in preventing the movement of the alkaline front in experiment Exp2, resulting in most of the copper precipitating as metal hydroxide in section S6. Therefore, AC was added to the RFM due to its affinity to the hydroxyl ions, preventing alkaline front transport toward the anode. Copper removal increased to 70.14% in Exp3 and further increased to 89.21% in Exp4 when the anolyte was recirculated to the cathode zone.

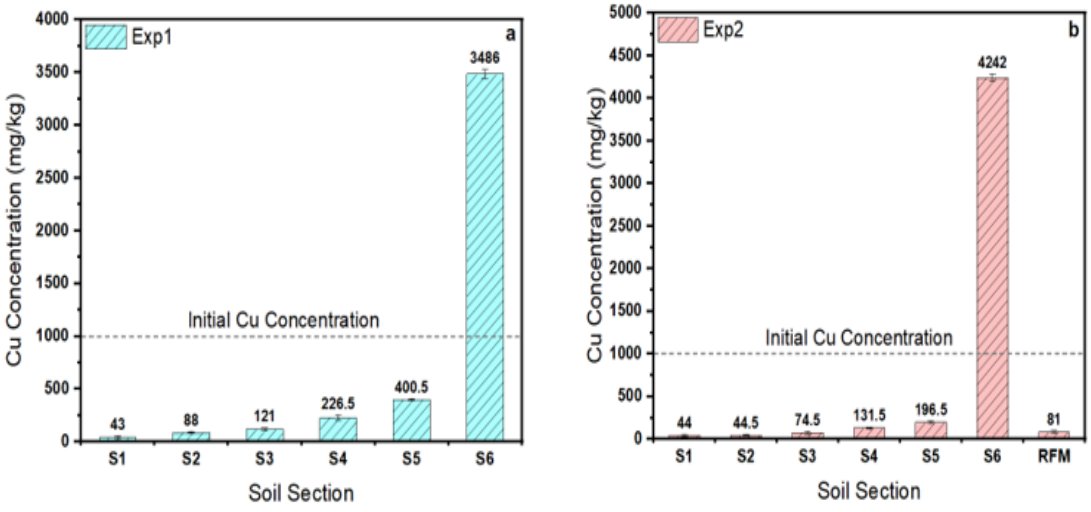

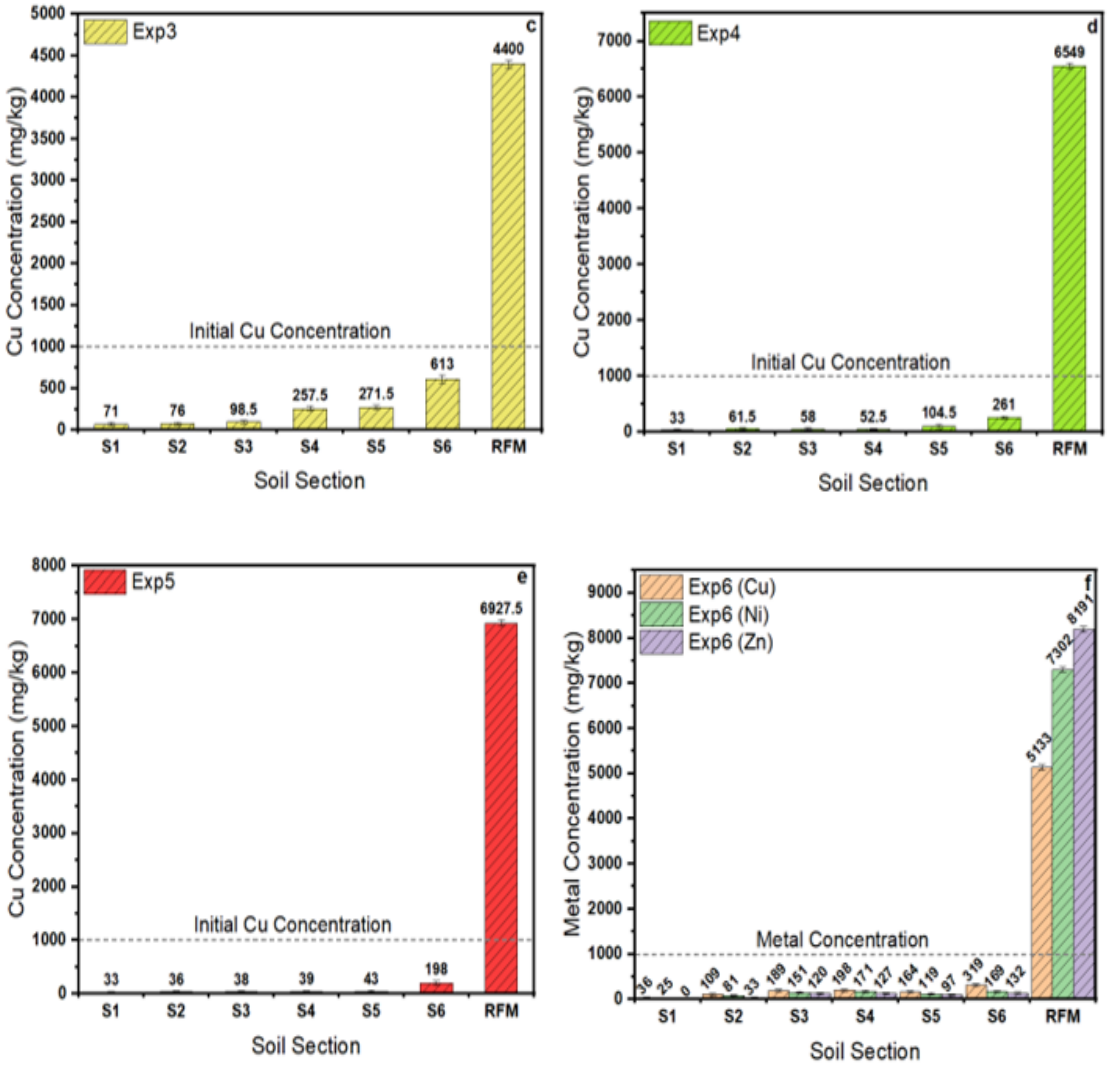
Exp3
c
Cu Concentration (mg/kg)
Initial Cu Concentration
71
76
98.5
257.5
271.5
613
4400
S1
S2
S3
S4
S5
S6
RFM
Soil Section
Exp4
d
6549
33
61.5
58
52.5
104.5
261
Exp5
e
6927.5
33
36
38
39
43
198
Exp6 (Cu)
Exp6 (Ni)
Exp6 (Zn)
f
Metal Concentration (mg/kg)
Metal Concentration
5133
7302
8191

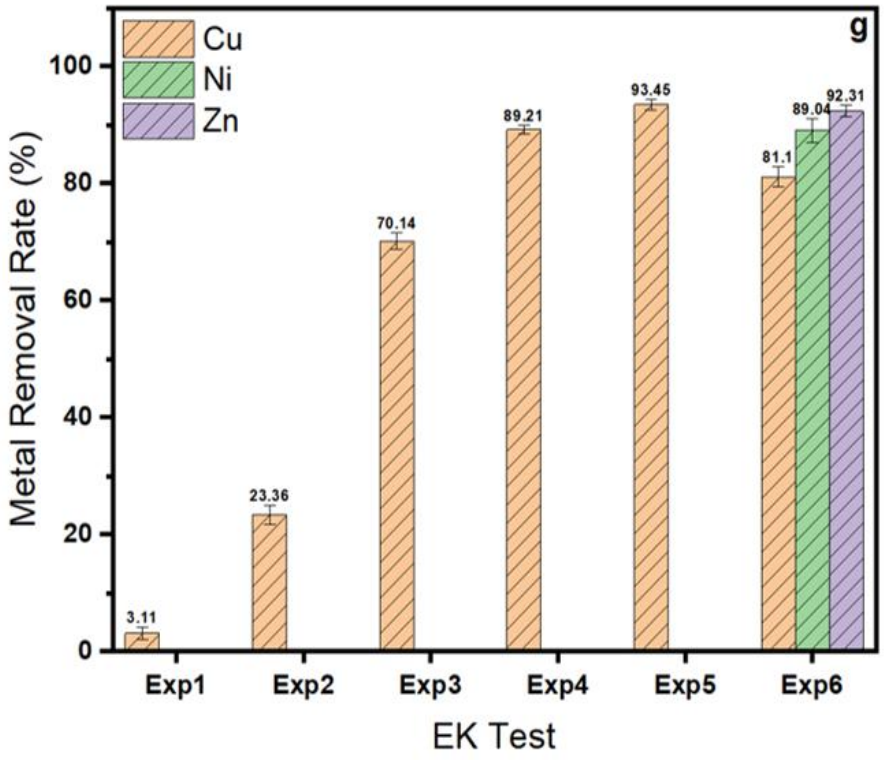

Figure 4.3: Cu in all experiments and Ni and Zn removal in experiment 6 at the end of the EK process.

Table 4.3: EK experimental conditions for copper removal and its mass balances. The concentration of metal ions is 1 g/kg, and tests were conducted at 22 °C.

Exp No	Metal ions	Residual metal ions in Soil (g)	Metal mass in RFM (g)	Mass Balance (%)	Removal (%)
Exp1	Cu	0.971	NA	102.97	3.11±0.23
Exp2	Cu	0.766	0.216	101.72	23.36±0.31
Exp3	Cu	0.297	0.625	103.27	70.14±0.28
Exp4	Cu	0.106	0.818	96.04	89.21±0.14
Exp5	Cu	0.065	0.844	97.88	93.45±0.19
	Cu	0.189	0.717	106.97	81.10±0.34

Exp6	Ni	0.109	0.839	102.98	89.04±0.39
	Zn	0.076	0.892	103.22	92.31±0.20

4.3.4. Characteristics of RFM

Steel slag, a solid waste, possesses a high specific surface area and considerable porosity. These characteristics make them a promising candidate as an inexpensive adsorbent for eliminating pollutants from soil. The effectiveness of steel slag in removing contaminants depends on its unique characteristics and chemical composition. Activated carbon has traditionally been an adsorbent for removing heavy metals from polluted soil and water (Ahmed et al., 2015; Ghobadi et al., 2020). In our study, we utilized a mixture of activated carbon and iron slag, known as the RFM (Remediation Filter Material), in the electrokinetic (EK) process to adsorb copper, nickel, and zinc. **Figure 4.4a** showcases the X-ray diffraction (XRD) outcome of the constituents of the iron slag produced in the steel-making process. The findings underscore the prevalence of iron oxide as the predominant element within the iron slag composition. It is noteworthy that iron oxide possesses a notable adsorption capability, rendering it effective in the removal of contaminants (Díaz-Piloneta et al., 2022). While the precise nature of the interaction between iron oxide and Cu, Ni, and Zn remains a topic of ongoing investigation, it is established that iron oxide has the capacity for adsorption or surface attachment interactions with these elements in the surrounding environment. This propensity is attributed to the inherent attributes of iron oxide, including its diminutive particle dimensions and pronounced porosity, which collectively bestow upon it a significant surface area, thereby positioning it as an excellent adsorbent. The central process governing the adsorption of Cu, Ni, and Zn onto iron oxide revolves around electrostatic interactions among the molecules of these metals. This interaction is succeeded by forming inner-sphere Fe-carboxylate complexes through

ligand exchange (Jain et al., 2018). The adsorption process involving Cu, Ni, and Zn onto iron oxide particles carries significant implications. Firstly, it diminishes the mobility of these elements within the environment, thereby mitigating the potential for groundwater contamination or seepage into the neighbouring regions. Moreover, this adsorption phenomenon can influence the behaviour and attributes of the iron oxide particles themselves. This influence extends to aspects encompassing stability and reactivity.

The functional properties of iron slag and iron slag/AC can be effectively assessed using FTIR spectra, which provide valuable information (Alhashimi and Aktas, 2017; Ghobadi et al., 2020). **Figure 4.4b** presents the FT-IR spectra of the new RFM, used RFM with iron slag, and used RFM with iron slag/AC. The FTIR spectra of both iron slag and iron slag/AC, both before and after the EK treatment, demonstrated similar characteristics. In contrast, the bands were more pronounced in the iron slag/AC before and after the EK treatment. This finding demonstrates the great promise of EK-iron slag/AC in eliminating copper, nickel, and zinc. After the EK treatment, the FTIR spectra of iron slag and iron slag/AC (refer to **Figure 4.4b**) exhibited peaks in the 3750, 2340, 1750, and 1550 cm^{-1} regions, indicating OH stretching. The band at 3750 cm^{-1} has diminished in Exp5 for Iron slag/AC; however, it has similar stretching in all the other experiments. The band at 2340 cm^{-1} has slightly increased in intensity after soil treatment with iron slag only in Exp2 due to the additional OH groups introduced by the iron slag, leading to a change in intensity. In all the experiments, this band has no visible change when the soil is treated with iron slag/AC. The FTIR band at 1750 cm^{-1} is diminished in Exp3 and Exp5 for iron slag/AC treatment, probably as a result of the adsorption of carbonyl groups (1750 cm^{-1}) by activated carbon (Stavropoulos et al., 2008).

SEM analysis combined with EDS (**Figure 4.4**) provided definitive evidence of the existence of copper, nickel, and zinc on the surfaces of RFMs following the electrokinetic

(EK) treatment. SEM images showing surface morphologies and EDS graphs for the RFMs are presented in **Figures 4.4c to 4.4f**. There is no presence of any contaminants on the surface of the RFMs. After treatment, contaminants observation was particularly evident in the iron slag and iron slag/AC specimens. The copper content in iron slag was lower than that in iron slag/AC RFM. According to the EDS results, the copper content was 1.19% in iron slag/AC and merely 0.34% in iron slag, indicating that copper removal through the EK treatment using iron slag/AC RFM was more effective than iron slag RFM. Significant changes in the surface morphology of RMSs are also observed after treatment with both methods, as evident from the SEM images in **Figures 4.4g to 4.4l**. The presence of copper, nickel and zinc is also apparent in these images, as indicated by the respective colours.

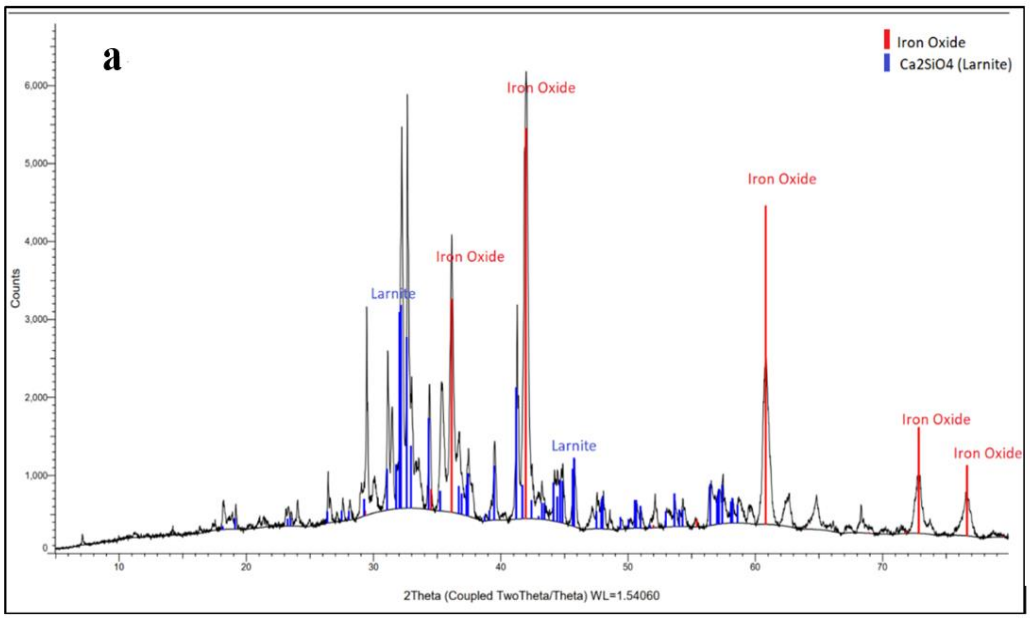

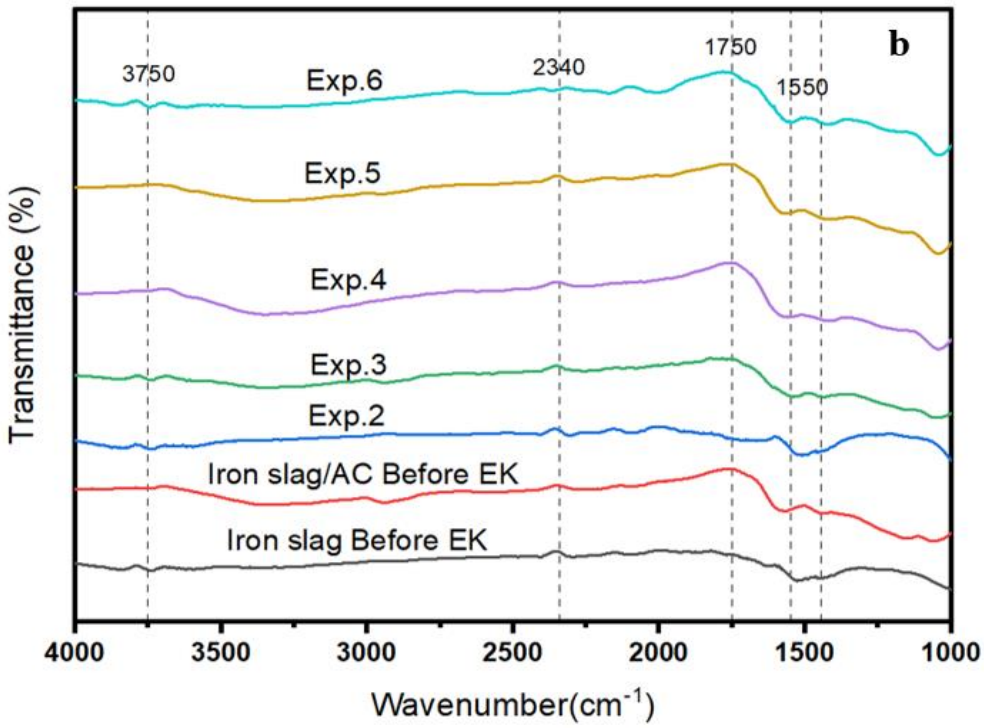
b
3750
2340
1750
1550
Exp.6
Exp.5
Exp.4
Exp.3
Exp.2
Iron slag/AC Before EK
Iron slag Before EK
Transmittance (%)
4000
3500
3000
2500
2000
1500
1000
Wavenumber(cm-1)

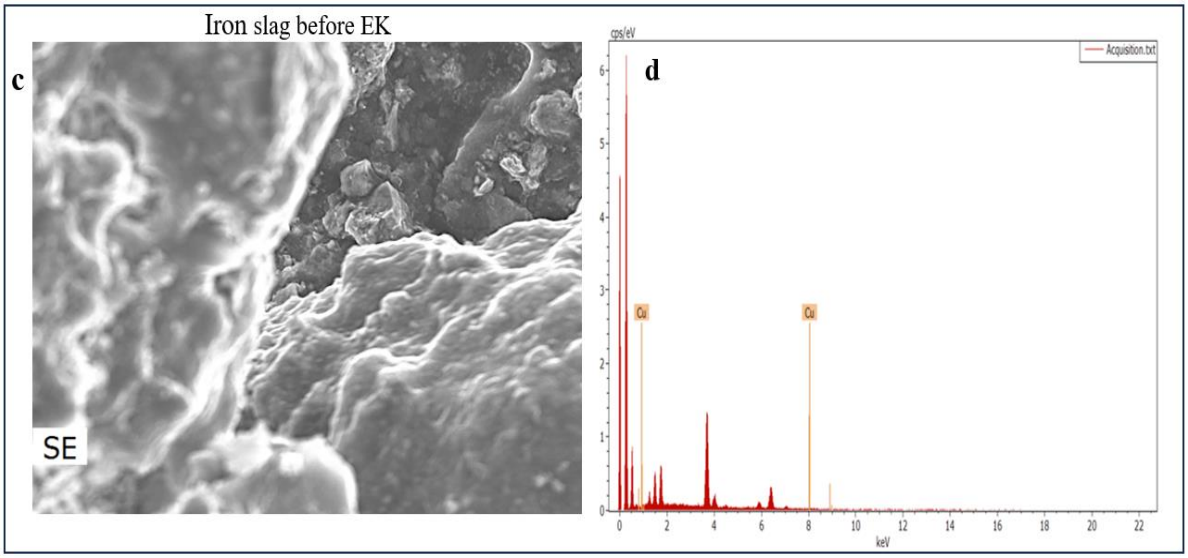
Iron slag before EK
c
SE
d
cps/eV
Acquisition.txt
Cu
Cu
keV

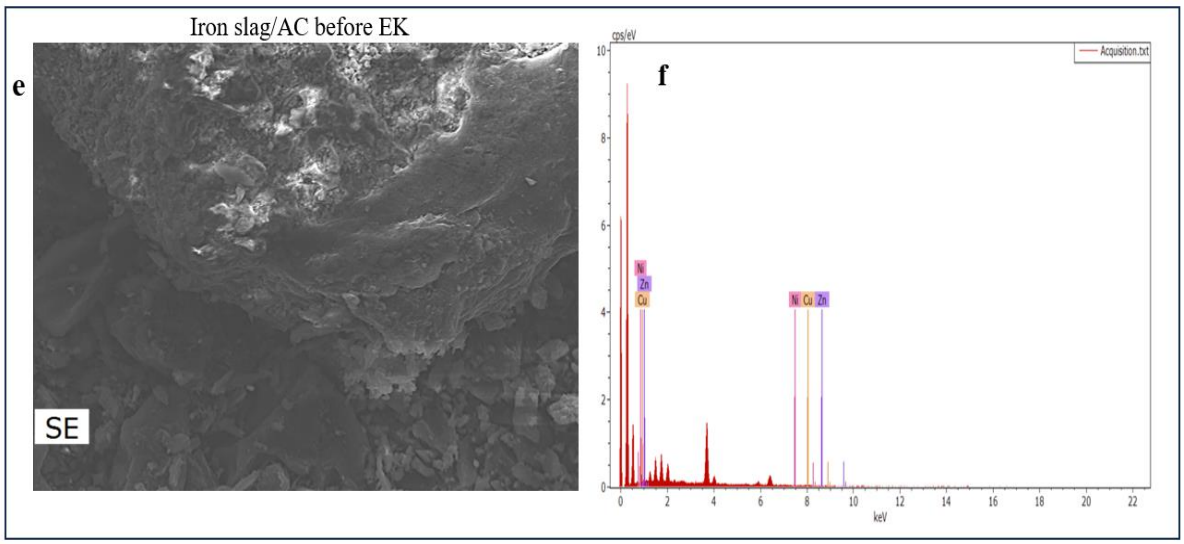
Iron slag/AC before EK
e
SE
f
cps/eV
Acquisition.txt
Ni
Zn
Cu
Ni Cu Zn
keV

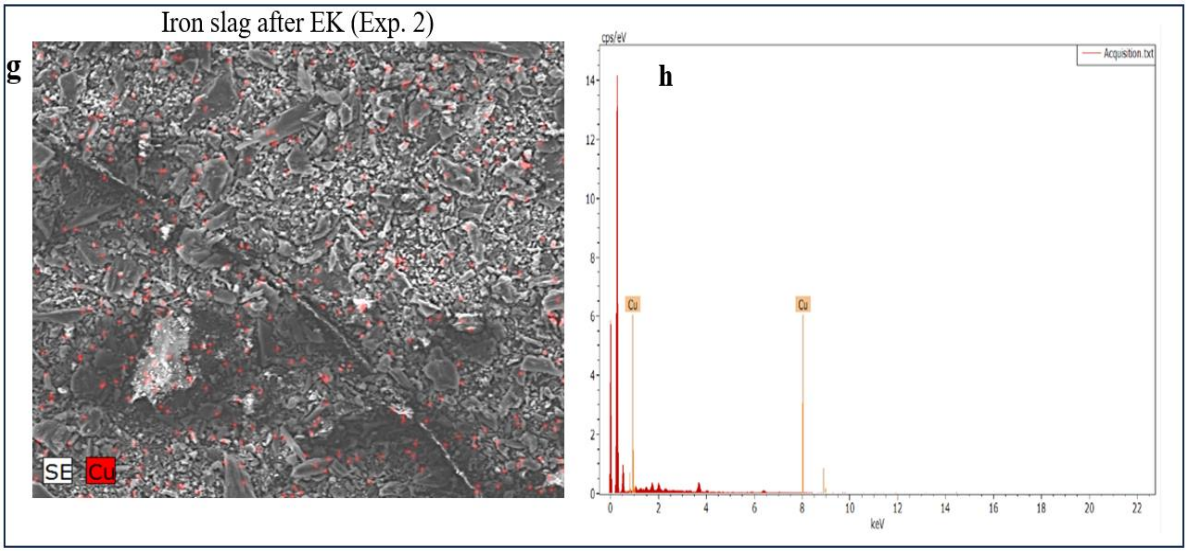
Iron slag after EK (Exp. 2)
g
SE Cu
h
cps/eV
Acquisition.txt
Cu
Cu
keV

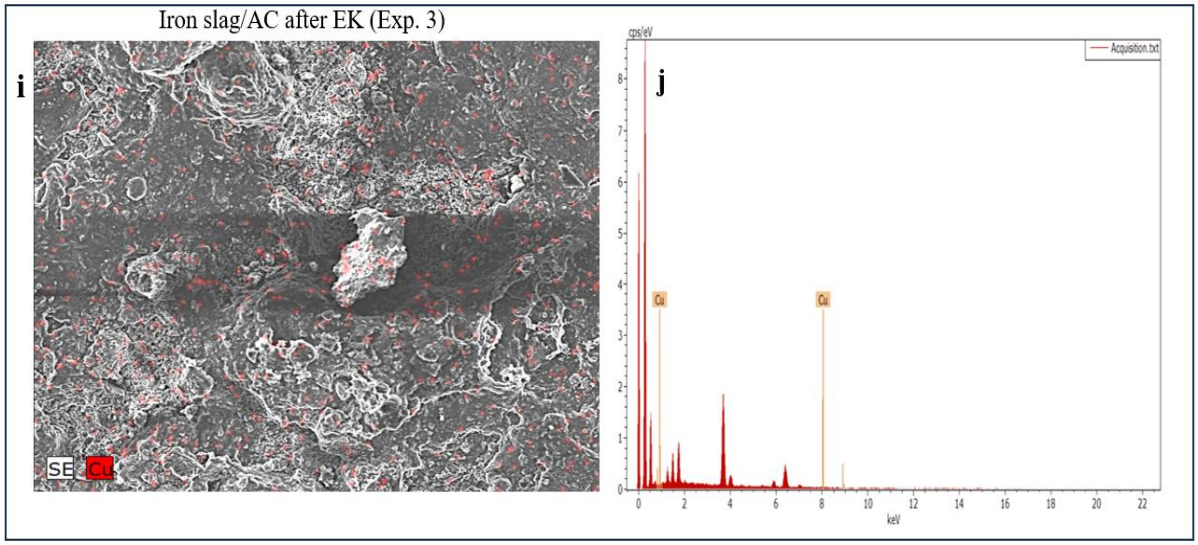

Figure 4.4: (a) the XRD spectrum of iron slag; (b) FTIR bands of iron slag, iron slag/AC before and after EK treatment; (c to l) iron slag, iron slag/AC SEM images with EDS before and after EK treatment.

4.3.5. RFM adsorption/desorption

The outcomes of dynamic adsorption trials utilizing iron slag/AC are portrayed in **Figures 4.5a and 4.5b**. The adsorption dynamics of heavy metals were exhaustively explored, revealing that iron slag achieves its highest adsorption capacity, amounting to 30.79 mg/g

within 90 minutes for copper sulfate. In the case of the mixed solution, the values were 29.16 mg/g for copper sulfate, 13.11 mg/g for nickel chloride, and 11.45 mg/g for zinc sulfate. Initially, the extraction of heavy metals transpires rapidly, signifying a notable adsorption velocity. Nonetheless, as the system nears equilibrium, the adsorption process gradually synchronizes with the desorption rate. The extent of heavy metal assimilation and the pace of adsorption is influenced by diverse factors, including the duration of contact and the specific attributes of the iron slag/AC (Kulal and Badalamoole, 2020; Zhuang et al., 2016).

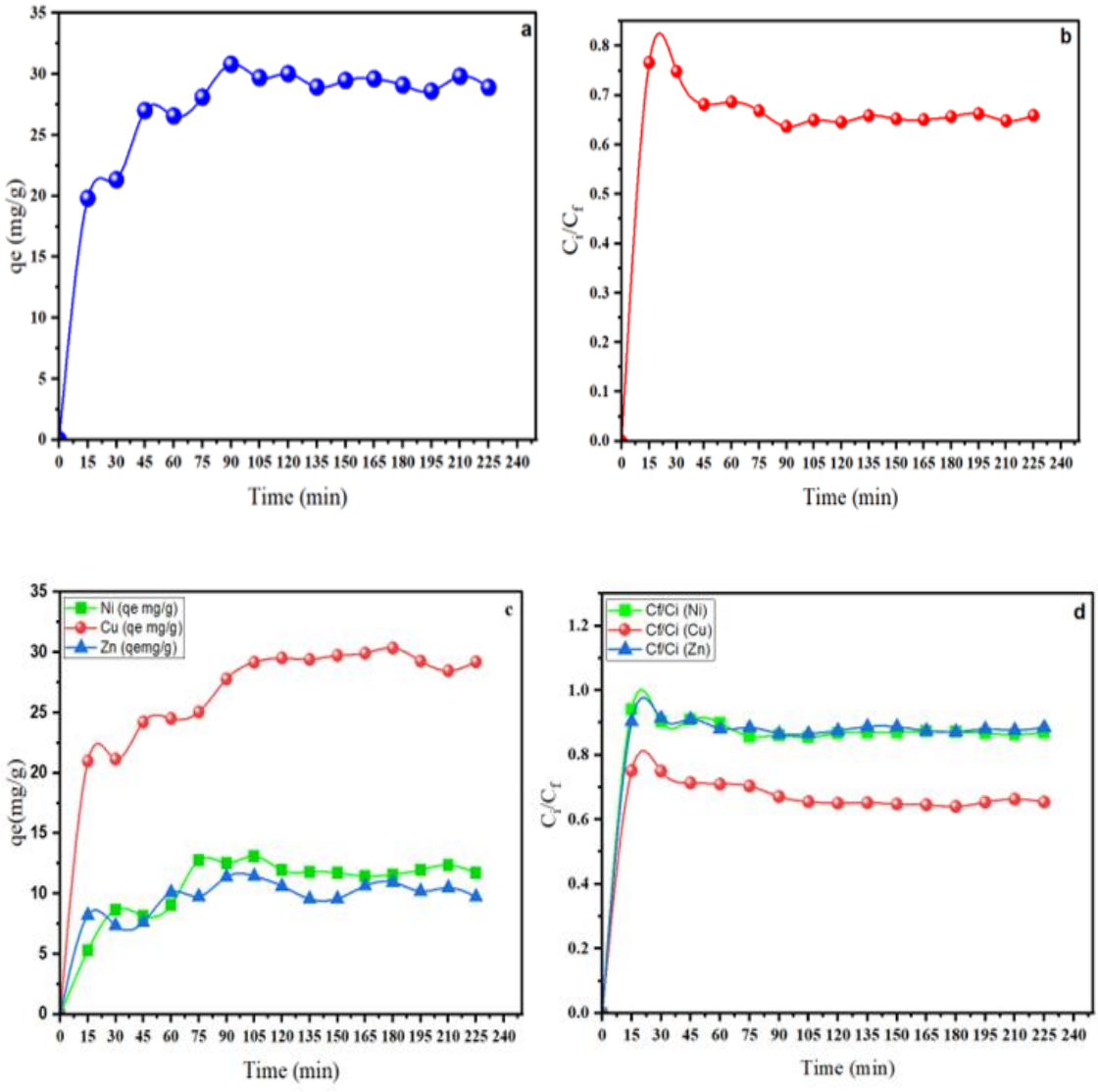

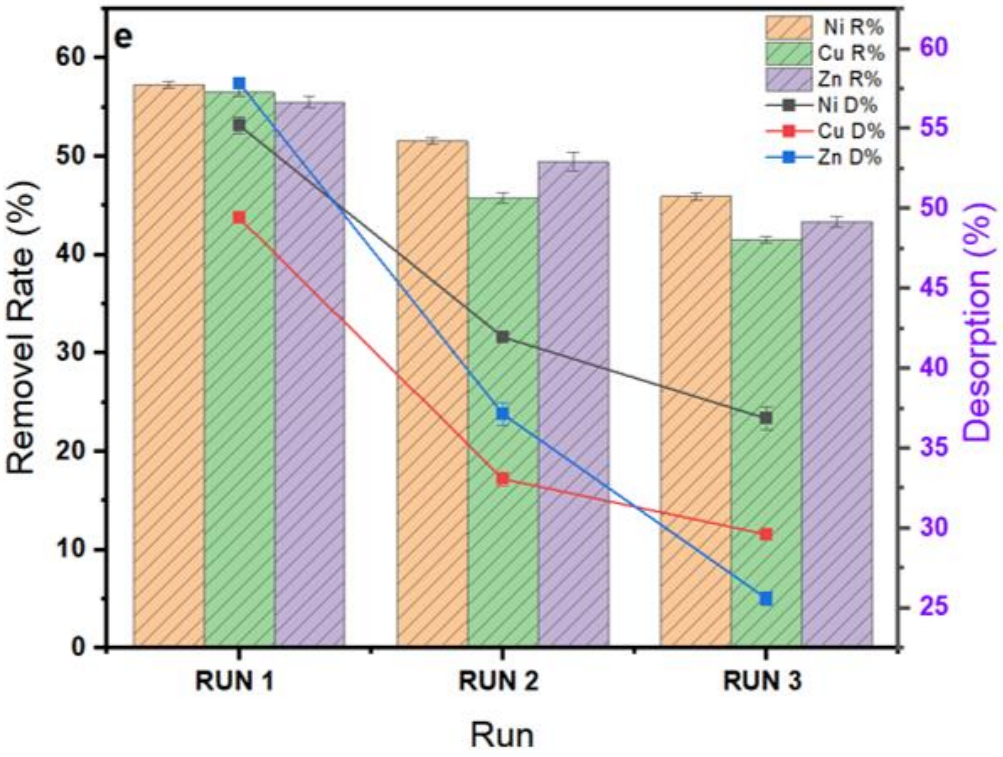

Figure 4.5: Copper and mixed solution adsorption experiments, a) impact of iron slag/AC adsorption of $CuSO_4$ with time, b) The impact of contact time on the adsorption of metal ion (Cu), c) impact of iron slag/AC adsorption of mixed solution (Cu, Ni, Zn) with time, d) The effect of contact time on the adsorption of metal ion (Cu, Ni, Zn), e) Adsorption and desorption of Cu, Ni, and Zn across three successive cycles.

The dynamic adsorption tests using iron slag/AC revealed outcomes in **Figures 4.5c and 4.5d**. Initially, metal ions were quickly removed, indicating strong adsorption. However, as the system approached equilibrium, this removal rate slowed due to the increasing occupation of adsorption sites. The interaction between adsorbate molecules at these sites and those in the bulk phase caused a deceleration. The adsorbate extraction rate from the solution depended on their transition within the adsorbent material, from surface to interior. Equilibrium, where adsorption and desorption rates are balanced, was reached

within 90 minutes for the studied metal ions (Rahchamani et al., 2011; Zhuang et al., 2016). Magnetite nanoparticles are electron contributors due to e^{2+} ions (Castro et al., 2018). The key approaches to extracting ions from water encompass electrostatic adsorption, the interaction of heavy metal ions with metal oxide surfaces, the exchange of metal ions in the solution with hydrogen derived from hydroxyl groups on the adsorbent's surface, and the creation of complexes. Adsorbents containing various chemical groups like carboxyl, hydroxyl, ester, aldehyde, and ketone can connect with metal ions. The strength of this connection depends on factors such as site count, accessibility, chemical structure, and binding nature (Jain et al., 2018).

Three adsorption-desorption cycles were executed with feed concentrations of 2.52 g/L, 2.21 g/L, and 2.51 g/L, each cycle lasting 24 hours to assess the sequential elimination of Cu, Ni, and Zn ions. Across the three cycles, the percentage of copper removal totalled 56.54%, 45.79%, and 41.96% of the initial Cu content. For nickel ions, the corresponding values were 57.3%, 51.54%, and 45.94%; for zinc, they were 55.54%, 49.46%, and 43.37%. Furthermore, the desorption concentrations after the three cycles were 49.42%, 33.09%, and 29.61% for copper, 55.22%, 41.96%, and 36.86% for nickel, and 57.86%, 37.15%, and 25.59% for zinc, as depicted in **Figure 4.5e**. The desorption process of iron slag/AC involves releasing previously held molecules or ions, occurring through mechanisms like diffusion, exchange reactions, solvent effects, and external triggers. Distribution follows concentration gradients, moving adsorbed species from high to low concentrations. Exchange reactions replace less-affine species with those having higher affinity. Solvents alter interactions between iron slag/AC and adsorbed species. External factors, such as variations in temperature, shifts in pH levels, structural adjustments, and the liberation of adsorbed species, can all lead to changes. In an acidic environment,

protons compete with binding sites, weakening interactions and releasing adsorbed metal ions, underscoring the role of solution conditions in desorption.

4.3.6. Specific Energy Consumption

The magnitude of the operating current plays a crucial role in the electrokinetic process, exerting a profound influence on both the power consumption and reaction kinetics involved (Ghobadi et al., 2021b). Instead of increasing the electric current, the experimental time was extended to 21 days to enhance heavy metals removal in experiments Exp5 and Exp6. Elevating electric current enhances heavy metals migration but could lead to electrolyte depletion, soil heating, and surface damage. Alternatively, extending processing time allows for gradual metal dissolution without such risks. Therefore, in the later EK tests Exp5 and Exp6, the experimental time was extended to 21 days to avoid any consequences due to the increased electric current. **Figure 4.6** illustrates the variations in the removal rate of total heavy metals (specifically Cu, Ni, and Zn) concerning the dry soil mass, along with the corresponding specific energy consumption during the whole experiment of the EK-RFM process. These changes are depicted under various experimental conditions and enhancement factors. The study examined the effects of processing time and current intensity to assess the removal rate and energy consumption. These factors were carefully investigated, and their impact is reflected in **Figure 4.6**. Significant removal rates of nickel (Ni), copper (Cu), and zinc (Zn) were observed in all tests that were conducted. The analysis of power consumption indicated a significant rise in specific energy consumption (SEC) within the EK-RFM system when altering the duration of treatment. The specific energy consumption (SEC) is at the high end, elevating from 0.055 kWh/kg to 0.14 kWh/kg for the treated soil. The comparison between Experiment 3 and Experiment 4 revealed that implementing anolyte recycling increased the overall copper removal rate. Significantly, this observed

enhancement in the removal rate was concomitant with a reduction in energy consumption, declining from 0.12 kWh/kg to 0.10 kWh/kg while maintaining a constant current of 20 mA. Experiment 5 exhibited a significant augmentation in energy consumption, reaching a value of 0.14 kWh/kg during the electrokinetic (EK) remediation procedure as the duration of processing was prolonged. Nevertheless, notwithstanding the escalated energy consumption, the overall removal rate remained consistently high, fluctuating between 89.21% and 93.45%.

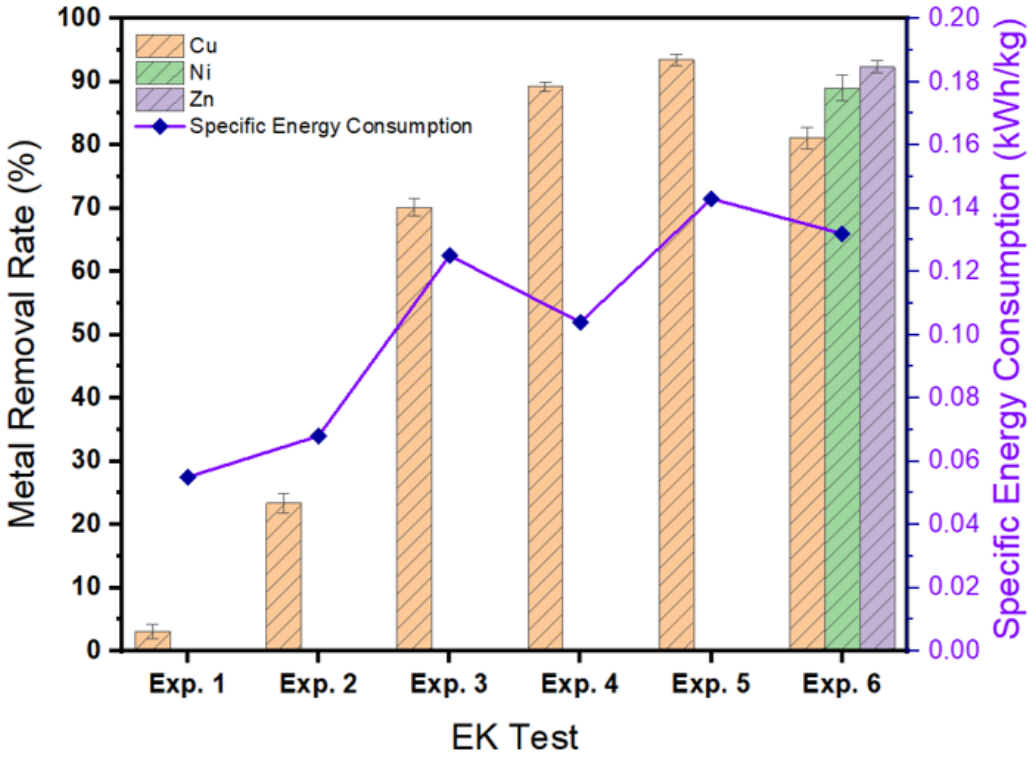

Figure 4.6: Total Cu, Ni, and Zn removal and specific energy consumption during EK.

The findings from the EK tests indicate a noteworthy decrease in power consumption due to the implementation of anolyte recycling. Typically, the incorporation of anolyte recycling within the electrokinetic (EK) process results in a reduction in specific power consumption. The findings from Experiment 6 underscored the importance of the electric current in the electrokinetic process. In the context of handling copper, nickel, and zinc

mixtures, the efficacy of completely removing copper declined from 93.45% to 81.10% due to the necessity to allocate the electric current across the three constituent elements. Previous studies by Ghobadi et al. (2021a and 2020) suggest that increasing the electric current would enhance the copper, nickel, and zinc treatment process.

Although EK tests with RFMs consumed higher energy, they achieved better heavy metals removal than the EK without RFMs. The higher electric conductivity of RFMs, 0.551 ms/cm to 0.643 ms/cm, compared to the kaolinite soil, 0.39 ms/cm, affected the power consumption in the EK process. Undoubtedly, the EK tests without RFMs required less energy to perform than those with the RFMs, but that was at the expense of heavy metal removal. RFM experiments achieved 23.36% to 93.45% copper removal compared to 3.11% in the EK without RFM. The higher energy consumption in experiments Exp5 and Exp6 also stems from extending the experimental time to 3 weeks.

4.4. Conclusion

The EK process was coupled with iron slag or iron slag-AC RFM for a single or a mixture of heavy metals removal from kaolinite soil. Heavy metals removal increased from 3.11% in the EK process to 23.26% in the iron slag-EK process. The alkaline pH of the iron slag promoted metal ions adsorption and precipitation. More significant copper removal was achieved in the EK process coupled with iron slag-AC RFM due to hydroxyl ions adsorption on the AC. Therefore, copper removal reached 70.14% in the EK process with iron slag-AC RFM. In conventional EK processes, enhancement agents are used to improve heavy metals removal, but that would be at the expense of the remediation cost. This study proposed anolyte recirculation to the cathode compartment to neutralize alkaline pH and enhance heavy metals removal. This method will reduce the operation cost, remediation efficiency, and risk of handling acid or alkaline chemicals. Copper removal increased from 70.14% in the RFM-EK process without anolyte recirculation to

89.21% in the RFM-EK with anolyte recirculation. More copper removal was achieved when the RFM-EK process was extended to 3 weeks, recording 93.45% copper removal. Besides, the RFM-EK with anolyte recirculation was evaluated for a mixture of heavy metals removal. Experimental results showed 81.1% copper removal, 89.04 nickel removal, and 92.31% zinc removal after a 3-week test. Heavy metals removal in the latter test corresponded to its solubility; hence, longer experimental time could be required for a greater removal. The RFM-EK with anolyte recirculation should be tested in a pilot plant in the future to demonstrate its field efficiency. Addressing the management of iron slag-AC RFM post-treatment is crucial, given its potential contamination with adsorbed heavy metals and pollutants. Safe disposal methods, such as recycling the slag for industrial applications or encapsulating it in inert materials, need exploration to prevent environmental hazards. Furthermore, future research should prioritize sustainable and eco-friendly strategies for managing waste from electrokinetic remediation processes, ensuring effective remediation while minimizing adverse environmental impacts.

CHAPTER FIVE:

BLACK TEA WASTE/IRON SLAG REACTIVE FILTER MEDIA-ELECTROKINETIC FOR MIXED HEAVY METALS TREATMENT FROM CONTAMINATED SITE

CHAPTER FIVE: BLACK TEA WASTE/IRON SLAG REACTIVE FILTER MEDIA-ELECTROKINETIC FOR MIXED HEAVY METALS TREATMENT FROM CONTAMINATED SITE

The content of this chapter is based on the following publication:

Hamdi, F.M., et al. (2025) "Black tea waste/iron slag reactive filter media-electrokinetic for mixed heavy metals treatment from contaminated site" Journal of Contaminant Hydrology, pp.104517–104517.

5.1. Introduction

The issue of soil contamination has become a significant environmental challenge on a global scale, presenting significant challenges for scientists and researchers. The rise of various pollutants, including organic and inorganic compounds, as well as heavy metals, is closely linked to industrial advancements (Cui et al., 2024; Hamdi et al., 2025, 2024; Zheng et al., 2024). Consequently, contamination of both groundwater and soil has become a serious issue. Despite remarkable progress in human life in recent years, rapid industrial expansion poses a significant threat to ecosystems, particularly through direct contamination of soil and groundwater. These contaminants are often carelessly disposed of into the environment, accumulating to concentrations that exceed international permissible limits (Acosta Hernández et al., 2024; Zheng et al., 2024). A variety of techniques are utilized for remediating contaminated sites, both in-situ and ex-situ (Hamdi et al., 2025; Yang et al., 2020). Importantly, the concentration and nature of the pollutant play crucial roles in selecting appropriate treatment techniques, along with the economic feasibility of such technologies (Cui et al., 2024; Wen et al., 2021). Among treatment techniques, the electrokinetic method stands out for its simplicity, cost-effectiveness, and high efficacy in removing pollutants. This method also boasts reduced

time requirements and lower voltage usage across cathode and anode electrodes (Cui et al., 2024; Ghobadi et al., 2021a).

In the last decade, contaminated sites have emerged as a prominent environmental concern, prompting heightened interest in technologies capable of removing environmental pollutants from soil. Among these techniques, reactive filter media (RFM) and electrokinetic (EK) remediation have garnered considerable interest for their eco-friendliness, adaptability, practicality, scalability, and cost-efficiency (Hamdi et al., 2024). Various techniques exist for addressing soil contamination stemming from activities such as oil extraction, petroleum mining, industrial chemical production, and agriculture practices. RFM and electrokinetic processes represent two such remediation approaches. In the RFM system, adsorption, precipitation, and degradation processes occur depending on the characteristics of the reactive material and the specific pollutants being addressed (Ganbat et al., 2023; Zheng et al., 2024). Various adsorbent materials, such as activated carbon, zero-valent iron, and atomizing slag, can be employed in the RFM. Among these, zero-valent iron is the predominant reactive substance because of its affordability (Cang et al., 2009b). Cang et al. (2009) explored the utilization of zero-valent iron (ZVI) as a reactive filter material (RFM) in conjunction with electrokinetic (EK) remediation to treat soil contaminated with chromium (Cr). Their findings revealed that the combined ZVI-RFM and electrochemical remediation approach achieved a maximum Cr removal efficiency of 72%. Additionally, the introduction of ZVI in the EK system led to a decrease in Cr present in both the anolyte and catholyte. In a study by Yuan and Chiang (2007), the feasibility of integrating EK with RFM for extracting arsenic (As) from contaminated soil was investigated. The RFM in their study comprised FeOOH and ZVI. Results demonstrated that the incorporation of RFM into the EK system enhanced As removal efficiency by 60–120% (Yuan and Chiang, 2007a). Yuan et al.

(2009) conducted further research on the EK-RFM system's efficacy in removing As from contaminated soil, employing a cobalt-coated carbon nanotube (CNT-Co) reactive barrier as the RFM. The experimental results revealed that the CNT-Co-based RFM, combined with EK remediation, successfully achieved As removal rates of 35% to 62% (Yuan and Chiang, 2007a).

To address these challenges, recent advancements have focused on integrating electrokinetic geosynthetics (EKG) and smart DC power sources into EK systems. EKG materials serve as multifunctional electrodes, enhancing contaminant removal while improving soil consolidation. Furthermore, the adoption of smart DC power sources allows for dynamic control of voltage and polarity, optimizing ion transport and reducing energy costs (Behrouzinia et al., 2022; Zhuang, 2021). In one study conducted by Behrouzinia et al. in 2022, this study will explore the use of electrokinetic geosynthetics (EKG) to enhance the consolidation of kaolinite and remove copper (Cu) contaminants. The results indicate that EKG accelerates the soil consolidation process and improves copper removal efficiency, achieving up to 97% removal. In a 2024 study by Cui et al., the research team achieved notable success in removing copper and zinc from contaminated environments using electrokinetic remediation with a sulfonic acid exchange resin (EKR-SER). The study reported total recovery rates of 95.47% for copper and 97.01% for zinc, significantly outperforming traditional electrokinetic remediation methods. The sulfonic acid exchange resin was instrumental in this process, as it effectively prevented metal precipitation and enhanced the overall metal removal efficiency in the EKR system (Cui et al., 2024). In two separate studies by Gobadi et al. (2021), the use of compost as RFM combined with EK treatment was assessed for its effectiveness in removing copper contamination from kaolinite soil and heavy metal mixtures from naturally contaminated soil. For kaolin soil, copper removal was

significantly higher, reaching 84.09%, primarily due to the RFM's capacity to buffer pH and facilitate the solubilization of copper ions. However, the natural soil presented greater challenges, particularly with metals like lead (Pb) and copper (Cu), which formed strong organic bonds, leading to lower removal rates of 28.2% and 29.1%, respectively. In contrast, metals such as zinc (Zn), cadmium (Cd), and manganese (Mn) were removed more effectively, with rates ranging from 51.6% to 72.1%. These differences highlight the added complexity of treating natural soils, where organic-metal interactions hinder the heavy metal extraction efficiency compared to kaolinite soil.

Recently, the performance of the EK process has seen significant enhancements through integration with recyclable waste RFMs, such as iron slag or its combination with activated carbon. Notably, iron slag with activated carbon has demonstrated superior efficiency in buffering soil pH compared to other RFMs, such as nano zero-valent iron (nZVI), biochar, and a mixture of biochar and compost. The high alkalinity of iron slag, with a pH of 11, facilitates the formation of metal precipitates when absorbed by the RFM. In a study by Hamdi et al. (2024), the EK process achieved impressive copper removal rates, reaching up to 93.45% with anolyte recirculation. Moreover, when tackling heavy metal mixtures in soil, substantial removal rates were observed, including 92.30% for zinc, 89% for nickel, and 81.10% for copper. These findings underscore the potential of EK-RFM systems, particularly those utilizing iron slag/activated carbon, to mitigate heavy metal contamination in soil effectively. Practically, iron slag is an industrial byproduct and, hence, more cost-effective than nZVI as an RFM.

This study aims to enhance heavy metal removal from contaminated soil using environmentally friendly and recyclable composite RFM. Black tea waste was selected as an effective heavy metals chelating agent when mixed with granules and powder iron

slag of alkaline pH to form superabsorbent material to sequester heavy metals in the EK process. Besides, the slightly acidic pH of tea waste (circa pH 5.5) was essential to prevent the rapid progression of the alkaline front developed at the cathode. To date, there is no study examining the use of iron slag coupled with black tea waste in the EK process. Granules and powder iron slag have different physicochemical properties, affecting their effectiveness for heavy metal adsorption. Cu^{2+}, Ni^{2+}, and Zn^{2+} were selected as the target pollutant due to their widespread presence in soil environments. One of the primary objectives of the study is to compare powder iron slag with granular iron slag coupled with black tea waste as a novel and recyclable RFM. Also, in this study, an innovative strategy is being developed to optimize the EK process for removing one element or mixing elements from kaolinite soil and heavy metal pollutants from natural soil. Kaolinite is being used as a representative soil model to analyze how experimental variables affect the effectiveness of the EK method. However, it is crucial to acknowledge that while kaolinite is a valuable model, it only partially represents the complete spectrum of complexities in actual soils. Natural soils possess a significantly higher level of intricacy than kaolinite, indicating that the efficiency observed in experiments may only partially mirror the real-world effectiveness of the EK process in natural soils. The findings of this research will offer insights into the most effective RFMs for heavy metal removal from soil through EKR technology.

5.2. Materials and methods

5.2.1. Preparation of samples and methods for analysis

Chapter 3 provides a detailed account of the materials, soil preparation methods, and apparatus used in the EK experiments. Kaolin soil is known for its high purity and low levels of organic and heavy metal pollutants. In contrast, natural soil samples from the sub-surface at a depth of 15 to 20 cm were obtained. Granular iron slag was provided by

the local steel manufacturing industry (Sydney, Australia). The reactive filter material (RFM) consisted of a mixture of granular or powder iron slag combined with black tea waste. The PIS/BTW and GIS/BTW RFMs were prepared as follows: black tea water was collected from used tea bags and dried in the oven at 90 ^{o}C for 1 hour. Then, the dried black team was pulverized using a granite mortar and pestle and mixed with either GIS or PIS. The mixture was put in a plastic container and shaken at 150 rpm for 2 hours. The chemical and physical properties of RFM are listed in **Table 5.1**. In contrast, **Tables 3.1 and 3.2** in (**Chapter 3**) provide a comprehensive overview of the characteristics of the kaolin soil and the natural soil used in the EK experiments.

During the filling process, a hand tamper was employed to compress the polluted soil in stages, guaranteeing the absence of any empty spaces. An investigation of the reactive filter media (RFMs) was conducted utilizing Energy Dispersive X-ray (EDX) analysis to evaluate its morphological and chemical features. The surface functional groups of the RFMs were analyzed using Fourier Transform Infrared Spectroscopy (FTIR), model Miracle-10 instrument (Shimadzu) before and after the EK process. In order to ascertain the surface area of the RFMs, Brunauer-Emmett-Teller (BET) nitrogen adsorption-desorption isotherm measurements were conducted both before and after the electrokinetic (EK) treatment. In addition, the Barrett-Joyner-Halenda (BJH) approach was employed for the examination of post-electrokinetic (EK) treatment. The Micromeritics 3-FlexTM surface characterization analyzer was used to perform the measurements at a temperature of 77K.

Table 5.1: Various physicochemical properties of RFM.

Parameter	**PIS**	**GIS**	**BTW**	**PIS/BTW**	**GIS/BTW**

Particle size analysis					
(%)	1.22	14.70	19.31	7.89	16.33
Greater than 2 mm	22.52	81.79	51.10	34.23	67.19
In between 1-2 mm	76.26	3.51	29.59	57.88	16.48
Less than 1mm					
Permeability (m/s)	1.67×10^{-3}	2.45×10^{-2}	8.33×10^{-4}	1.35×10^{-3}	4.81×10^{-2}
Density (g/cm^3)	2.45	2.21	0.2	0.37	0.366
Surface area (m^2/g)	0.493	0.037	0.129	0.311	0.083
TDS (mg/L)	461.5	981.9	394.5	387.5	417.6
pH	11.38 ± 0.02	11.13 ± 0.03	5.5 ± 0.02	10.37 ± 0.03	8.86 ± 0.03
EC (mS/cm)	0.643 ± 0.02	0.359 ± 0.01	0.654 ± 0.03	0.476 ± 0.02	0.441 ± 0.02

[PIS - powder iron slag; GIS - granular iron slag; BTW - black tea waste; TDS - total dissolved solids; EC - electrical conductivity]

5.2.2. EK cell experimental setup

The experimental setup involved constructing a reactor made of plexiglass with dimensions of (23L x 8W x 11H) cm, designed for optical monitoring and featuring compartments for electrodes at both ends, along with a central compartment for the contaminated soil. An EAPS-3015-11B power supply was utilized to deliver electric current via graphite rod electrodes (15 cm x 1 cm) positioned at both ends of the reactor. Cellulose filter sheets (pore size 5-13 μm, LLG Labware) were placed between the electrode compartments and the soil to prevent soil particles from entering the electrolyte. The moisture content of the soil was 100% in all experiments. A perforated plexiglass plate was used to provide support for the filter sheets. The Reactive Filter Media (RFM) was positioned near the cathode compartment within the soil. Throughout the experiment, (Milli-Q water) was periodically introduced into the anolyte compartment to counterbalance water depletion caused by electrolysis and electroosmotic flow. Continuous monitoring was conducted with hourly current measurements using a Keithley 175 auto-ranging multimeter. **Figure 3.1** illustrates a detailed schematic of the experimental setup for electrokinetic (EK) experiments conducted in this study.

5.2.3. Test design

The EK studies investigated the extraction of an individual pollutant (Cu) and combined heavy metals (Cu, Ni, and Zn) from contaminated kaolinite soil and naturally contaminated soil. Each trial aimed to evaluate the efficiency of electrokinetic remediation under varying conditions and different metal mixtures. The first five experiments focused on copper recovery, comparing the EK process efficiency with and without RFM and evaluating the feasibility of reusing the RFM in the EK process. These trials also evaluated the performance differences between granular iron slag/black tea waste (GIS/BTW) and powder iron slag/black tea waste (PIS/BTW). Experiment six expanded the scope to target the removal of a mixture of Cu^{2+}, Ni^{2+}, and Zn^{2+} pollutants from kaolin soil using EK with PIS/BTW as RFM. In the seventh experiment, heavy metals contaminated natural soil were treated in the EK with PIS/BTW (**Table 5.2)**. Based on the previous EK studies (Hamdi et al., 2024; Ghobadi et al., 2021a), the applied electric current was 20 mA in experiment Exp1, equivalent to 0.25 mA/cm^2 current density. However, due to unsatisfactory heavy metal removal in Exp1, the electric current was increased to 25 mA in experiments Exp2 through Exp7 employed, or equivalent to 0.3125 mA/cm^2 current density. The duration for experiments Exp2 to Exp5 was set at 21 days, while Experiments Exp6 and Exp7 were extended to 28 days and 35 days, respectively, to allow adequate removal time of the heavy metals mixture. The tests were conducted with an initial concentration of 1000 mg kg^{-1} for Cu^{2+}, Ni^{2+}, and Zn^{2+}, 120 to 130 g of RFM positioned near the cathode. Experiment Exp1 was a baseline electrokinetic test using kaolinite, with 1000 mg/kg of Cu^{2+} introduced and a 20 mA electric current. Experiments Exp2 and Exp3 were conducted to compare the effects of granular versus powder iron slag, when mixed with black tea waste as RFM, on the removal of Cu^{2+} from kaolinite soils. Experiments Exp4 and Exp5 evaluated the performance of recycled

granulated and powder iron slag mixed with black tea waste as RFM in the removal of Cu^{2+} from kaolinite. Briefly, the used RFM was extracted from the soil at the end of the EK process for heavy metals desorption, as explained in section 2.4. Then, the desorbed RFM was rinsed with DI water and repacked in the EK cell. New RFM materials were added to the reused one to compensate for the small RFM amount taken for EDX and FTIR analysis. Experiments Exp6 involved a powder iron slag/black tea waste (PIS/BTW) RFM-EK process conducted over 28 days to assess the effectiveness of removing Cu^{2+}, Ni^{2+}, and Zn^{2+} from kaolinite. Finally, Experiment Exp7 utilized an RFM-EK process with PIS/BTW, conducted over 35 days to assess the efficiency of Cu^{2+}, Ni^{2+}, and Zn^{2+} mixture removal from natural soil. After finishing the trials, the liquid samples were gathered from the anode, cathode and electrode assemblies for analysis. The kaolin soil was partitioned into six equidistant portions, each after that placed within a designated plastic bag. Subsequently, every portion was uniformly mixed before being sampled for metal ion analysis. The pH, conductivity, and concentrations of Cu^{2+}, Ni^{2+}, and Zn^{2+} in each soil sample were measured in triplicate.

Table 5.2: Shows the conditions under which the different EK tests.

Exp	Type of soil	Type of experiment	Metals	RFM	Metal concent. (mg/kg)	Electrical current (mA)	Time (day)
Exp1	Kaolin Soil	EK only	Cu	N/A	1000	20	14
Exp2	Kaolin Soil	EK- (50% GIS + 50% BTW)	Cu	Granular iron slag + black tea waste	1000	25	21
Exp3	Kaolin Soil	EK- (50% PIS + 50%BTW)	Cu	Powder iron slag + black tea waste	1000	25	21
Exp4	Kaolin Soil	EK- RC (50% PIS + 50%BTW)	Cu	Recycled powder iron slag + black tea waste	1000	25	21

Exp5	Kaolin Soil	EK- RC (50% GIS + 50% BTW)	Cu	Recycled granular iron slag + black tea waste	1000	25	21
Exp6	Kaolin Soil	EK- (50% PIS + 50%BTW)	Cu, Ni, and Zn	Powder iron slag + black tea waste	1000	25	28
Exp7	Real Soil	EK- (50% PIS + 50%BTW)	Cu, Ni, and Zn	Powder iron slag + black tea waste	430, 325, and 652	25	35

[EK – electrokinetic; PIS - powder iron slag; GIS - granular iron slag; BTW - black tea waste; RC – recycled]

5.3. Results and discussion

5.3.1. Electric current

The applied electric current during the EK process plays a crucial role in the migration of pollutants through the soil and is directly related to the concentration of free ions (Hamdi et al., 2024). As such, one of the key variables that directly affects how well contaminants migrate through the soil is the electric current (Hamdi et al., 2024; Hawal et al., 2023). In the EK experiments, the current was 20 mA for experiment Exp1 and 25 mA for experiments Exp2 to Exp7. **Figure 5.1a** depicts the decrease of electric current across experiments Exp1 to Exp7 in the Ek study. Water electrolysis generates H^+ ions at the anode and OH^- ions at the cathode. The electric current intensifies as the ions migrate toward the electrode with an opposing charge (Fardin et al., 2021; Zheng et al., 2024). The dissolution of metal ions is caused by the acid front advancing toward the cathode, which leads to an increase in the ionic strength of the pore fluid. However, the presence of ionic species gradually diminishes over time as a result of the acid and base neutralization that occurs when they come into contact and the precipitation of metal ions (Ganbat et al., 2023; Hamdi et al., 2024).

The EK electric current diminishes with time as a result of the deposition of metal ions near the cathode region in soil with an alkaline pH. Possible causes for the reduction in electric current include the formation of metal hydroxide precipitates, the accumulation

of deposits on the electrodes, or the convergence of acid and hydroxide ions near the cathode. There was a decrease in experiments Exp1 to Exp5 electric current after 48 hours, while in experiments Exp6 and Exp7, there was a decrease after 120 hours. Experiment Exp1 served as a baseline to investigate the EK process without the inclusion of any RFM. The initial electrical current was set at 20 mA and remained unchanged for the first 24 hours, then significantly decreased as time progressed and recorded a 2 mA after 336 hr. The results indicated reduced ion migration and metal hydroxide precipitation in the soil, demonstrating the limited efficiency of the EK process without RFMs to facilitate ion movement. Experiment Exp2 aimed to study the effect of GIS/BTW RFM on copper removal at 25 mA. The electrical current gradually decreased during the first 24 hours until it reached 13.5 mA after 144 hours and then stabilized throughout the EK treatment. Experiment Exp3 was performed using the PIS/BTW RFM in an EK process for Cu^{2+} removal. The initial current was set at 25 mA, remained constant during the first two days of treatment, gradually decreased and reached 12 mA after 190 h, then stabilized to the end of the EK process. GIS/BTW and PIS/BTW RFMs maintained a higher electric current compared to the control experiment Exp1 as a result of slowing down the movement of the alkaline front in the soil and facilitating ions movement.

Experiment Exp4 evaluated the performance of reusing the RFM from experiment Exp3, which is the PIS/BTW recovered after the Cu^{2+} acid extraction at the conclusion of the EK process. The current remained stable for 72 hours, dropped to 14 mA after 168 hours, and then gradually reduced until it reached 11.5 mA by the end of the test. The recycled PIS/BTW RFM resulted in an initial peak current slightly lower than experiment Exp3, probably due to the slight difference in the functional groups and characteristics of the recycled PIS/BTW RFM (Section 3.4). Experiment Exp5 investigated the performance

of recycled GIS/BTW RFM for Cu^{2+} removal by the EK process. Although the experiment was performed under the same conditions as experiment Exp4, the electrical current was initially slightly less than 25 mA, dropped to 14 mA after 168 hours, and reached 12.5 mA by the conclusion of the EK process.

Experiment Exp6 was carried out over four weeks to assess the EK effectiveness in remediating kaolinite polluted with a mixture of Cu^{2+}, Ni^{2+}, and Zn^{2+}. An electric current of 25 mA continued for 144 hours owing to the elevated ionic strength in the natural soil. After 144 hours, the electrical current exhibited a progressive decline, ultimately reaching 9.5 mA. Subsequently, the current continued to fall, recording 7.8 mA at the conclusion of the test. Compared to previous experiments, the steep decrease in electric current at the conclusion of the experiment Exp6 was attributed to the precipitation of metal ions of various solubilities near the cathode chamber. The deposition of Cu^{2+}, Ni^{2+}, and Zn^{2+} ions at varying pH levels resulted in an elevation of soil resistivity, leading to a greater reduction in the electric current seen in experiment Exp6 compared to other experiments. Experiment Exp7 was conducted for five weeks to assess the efficacy of the EK process in treating natural soil polluted with Cu^{2+}, Ni^{2+}, and Zn^{2+}ions. The 25 mA current lasted for 192 hours because of the higher ionic strength in natural soil compared to all previous experiments. After 192 hours, the electric current showed a gradual decrease, reaching 7.80 mA at 432 hours, and recorded 7.5 mA at the conclusion of the experiment after 550 hours. Similarly to experiment Exp6, the electric current at the conclusion of experiment Exp7 was lower than in other tests attributed to differential precipitation of various metal ions in the natural soil.

Figure 5.1b shows a clear inverse relationship between electric current and change in voltage. The accumulation of metal ions reduced the electric current, leading to an increase in voltage as a result of the higher resistivity of the soil. During the initial 24

hours of all EK tests, the voltage fell due to the solubilization of metal ions, which led to an increase in the ionic strength of the pore fluid. The initial voltage ranged from 12.5 to 26.8 V and, after that, fell to approximately 7.8 V after 24 hours. In tests Exp1, Exp4, and Exp5, the voltage rose to around 35 V after 48 hours. Similarly, in experiments Exp2 and Exp3, the voltage increased after 72 hours, while in experiments Exp6 and Exp7, the voltage increased after 144 hours because of the elevated soil ionic strength and conductivity. The control experiment Exp.1 showed a lower electric current (5-6 mA) than other experiments with the RFMs, highlighting the limitations of the EK process without RFMs. Both new and recycled RFMs (granular and powder) showed a better performance than experiment Exp1, demonstrating their effectiveness in enhancing the EK process and their prospect for sustainable and cost-effective use.

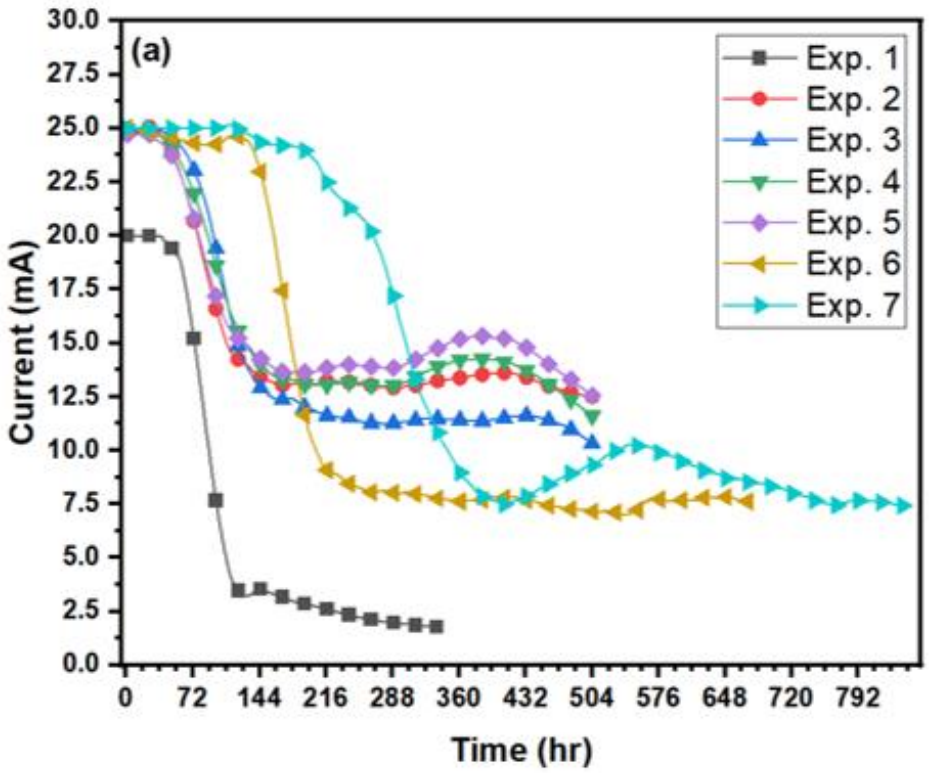

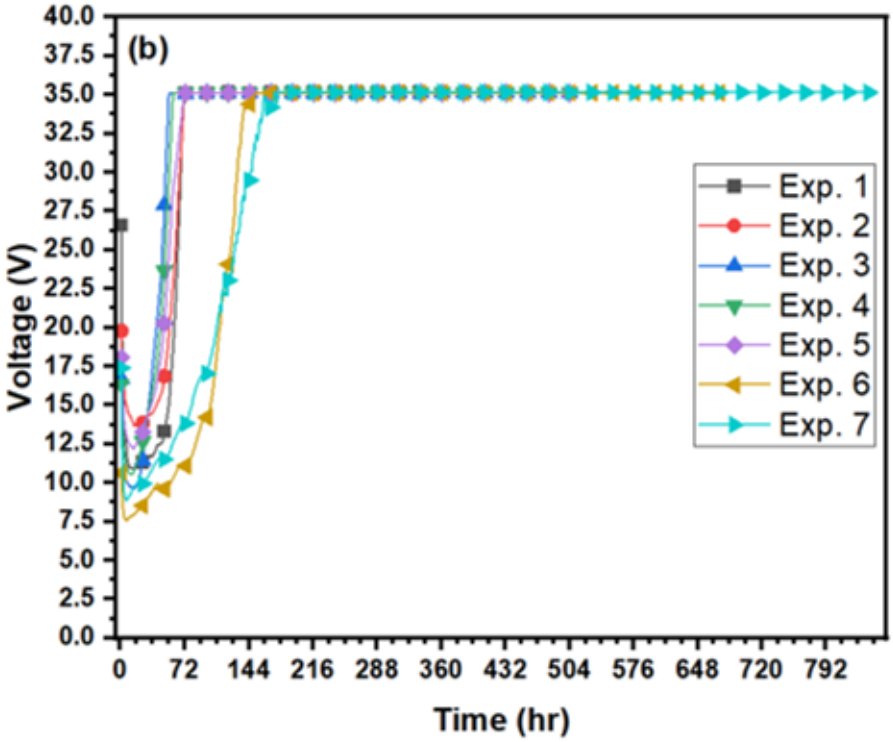

Figure 5.1: (a) The electrokinetic tests' current change (mA) and (b) the voltage change (V). A direct current of 25 mA was used for the experiments.

5.3.2. pH and electrical conductivity of soil

The pH and electric conductivity of the soil were measured at the conclusion of the (EK) experiments. The soil pH refers to the level of acidity or alkalinity in the soil, while the electric conductivity measures the soil's capacity to conduct electrical current. The pH values of soil sections S1 through S7, as well as the RFMs in Exp2 through Exp7, are shown in **Figure 3a**. The following reactions illustrate the main electrochemical processes that occur at the anode and cathode, producing H^+ and OH^- ions, respectively:

$$2H_2O - 4e^- \Rightarrow O_2 + 4H^+ \quad (5.1)$$

$$4H_2O + 4e^- \Rightarrow 2H_2 + 4OH^- \quad (5.2)$$

As per Equation (5.1), the electrolytic reaction occurring at the anode produces H^+ ions that move toward the cathode, causing a drop in soil pH. In contrast, the high pH level observed at the cathode is a consequence of the production of OH^- and their subsequent movement towards the anode area, as explained by Equation (5.2). The ionic mobility of H^+ ions is roughly 1.8-fold greater than that of OH^- ions, suggesting that H^+ ions can move and displace more easily within the soil than OH^- ions (Hamdi et al., 2024).

The soil's initial pH was approximately 4.45. In all experiments, the soil pH dropped below this initial value of 4.45 in sections S1 to S6, except for section S6 in Experiment Exp1. The soil pH in section S6 increased to near pH 6.5 in experiment Exp1 due to the progression of the alkaline front in the soil. In contrast, in experiment Exp2 to Exp7, the pH in section S6 was slightly below the initial soil pH (**Figure 5.2a**). In experiments Exp3 and Exp5, the soil pH in section S1 was around 2.5, but showed a little increase in sections S2 and S3 and reached a pH of 3 in section S4. In comparison to experiment Exp1, the addition of PIS/BTW and GIS/BTW RFMs mitigated the soil pH near the cathode by impeding alkaline front progression to the anode. Consequently, the acid front moved across the soil sections to the cathode region.

In these experiments, a combination of 50%-50% PIS and BTW was used as the RFM for Exp3, Exp4, Exp6, and Exp7, whereas experiments Exp2 and Exp5 utilized a 50%-50% GIS and BTW RFM. Both RFMs were positioned adjacent to the cathode within the RFM. The duration of experiments varied: Exp2 through Exp5 were conducted for three weeks, Exp6 was extended to four weeks, and Exp7, focused on remediating natural soil, spanned over five weeks. In experiments Exp2 and Exp5, the soil pH gradually rose from approximately 2.8 in section S1 to around 3.5 in sections S5 to S6 (**Figure 5.2a**). In experiment Exp3, the pH gradually increased from section S1 to section S3, reaching pH 3.25, after which it remained constant from sections S4 to S6. Unlike the later tests, the

soil pH in experiment Exp6 remained relatively stable at around pH 3 in sections S1 to S5. This stability resulted from the acid front moving quickly through the soil. However, in section S6, the soil pH increased, reaching a pH of 3.60. Overall, the soil pH was reduced below its initial level, leading to a positive charge on the soil surface, which in turn decreased the adsorption of metal ions.

Figure 5.2b illustrates the electrical conductivity (EC) for all EK experiments. In experiments Exp1-Exp6, the soil's EC in sections S1-S2 exceeded the initial EC of kaolinite soil. This increase can be attributed to the elevated ionic strength of the pore fluid, which is a result of the solubilization of metal ions by the advancing acid front in sections S1 through S2 in Exp1 through Exp6. Conversely, the EC in sections S3 to S6 gradually declined due to the precipitation or migration of metal ions toward the cathode region. In experiment Exp7, which utilized natural soil, a decrease in electrical conductivity was observed across all soil sections, with values falling below the initial EC of the natural soil (**Table 3.1**). This decline is attributed to the migration and precipitation of the soil's ionic species toward the cathode. Similarly, in all tests, the EC in sections S4 through S6 remained lower than the initial soil EC due to the precipitation of ions near the cathode region.

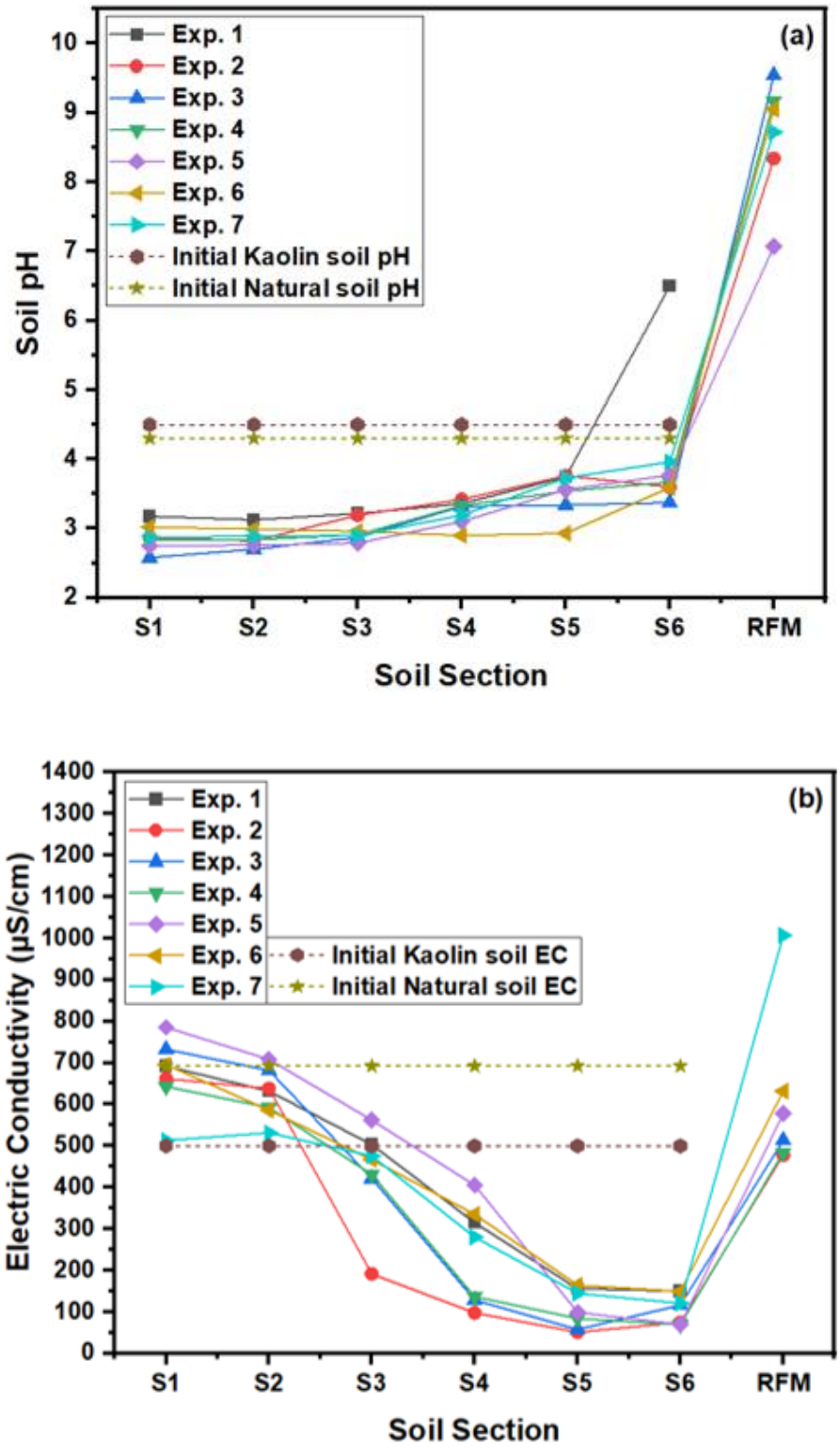

Figure 5.2: Soil pH and electrical conductivity were assessed after the electrokinetic tests.

5.3.3. Heavy metal removal rate

Seven EK investigations were carried out to assess the removal of single (Cu^{2+}) and mixtures of heavy metals (Cu^{2+}, Ni^{2+}, and Zn^{2+}) from polluted kaolinite and natural soil (**Table 5.2**). Experiment Exp1 spanned 2 weeks, while Exp2 through Exp5 extended to 3 weeks, and Exp6 and Exp7 lasted 4 and 5 weeks, respectively. These latter trials specifically target the remediation of heavy metals mixture from kaolinite and natural soils. Positioning the RFM near the cathode chamber is to capture heavy metals, Cu^{2+}, Ni^{2+}, and Zn^{2+}, which are expected to migrate toward the cathode and facilitate their adsorption and removal from the soil. By doing so, the RFM serves as an effective medium to accumulate and extract heavy metals, improving the overall efficiency of the EK experiment and making it easier to recover these pollutants at the conclusion of the treatment (Hamdi et al., 2024).

Metal ions migrated through the soil from the anode, accumulating in areas near the cathode based on their solubility factor. This movement occurred after they were dissolved by the acid front generated at the anode during the electrolysis reaction. In the Exp1 experiment, Cu^{2+} ions were solubilized by the acidic front and translocated from section S1 to S5 as soil pH decreased below pH 4 and accumulated in section S6 due to the pH increase over pH 6. Acid front sweeping across the soil led to a near-complete removal of Cu^{2+} in section S1, with concentrations gradually rising in sections S2 to S5 and accumulation in section S6 at 3989 mg/L (**Figure 5.3a**). Conversely, the Cu^{2+} extracted from the soil was 3.46% only due to high alkalinity in section S6 and short EK processing time (**Figure 5.3h**). Experiment Exp2 used a 50%-50% mixture of GIS and BTW as the RFM and the EK duration extended to 3 weeks. The Cu^{2+} concentrations across soil sections S1 to S6 exhibited ranged from 98 to 104 mg/L (**Figure 5.3b**). Meanwhile, 6972.5 mg/L of Cu^{2+} was captured in the RFM, resulting in a staggering

removal of 90.06% (**Table 5.3**). In experiment Exp3, applying the PIS/BTW as the RFM near the cathode enhanced Cu^{2+} removal across soil sections S1 to S6 (**Figure 5.3c**). The majority of the Cu^{2+} ions were precipitated in the RFM as the soil pH shifted to alkaline conditions, > pH 9 (**Figure 5.3a**). In section S1, the Cu^{2+} concentration was 4.5 mg/L, increasing to 57 mg/L in section S6, and reached 8147.5 mg/L in PIS/BTW RFM. Cu^{2+} removal in experiment Exp 3 was 98.75% rate (**Figure 5.3h & Table 5.3**), with 97.7% of the Cu^{2+} being accumulated in the RFM. Iron oxide, the primary constituent of iron slag, exhibits a significant adsorption capability for metal ions. Its retention mechanisms encompass precipitation, electrostatic interactions, and surface complexation (Hamdi et al., 2024; Yeongkyoo, 2018). The alkaline pH of iron oxide, around pH 11, facilitates Cu^{2+} precipitation in the RFM (**Table 5.1**). The deprotonation of hydroxyl (-OH) groups in iron slag enhances Cu^{2+} adsorption. Losing protons will acquire -OH groups a negative charge, increasing their electrostatic attraction to Cu^{2+} ions. Also, black tea waste was selected as an effective heavy metals chelating agent, with polyphenols, proteins, and fibers acting as natural adsorbents. These compounds have hydroxyl and carboxyl functional groups that can bind metal ions by mechanisms such as ion exchange, chelation, and surface adsorption. Compared to experiment Exp2, Cu^{2+} removal was 9.6% higher in experiment Exp3 with PIS/BTW RFM because of the larger surface area of the RFM, 0.493 m^2/g (**Table 5.1**).

In experiment Exp4, reusing recycled PIS/BTW as the RFM resulted in an increase in Cu^{2+} concentration from 5.5 mg/L in section S1 to 463.5 mg/L in section S6, with 7448 mg/L accumulated in the RFM (**Figure 5.3d**). PIS/BTW RFM reuse led to a reduction in Cu^{2+} removal compared to experiment Exp3. The total Cu^{2+} removal in experiment Exp4 was 91.28%, with 89.4% of the Cu^{2+} being sequestered in the RFM (**Table 5.3**). The decrease in removal efficiency from 98.75% in Exp3 to 91.28% in Exp4 is likely due to

factors such as saturation of adsorption sites, decreased reactivity of the RFM, and changes in pH that affect Cu^{2+} precipitation. The adsorption capacity of PIS/BTW RFM was compromised after recycling due to the cleavage of carboxyl and hydroxyl groups in the black tea waste, as shown in the FTIR analysis (**Figures 5.4a and 5.4b**). FTIR results also reveal that sulphate and silicate in the recycled iron slag suffered structural modifications by thermal or chemical mechanisms, which affected their adsorption efficiency. In experiment Exp5, a reused RFM composed of GIS/BTW was employed. Cu^{2+} concentrations across soil sections S1 to S6 exhibited a slight increase compared to experiment Exp2, ranging from 124.5 to 190.5 mg/L (**Figure 5.3e**). **Table 5.3** shows that Cu^{2+} ions in the RFM dropped from 6972.5 to 5626 mg/L, resulting in a reduced overall removal efficiency of 84.90%. Acid washing would likely cause the loss of some of the surface reactivity of the RFM, as explained above. Generally, adsorption and desorption tests indicated that PIS/BTW exhibited superior performance in metal removal compared to GIS/BTW (**Figure 5.5e**) due to its larger surface area and improved porosity (**Table 5.1**). These factors contribute to more efficient adsorption processes, allowing powder slag to capture contaminants more effectively.

The experiment Exp6 assessed the effectiveness of the EK method when combined with PIS/BTW as RFM by extending the treatment duration to 4 weeks. Cu^{2+}, Ni^{2+}, and Zn^{2+} were spiked into the kaolinite soil at a concentration of 1000 mg/kg each to evaluate the EK process of treating a mixture of pollutants. In Exp6, Cu^{2+}, Ni^{2+}, and Zn^{2+} ions were transported to the RFM close to the cathode region by the acid front that swept across the soil (**Figure 5.3f**). In the soil sections S1 to S6, between 16 and 33.5 mg/L of Cu^{2+}, Ni^{2+}, and Zn^{2+} was detected, while most of the heavy metals were accumulated in the RFM close to the cathode. In the RFM, the concentrations of Cu^{2+} was 7840.5 (mg/L), Ni^{2+} was 8120.5 (mg/L), and Zn^{2+} was 7748 (mg/L). Indeed, the RFM captured 94.1% of copper,

97.4% of nickel, and 93.1% of zinc (**Table 5.3**). At the end of the EK process, Cu^{2+}, Ni^{2+}, and Zn^{2+} ions were removed at rates of 97.15%, 98.30%, and 96.68%, respectively. Experiment Exp7 evaluated the effectiveness of the EK combined with PIS/BTW RFM for Cu^{2+}, Ni^{2+}, and Zn^{2+} ions removal from naturally contaminated soil. The initial concentrations of Cu^{2+}, Ni^{2+}, and Zn^{2+} in natural soil were 430, 325, and 652 mg/L, respectively (**Table 3.2**). This experiment considered an extended treatment duration of 5 weeks to allow sufficient time for metal ions removal. The concentration of Cu^{2+} in soil sections S1 to S6 ranged from 0.85 to 656 mg/L, while Ni^{2+} and Zn^{2+} concentrations were lower than Cu^{2+}. Ni^{2+} concentrations ranged from 6.3 mg/L in S1 to 120.95 mg/L in S6, and Zn^{2+} concentrations ranged from 1.35 mg/L in S1 to 201.5 mg/L in S6. The concentrations of Cu^{2+}, Ni^{2+}, and Zn^{2+} in the RFM were measured at 532.7 mg/L, 2044.8 mg/L, and 3869.8 mg/L. The RFM was effective in capturing 14.84% of Cu^{2+}, 88.09% of Ni^{2+}, and 83.06% of Zn^{2+} (**Table 5.3**). By the end of the EK process, the overall removal rates for Cu^{2+}, Ni^{2+}, and Zn^{2+} reached 16.39%, 89.22%, and 84.38%, respectively. The results indicate that Cu^{2+} removal was lower than that of Ni^{2+} and Zn^{2+} due to its stronger affinity for soil particles, particularly organic matter and clay minerals. Cu^{2+} binds more tightly through chemisorption, forming complexes with soil organic matter, hydroxides, and sulfides. This strong binding makes Cu^{2+} less mobile and harder to displace during EK remediation. In contrast, Ni^{2+} and Zn^{2+} form weaker bonds with soil components, allowing for easier removal through the EK process. Also, Cu^{2+} tends to precipitate in soils with higher pH levels, forming precipitate more readily as hydroxides or oxides, making it less soluble than Ni^{2+} and Zn^{2+}. These precipitates further limit Cu^{2+} mobility, reducing its availability for removal by the EK. Instead, Ni^{2+} and Zn^{2+} remain in more soluble forms under similar conditions, making them easier to mobilize and remove.

In a nutshell, the alkaline front in experiment Exp1 moved beyond section S6, leading to the deposition of most of the Cu^{2+} in the form of metal hydroxide. However, the incorporation of PIS or GIS/BTW RFM in experiments Exp2 to Exp7 significantly enhanced heavy metals removal. The addition of RFM improved the EK process's ability to capture and immobilize heavy metals, ensuring more efficient extraction and overall higher metal removal efficiency compared to the EK process without RFM. As shown in **Table 5.2**, the EK process utilizing PIS/BTW RFM exhibited the highest Cu^{2+} removal rate of 98.75%. In experiments involving the PIS/BTW RFM in kaolinite soil, the removal rates were 97.15%, 98.30%, and 96.68% for Cu^{2+}, Ni^{2+}, and Zn^{2+}, respectively. Recycling the PIS/BTW as the RFM resulted in a slightly lower copper removal rate of 91.28%.

Conversely, GIS/BTW recorded a 90.06% Cu^{2+} removal in new RFM and 84.90% in recycled RFM. In experiment Exp7, which tested Cu^{2+}, Ni^{2+}, and Zn^{2+} ions removal from natural soil, the PIS/BTW-EK system achieved 16.39%, 89.22%, and 84.38% removal rates, respectively. Without the enhancement of RFM, the EK process demonstrated low effectiveness, with a total copper removal of only 3.46% in experiment Exp1. These results underscore the superior performance of powder iron slag over granular forms and emphasize the importance of RFM composition and reuse strategies.

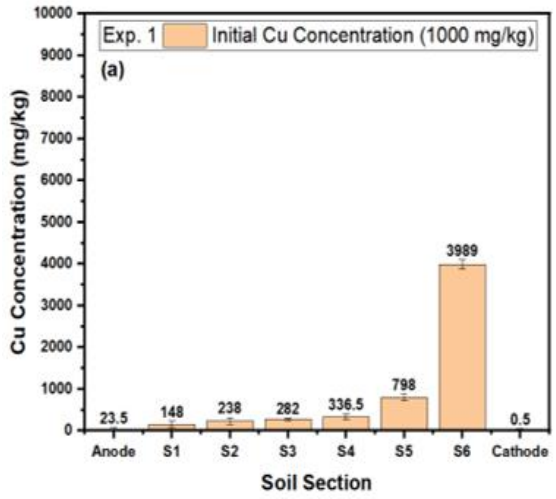
Exp. 1
Initial Cu Concentration (1000 mg/kg)
(a)
Cu Concentration (mg/kg)
Soil Section
Anode
S1
S2
S3
S4
S5
S6
Cathode
23.5
148
238
282
336.5
798
3989
0.5

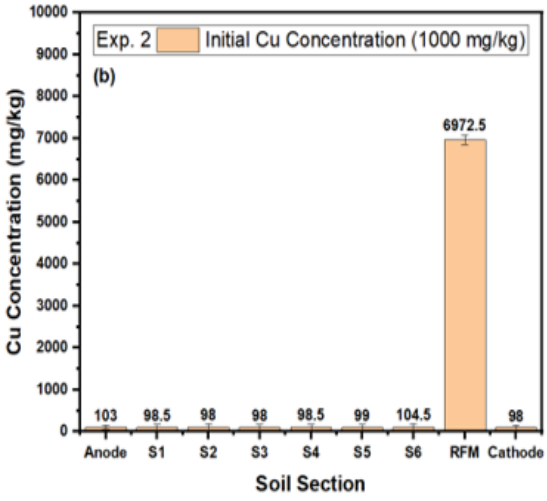
Exp. 2
Initial Cu Concentration (1000 mg/kg)
(b)
Cu Concentration (mg/kg)
Soil Section
Anode
S1
S2
S3
S4
S5
S6
RFM
Cathode
103
98.5
98
98
98.5
99
104.5
6972.5
98

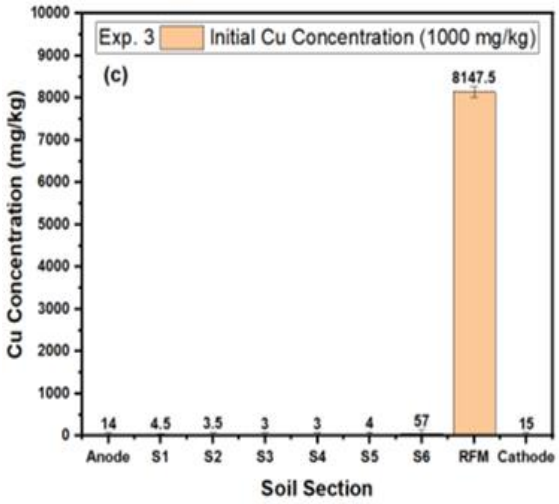
Exp. 3
Initial Cu Concentration (1000 mg/kg)
(c)
Cu Concentration (mg/kg)
Soil Section
Anode
S1
S2
S3
S4
S5
S6
RFM
Cathode
14
4.5
3.5
3
3
4
57
8147.5
15

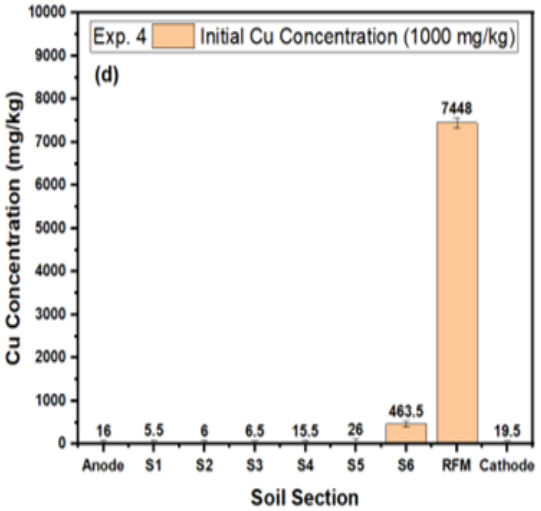
Exp. 4
Initial Cu Concentration (1000 mg/kg)
(d)
Cu Concentration (mg/kg)
Soil Section
Anode
S1
S2
S3
S4
S5
S6
RFM
Cathode
16
5.5
6
6.5
15.5
26
463.5
7448
19.5

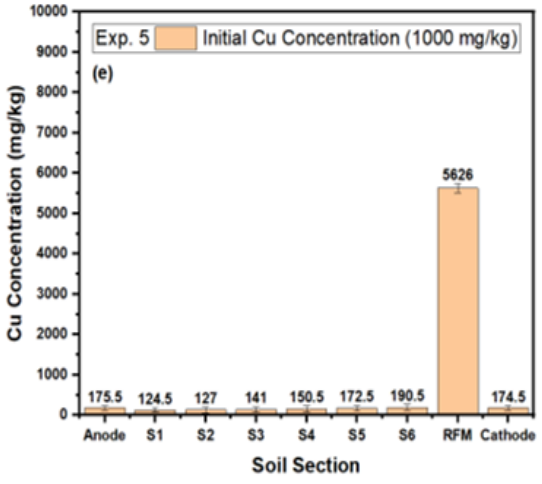
Exp. 5
Initial Cu Concentration (1000 mg/kg)
(e)
Cu Concentration (mg/kg)
Soil Section
Anode
S1
S2
S3
S4
S5
S6
RFM
Cathode
175.5
124.5
127
141
150.5
172.5
190.5
5626
174.5

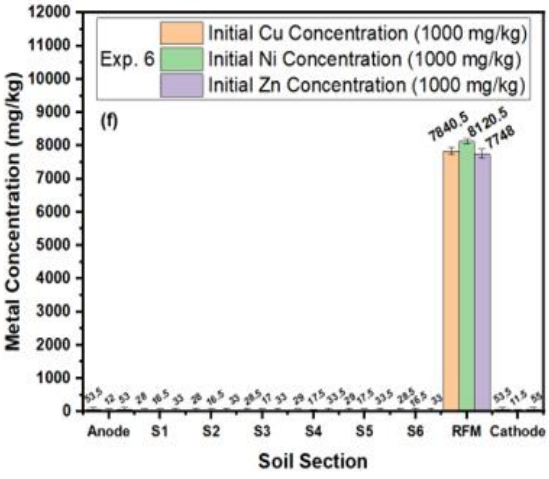
Exp. 6
Initial Cu Concentration (1000 mg/kg)
Initial Ni Concentration (1000 mg/kg)
Initial Zn Concentration (1000 mg/kg)
(f)
Metal Concentration (mg/kg)
Soil Section
Anode
S1
S2
S3
S4
S5
S6
RFM
Cathode
7840.5
8120.5
7748

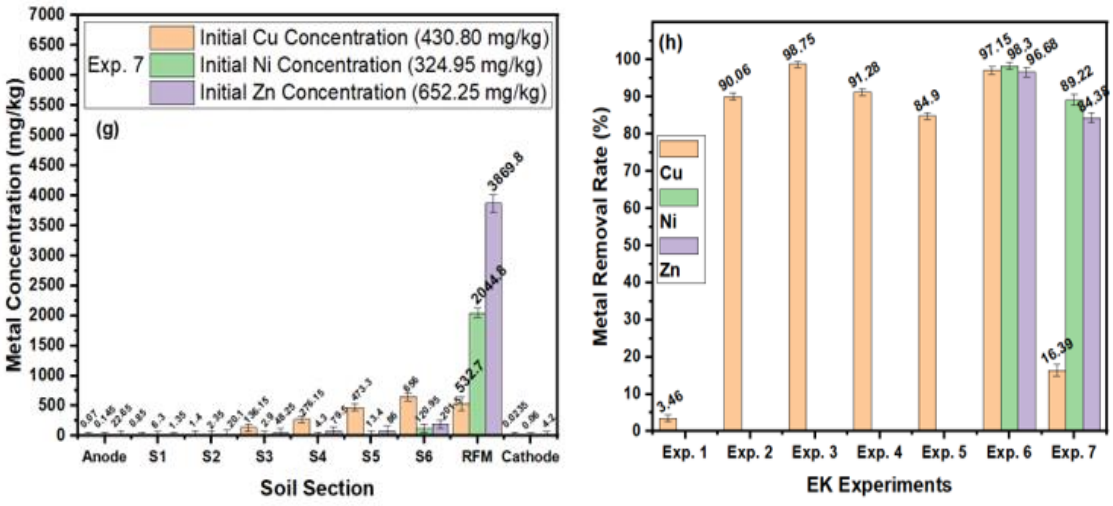

Figure 5.3: Shows (a) to (f) the removal of single and mixed elements from kaolin soil, (g) the removal of mixed elements from natural soil, and (h) the total metal removal for all experiments.

Table 5.3: Removal efficiency and Mass Balance of EK tests.

Exp No	Type of soil	Metal ions	Initial Metal in soil (mg/kg)	Residual Metal in Soil (mg)	Metal mass in RFM (mg)	Mass Balance (%)	Total removal (%)
Exp1	Kaolin Soil	Cu	1000	965.44	N/A	103.39	3.46±0.21
Exp2	Kaolin Soil	Cu	1000	99.42	836.7	100.02	90.06±0.19
Exp3	Kaolin Soil	Cu	1000	12.50	977.7	100.34	98.75±0.22
Exp4	Kaolin Soil	Cu	1000	87.17	893.76	100.56	91.28±0.16
Exp5	Kaolin Soil	Cu	1000	151.01	675.12	99.98	84.90±0.20
		Cu	1000	28.50	940.86	100.33	97.15±0.21
Exp6	Kaolin Soil	Ni	1000	16.92	974.46	100.25	98.30±0.18
		Zn	1000	33.17	929.76	100.77	96.68±0.22

Exp7	Real Soil	Cu	430	360.18	14.84	99.10	16.39±0.29
		Ni	325	35.04	88.09	101.13	89.22±0.26
		Zn	652	101.88	83.06	101.09	84.38±0.25

5.3.4. Characteristics of RFM

Steel slag is a solid waste that has a significant porosity and high specific surface area. These qualities make them a viable option for use as an affordable adsorbent to remove contaminants from soil. The distinct qualities and chemical makeup of steel slag determine how well it removes impurities (Ganbat et al., 2023; Hamdi et al., 2024). Black tea waste refers to the organic residue left after brewing black tea, primarily composed of tea leaves. It is rich in organic compounds such as tannins, cellulose, lignin, and polyphenols, making it a valuable adsorbent material for environmental applications, particularly for the removal of heavy metals from water (Gupta and Suhas, 2009). Our study employed a combination of black tea waste with granular or powder iron slag, referred to as RFM, in the electrokinetic (EK) process for the absorption of heavy metals. Iron oxide has been shown to have the ability to form surface attachment or adsorption contacts with heavy metal in the surrounding environment; however, the exact nature of these interactions is still being investigated. This tendency is ascribed to the intrinsic characteristics of iron oxide, such as its small particle size and prominent porosity, which together confer a substantial surface area and establish it as a superior adsorbent. Electrostatic interactions between the molecules of Cu^{2+}, Ni^{2+}, and Zn^{2+} are the primary mechanisms regulating their adsorption onto iron oxide. The formation of inner-sphere Fe-carboxylate complexes by ligand exchange facilitates this interaction(Jain et al., 2018). There are important consequences associated with the adsorption of Cu^{2+}, Ni^{2+},

and Zn^{2+} onto iron oxide particles. In the first place, it reduces these substances' mobility, which lessens the chance of groundwater being polluted or that it will seep into nearby areas. Furthermore, the behavior and characteristics of the iron oxide particles themselves might be impacted by this adsorption phenomenon. This impact also includes elements related to responsiveness and stability.

The FTIR study of PIS/BTW and GIS/BTW RFMs conducted for both pre-and post-electrokinetic treatment and recycled (RC) RFM reveals distinct variations in their chemical structure and surface properties (**Figures 5.4a and 5.4b**). The PIS samples have more well-defined peaks owing to their greater surface area, especially in the Fe-O stretching region around 500 cm^{-1}, in contrast to the GIS samples, where smaller particles, such as powders, often display larger surface areas and more prominent peaks. The O-H stretching band at 3200–3600 cm^{-1}, linked to hydroxyl groups, has more intensity in the PIS/BTW spectra, indicating an increased abundance of water or surface hydroxyl groups, which are more readily available in powder form. Post-EK treatment, both PIS and GIS exhibit a diminution in the O-H and C=O stretching peaks at 1600–1650 cm^{-1}, implying that the treatment may have induced dehydration or alteration of the organic constituents, including black tea waste, through the cleavage of carboxyl and hydroxyl groups, as evidenced by the reduction in intensity. The Fe-O peak at around 500 cm^{-1} is more pronounced in EK-treated samples, suggesting a potential reorganization or enhanced exposure of iron oxide groups after EK processes, which may facilitate ion transport within the matrix and result in the rearrangement of iron species. In recycled (RC) samples, the O-H and C=O peaks persist and diminish, indicating the partial decomposition of organic materials. Besides, alterations in the S=O stretching peak at 1220–1270 cm^{-1} and Si-O stretching peaks at 1000–1100 cm^{-1} signify structural changes within the slag constituents. These changes indicate that the recycling process may

modify the sulphate and silicate structures in the slag, perhaps via thermal or chemical mechanisms. The modifications in various treatments demonstrate the impact of particle size, electrokinetic treatment, and recycling on the chemical properties and structural stability of iron slag/black tea waste composites (Çelebi et al., 2020; Faisal et al., 2019; Stumpe et al., 2012).

The combination of SEM and EDS (**Figure 5.4**) showed for sure that Cu^{2+}, Ni^{2+}, and Zn^{2+} were present on the surfaces of RFMs after the EK process. The RFMs before treatment are shown in **Figures 5.4c to 5.4n,** with SEM pictures and EDS graphs showing their surface shapes. The RFMs after treatment are shown in **Figures 5.4o to 5.4z**. These pictures show how the RFMs' surface features and chemical makeup changed before and after electrokinetic treatment. Post-treatment observations of contaminants were notably pronounced in the GIS/BTW and PIS/BTW samples. The Cu^{2+} concentration in the GIS/BTW was significantly lower than in the PIS/BTW RFM. EDS analysis revealed that Cu^{2+} content was 8.65% in the PIS/BTW (**Figure 5.4r**) and only 0.67% in the GIS/BTW (**Figure 5.4p**), demonstrating that Cu^{2+} removal was more efficient with the PIS/BTW RFM during the EK treatment compared to the GIS/BTW RFM.

Powder iron slag demonstrated superior performance in metal removal compared to granular iron slag, primarily due to its higher surface area and better reactivity. While RFM materials can be reused after acid washing, their adsorption capacity diminishes over time, indicating the need for better regeneration processes. Black tea waste enhances metal ion adsorption, but the overall system's effectiveness is influenced significantly by the form and condition of the iron slag used. The inferior performance of granular iron slag compared to powder iron slag can be attributed to its lower surface area, reduced porosity, and fewer active sites. The granular structure limits the diffusion of ions, making it less effective for adsorbing heavy metals. Black tea waste likely contributed positively

but could not compensate for the limitations of the granular material. The high surface area and porosity of powder iron slag allow for enhanced adsorption, making this material highly effective. The use of black tea waste, rich in tannins, also contributed to better copper ion adsorption due to its chelating properties.

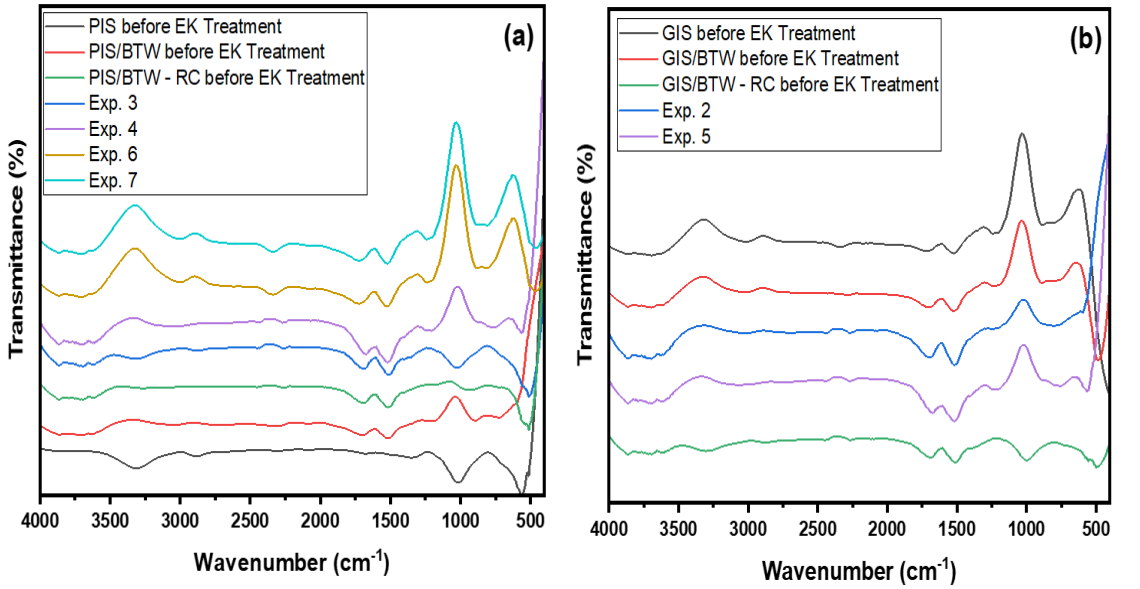

(c)

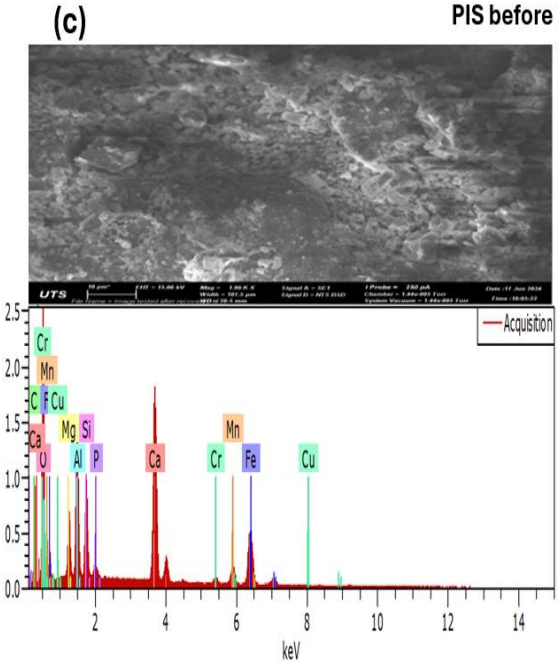

(d)

El	AN	Series	unn. C [wt.%]	norm. C [wt.%]	Atom. C [at.%]	Error (1 Sigma) [wt.%]
O	8	K-series	34.78	35.89	54.42	4.30
Ca	20	K-series	18.43	19.02	11.51	0.58
C	6	K-series	4.28	4.42	8.93	0.81
Fe	26	K-series	17.89	18.46	8.02	0.57
Al	13	K-series	6.83	7.04	6.33	0.35
Si	14	K-series	4.67	4.82	4.16	0.23
Mg	12	K-series	3.05	3.15	3.14	0.19
Mn	25	K-series	4.80	4.95	2.19	0.18
Cr	24	K-series	1.41	1.46	0.68	0.08
P	15	K-series	0.76	0.78	0.61	0.06
		Total:	96.91	100.00	100.00	

(e) **GIS before EK Treatment** (f)

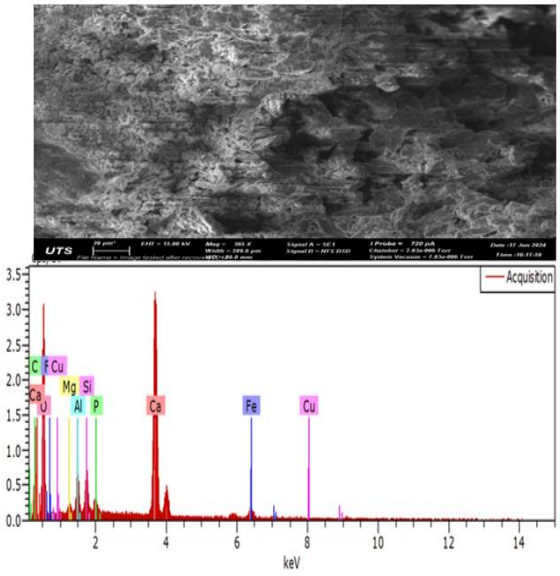

El	AN	Series	unn. C [wt.%]	norm. C [wt.%]	Atom. C [at.%]	Error (1 Sigma) [wt.%]
O	8	K-series	47.86	49.41	62.56	8.90
C	6	K-series	8.89	9.18	15.48	2.55
Ca	20	K-series	29.52	30.47	15.40	1.03
Al	13	K-series	2.60	2.69	2.02	0.21
Si	14	K-series	2.64	2.73	1.97	0.20
Fe	26	K-series	3.76	3.89	1.41	0.32
P	15	K-series	1.10	1.14	0.74	0.12
Mg	12	K-series	0.49	0.51	0.42	0.09
		Total:	96.87	100.00	100.00	

(g) **PIS/BTW before EK Treatment** (h)

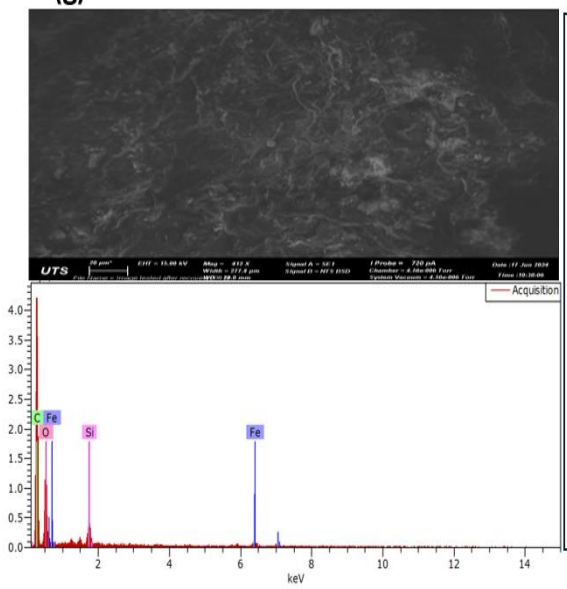

El	AN	Series	unn. C [wt.%]	norm. C [wt.%]	Atom. C [at.%]	Error (1 Sigma) [wt.%]
C	6	K-series	59.43	59.43	68.30	9.14
O	8	K-series	34.32	34.32	29.61	6.53
Si	14	K-series	2.24	2.24	1.10	0.16
Fe	26	K-series	4.00	4.00	0.99	0.32
		Total:	100.00	100.00	100.00	

(i) **GIS/BTW before EK Treatment** (j)

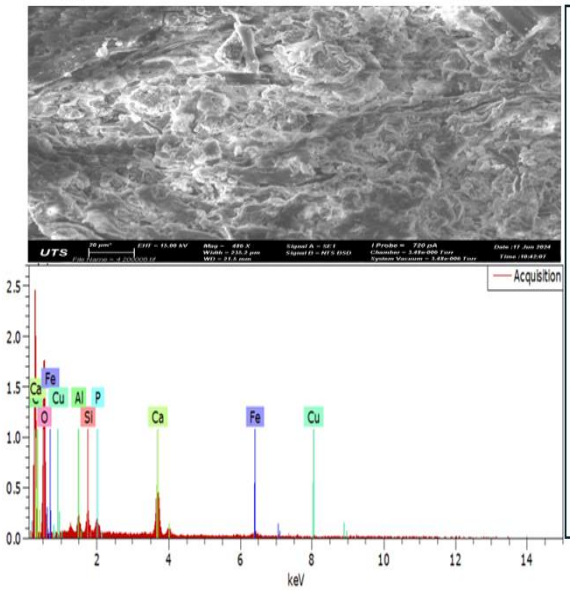

El	AN	Series	unn. C [wt.%]	norm. C [wt.%]	Atom. C [at.%]	Error (1 Sigma) [wt.%]
C	6	K-series	39.90	41.02	51.81	5.86
O	8	K-series	43.74	44.97	42.64	6.62
Ca	20	K-series	8.06	8.29	3.14	0.31
Si	14	K-series	1.34	1.38	0.75	0.10
Fe	26	K-series	2.36	2.43	0.66	0.17
Al	13	K-series	1.03	1.05	0.59	0.09
P	15	K-series	0.83	0.85	0.42	0.08
		Total:	97.27	100.00	100.00	

(k) **PIS/BTW before EK Treatment (Recycling)** (l)

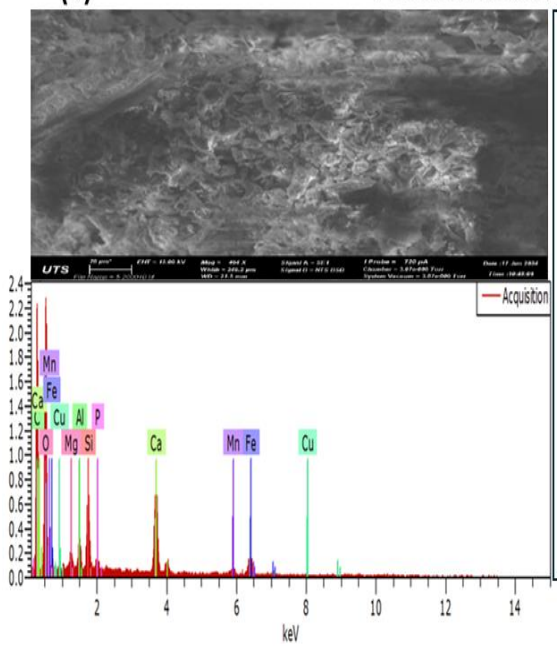

El	AN	Series	unn. C [wt.%]	norm. C [wt.%]	Atom. C [at.%]	Error (1 Sigma) [wt.%]
C	6	K-series	34.91	34.68	46.89	5.50
O	8	K-series	43.12	42.84	43.48	6.59
Ca	20	K-series	8.97	8.91	3.61	0.35
Si	14	K-series	3.91	3.89	2.25	0.22
Fe	26	K-series	5.50	5.46	1.59	0.29
Al	13	K-series	1.52	1.51	0.91	0.13
Mg	12	K-series	0.92	0.91	0.61	0.10
Mn	25	K-series	1.24	1.23	0.36	0.12
P	15	K-series	0.58	0.57	0.30	0.07
		Total:	100.66	100.00	100.00	

(m) GIS/BTW before EK Treatment (Recycling) (n)

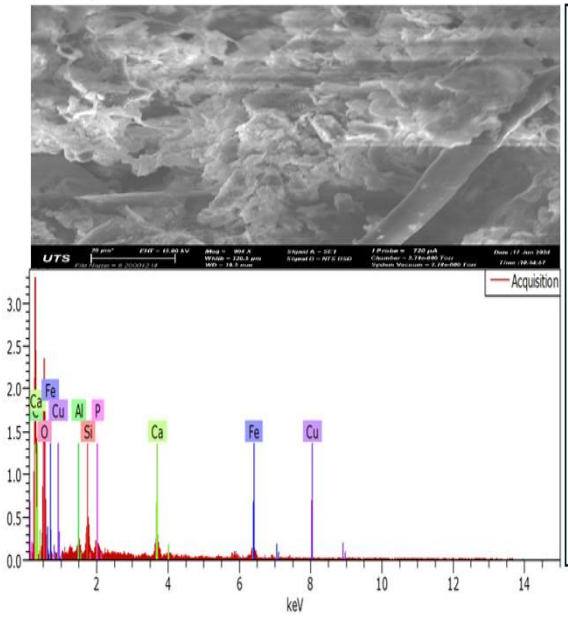

El	AN	Series	unn. C [wt.%]	norm. C [wt.%]	Atom. C [at.%]	Error (1 Sigma) [wt.%]
C	6	K-series	39.06	46.60	57.03	7.03
O	8	K-series	35.48	42.32	38.88	6.87
Fe	26	K-series	3.89	4.64	1.22	0.35
Ca	20	K-series	2.62	3.12	1.15	0.19
Si	14	K-series	1.67	1.99	1.04	0.14
Al	13	K-series	0.54	0.65	0.35	0.08
P	15	K-series	0.57	0.67	0.32	0.08
		Total:	83.83	100.00	100.00	

(o) GIS/BTW after EK Treatment (Exp2) (p)

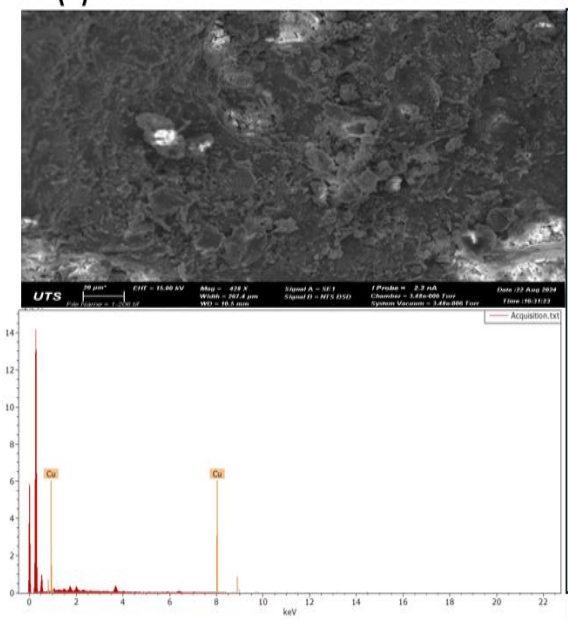

El	AN	Series	unn. C [wt.%]	norm. C [wt.%]	Atom. C [at.%]	Error (1 Sigma) [wt.%]
Cu	29	K-series	0.67	100.00	100.00	0.08
		Total:	0.67	100.00	100.00	

(q) PIS/BTW after EK Treatment (Exp3) (r)

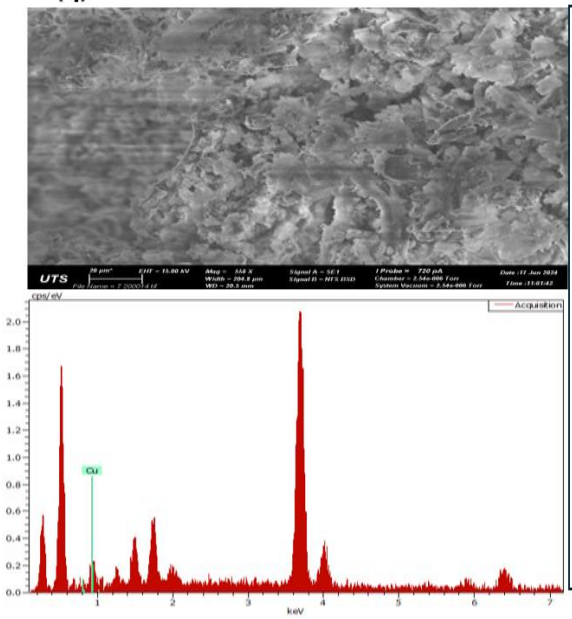

El	AN	Series	unn. C [wt.%]	norm. C [wt.%]	Atom. C [at.%]	Error (1 Sigma) [wt.%]
Cu	29	K-series	8.65	100.00	100.00	1.08
Total:			8.65	100.00	100.00	

(s) PIS/BTW - RC after EK Treatment (Exp4) (t)

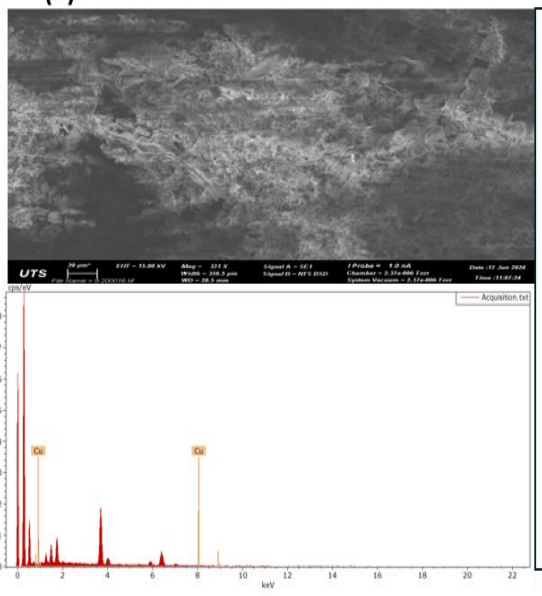

El	AN	Series	unn. C [wt.%]	norm. C [wt.%]	Atom. C [at.%]	Error (1 Sigma) [wt.%]
Cu	29	K-series	0.34	100.00	100.00	0.07
Total:			0.34	100.00	100.00	

(u) GIS/BTW - RC after EK Treatment (Exp5) (v)

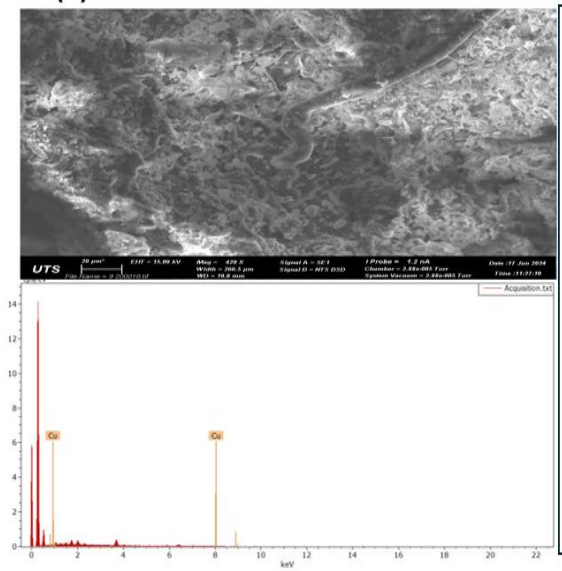

El	AN	Series	unn. C [wt.%]	norm. C [wt.%]	Atom. C [at.%]	Error (1 Sigma) [wt.%]
Cu	29	K-series	0.19	100.00	100.00	0.05
Total:			0.19	100.00	100.00	

(w) PIS/BTW after EK Treatment (Exp6) (x)

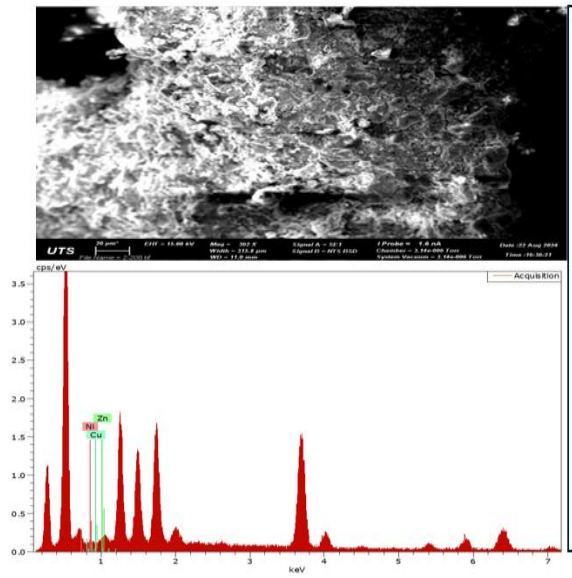

El	AN	Series	unn. C [wt.%]	norm. C [wt.%]	Atom. C [at.%]	Error (1 Sigma) [wt.%]
Cu	29	K-series	1.19	57.57	56.80	0.14
Ni	28	K-series	0.48	23.13	24.70	0.08
Zn	30	K-series	0.40	19.30	18.50	0.09
Total:			2.06	100.00	100.00	

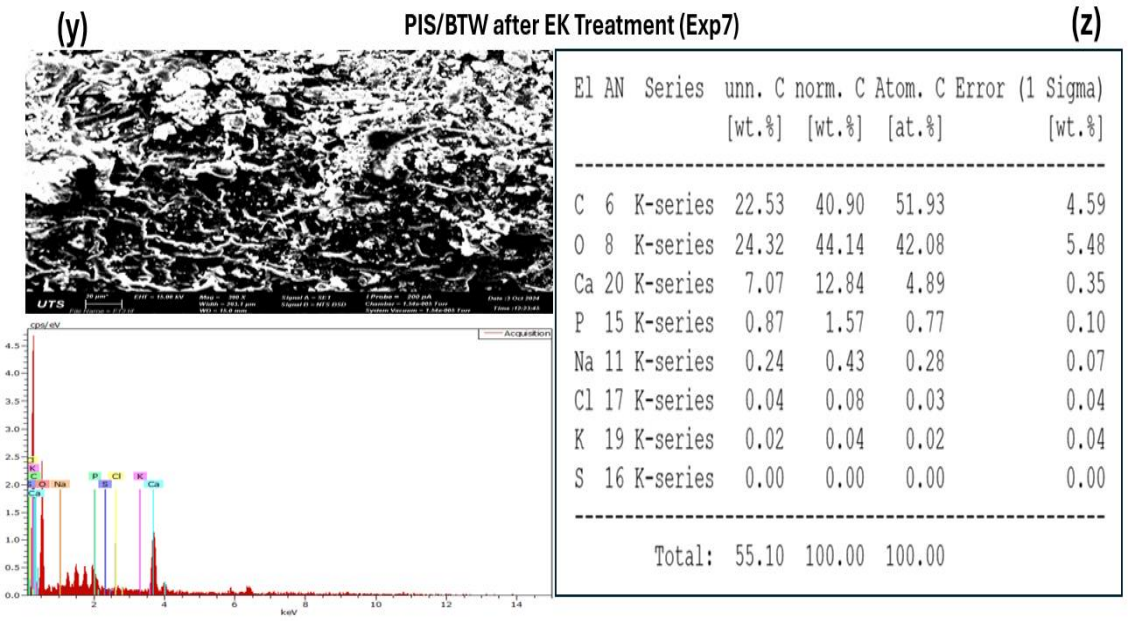

Figure 5.4: FTIR spectra of (a & b) PIS/BTW and GIS/BTW before and after EK, and SEM and EDS of (c to n) PIS, GIS, PIS/BTW, and GIS/BTW before EK, and SEM and EDS of (o to z) PIS/BTW and GIS/BTW after EK.

5.3.5. RFM adsorption/desorption

The results of dynamic adsorption experiments using PIS/BTW and GIS/BTW are illustrated in **Figures 5.5a and 5.5b**. The adsorption behavior of heavy metals was thoroughly analyzed, demonstrating that PIS/BTW achieved its maximum adsorption capacity of 66.80 mg/g for Cu^{2+} within 60 minutes. In comparison, GIS/BTW reached its peak capacity of 63.81 mg/g for Cu^{2+} over 135 minutes. In the mixed metal solution, PIS/BTW exhibited adsorption capacities of 56.67 mg/g for Cu^{2+} at 14 minutes, 55.83 mg/g for Ni at 135 minutes, and 54.92 mg/g for Zn at 30 minutes. Initially, the removal of Cu^{2+}, Ni^{2+}, and Zn^{2+} occurred rapidly, indicating a fast adsorption rate. However, as equilibrium approached, the adsorption process slowed down, balancing with the desorption rate. The overall metal uptake and adsorption speed were influenced by several factors, such as contact time and the unique properties of PIS/BTW and GIS/BTW.

The dynamic adsorption tests with PIS/BTW, shown in **Figures 5.5c and 5.5d**, demonstrated an initially rapid uptake of metal ions, indicating efficient adsorption. However, as equilibrium was approached, the rate of removal began to slow due to the progressive occupation of available adsorption sites. This slowdown resulted from interactions between the adsorbed molecules and those in the bulk solution. The extraction rate of adsorbates depended on their movement from the surface to the inner layers of the adsorbent. The metal ions that were investigated reached equilibrium, where the rates of adsorption and desorption were equal in under fifteen minutes (Kulal and Badalamoole, 2020; Rahchamani et al., 2011; Zhuang et al., 2016). The magnetite nanoparticles with embedded Fe^{2+} ions serve as electron donors. The primary techniques utilized for ions removal from solution include electrostatic adsorption, metal ions binding to surfaces of metal oxide, and ion exchange with H^+ from OH^- groups on the surface of the adsorbent, forming complexes. Adsorbents possessing various chemical functionalities like carboxyl, aldehyde, ester, hydroxyl, and ketone groups can interact with metal ions. The effectiveness of this interaction depends on variables such as the number of binding sites, accessibility, chemical structure, and the binding involved (Castro et al., 2018; Jain et al., 2018).

Over the three cycles, the Cu^{2+} removal efficiency using PIS/BTW was 67.54%, 58.79%, and 49.56% of the initial Cu^{2+} content, while GIS/BTW achieved 61.54%, 56.79%, and 48.90%, respectively. The desorption rates for Cu^{2+} over these cycles were 59.42%, 40.09%, and 30.61%, while GIS/BTW showed desorption rates of 56.42%, 39.09%, and 29.61%, as shown in **Figure 5.5e** for comparison between PIS/BTW and GIS/BTW. For the mixed heavy metal solution, Cu^{2+} removal with PIS/BTW reached 59.01%, 48.54%, and 41.94% across the three cycles. Ni^{2+} removal rates were 58.54%, 49.79%, and 42.16%, and for Zn^{2+}, they were 59.54%, 48.60%, and 40.37%. Desorption

concentrations for Cu^{2+} were 50.22%, 43.09%, and 29.61%, while Ni^{2+} were 52.42%, 44.10%, and 30.51%, and Zn^{2+} were 50.86%, 40.15%, and 29.60%, as shown in **Figure 5.5f**. The desorption process in GIS or PIS with BTW involves the release of molecules or ions that were previously adsorbed through mechanisms like diffusion, exchange reactions, solvent interactions, or external influences. The movement of adsorbed species follows concentration gradients from areas of high to low concentration. Exchange reactions occur when species with a higher affinity replace those with a lower affinity. Solvents can alter interactions between PIS/BTW and the adsorbed substances. Additionally, external factors like temperature changes, pH shifts, or structural modifications can impact the process. In acidic conditions, protons compete for binding sites, reducing interactions and causing the release of adsorbed metal ions.

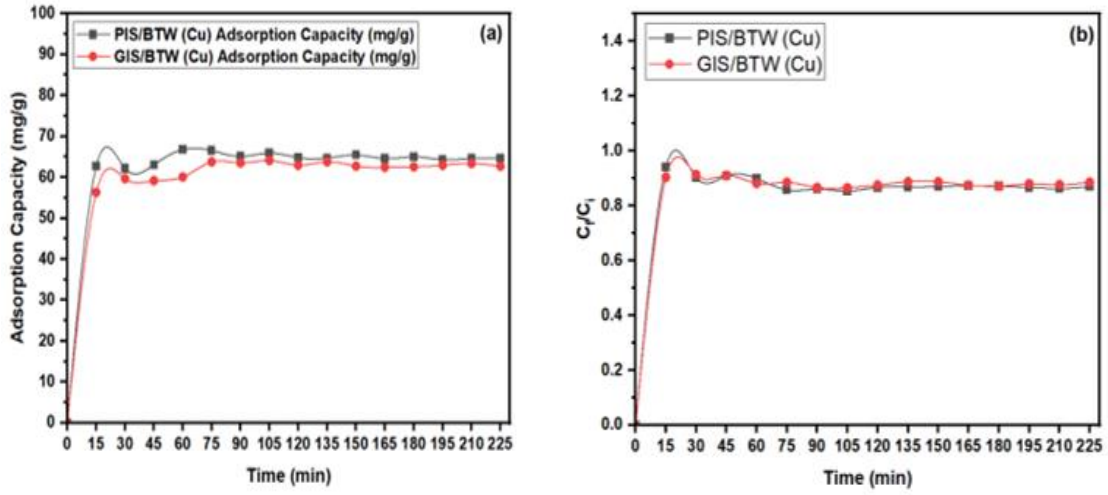

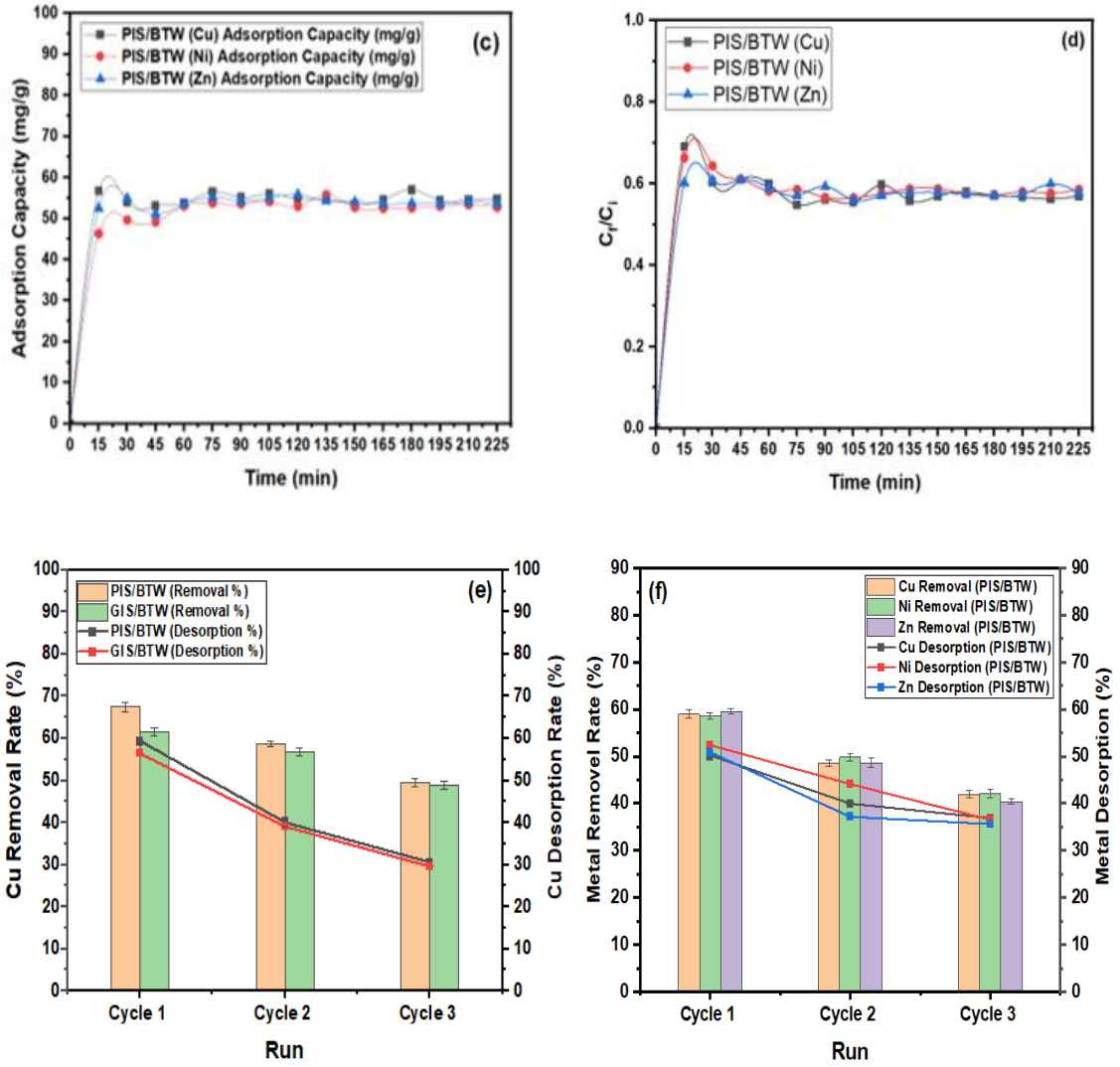

Figure 5.5: (a) Influence of PIS/BTW and GIS/BTW on copper adsorption over time, (b) Effect of contact duration on copper ion adsorption efficiency. (c) Adsorption of meatl from mixed solutions by PIS/BTW over time. (d) Influence of contact duration on the adsorption of metal ions, and (e&f) Adsorption/desorption behavior of metal across three consecutive cycles.

5.3.6. Specific energy consumption

The intensity of the operating electrical current is pivotal in the electrokinetic process, significantly affecting both reaction kinetics and power consumption (Ganbat et al., 2023; Hamdi et al., 2024). Apart from experiment Exp1, which used 20 mA, the electric current

was 25 mA in experiments Exp2 to Exp7. Also, the duration of experiments Exp2 to Exp5 was extended to 3 weeks to allow more time for copper removal and was further extended to 28 and 35 days in experiments Exp6 and Exp7 to enhance the removal of multiple heavy metals in kaolinite and natural soils. Increasing electric current accelerates the transport of heavy metals yet may result in electrolyte depletion, surface degradation, and soil heating. Alternatively, increasing the processing time allows for gradual metal breakdown and dissolution with fewer risks (Hamdi et al., 2024). **Figure 5.6** depicts the fluctuations in the removal rate of total metal in relation to the dry soil mass, alongside the associated specific energy consumption in the EK process. In all EK experiments, high Cu^{2+}, Ni^{2+}, and Zn^{2+} ions removal rates were noted in the kaolinite soil. The percentage of Cu^{2+} removal decreased in experiment Exp7 with the natural soil (**Figure 5.6**). The analysis of power consumption during the EK-RFM system revealed a significant increase in specific energy consumption (SEC) when both electric current and processing duration were extended. For example, SEC in experiment EXP2 increased sharply compared to Exp1 due to the longer EK processing time and the higher electric current.

The SEC was in the range from 0.055 to 0.340 kWh kg^{-1}. Comparing experiments Exp2 and Exp3, which were both conducted at 25 mA for 3 weeks, showed that the implementation of PIS/BTW improved Cu^{2+} removal rates while simultaneously reducing energy consumption from 0.237 kWh kg^{-1} to 0.227 kWh kg^{-1}. Experiment Exp6 energy consumption as 0.224 kWh/kg for Cu^{2+}, Ni^{2+}, and Zn^{2+} removal in 4 weeks. However, the energy consumption Exp7 was 0.344 kWh kg^{-1} when natural soil was used instead of kaolinite soil due to the extended EK processing time of 5 weeks. Cu^{2+}, Ni^{2+}, and Zn^{2+} ions removal in Exp7 were lower than in Exp6 despite the longer processing time. Natural soil's heterogeneity, higher organic content, and stronger metal-binding properties make

it more resistant to electrokinetic treatment, requiring more energy to break down these bonds. Additionally, the presence of various competing ions and the extended treatment duration (5 weeks) contributed to the higher energy demands, resulting in a significant rise in SEC compared to experiments using kaolin soil.

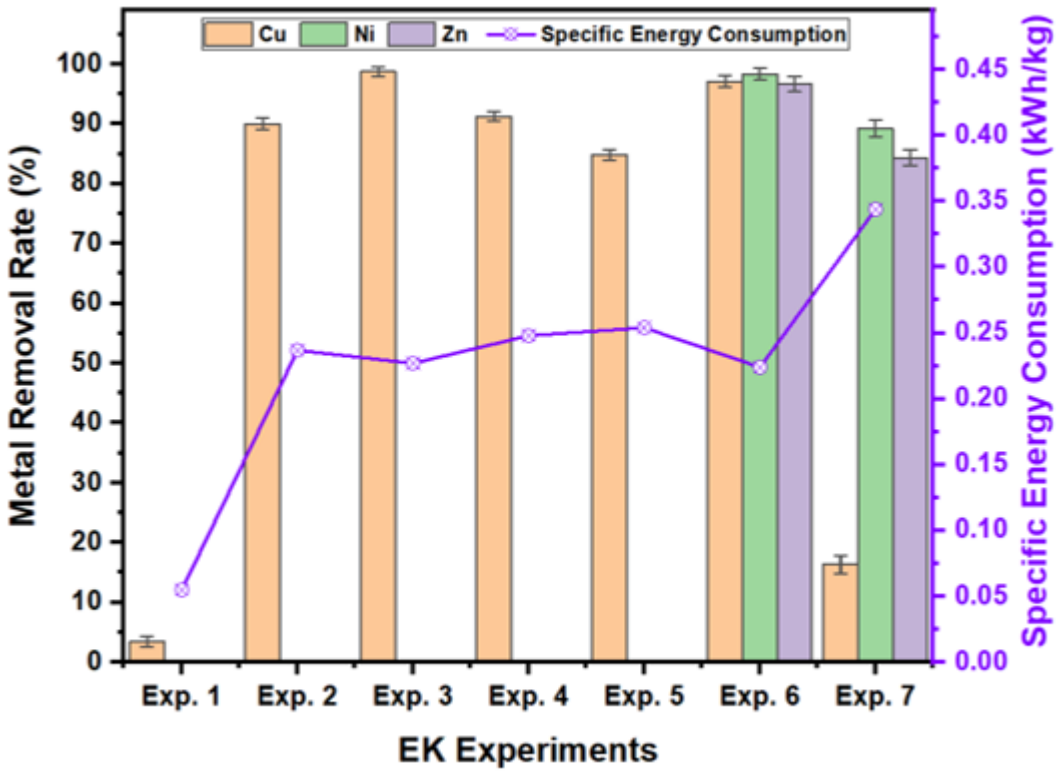

Figure 5.6: Total metal removal rate and specific energy consumption during EK experiments.

5.4. Conclusion

This study explored the integration of EK remediation with RFM, using powder iron slag/black tea waste (PIS/BTW) and granular iron slag/black tea waste (GIS/BTW) for the removal of single and mixed heavy metals from kaolinite and natural soils. The results demonstrated that PIS/BTW significantly outperformed GIS/BTW due to its higher surface area and reactivity, particularly in kaolinite soil. Heavy metal removal rates

increased from 3.46% in the standalone EK to 90.06% when combined with GIS/BTW. Copper removal was notably higher with PIS/BTW, reaching 98.75%, due to the enhanced adsorption of hydroxyl ions. Recycling the RFM in the EK process maintained high pollutant removal efficiency, with copper removal rates of 91.28% for PIS/BTW and 84.90% for GIS/BTW during a 3-week treatment. Energy consumption analysis revealed that specific energy consumption (SEC) increased with longer treatment durations and higher electric currents. SEC ranged from 0.055 kWh kg^{-1} to 0.254 kWh kg^{-1} in kaolin soil treatments, while extending the treatment period for natural soil to 5 weeks increased to 0.344 kWh kg^{-1}. In kaolinite soil, a mixture of heavy metals was successfully removed, with 97.15% for copper, 98.30% for nickel, and 96.68% for zinc. In the natural soil, the removal rates were lower, with 16.39% for copper, 89.22% for nickel, and 84.38% for zinc due to the complicated chemistry of natural soils and the interaction between pollutants and soil's organic matter. The alkaline pH of the RFMs contributed to the adsorption and precipitation of metal ions, enhancing their immobilization. Proper post-treatment management of RFMs is crucial due to potential heavy metal contamination, and safe disposal or recycling methods must be explored to minimize environmental risks. This study highlights the potential of using environmentally friendly and recyclable composite RFMs to improve EK-based heavy metal remediation while reducing remediation costs.

CHAPTER SIX:

DECONTAMINATION OF HEAVY METALS FROM SOIL BY ELECTROKINETIC COMBINED WITH REACTIVE FILTER MEDIA FROM INDUSTRIAL WASTES

CHAPTER SIX: DECONTAMINATION OF HEAVY METALS FROM SOIL BY ELECTROKINETIC COMBINED WITH REACTIVE FILTER MEDIA FROM INDUSTRIAL WASTES

The content of this chapter is based on the following publication:

Hamdi, F.M., et al. (2025) "Decontamination of heavy metals from soil by electrokinetic combined with reactive filter media from industrial wastes," Water, Air, & Soil Pollution**,** 236(9).

6.1. Introduction

Contaminated soils by various heavy metals are an urgent and prominent global environmental matter, presenting a substantial threat to the natural ecosystem and human well-being (Ganbat et al., 2023; Hamdi et al., 2024; Wen et al., 2021). Soil samples, for example, were collected from a previous wood impregnation site in the northern region of Copenhagen, Denmark, and exhibited elevated levels of copper, reaching concentrations as high as 1662 mg/kg, along with diverse other heavy metals. Similarly, soil from vineyards in France exhibited copper levels of up to 800 mg/kg (Fagnano et al., 2020; Frick et al., 2019). Consequently, there is an urgent need for remediation technologies that can effectively eliminate heavy metals while minimizing harm to the soil ecosystem (Turan, 2024). One promising approach for remediating soils with low permeability, which are traditionally challenging to clean, is Electrokinetic (EK) treatment. This method entails the application of a low electric current between electrodes inserted into the contaminated soil. Studies (Gholizadeh and Hu, 2021; Wen et al., 2021; Ghobadi et al., 2021a; Yuan et al., 2016) highlighted the effectiveness of EK treatment in addressing soil contamination.

During the electrokinetic (EK) process, heavy metals dissolve in the acidic regions of the soil and accumulate near the cathode. Thus, there is a growing need to improve EK methods by slowing the advance of the alkaline front to facilitate heavy metal removal (Wen et al., 2021). Reducing the pH level promotes the extraction of inorganic contaminants from polluted soils by increasing the release of these metals from the soil's surface (Ganbat et al., 2023; Gholizadeh and Hu, 2021). Enhancement agents are often applied to adjust the catholyte pH and promote acid transport (Fu et al., 2017; Ganbat et al., 2023; Xue et al., 2017; Yu et al., 2019). A study by Bahemmat and co-workers (2016) investigated heavy metal-contaminated soil treatment by catholyte conditioning with 0.1M HNO_3. Results showed a two to three-fold enhancement in heavy metal remediation efficiency after 3 weeks compared to the unenhanced EK process. Yuan et al. (2016) suggested using $CaCl_2$ and citric acid to remove inorganic pollutants, reporting better EK remediation results, reduced power consumption, and lowered environmental risks. In a study on chromium waste from industry, Fu et al. (2017) looked at polyaspartic acid and citric acid as two different conditioning electrolytes for EK remediation. The study found citric acid was particularly effective for total chromium removal. Compared to DI water as the electrolyte, citric acid increased energy due to water electrolysis and heat loss. While strong acids can effectively counteract the alkaline front advancement in soil, they come with trade-offs, including increased energy consumption and the EK treatment period (Fu et al., 2017). Adding conditioning agents can alter specific soil characteristics, including pH levels and conductivity, as observed in the study by Bahemmat et al. (2016). Additionally, it's crucial to consider the electrolyte recovery following EK treatment to manage remediation costs effectively.

To address the limitations associated with conventional EK processes utilizing chemical agents, researchers have explored the use of Reactive Filter Media (RFM) made from

materials such as compost, zero-valent iron, activated carbon, and activated bamboo charcoal (Ghobadi et al., 2021b, 2021a, 2020; Xue et al., 2017). These RFMs have demonstrated enhanced performance when compared to traditional EK methods. However, the practical application of these RFMs may need to be improved by cost, availability, and, notably, their life cycle. Consequently, this combined approach to treating EK may need to be more cost-effective (Ganbat et al., 2023; Wen et al., 2021). Recent research has significantly emphasized the development of environmentally sustainable methods to improve EK processes. Research into RFM-enhanced electrokinetics has yielded promising outcomes in various laboratory-scale tests, particularly when employing industrial or agricultural waste materials as the RFM. This approach offers practicality and sustainability by repurposing waste materials (Ganbat et al., 2023; Ghobadi et al., 2021a).

Tests involving RFM-improved EK processes have shown successful application in soils polluted with organic chemicals. For instance, carbonized food waste was utilized in EK processes for copper extraction, showcasing average treatment efficiencies ranging from 53.4% to 84.6% (Han et al., 2010). Compost was also used as an RFM in EK processes for copper removal in a laboratory-scale study, resulting in an impressive removal efficiency of 84.09%. After two cycles of renewal and reuse, the elimination effectiveness remained steady at 74.11% (Ghobadi et al., 2021b). RFMs present numerous advantages in EK processes, such as the adsorption, immobilization, or degradation of contaminants in situ without surface extraction (Cameselle and Reddy, 2012). In this context, investigators have investigated the application of cost-effective, environmentally compatible, and easy-to-regenerate RFMs, such as compost, biochar, and granular activated carbon, which serve as environmentally sustainable methods to improve the EK process (Ghobadi et al., 2021b, 2020). In another study, soil contaminated with heavy

metals from wastewater irrigation of arable lands was treated with charcoal adsorbent from rice stubble (Farhad et al., 2024).

This study utilizes sustainable sawdust (as a cellulose source)/iron slag hybrid RFM to remove copper from kaolinite and heavy metals from contaminated natural soil by the electrokinetic process. Kaolinite was used as a representative model soil to study the effect of experimental factors, without interferences of soil organic and inorganic substances, on the efficiency of the EK before its application to the soil obtained from a contaminated site. Copper was selected as the target contaminant, driven by its widespread presence in contaminated soil (Ghobadi et al., 2021b, 2020). Sawdust and iron slag, waste materials with outstanding adsorption capacity for heavy metals, were mixed to formulate an RFM of desirable physicochemical properties for heavy metals removal by the EK process. Although sawdust's poor conductance to electric current, the excellent electric conductivity of iron slag renders the RFM suitable for the EK application. The elevated alkalinity (pH of 11.38) of the RFM facilitates capturing metal ions but cannot deter the advancement of the alkaline front generated at the cathode. The iron slag/sawdust was crosslinked with glutaraldehyde, and sawdust was functionalized with HCl to enhance the RFM retention capacity to heavy metals and alkaline pH movement in the soil. The study's novelty lies in introducing an environmentally sustainable method of soil treatment by coupling the EK process with a hybrid organic-inorganic sawdust/iron slag RFM. Also, to develop an innovative technique to optimize the electrokinetic process for the removal of copper from kaolinite soil and heavy metal contaminants from natural soil. The research questions are: i) what is the comparative efficiency of removing copper ions from kaolinite with and without the sawdust/iron slag RFM? ii) how does crosslinked glutaraldehyde sawdust/iron slag RFM affect heavy metals adsorption and alkaline front movement in the soil? iii) what are the environmental

and soil remediation process implications of implementing the RFM-EK hybrid system? The experiments also explored the impact of electric current intensity and the duration of the EK process on copper extraction from kaolinite soil. The results of this research will provide insights into the most efficient RFMs for the removal of heavy metals from soil using EKR technology.

6.2. Materials

6.2.1. Sample Preparation

The kaolinite soil was sourced from Keane Ceramic Pty, Australia. This soil type was chosen as a standard material for conducting EK tests due to its well-characterized properties. This choice was made due to specific attributes of the soil, namely its minimal organic content, low permeability, and cation exchange capacity. While natural soil samples from the sub-surface at a depth of 15 to 20 cm were obtained from a contaminated site in Sydney (Australia), upon the removal of debris, roots, and stones, the soil was initially air-dried and subsequently sifted through a 600 μm sieve. **Table 6.1** provides detailed information on the characteristics of both the RFM, kaolin soil, and natural soil used in the experiments. The lack of organic matter and the inert nature of the kaolin soil render it exceptionally suitable for investigating the mobility of copper within the EK system under direct electric fields, free from external influences.

For the RFM, in this study, sawdust was combined with iron slag obtained from an electric arc steel-making furnace at InfraBuild, Australia, and sawdust from a construction project by the Labour Revolution Company, Australia. Electrical conductivity and pH level of the soil were measured using a multimeter model Thermo Scientific (EUTECH PC 450). The readings were acquired by formulating slurries with a dry soil-to-water ratio of 1:5 (weight-to-volume) (Ghobadi et al., 2020). A variety of analytical methods were used to investigate the physical and chemical characteristics of RFMs comprehensively. Data was

collected using Energy Dispersive X-ray Spectroscopy (EDX), Zeiss Evo-SEM, and Scanning Electron Microscopy (SEM) techniques. This combination allowed for comprehensive microchemical analysis. Shimadzu Miracle-10 instrument was employed for Fourier Transform Infrared Spectroscopy (FTIR) to examine the RFMs surface functional groups in pre and post-electrokinetic (EK) experiments. The analyses were conducted using a Micrometrics 3Flex surface characterization analyzer operating at 77K.

Table 6.1: Characteristics of RFM, Kaolin, and Natural soil.

Parameter	kaolin soil	Natural soil	Iron slag	Sawdust/Iron slag	Treated Sawdust/Iron slag	Crosslinked glutaraldehyde sawdust/Iron slag
Particle size analysis (%)						
Less than 1 mm	46.8	13.8	24.89	17.8	17.8	17.8
In between 1 to 2 mm	51.1	65.7	72.5	79.4	79.4	79.4
Greater than 2 mm	2.1	20.5	2.61	2.8	2.8	2.8
Permeability (m/s)	3.95×10^{-10}	1.0×10^{-6}	1.67×10^{-3}	2.35×10^{-2}	2.28×10^{-2}	2.36×10^{-2}
Density (g/cm^3)	1.35	1.42	2.45	1.52	1.51	1.65
TDS (mg/L)	144	303.6	461.5	350.7	348.9	139.4
pH	4.5 ± 0.04	4.76± 0.2	11.38± 0.04	10.19 ± 0.03	9.24 ± 0.03	9.55 ± 0.05
EC (mS/cm)	0.40 ± 0.05	0.292± 0.2	0.643± 0.02	0.557 ± 0.02	0.483 ± 0.02	1.478 ± 0.03
Elemental composition (%)						
C		5.85	-	-	-	-
O		91.29	-	-	-	-
Fe	Negligible	2.36	-	-	-	-
Others		1.2	-	-	-	-
Initial metal concentration (mg/kg)						
Cu	1000	216	-	-	-	-
Ni	-	581	-	-	-	-
Zn	-	733	-	-	-	-

6.2.2. EK cell experimental setup and design

The experimental arrangement for EK is depicted in **Figure 6.1**. EK experiments utilize a plexiglass reactor with dimensions (cm) of 23 L, 8 D x 11 W. This reactor is designed with two electrode compartments: one for soil and the other for RFM. Inside the soil

compartment, positioned at the boundary between the soil and the cathode chamber, a 1.5 to 2 cm RFM is placed between two filter papers. A perforated plexiglass plate reinforces the filter paper, size 5-13 μm (LLG Labware), acting as a barrier, separating the soil compartment from the electrode chamber to stop soil from infiltrating the electrolyte chambers. A steady electrical current was employed to uphold experimental integrity, facilitated by a direct current power supply, model EA-PS 3015-11B. Hourly measurements and recording of electric current and voltage were carried out by a multimeter (Keithley 175). The reactor's electrode compartments flanking the reactor were equipped with 15 cm x 1 cm (graphite rod electrodes) obtained from Graphite Australia Pty Ltd. Deionized water was employed in both the anolyte and catholyte chambers. To maintain water levels depleted by electroosmotic flow, periodic infusions of ultrapure water were added to the anolyte compartment. The experiment consistently monitored and measured the electroosmotic flow and current intensity. EK tests were conducted at room temperature in the laboratory using constant currents of 20 mA, 25 mA, and 30 mA without controlling the pH level. **Table 6.2** furnishes detailed information on the eight EK experiments. Milli-Q water served as the anolyte, and the solution level in the inflow reservoir was meticulously controlled to sustain a consistent level, ensuring a constant hydraulic gradient across the soil sample. The EK experiments persisted for durations spanning two to three weeks.

To assess the efficacy of the enhanced RFM-EK test, Exp1 served as a baseline experiment, focusing on Cu removal from kaolin soil without an RFM at 20 mA steady currents. Exp2 delved into the effect of a standalone iron slag RFM at 20 mA electric currents for copper extraction from the contaminated soil. Exp3 investigated the impact of a mixture of sawdust/iron slag-RFM at 20 mA current intensity. Exp4 and Exp5 studied the impact of raising the electric current from 20 mA to 30 mA on the efficiency of the

sawdust/iron slag RFM-EK system for copper treatment. Exp6 scrutinized the influence of treating sawdust with HCl to lower its pH in the sawdust/iron slag RFM-EK system at 25 mA electric currents for copper treatment. Exp7 studied glutaraldehyde (Sigma-Aldrich, Australia) crosslinking with sawdust in the RFM. A 2% glutaraldehyde was mixed with sawdust and iron slag to ensure homogeneity of the RFM in the EK process operating at a 25 mA electric current. The concentration of glutaraldehyde was 2% i) to reduce the environmental toxicity of glutaraldehyde, ii) to maintain a desirable biodegradability of glutaraldehyde compounds in soil, iii) over-crosslinking will reduce the RFM flexibility and surface area, block active functional groups, and change the surface charge of the crosslinked RFM. Finally, Exp8 utilized an RFM-EK process with sawdust/iron slag and 2% glutaraldehyde, conducted over 35 days for Cu^{2+}, Ni^{2+}, and Zn^{2+} mixture removal from a contaminated site. EK optimization considered the following critical operating factors: RFM use, electrical current, sawdust pH adjustment, and EK operating time.

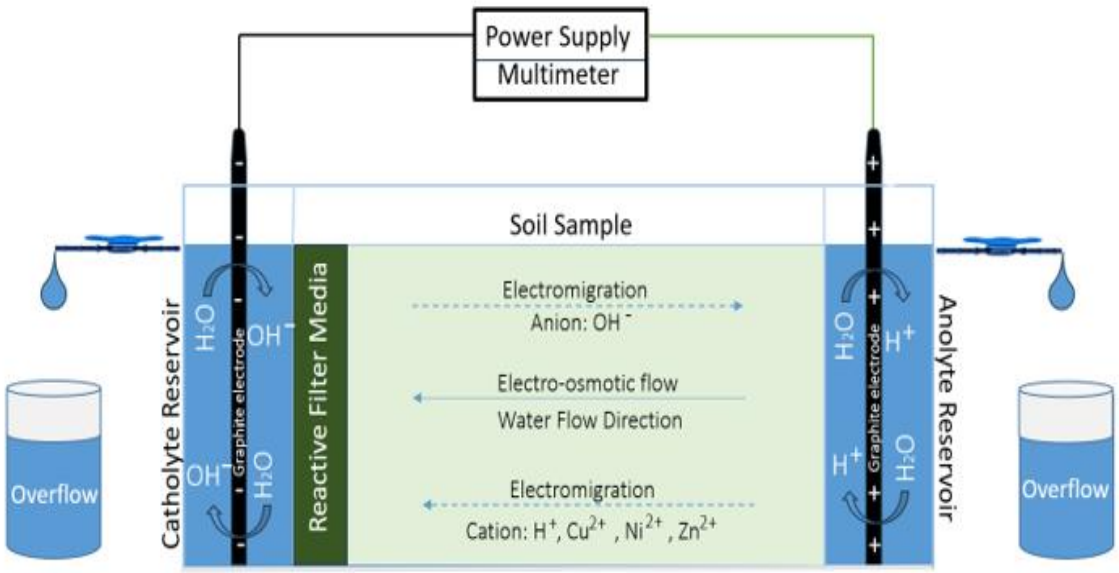

Figure 6.1: Schematic illustration of metal treatment by EK-RFM hybrid system.

Table 6.2: Description of the EK-RFM system.

Experiment	Type of soil	RFM type	Metals	Metal (mg/kg)	RFM	Current (mA)	Period (day)
Exp1	Kaolin Soil	EK only	Cu	1000	NA	20	14
Exp2	Kaolin Soil	EK- Iron slag	Cu	1000	100% Iron slag	20	14
Exp3	Kaolin Soil	EK- SD/Iron slag	Cu	1000	50% Sawdust+50% Iron slag	20	21
Exp4	Kaolin Soil	EK- SD/Iron slag	Cu	1000	50% Sawdust+50% Iron slag	25	21
Exp5	Kaolin Soil	EK- SD/Iron slag	Cu	1000	50% Sawdust+50% Iron slag	30	21
Exp6	Kaolin Soil	EK- TSD/Iron slag	Cu	1000	50% Treated Sawdust+50% Iron slag	25	21
Exp7	Kaolin Soil	EK- SD/Iron slag + GA	Cu	1000	50% Sawdust+50% Iron slag and 2% glutaraldehyde	25	21
Exp8	Natural Soil	EK- SD/Iron slag + GA	Cu, Ni, and Zn	216,581, and 733	50% Sawdust+50% Iron slag and 2% glutaraldehyde	25	35

6.3. Results and Discussion

6.3.1. The Electric Current

During water electrolysis, hydronium ions (H_3O^+) are generated at the anode, while hydroxide ions (OH^-) are produced at the cathode electrode. Consequently, an acid and alkaline front emerges, migrating toward their respective electrodes within the soil (Hamdi et al., 2024; Hawal et al., 2023). Acid front transport through the soil solubilizes metal ions and carries them toward the cathode. **Figure 6.2** illustrates soil voltage and electric current variations across different EK tests. A clear connection exists between the electric current and the quantity of electric charge moving through the soil pores, exhibiting an inverse relationship with the transfer of electrons (Hamdi et al., 2024; Hawal et al., 2023).

At the onset of different EK experiments, the initial electric currents were approximately 20 mA, 25 mA, and 30 mA (**Table 6.2**) and gradually declined after 48 to 96 hours. The correlation between the electric current in the soil's EK cell and the concentration of free ions underscores the significant impact of electric current on the movement of contaminants through the soil. The initial stability in electric current for several hours can be attributed to the occurring anode electrolysis reaction and the subsequent increase in dissolved ions within the solution pores. Nevertheless, an overtime decrease in electric current results from the merging of acid and alkaline fronts and the buildup of charged molecules within the soil sample. The reduction in charged particles in the soil led to a decrease in the electric current. Therefore, the presence of charged soil particles decreased, reducing the electric current (Ganbat et al., 2023, 2022; Hamdi et al., 2024; Hawal et al., 2023).

Figure 6.2a depicts a noticeable decline in electric current between 48 and 96 hours across Experiments 1-8. The most pronounced drop was observed in Exp1, conducted without RFM, facilitating alkaline front progression near the cathode zone within the soil. A similar trend was observed in Experiment 2, where all iron slag RFM was used. In this instance, after 72 hours of operation, the electrical current decreased from an initial 20 mA to 17 mA and further dropped to 3.10 mA after 240 hours. Subsequently, an unexpected increase occurred, rising to 4.20 mA after 264 hours and eventually reaching 4.80 mA by the end of the experiment, possibly attributed to the dissolution of ionic components due to the advancing acid front in the later stages of the EK test. Exp3 aimed to mitigate the progression of the alkaline front by utilizing a mixture of 50% sawdust (SD) and 50% iron slag, coupled with an extension of the EK duration to three weeks. During Experiment 3, which extended over three weeks and involved mixing iron slag with sawdust, the electric current held steady at 20 mA for 96 hours. The lower pH of

SD-iron slag RMF in Experiment Exp3 than in Exp2 suppressed the alkaline from movement in the soil and maintained the electric current for a longer time. Subsequently, electric current experienced a gradual decrease, dropping to 7.5 mA by the third week attributed to metal hydroxide precipitation and the interaction between alkaline and acid fronts in the soil.

Exp4 replicated the operating conditions of Exp3, with an increase in the electrical current to 25 mA to facilitate the acid front transport through the Kaolin soil. The electric current experienced a significant decline from 25 mA to 20.2 mA after 48 hours due to the precipitation of metal hydroxides and the convergence of the acid and alkaline fronts within the soil. Following this, it continued to decrease to 17.1 mA after 72 hours and ultimately reached 6 mA by the conclusion of the experiment. During Experiment 5, when the EK electric current was raised to 30 mA, it initially held at 29.49 mA for 24 hours, gradually decreased to 12.6 mA after 120 hours, and subsequently fluctuated between 9.10 and 11 mA. Exp6 was conducted at an electric current of 25 mA, treating sawdust with HCl to lower the pH of the RFM, aiming to mitigate the progression of the alkaline front in the soil. The maximum electric current reached 24.26 mA, slightly lower than that observed in Experiment 4. This reduction can be attributed to the reduced EC of the RFM used in Exp6 (**Table 6.1)**. Notably, there was a significant decline in the electric current, dropping from 24.26 mA to 15 mA after 96 hours. This decline likely resulted from the precipitation of metal hydroxides and the convergence of the acid and alkaline fronts. By the conclusion of Exp6, the electric current had decreased even further to 4.5 mA. Exp7 was conducted at 25 mA, using an RFM composed of a 50% sawdust (SD) and 50% iron slag mixture. The mixture was treated with a 2% glutaraldehyde to enhance its adsorption properties. The primary objective of this experiment was to mitigate the progression of the alkaline front in the soil, which is a common challenge in electrokinetic

treatments. The use of glutaraldehyde aimed to improve the structural integrity and reactivity of the RFM, enhancing its ability to capture and immobilize metal ions while controlling the pH changes in the soil section near the cathode. The electric current remained constant at 23 mA for 72 hours, then gradually decreased and stabilized at around 10 mA until the end of the experiment. In Exp8, conditions from Exp7 were replicated with a key modification that the duration was extended to 5 weeks, and natural soil replaced kaolinite to evaluate the effectiveness of the EK process in removing Cu^{2+}, Ni^{2+}, and Zn^{2+} ions from a contaminated site. The electric current initially dropped from 25 mA to 19.35 mA after 168 hours, then fluctuated slightly before declining again due to metal hydroxide precipitation and the convergence of acid and alkaline fronts in the soil. By the experiment's end, the current had decreased further to 6.45 mA.

As illustrated in **Figure 6.2b**, there is a discernible adverse correlation between the electric current and the voltage change. The precipitation of metal ions decreased the electric current while simultaneously leading to an increase in voltage, which can be attributed to the heightened soil resistivity. Across all EK tests, a consistent trend was observed wherein the voltage declined initially within the initial 24-hour period. This decline was probably attributed to the solubilization of metal ions and a subsequent rise in the concentration of ions within the soil's pore fluid. Initial voltage readings ranged from 10.44 to 20.5 V, declining to approximately 9 V after 24 hours.

Interestingly, a subsequent voltage surge to nearly 35.12 V was observed in Experiments 1, 2, 4, and 5 after 48 hours and in Experiments 3, 6, 7, and 8 after 120 hours. This increase was attributed to the greater soil conductivity and ionic strength observed in Experiments 3, 6, 7, and 8. Compared to standard processes, EK experiments involving RFM exhibited higher electric currents since the alkaline front movement was slowed down, preventing early metal ions precipitation in the soil.

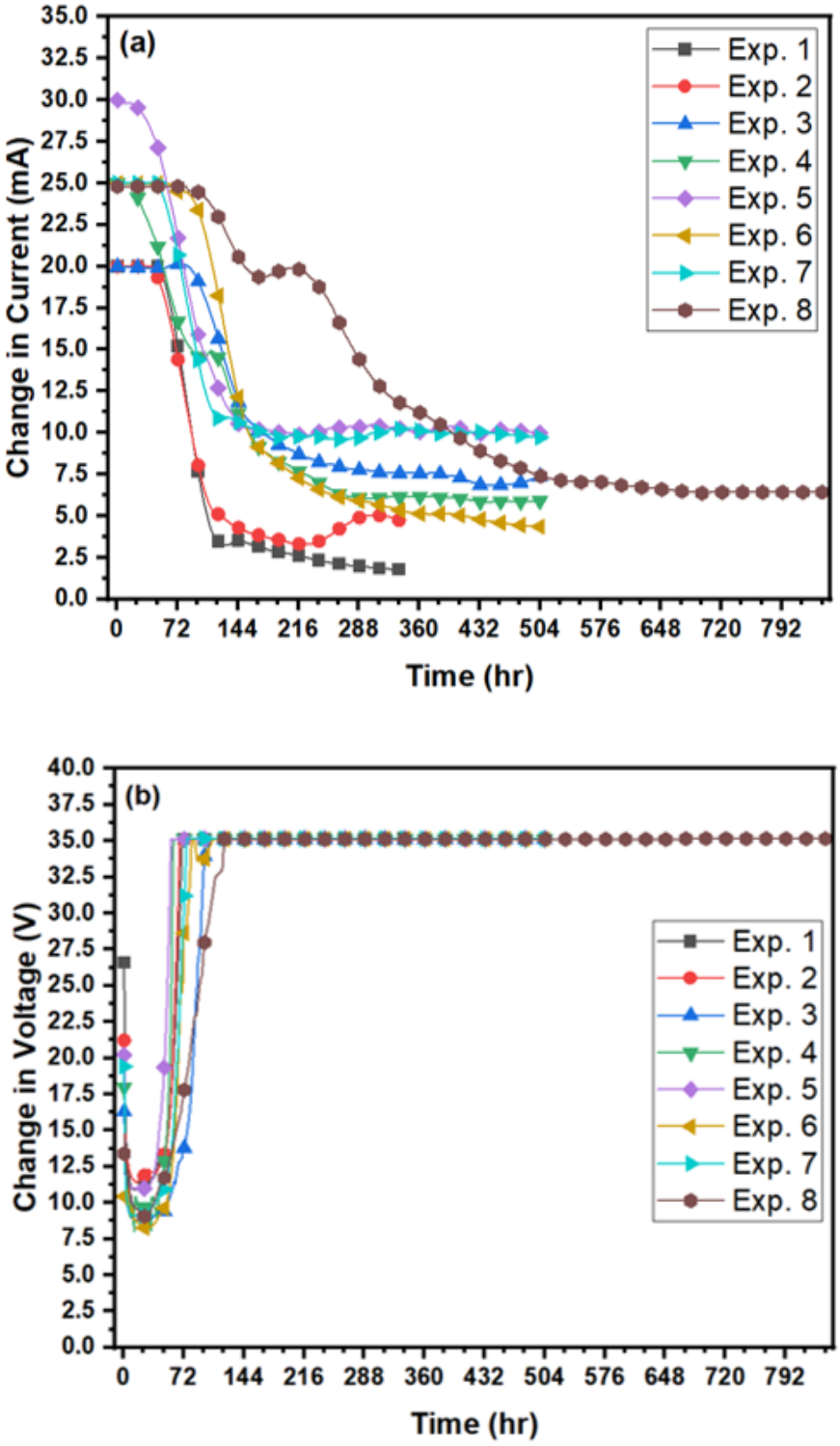

Figure 6.2: (a) Electric current variation during EK tests at 20, 25, and 30 mA. (b) Corresponding voltage changes, showing the influence of current and soil interactions on EK efficiency.

6.3.2. Electric conductivity and pH

Figure 6.3a illustrates the pH distribution across soil sections S1 through S6, ranging from the anode to the cathode, after the EK tests. It is essential to highlight that the EK tests were conducted without controlling the pH. By the conclusion of the EK treatment, the pH of the soil in regions proximal to the anode compartment decreased below the initial pH, subsequently increasing gradually towards the cathode zone. At the anode, soil sections S1 to S3 displayed acidity due to the advancement of the acid front resulting from electrolysis, leading to the generation of H^+ ions. This phenomenon is influenced by the higher ionic mobility of hydrogen ions, which move approximately 1.8 times faster than hydroxide ions (Ganbat et al., 2023; Ghobadi et al., 2021b).

Figure 6.3a represents pH differences in the soil sections Exp1 and RFM-enhanced Exp2 to Exp8. In Exp1, soil sections S1 to S5 consistently maintained acidic pH levels. In contrast, section S6, close to the cathode, recorded a pH of 6.5 due to the rapid migration of OH^- ions. On the contrary, in RFM-enhanced Exp2, a discernible pH increase is observed from the soil section S1 toward the RFM. The high pH of the RFM is due to its initial alkalinity of 11.38 (**Table 6.1)**, which negatively affected the transport of H^+ ions close to the cathode. Interestingly, the pH in the cathode tank remains stable at pH 12.71, while the pH of sections S4 to S6 adjacent to the cathode fluctuates. Specifically, in Exp2, the pH across soil sections S1 to S5 increased from 2.20 to 4.08. In contrast, the alkaline nature of the RFM facilitated the rapid migration of OH^- ions in the soil, resulting in section S6 reaching a pH of 7.04.

However, the incorporation of 50% sawdust into the iron slag RFM acted as a buffer, impeding the movement of alkaline pH toward the anode. Sawdust contains cellulose that interacts with hydroxyl ions in an alkaline solution, potentially reducing pH through

absorption. The cellulose hydroxyl groups have an affinity to the hydroxyl generated at the cathode, slowing down alkaline from movement in the soil. As a result, the acid front progressed faster towards the cathode in Exp3 compared to Exp2. In Exp3, pH levels ranged from 3.00 to 4.06 across soil sections S1 to S5, while section S6 reached a pH of 5.43. The lower pH of section S6 in Exp3 is attributed to the RFM pH of 10.19 compared to the RFM pH of 11.38 in Exp2. The lower RFM pH in Exp3 hindered the rapid movement of the alkaline front in the soil, thereby enabling the propagation of the acid front in soil section S6. In Exp4, the electrical current was increased to 25 mA. It was observed that there was a decrease in soil pH of sections S1 and S2, reaching pH 2.6, while for sections S3 to S6, the pH ranged between 3.15 and 4.60. Notably, the RFM's pH was 9.63, which decreased from the initial pH of 10.19. The decline in soil pH likely resulted from increased electrical currents, facilitating the movement of acidic components toward the cathode zone. However, raising the electric current to 30 mA in Exp5 slightly increased sections S1 and S2 pH to 3.15 compared to pH 2.6 in Exp4. For sections S3 to S6, the pH ranged between 3.70 and 4.80. Also, the pH of the RFM was 10.25 at the end of the test. In Exp6, the sawdust was treated with HCl to lower its pH from 8.11 to 5 before mixing with iron slag to reduce the RMF pH to 9.24 (**Table 6.1**). Sections S1 to S5 recorded pH values lower than the initial pH, ranging from 2.50 to 3.30, while section S6 showed a slightly higher pH than the initial value, measuring pH 4.57.

Nevertheless, the integration of 50% sawdust with 50% iron slag RFM and 2% Glutaraldehyde in Exp7 facilitated slowing down the advancement of the alkaline pH toward the anode. All sections from S1 to S6 exhibited pH levels lower than the initial value, ranging between 2.80 and 4.10. Compared to other experiments, Exp7 demonstrated the lowest range of pH level in S1-S6 because of the initial RFM low pH of 9.55, deterring alkaline front rapid movement in the soil and enabling the mobility of

H^+ ions toward the cathode. Notably, the elevated pH levels in soil sections adjacent to the cathode result in a negative soil surface charge, thereby enhancing the adsorption of Cu^{2+} through increased electrostatic interaction with the positively charged Cu^{2+} ions (Ghobadi et al., 2021b). In Exp8, the sawdust/iron slag was crosslinked with 2% Glutaraldehyde to effectively slow down the advancement of the alkaline pH toward the anode and reduce the RMF pH to 9.55 (**Table 6.1**). Sections S1 to S5 recorded pH values lower than the initial pH, ranging from 3.36 to 4.02, while section S6 showed a higher pH than the initial value, measuring pH 6.60.

As depicted in **Figure 6.3a**, in Exp1 without RFM, soil pH in sections (S1-S5) was acidic (ranging from pH 3.18 to pH 3.75) and increased toward the cathode, reaching pH 6.5 in section S6. In Exp2 (**Figure 6.3b**), the pHs of sections (S1-S5), from 2.20 to 4.08, were lower than the initial soil pH and increased to 7.04 in S6. The elevated pH level in the cathode zone of Exp2 is likely due to the higher iron slag content in the RFM. In **Figure 6.3c**, Exp3 displayed soil pH from 3.00 to 4.06 in sections (S1 to S5), increasing to pH 5.43 in section S6. The decrease in pH of soil S6 was likely due to the lower pH of the sawdust/iron slag RFM (10.19), contributing to the acid front advancement in the soil. In Exp4 (**Figure 6.3d**), sections (S1 to S5) recorded pH values from pH 2.49 to 3.73, slightly increasing to 4.60 in soil section S6 near the cathode. **Figure 6.3e** illustrates that in Exp5, the pH in sections (S1 to S5) ranged from pH 3.12 to 3.93, significantly increasing to pH 4.80 in section S6. Exp6 (**Figure 6.3f**) exhibited a low pH of 2.56 to 2.80 in soil sections S1 to S3, increasing to pH 3.14 and 3.29 in sections S4 and S5 and further increasing to pH 4.57 in section S6. Exp 7 (**Figure 6.3g**), the pH levels across sections (S1 to S6) were consistently low, ranging from 2.80 to 4.10, which was lower than the initial pH. In Exp8 (**Figure 6.3h**), the pH across sections S1 to S5 remained consistently low, ranging from 3.36 to 4.02, below the initial pH of 4.76 (**Table 6.1**), while section S6 pH was 6.60.

Prior studies corroborate these results, suggesting an inverse relationship between soil pH and soil electrical conductivity (EC) (Ghobadi et al., 2021b, 2021a; Hamdi et al., 2024). The EC of soil is pivotal in the electrokinetic (EK) process, facilitating the migration of pollutants and charged particles in response to direct electric current. Throughout the EK process, the migration of charged particles towards the positive and negative electrodes establishes a gradient in concentration, influencing soil resistivity and pH modification. When the soil has high electrical conductivity (EC), it can conduct electrical charges. However, the removal of ionic species during EK treatment can lead to a decrease in EC. In this study, an SD-iron slag, strategically placed near the cathode to capture metal ions and prevent the advancement of an alkaline front, exhibited slightly higher conductivity than the kaolinite soil (**Table 6.1**). **Figure 6.3** indicates a lower EC in soil with low ion concentrations. Soil's EC exhibited a consistent decrease from the anode to the cathode zone across Exp1 to Exp8, indicating a higher concentration of free ions near the anode. Generally, using RFM with acid-treated sawdust mixed with iron slag assisted in maintaining the soil pH below the initial levels in all sections and prevented the advancement of the alkaline front in the soil (**Figure 6.3f**). The EC of soil S1-S3 in all EK experiments increased, resulting from the increase of ionic species, notably associated with free protons. Across all experiments, a decline in EC was observed in soil S4-S6, attributed to the convergence of acid and alkaline fronts close to the cathode zone.

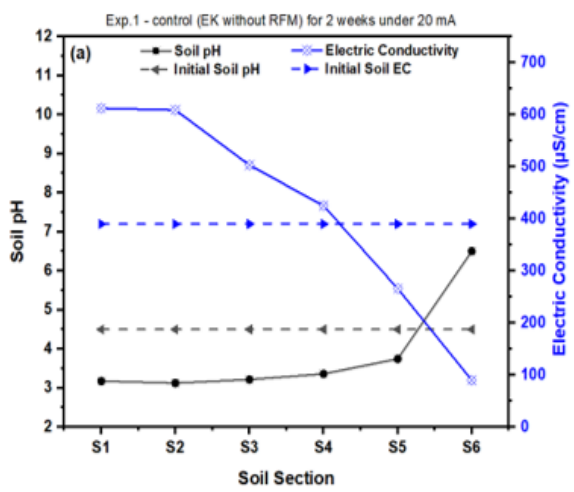
Exp.1 - control (EK without RFM) for 2 weeks under 20 mA
(a)
Soil pH
Initial Soil pH
Electric Conductivity
Initial Soil EC
Soil pH
Electric Conductivity (µS/cm)
S1
S2
S3
S4
S5
S6
Soil Section

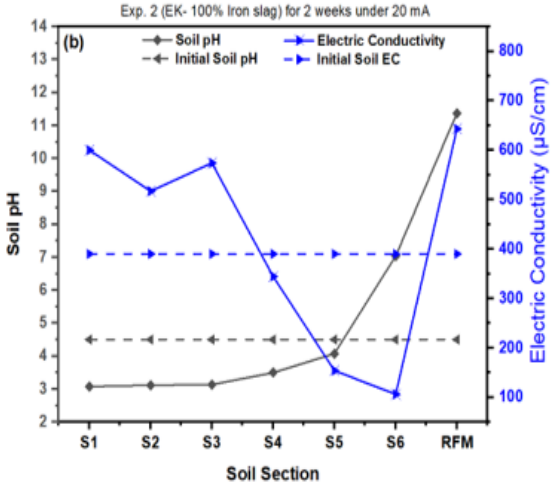
Exp. 2 (EK- 100% Iron slag) for 2 weeks under 20 mA
(b)
Soil pH
Initial Soil pH
Electric Conductivity
Initial Soil EC
Soil pH
Electric Conductivity (µS/cm)
S1
S2
S3
S4
S5
S6
RFM
Soil Section

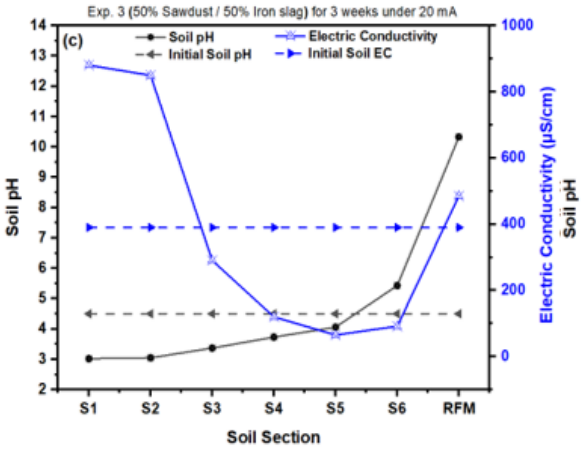
Exp. 3 (50% Sawdust / 50% Iron slag) for 3 weeks under 20 mA
(c)
Soil pH
Initial Soil pH
Electric Conductivity
Initial Soil EC
Soil pH
Electric Conductivity (µS/cm)
S1
S2
S3
S4
S5
S6
RFM
Soil Section

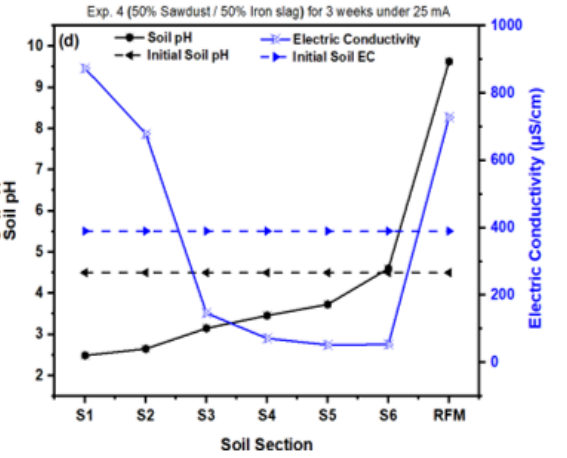
Exp. 4 (50% Sawdust / 50% Iron slag) for 3 weeks under 25 mA
(d)
Soil pH
Initial Soil pH
Electric Conductivity
Initial Soil EC
Soil pH
Electric Conductivity (µS/cm)
S1
S2
S3
S4
S5
S6
RFM
Soil Section

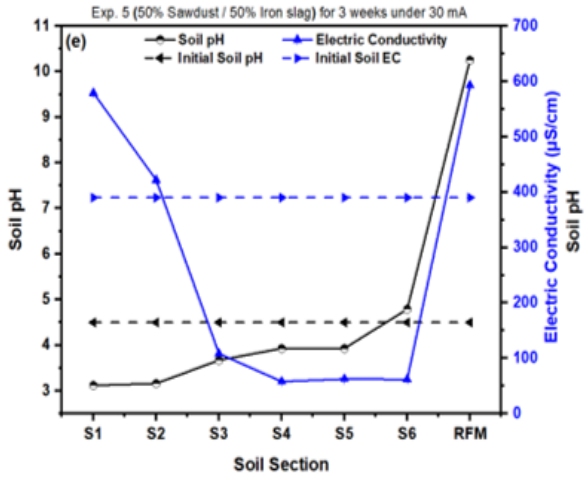
Exp. 5 (50% Sawdust / 50% Iron slag) for 3 weeks under 30 mA
(e)
Soil pH
Initial Soil pH
Electric Conductivity
Initial Soil EC
Soil pH
Electric Conductivity (µS/cm)
S1
S2
S3
S4
S5
S6
RFM
Soil Section

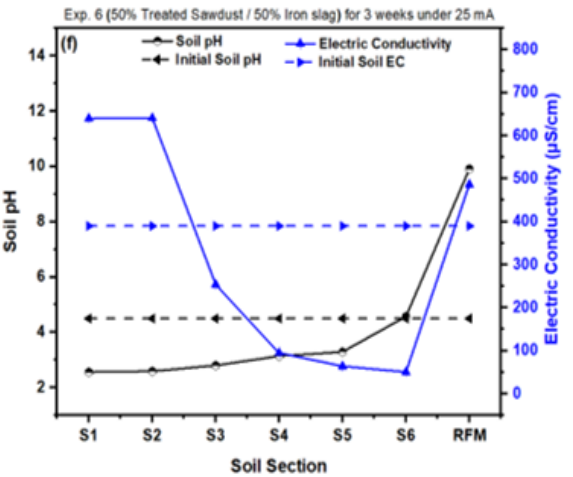
Exp. 6 (50% Treated Sawdust / 50% Iron slag) for 3 weeks under 25 mA
(f)
Soil pH
Initial Soil pH
Electric Conductivity
Initial Soil EC
Soil pH
Electric Conductivity (µS/cm)
S1
S2
S3
S4
S5
S6
RFM
Soil Section

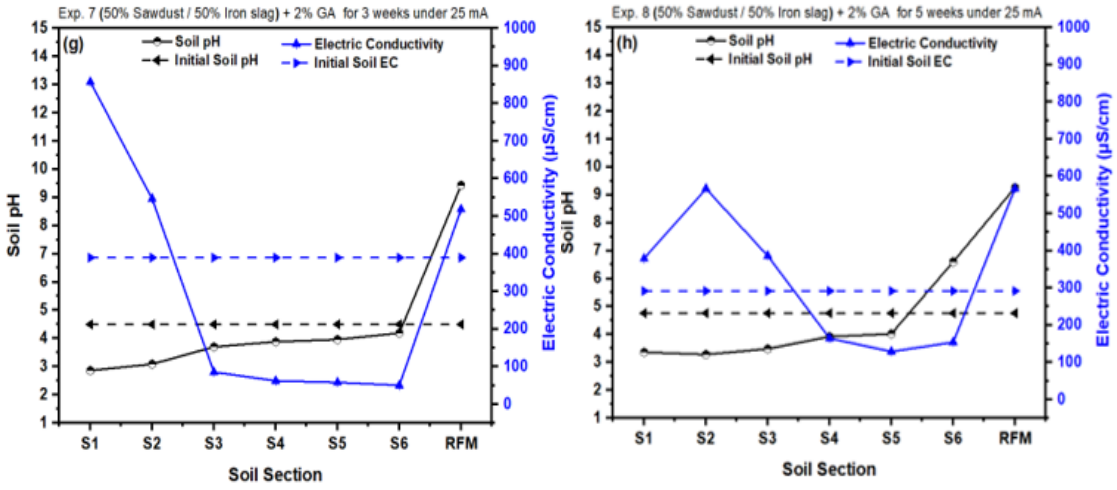

Figure 6.3: pH and EC of the soil post-remediation across the sections from the anode to the cathode (a) Exp1 (control) (b) Exp2 (c) Exp3 (d) Exp4 (e) Exp5 (f) Exp6 (g) Exp7 (h) Exp8.

6.3.3. Removal of contaminant

Figure 6.4a shows the distribution of Cu^{2+} across kaolinite soil sections and the RFM, while **Figure 6.4b** presents the distribution of Cu^{2+}, Ni^{2+}, and Zn^{2+} ions across natural soil sections and the RFM at the end of the EK process. The positively charged Cu^{2+}, Ni^{2+}, and Zn^{2+} ions dissolved and migrated toward the cathode. In the Ek tests without RFM, significant deposition of Cu^{2+} occurred near the cathode due to the alkaline pH, leading to the precipitation of metal hydroxides (Ghobadi et al., 2021b, 2021a; Hamdi et al., 2024; Hawal et al., 2023). Based on these results, iron slag and sawdust/iron slag RFMs were employed to capture metal ions in experiments Exp2 to Exp8. **Figures 6.4a&6.4b** show a substantial Cu^{2+}, Ni^{2+}, and Zn^{2+} migration and accumulation near the soil section 6 and in the RFM.

Exp1 to Exp7 were conducted to extract Cu^{2+} ions from the polluted kaolinite soil, and Exp8 was conducted to extract Cu^{2+}, Ni^{2+}, and Zn^{2+} ions from a contaminated site (**Table 6.2**). In Exp1 to Exp3, an electric current was 20 mA, while Exp4, Exp6, Exp7, and Exp8

employed 25 mA, and Exp5 used 30 mA to study the impact of increasing electric current and RFM on EK performance. Exp1 and Exp2 had a duration of 2 weeks, whereas Exp3 to Exp7 were carried out over 3 weeks, and Exp8 was 5 weeks with natural soil. In Exp1, copper concentration was nearly eliminated from section S1, gradually increasing across sections S2-5 and spiking to 3486 mg. L^{-1} in section S6 (**Figure 6.4a**). Nevertheless, the total depletion of copper from the soil amounted to approximately 3.21% (**Figure 6.4c**). In Exp2, iron slag RFM closed to the cathode notably boosted the removal of Cu^{2+} throughout soil sections S1 to S5. A considerable amount of copper precipitated in section S6, which is attributed to the alkaline pH of the soil. The concentration of Copper ranged from 44 mg. L^{-1} in S1 to 4242 mg. L^{-1} in S6. The alkaline conditions in S6 promoted the precipitation and adsorption of copper onto the soil surface. The correlation between soil pH and Cu^{2+} adsorption confirms that Cu^{2+} adsorption is pH-dependent (Ghobadi et al., 2021b; Hamdi et al., 2024). When pH levels fall below the point of zero charge (pHzpc), the soil exhibits a positive charge, which shifts to a negative charge as the pH surpasses the pHzpc. Cu^{2+} adsorption intensifies when the soil exhibits a negative charge near the cathode region, characterized by a pH higher than the pHzpc of 4.5. Conversely, Cu adsorption diminishes in the vicinity of the cathode area due to the elevated soil pH, exceeding the pHzpc of 4.5. Only 216.4 mg. L^{-1} of copper concentration was detected in the iron slag RFM. Iron oxide, the predominant component of iron slag, demonstrates a strong affinity for adsorbing heavy metals (Yeongkyoo, 2018). Iron oxide retains heavy metals through mechanisms such as surface complexation, electrostatic interactions, and precipitation (Hu et al., 2018). While achieving a higher rate of removing copper (seven times higher than Exp1), Exp2 still exhibited a relatively low removal efficiency, capturing approximately 21.76% of the Cu^{2+} in the RFM (**Table 6.3**). Moreover, the alkaline pH of RFM promoted the movement and propagation of OH^- ions from the

cathode to the anode. Exp3 utilized sawdust with iron slag to reduce the RFM pH from 11.38 to 10.19, slowing the rapid movement of the alkaline front from the cathode (**Table 6.1**). Sawdust also releases acidic components when exposed to hydroxyl ions. Its alkaline nature helps neutralize excess hydroxyl ions, maintaining a stable pH environment. Exp3 achieved a notable removal improvement of copper across the majority of soil sections, with 67.66% of the copper accumulating in the RFM and achieving an overall removal rate of 71.8% (**Table 6.3**). The concentration of copper decreased from 21.5 mg. L^{-1} in soil S1 to 1539.5 mg. L^{-1} in S6, achieving 5638.5 mg. L^{-1} in the RFM (**Figure 6.4a**). The predominant acidic conditions observed in the majority of soil sections during Exp3 significantly improved the extraction of copper compared to Exp2.

The electric current was increased in Exp4 to Exp8 to enhance the electrolysis reaction and copper, nickel and zinc removal from the soil. As depicted in **Figures 6.4a&6.4b**, copper was extracted from soil S1-6 and gathered in the RFM during Exp4. Copper concentration in S1 was 16 mg. L^{-1} and increased incrementally in subsequent sections, peaking at 646.5 mg. L^{-1} in S6 and reaching 6801.5 mg. L^{-1} in the RFM. Approximately 82.22% of the copper was retained in the RFM (**Table 6.3**), resulting in an overall copper removal rate of 88.10% for Exp4. The improved extraction of copper noted in Exp4, compared to Exp3, was attributed to the rise in electric current from 20 to 25 mA. This increase effectively bolstered the progression of the acid front within the soil. Consequently, the acid front propagated through the soil, solubilizing and transporting the copper ions towards the RFM. Increasing the electrical current from 25 mA to 30 mA in Exp5 did not lead to a significant improvement in copper concentration **(Figure 6.4a)**. The copper concentration for sections S1 to S6 was slightly less than that for the soil sections in Exp 4, and it reached 6939 mg. L^{-1} in S6. The RFM accumulated 83.27% of the copper, resulting in a total copper removal of 88.91% by the end of Exp5 (**Table 6.3**),

approximately 1% higher than in Exp4. EK experiments show that increasing the electric current from 25 mA to 30 mA led to only a slight improvement in copper removal (< 1%) from 88.10% to 88.91%, highlighting a non-linear relationship between current intensity and EK efficiency. While higher currents can boost ion migration and electroosmotic flow, they also intensify water electrolysis, creating sharp pH gradients that may cause Cu^{2+} precipitation or immobilization before reaching the RFM. Additionally, increased current raises energy consumption and costs without proportional gains in performance. Issues like electrode polarization and overheating may also arise. The results suggest that a 25 mA electric current is more effective for running the EK-RFM system, while a higher electric current offers no benefit. Thus, careful current optimization is crucial to balance efficiency, energy use, and system stability. Therefore, Exp6 was conducted at 25 mA electric current, with sawdust treated with HCl to lower the pH of the RFM, aimed at buffering the advancement of the alkaline front. The concentration of Cu^{2+} in (S1) was 15.5 mg. L^{-1} and increased to 490 mg. L^{-1} in S6 while reaching 7011.5 mg. L^{-1} in the RFM, as shown in **Figure 6.4a**. The RFM accumulated 84.14% of the copper, resulting in a total copper removal of 90.30% at the end of the 3-week EK process (**Figure 6.4c**). In addition, the introduction of glutaraldehyde to sawdust/iron slag RFM in Exp7 significantly improved the efficiency of Cu^{2+} removal. Glutaraldehyde created a homogenized and reactive composite material, enhancing the adsorption capacity of the sawdust/iron slag RFM (**Figure 6.6c**), leading to more effective immobilization of Cu^{+2}, thereby increasing the overall efficiency of the EK process compared to experiments Exp1 to Exp6. Introducing glutaraldehyde in Exp7 modified the surface property of RFM by increasing surface polarity and enhancing interactions with OH^- ions through hydrogen bonding or electrostatic attraction. Thus impeding alkaline front migration toward the anode and maintaining a lower pH throughout the experiment. This reduction in pH was responsible for enhancing the removal of Cu^{2+}, creating an acidic environment conducive to the dissolution and

migration of metal ions, and ultimately improving the efficiency of the EK process. The concentration of copper in S1 was 0.155 mg. L^{-1} and increased to 123.5 mg. L^{-1} in S6 while reaching 8133.5 mg. L^{-1} in the RFM (**Figure 6.4a)**. The RFM captured 97.60% of the Cu^{2+}, resulting in 97.92% removal (**Table 6.3**).

Exp8 evaluated the effectiveness of the EK combined with sawdust with iron slag RFM and glutaraldehyde for Cu^{2+}, Ni^{2+}, and Zn^{2+} ions removal from contaminated soil. The concentrations of Cu^{2+}, Ni^{2+}, and Zn^{2+} were 216, 581, and 733 mg. L^{-1}, respectively (**Table 6.1**). The concentration of Cu^{2+} in soil sections S1 to S6 ranged from 35.5 to 291.5 mg. L^{-1}, while Ni^{2+} and Zn^{2+} concentrations were lower than Cu^{2+}. Ni^{2+} concentrations ranged from 4.75 mg. L^{-1} in S1 to 1107.5 mg. L^{-1} in S6 and Zn^{2+} concentrations ranged from 5.5 mg. L^{-1} in S1 to 1305 mg. L^{-1} in S6. The concentrations of Cu^{2+}, Ni^{2+}, and Zn^{2+} in the RFM were measured at 199, 1469.5, and 1984.5 mg. L^{-1}. The RFM was effective in capturing 21.03% of Cu^{2+}, 50.58% of Ni^{2+}, and 54.14% of Zn^{2+} (**Table 6.3**), achieving 26.72%, 54.36%, and 56.44% removal for Cu^{2+}, Ni^{2+}, and Zn^{2+} by the end of the EK process (**Figure 6.4c**).

The application of sawdust-iron slag RFM significantly enhanced copper removal across Experiments 3 to 7. Initially, copper removal was 3.21% in Exp1, increasing to 23.76% in Exp2 with the introduction of iron slag RFM. Exp3 demonstrated further improvement in copper removal by combining sawdust with iron slag, leveraging sawdust's affinity for alkaline pH. In Exp4, increasing the electric current to 25 mA achieved 88.10% removal. Exp5 showed marginal enhancement in copper elimination with an electric current of 30 mA, indicating non-linear effects that should be optimized during the EK process. Exp6, where sawdust was treated with HCl to lower RFM pH, achieved a total copper removal of 90.30%. Exp7, the integration of sawdust with iron slag RFM and glutaraldehyde effectively slowed down the advancement of the alkaline pH towards the anode, achieving

a total copper removal of 97.92%. These results highlight the critical role of optimizing both the electric current and the process duration to achieve the desired removal rates efficiently. In Exp8, the crosslinked sawdust/iron slag RFM-EK system achieved 26.72%, 54.36%, and 56.44% removal, respectively.

While EK tests with kaolinite achieved excellent removal of metal ions, the decontamination of real soils is far more complex due to the presence of organic matter, microbial activity, and mineralogy that can affect metal mobility and binding. These factors may reduce the decontamination efficiency by altering metal behavior. Since heavy metals removal from the soil is a dynamic process during the EK process, the efficiency of the EK will be affected by several factors, such as various in the pH of the soil and other organic and inorganic metal ions in the soil that may interfere with the removal of metal ions. Therefore, pilot-scale studies in heterogeneous soils are essential to assess the practical applicability of the EK-RFM system under realistic conditions.

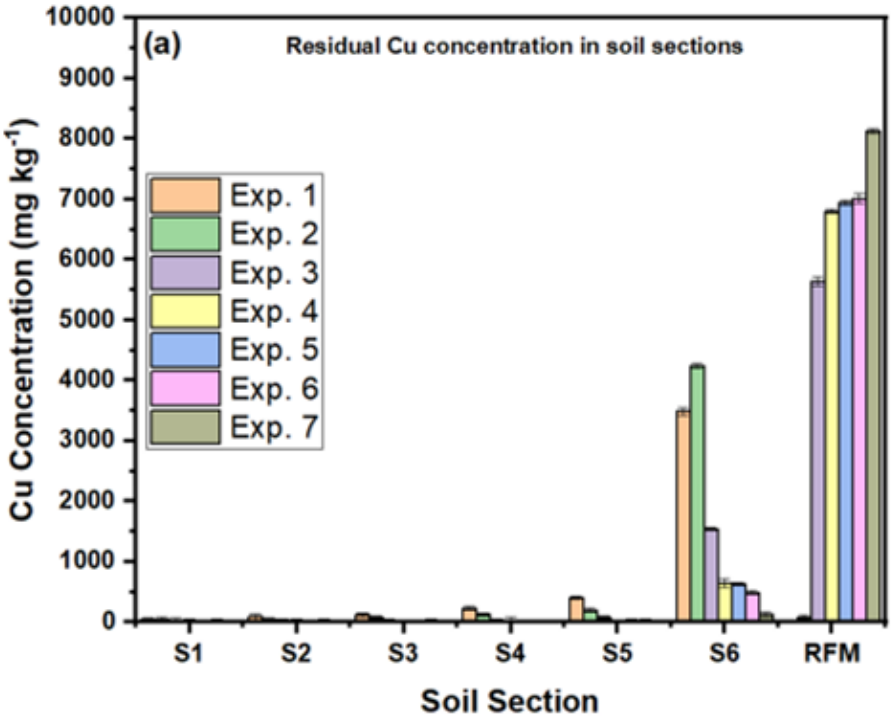

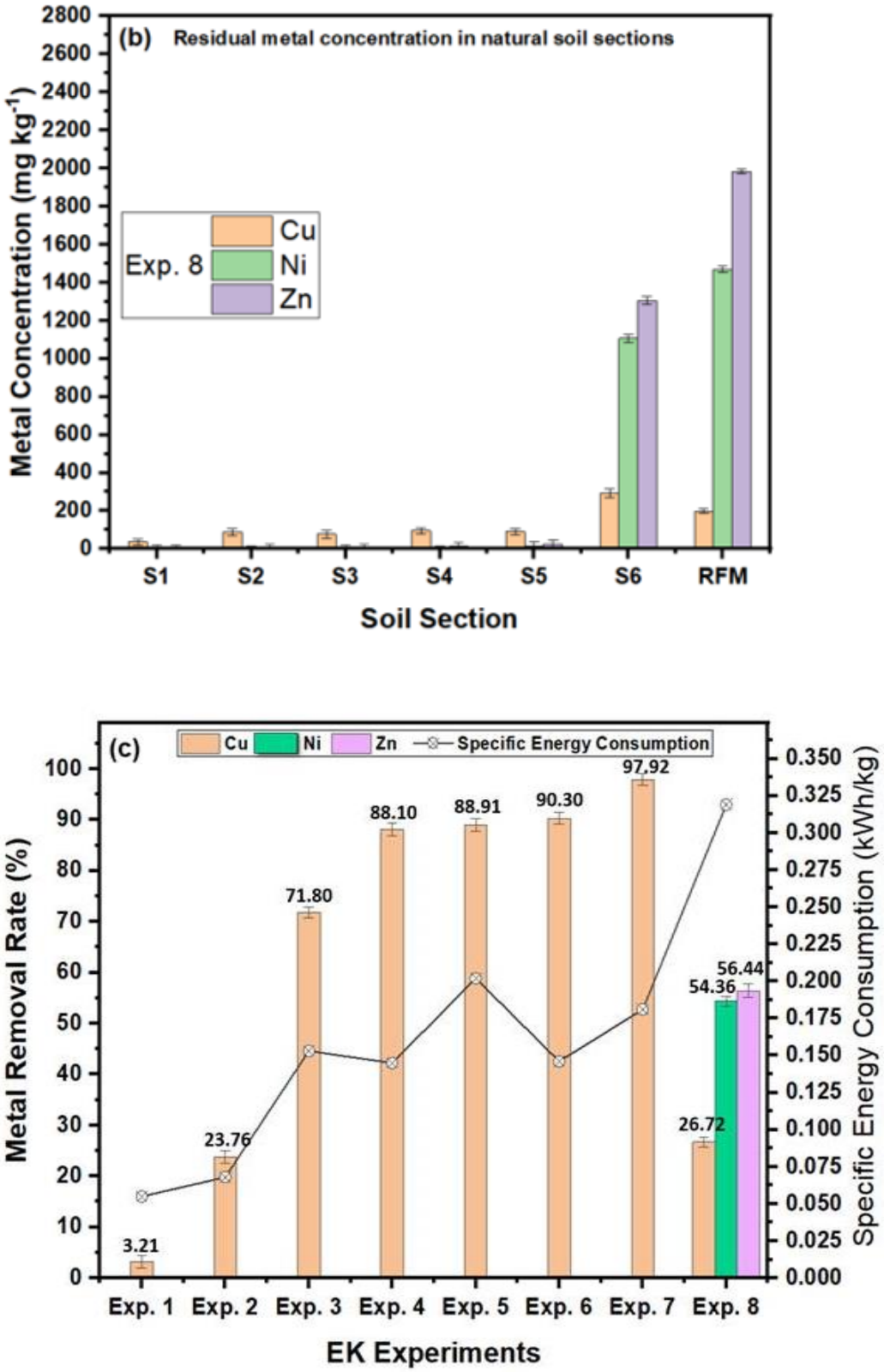

Figure 6.4: (a&b) Residual metal concentration in soil sections/RFM after EK, and (c) Total metal removal/Specific Energy Consumption at the end of the EK.

Table 6.3: Removal efficiency and Mass Balance of EK experiments.

Exp No	Type of soil	Metal ions	Initial Metal in soil (mg)	Residual Metal in Soil (mg)	Metal in RFM (mg)	Electrolyte/ pore water Metal (mg)	Mass Balance (%)	Total metal removal (%)
Exp1	Kaolin Soil	Cu	1000	968.19	N/A	1.5	102.17	3.21±0.31
Exp2	Kaolin Soil	Cu	1000	761.94	216.4	0	101.72	23.76±0.38
Exp3	Kaolin Soil	Cu	1000	281.50	676.62	4.5	101.15	71.80±0.19
Exp4	Kaolin Soil	Cu	1000	118.58	822.18	4.5	102.50	88.10±0.30
Exp5	Kaolin Soil	Cu	1000	111.00	832.68	1	101.88	88.91±0.24
Exp6	Kaolin Soil	Cu	1000	97.25	841.38	1.5	102.48	90.30±0.20
Exp7	Kaolin Soil	Cu	1000	20.82	976.02	0.5	100.29	97.92±0.23
		Cu	216	158.29	209.69	0.2	103.30	26.72±0.26
Exp8	Natural Soil	Ni	581	265.14	505.85	0.1	101.92	54.36±0.25
		Zn	733	319.27	514.41	0.1	100.80	56.44±0.29

6.3.4. Specific Energy Consumption

It is essential to determine the specific energy consumption (SEC) to evaluate the overall energy usage and treatment expenses, as described in **Equation 3.6.** This equation computes the SEC across all experimental scenarios (Ghobadi et al., 2021a, 2021b). The fluctuations in the copper removal (Cu^{2+}) and the corresponding energy requirement

throughout the RFM-EK experiments are shown in **Figure 6.4c**. These variations are illustrated across different experimental conditions in **Table 6.2**. The investigation examined how higher electrical current and extended processing time affect the removal rate of Cu^{2+} and energy consumption. A thorough examination of these factors was conducted, and their influence is depicted in **Figure 6.4c**. Substantial Cu^{2+} removal was observed across all tests, and the power consumption analysis revealed a notable increase in energy requirements of the EK process when the electrical current changed from 20 mA to 30 mA in Exp3 to Exp5.

A comparison of Exp 3 and Exp 4 revealed a general increase in the removal rate of Cu^{2+} with the transition of the electrical current from 20 mA to 25 mA at the experiment's outset. Notably, the improvement in copper removal coincided with an energy consumption decrease from 0.153 kWh. Kg^{-1} to 0.145 kWh. Kg^{-1}. As the electrical current was increased to 30 mA in Exp5, the energy consumption reached 0.202 kWh/kg, with a slight increase in the Cu^{2+} removal from 88.1% in Exp4 to 88.91 in Exp5.

In contrast, the energy consumption in Exp6 conducted at 25 mA electric current was 0.146 kWh/kg, and total copper removal reached 90.30%. Results reveal that Exp6 achieved higher Cu^{2+} removal than Exp4, conducted at the same electric current, but energy consumption was the same in both experiments. Contrarily, the Cu^{2+} removal increased at 25 mA in Exp4 compared to 30 mA in Exp5; all was achieved at higher energy consumption (**Figure 6.4c**). The higher SEC in Exp8 is attributed to the greater complexity of heavy metals removal from contaminated sites where soil heterogeneity, elevated organic content, and stronger metal-binding properties increase resistance to EK treatment, necessitating more energy to disrupt these bonds. The presence of competing ions and the longer treatment duration (35 days) further raised energy requirements, leading to a substantial SEC increase relative to kaolinite-based experiments.

6.3.5. Characteristics of RFM

Sawdust garners significant attention among agricultural byproducts due to its cost-effectiveness and remarkable efficacy in eliminating heavy metals from wastewater. Its composition, comprising cellulose, lignin, and carboxyl groups, enhances its capacity to attract cations to its active sites, rendering it an intriguing candidate for water purification purposes. The heavy metals' adsorption onto sawdust follows the Freundlich or Langmuir isotherms, demonstrating the potential for adsorption in single-layer and multiple-layer arrangements. Typically, the adsorption mechanism on sawdust follows the pseudo-second-order kinetic model, indicating a chemisorption process (Meez et al., 2021). Treatment with glutaraldehyde crosslinks the hydroxyl groups in sawdust, enhancing its structural integrity, reducing biodegradability, and introducing aldehyde (-CHO) groups that further facilitate metal binding. Acid treatment, typically using dilute mineral acids, removes impurities, increases the surface area, and exposes more reactive sites on both sawdust and iron slag. These chemical modifications improve the material's porosity, surface reactivity, and overall metal uptake capacity, thereby increasing the effectiveness and durability of the RFM in copper removal. Moreover, iron slag exhibits notable features of excellent specific surface area and significant porosity, making it a cost-effective adsorbent for soil treatment. The efficacy of iron slag in metal ions removal depends on its distinctive properties and chemical composition (Ganbat et al., 2023; Hamdi et al., 2024). This investigation employed a blend of sawdust and iron slag RFM to maximize Cu^{2+} adsorption by the RFM. Ligning in the sawdust contains hydroxyl, carboxyl, and methoxy groups, which can act as binding sites for heavy metal ions through complexation. Interaction between copper and ligning can involve coordination between the metal ions and the oxygen atoms in the functional groups of lignin, forming complexes known as chelates. These chelates are typically more stable than simple ion

interactions. Further, oxides and hydroxides functional groups in iron slag adsorb copper iron through electrostatic attraction and complexation reactions. Iron slag also induces copper precipitation due to its alkaline pH (**Table 6.1**).

Figure 6.5a displays the outcomes of X-ray diffraction (XRD) analysis regarding the iron slag's composition originating from the steel-making procedure. The data indicate that iron oxide is the primary component in the slag waste matrix. Iron oxide exhibits notable adsorption capabilities, effectively removing contaminants (Díaz-Piloneta et al., 2022). Although the specific mechanism by which heavy metals interact with iron oxide is still being studied, it is known that iron oxide can bind to or adsorb these elements on its surface. This ability is attributed to iron oxide's inherent properties, including its infinitesimal particles and notable porous nature that provide a substantial surface area, making it a remarkable RFM. Heavy metal adsorption onto iron oxide is characterized by electrostatic interactions among the metal molecules, which are subsequently followed by developing inner-sphere Fe-carboxylate complexes via ligand exchange (Jain et al., 2018).

Figure 6.5b illustrates the FTIR spectra of untreated RFMs, iron-slag-treated RFM, sawdust/iron-slag-treated RFM, and treated sawdust/iron RFM. The FTIR bands of iron slag, sawdust/iron slag, treated sawdust/iron, and sawdust/iron slag with 2% glutaraldehyde before and after EK treatment showed comparable features. Nevertheless, the bands exhibited greater prominence in the sawdust/iron slag both before and after EK treatment, underscoring the considerable efficacy of EK-treated sawdust/iron slag in removing Cu^{2+}. Following EK tests, the FTIR bands of slag, sawdust/slag, and treated sawdust/slag (**Figure 6.5b**) displayed peaks in 3787, 3743, 1603, and 1525 cm^{-1} regions, indicative of OH^- stretch. The band 3787 cm^{-1} showed diminished intensity in Exp2, although it exhibited similar stretching in most EK tests. The band 3743 cm^{-1} intensity,

to some extent, increased after the EK treatment in Exp5 and Exp6, attributed to added OH^- groups introduced by the sawdust/slag, causing intensity changes. In all experiments, there was no observable alteration in this band when the soil was treated with sawdust or iron slag. Additionally, in Experiment 2 with iron slag RFM, the FTIR band at 1603 cm^{-1} decreased.

Figures 6.5c to 6.5x present the results of the scanning electron microscope (SEM) with energy-dispersive X-ray spectroscopy (EDS) analysis performed on various configurations of RFM, including iron slag, sawdust/iron slag, treated sawdust/iron slag, and sawdust/iron slag mixed with a 2% glutaraldehyde solution. These analyses were conducted before and after the EK treatment to examine the changes in surface morphology. In **Figure 6.5k**, the SEM analysis of the iron slag RFM exhibits semi-smooth surfaces and solid structures after the EK treatment. In contrast, **Figures 6.5m to 6.5r** display rougher surfaces for the sawdust/iron slag combination after the EK treatment. **Figure 6.5s** shows similar rough surfaces for the treated sawdust/iron slag. These observations suggest that the treatment led to an increase in the surface area of the sawdust/iron slag, thereby enhancing its sorption capacity. The rougher surface morphology indicates that the material's ability to adsorb contaminants was improved due to the increased surface area available for interaction. The treatment of sawdust/iron slag with 2% glutaraldehyde solution enhances its surface properties, making it more effective for contaminant adsorption. The aldehyde groups in glutaraldehyde likely react with functional groups on the sawdust and iron slag, such as hydroxyl and carboxyl groups, leading to cross-linking or chemical modification. This process can result in the formation of additional active sites and a more uniform surface morphology, as observed in **Figure 6.5u to 6.5x**.

Generally, sawdust possesses a porous structure ideal for adsorption applications, enabling it to bind heavy metal ions effectively. Its efficacy as an adsorbent in heavy metal removal has been well-established in wastewater treatment (Božić et al., 2009; Meez et al., 2021). Sawdust is also characterized by its composition, which includes cellulose, lignin, and carboxyl groups, which enhances its ability to homogenize with iron slag. Iron slag also has features that contribute to the homogenization process, including its high surface area and extensive porosity. These properties make it a desirable choice as a material that can be homogenized with other materials. However, the introduction of 2% glutaraldehyde into sawdust and iron slag significantly improved the adsorption process and Cu^{2+} removal efficiency. The glutaraldehyde helped to form a more homogeneous and reactive composite material, which enhanced the adsorption capacities of the sawdust and iron slag, resulting in a more effective stabilization of Cu^{+2}, thus increasing the overall efficiency of the electrical process comparatively. The comparative analysis confirmed that the glutaraldehyde-treated composite exhibited superior adsorption capacity compared to untreated combinations of sawdust and iron slag or their components. This indicates that glutaraldehyde not only enhances surface properties but also promotes synergistic effects within the composite, making it an effective solution for heavy metal remediation in EK systems, as observed in **Figure 6.6c**. The glutaraldehyde also contributed to the pH reduction by crosslinking with the cellulose in the sawdust. This crosslinking process likely stabilizes the RFM mixture, thus reducing alkaline migration toward the anode and maintaining a lower pH throughout the experiment. This decrease in pH can be beneficial to enhance the removal of Cu^{2+}.

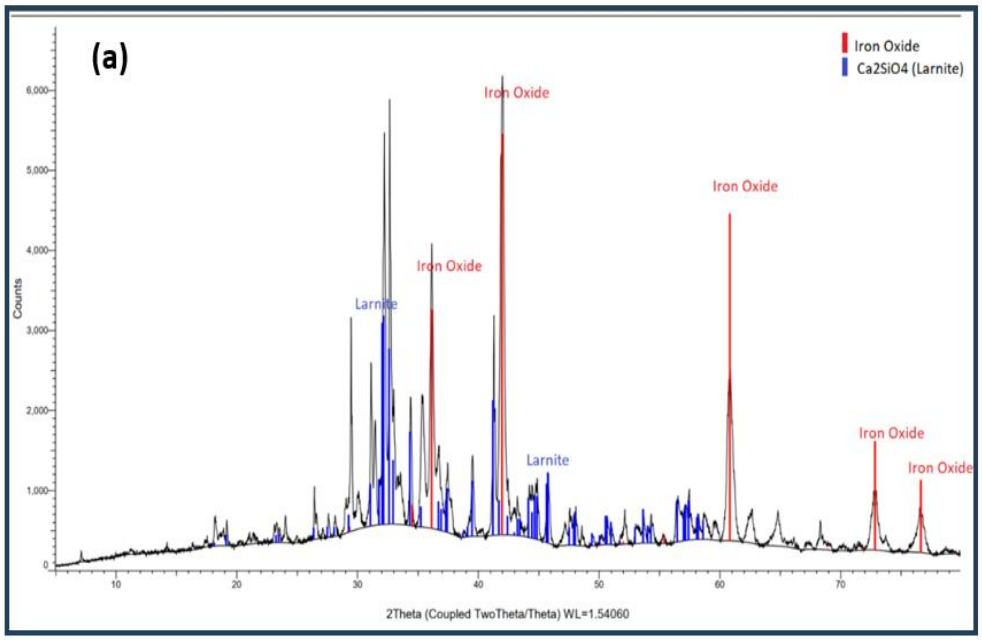
(a)
Iron Oxide
Ca2SiO4 (Larnite)
Iron Oxide
Iron Oxide
Iron Oxide
Larnite
Larnite
Iron Oxide
Iron Oxide
Counts
2Theta (Coupled TwoTheta/Theta) WL=1.54060

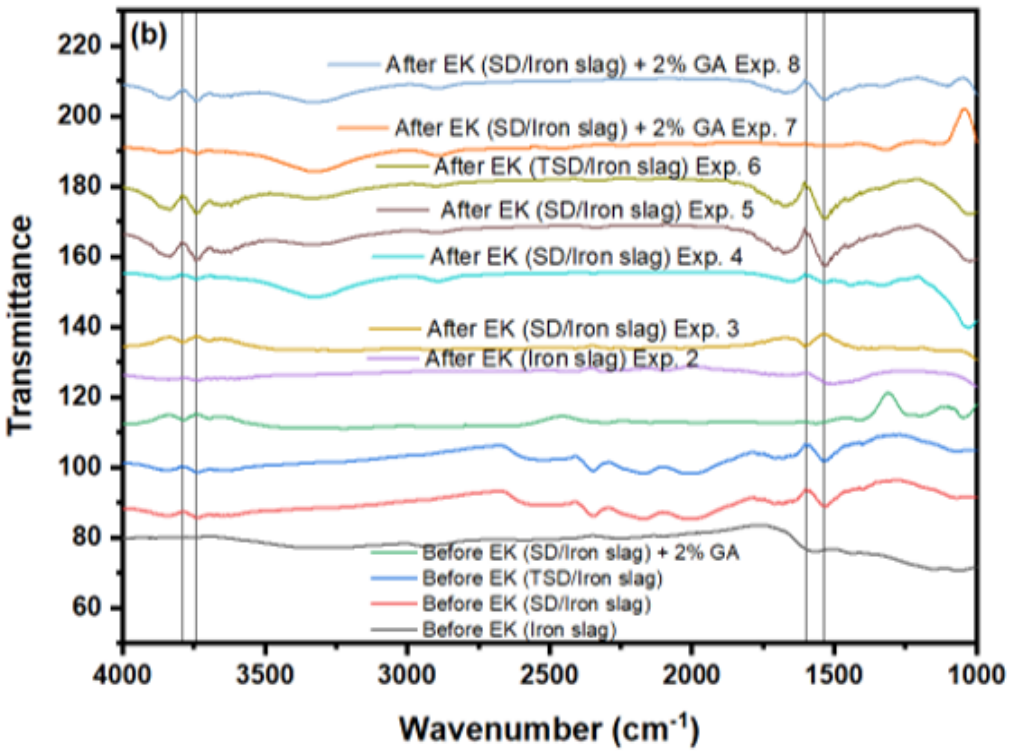
(b)
After EK (SD/Iron slag) + 2% GA Exp. 8
After EK (SD/Iron slag) + 2% GA Exp. 7
After EK (TSD/Iron slag) Exp. 6
After EK (SD/Iron slag) Exp. 5
After EK (SD/Iron slag) Exp. 4
After EK (SD/Iron slag) Exp. 3
After EK (Iron slag) Exp. 2
Before EK (SD/Iron slag) + 2% GA
Before EK (TSD/Iron slag)
Before EK (SD/Iron slag)
Before EK (Iron slag)
Transmittance
Wavenumber (cm-1)

(c) Iron slag before EK Treatment (d)

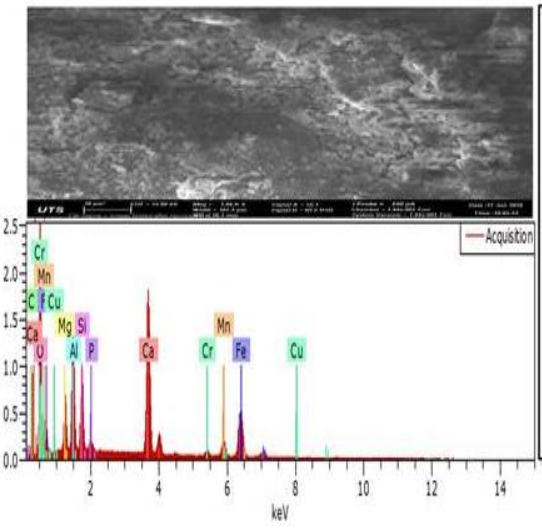

El	AN	Series	unn. C [wt.%]	norm. C [wt.%]	Atom. C [at.%]	Error (1 Sigma) [wt.%]
O	8	K-series	34.78	35.89	54.42	4.30
Ca	20	K-series	18.43	19.02	11.51	0.58
C	6	K-series	4.28	4.42	8.93	0.81
Fe	26	K-series	17.89	18.46	8.02	0.57
Al	13	K-series	6.83	7.04	6.33	0.35
Si	14	K-series	4.67	4.82	4.16	0.23
Mg	12	K-series	3.05	3.15	3.14	0.19
Mn	25	K-series	4.80	4.95	2.19	0.18
Cr	24	K-series	1.41	1.46	0.68	0.08
P	15	K-series	0.76	0.78	0.61	0.06
		Total:	96.91	100.00	100.00	

(e) SD/Iron slag Before EK Treatment (f)

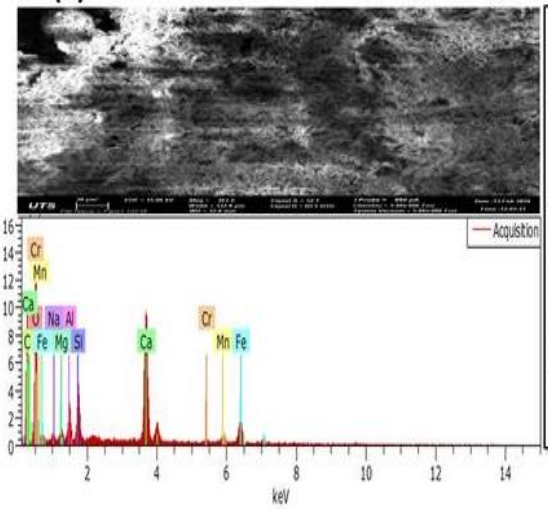

El	AN	Series	unn. C [wt.%]	norm. C [wt.%]	Atom. C [at.%]	Error (1 Sigma) [wt.%]
C	6	K-series	18.16	18.16	33.83	0.65
O	8	K-series	23.82	23.82	33.31	0.80
Ca	20	K-series	33.16	33.16	18.52	1.08
Si	14	K-series	6.37	6.37	5.07	0.15
Fe	26	K-series	11.02	11.02	4.42	0.45
Al	13	K-series	3.30	3.30	2.73	0.16
Mn	25	K-series	2.29	2.29	0.93	0.16
Cr	24	K-series	1.15	1.15	0.50	0.11
Mg	12	K-series	0.41	0.41	0.38	0.06
Na	11	K-series	0.32	0.32	0.31	0.05
		Total:	100.00	100.00	100.00	

(g) TSD/Iron slag Before EK Treatment (h)

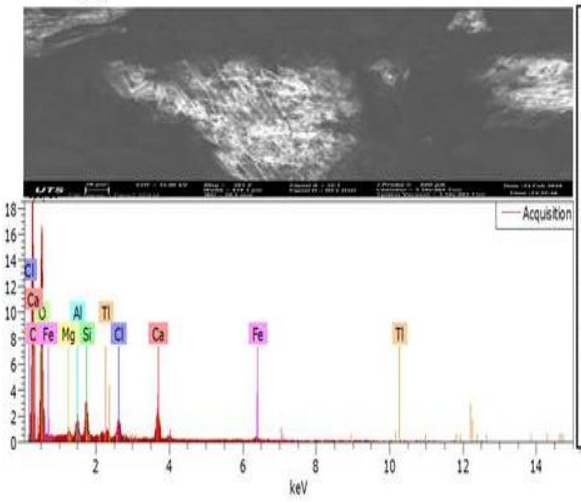

El	AN	Series	unn. C [wt.%]	norm. C [wt.%]	Atom. C [at.%]	Error (1 Sigma) [wt.%]
C	6	K-series	45.94	45.94	60.39	1.48
O	8	K-series	30.12	30.12	29.72	0.98
Ca	20	K-series	7.84	7.84	3.09	0.31
Si	14	K-series	4.95	4.95	2.78	0.13
Cl	17	K-series	3.27	3.27	1.46	0.16
Al	13	K-series	2.35	2.35	1.37	0.12
Fe	26	K-series	2.13	2.13	0.60	0.15
Mg	12	K-series	0.57	0.57	0.37	0.06
Tl	81	M-series	2.83	2.83	0.22	0.61
Total:			100.00	100.00	100.00	

(i) SD/Iron slag + 2% GA Before EK Treatment (j)

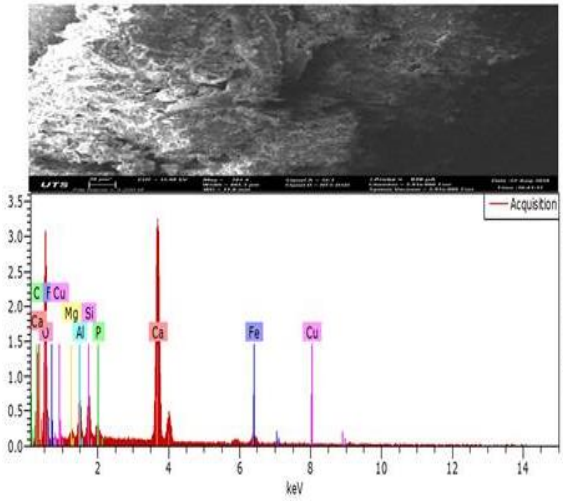

El	AN	Series	unn. C [wt.%]	norm. C [wt.%]	Atom. C [at.%]	Error (1 Sigma) [wt.%]
O	8	K-series	47.86	49.41	62.56	8.90
C	6	K-series	8.89	9.18	15.48	2.55
Ca	20	K-series	29.52	30.47	15.40	1.03
Al	13	K-series	2.60	2.69	2.02	0.21
Si	14	K-series	2.64	2.73	1.97	0.20
Fe	26	K-series	3.76	3.89	1.41	0.32
P	15	K-series	1.10	1.14	0.74	0.12
Mg	12	K-series	0.49	0.51	0.42	0.09
Total:			96.87	100.00	100.00	

(k) Iron slag After EK Treatment (Exp. 2) (l)

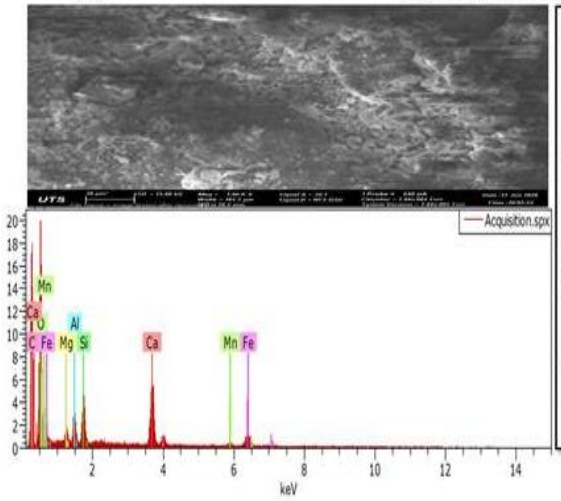

El	AN	Series	unn. C [wt.%]	norm. C [wt.%]	Atom. C [at.%]	Error (1 Sigma) [wt.%]
C	6	K-series	36.26	36.26	52.37	1.19
O	8	K-series	28.70	28.70	31.12	0.93
Ca	20	K-series	16.89	16.89	7.31	0.58
Si	14	K-series	5.81	5.81	3.59	0.14
Al	13	K-series	3.45	3.45	2.22	0.16
Fe	26	K-series	5.99	5.99	1.86	0.28
Mg	12	K-series	1.54	1.54	1.10	0.10
Mn	25	K-series	1.35	1.35	0.43	0.12
Total:			100.00	100.00	100.00	

(m) SD/Iron slag After EK Treatment (Exp. 3) (n)

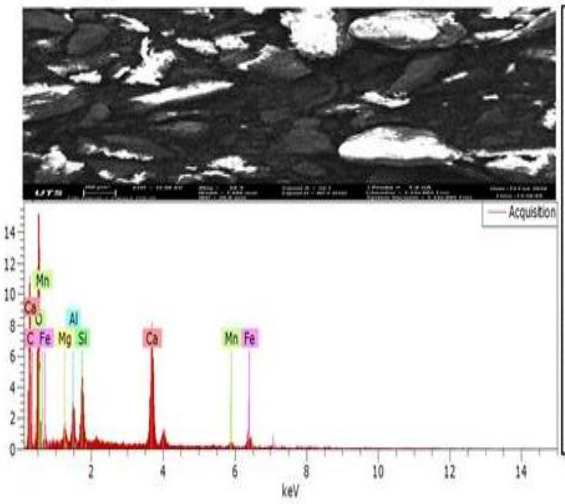

El	AN	Series	unn. C [wt.%]	norm. C [wt.%]	Atom. C [at.%]	Error (1 Sigma) [wt.%]
O	8	K-series	46.48	45.28	48.86	6.70
C	6	K-series	27.51	26.80	38.52	4.29
Ca	20	K-series	16.53	16.11	6.94	0.56
Si	14	K-series	3.22	3.14	1.93	0.18
Fe	26	K-series	4.86	4.74	1.46	0.25
Al	13	K-series	2.02	1.97	1.26	0.14
Mg	12	K-series	1.06	1.03	0.73	0.10
Mn	25	K-series	0.96	0.93	0.29	0.09
		Total:	102.64	100.00	100.00	

(o) SD/Iron slag After EK Treatment (Exp. 4) (p)

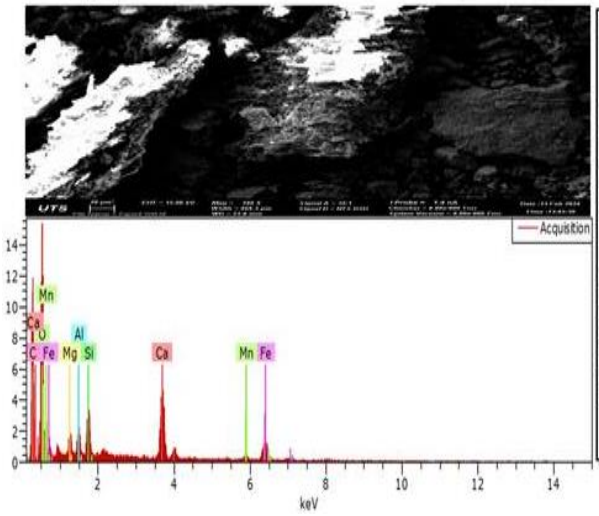

El	AN	Series	unn. C [wt.%]	norm. C [wt.%]	Atom. C [at.%]	Error (1 Sigma) [wt.%]
O	8	K-series	38.57	43.56	46.01	5.53
C	6	K-series	27.02	30.52	42.93	4.10
Ca	20	K-series	8.86	10.01	4.22	0.32
Fe	26	K-series	7.23	8.16	2.47	0.31
Si	14	K-series	2.62	2.95	1.78	0.15
Mg	12	K-series	1.35	1.53	1.06	0.12
Al	13	K-series	1.47	1.66	1.04	0.11
Mn	25	K-series	1.42	1.60	0.49	0.11
		Total:	88.53	100.00	100.00	

(q) SD/Iron slag After EK Treatment (Exp. 5) (r)

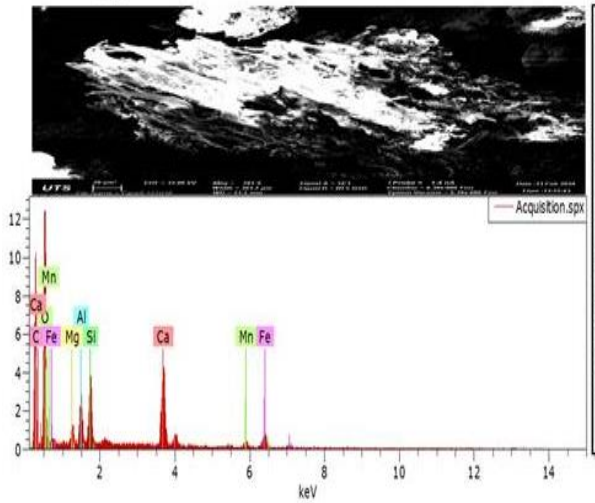

El	AN	Series	unn. C [wt.%]	norm. C [wt.%]	Atom. C [at.%]	Error (1 Sigma) [wt.%]
C	6	K-series	31.18	31.18	47.35	1.04
O	8	K-series	27.90	27.90	31.81	0.91
Ca	20	K-series	18.67	18.67	8.50	0.64
Si	14	K-series	8.13	8.13	5.28	0.16
Al	13	K-series	4.80	4.80	3.25	0.20
Fe	26	K-series	6.09	6.09	1.99	0.29
Mg	12	K-series	1.81	1.81	1.36	0.11
Mn	25	K-series	1.41	1.41	0.47	0.12
		Total:	100.00	100.00	100.00	

(s) TSD/Iron slag After EK Treatment (Exp. 6) (t)

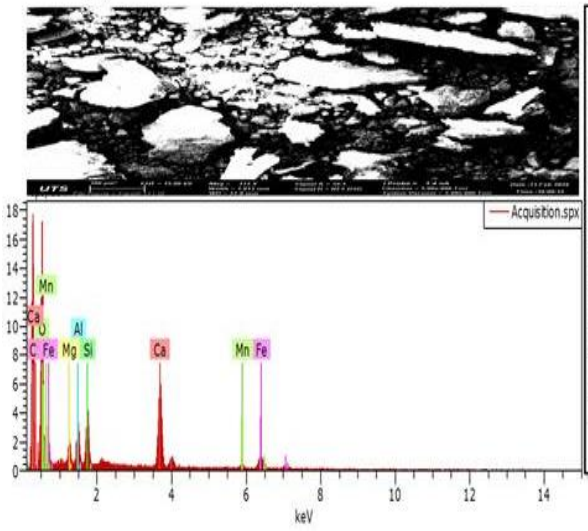

El	AN	Series	unn. C [wt.%]	norm. C [wt.%]	Atom. C [at.%]	Error (1 Sigma) [wt.%]
C	6	K-series	37.95	37.95	54.77	1.24
O	8	K-series	25.87	25.87	28.03	0.85
Ca	20	K-series	17.65	17.65	7.63	0.61
Si	14	K-series	5.66	5.66	3.49	0.14
Al	13	K-series	3.93	3.93	2.53	0.17
Fe	26	K-series	5.59	5.59	1.74	0.27
Mg	12	K-series	1.89	1.89	1.35	0.11
Mn	25	K-series	1.47	1.47	0.46	0.12
Total:			100.00	100.00	100.00	

(u) SD/Iron slag + 2% GA After EK Treatment (Exp. 7) (v)

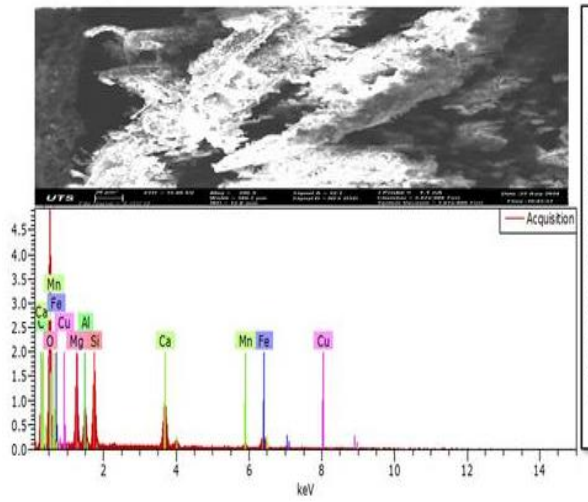

El	AN	Series	unn. C [wt.%]	norm. C [wt.%]	Atom. C [at.%]	Error (1 Sigma) [wt.%]
O	8	K-series	54.32	50.57	56.75	7.91
C	6	K-series	17.96	16.72	25.00	3.66
Mg	12	K-series	8.03	7.48	5.52	0.50
Si	14	K-series	7.53	7.01	4.48	0.38
Ca	20	K-series	8.13	7.56	3.39	0.33
Al	13	K-series	4.44	4.13	2.75	0.27
Fe	26	K-series	5.59	5.20	1.67	0.30
Mn	25	K-series	1.42	1.33	0.43	0.13
Total:			107.42	100.00	100.00	

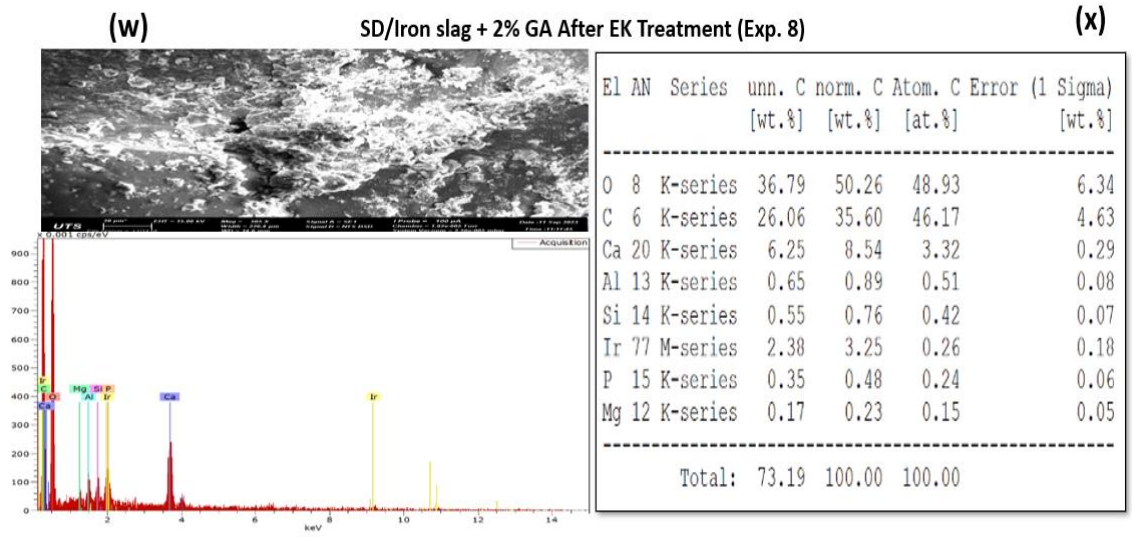

Figure 6.5: (a) the XRD spectrum of iron slag, (b) FTIR bands of iron slag, SD/iron slag, TSD/iron slag, and SD/iron slag mix with 2% GA before and after EK treatment, and (c to x) iron slag, SD/iron slag, TSD/iron slag, and SD/iron slag mix with 2% GA SEM images with EDS before and at the end of the EK treatment.

6.3.6. RFM adsorption/desorption

Figures 6.6a and 6.6b illustrate the results of dynamic adsorption using a combination of sawdust and iron slag. A pseudo-second-order (PSO) adsorption model was employed to evaluate the adsorption of metal ions onto the surface of RFM. This model is based on the following assumptions: i) the adsorbent surface is homogeneous, ii) the adsorption of metal ions onto RFM is governed by chemisorption, and iii) the reaction rate depends on the availability of active sites. The Cu^{2+} behaviour during adsorption was thoroughly investigated, revealing that the highest adsorption capacity, reaching 26.66 mg/g Cu^{2+}, is achieved within 20 minutes using sawdust or HCl-treated sawdust combined with iron slag and sawdust/iron slag mix with 2% GA solution. At first, the absorption of Cu^{2+} happens swiftly, demonstrating a notable rate of adsorption. However, as equilibrium is approached, the adsorption and desorption rates gradually equalise. Variables such as the

contact duration and the distinct properties of the sawdust/ slag blend influence the extent of Cu^{2+} adsorption and the absorption rate (Kulal and Badalamoole, 2020).

The slowing down of adsorbate interactions at specific sites compared to those in the bulk phase influenced the extraction rate. The speed at which adsorbate molecules were removed from the solution varied based on their movement in the adsorbent from the surface to the inside. Characterized by a balance between adsorption and desorption rates, equilibrium was achieved within 200 min for the Cu^{2+} (Rahchamani et al., 2011; Zhuang et al., 2016). The magnetite nanoparticles with embedded Fe^{2+} ions serve as electron donors (Castro et al., 2018). The primary techniques utilized for ions removal from solution include electrostatic adsorption, Cu^{2+} binding to surfaces of metal oxide, and ion exchange with H^{+} from OH^{-} groups on the surface of the adsorbent, forming complexes. Adsorbents possessing various chemical functionalities like carboxyl, aldehyde, ester, hydroxyl, and ketone groups can interact with copper ions. The effectiveness of this interaction depends on variables such as the number of binding sites, accessibility, chemical structure, and the binding involved (Jain et al., 2018).

Three cycles of adsorption and desorption were conducted using a feed concentration of 2.52 g/L of Cu^{2+} ions, 24 hours each cycle, aimed at evaluating the sequential removal process. Throughout the adsorption cycles, the removal percentages of Cu^{2+} ions from the initial content in sawdust/iron slag were 57%, 48.54%, and 41.94% in cycles 1 to 3. Similar results were obtained for sawdust/iron slag mix with 2% GA solution, with removal percentages of 58.54%, 48.60%, and 40.37% in cycles 1 to 3. Additionally, the desorption concentrations at the end of the three cycles were 50.22%, 39.96%, and 36.86% for sawdust/iron slag and 50.86%, 37.15%, and 35.59% for sawdust/iron slag with 2% GA (**Figure 6.6c)**. The desorption process of sawdust/slag includes the release of formerly bound molecules/ions, which occurs via various methods such as diffusion,

exchange reactions, and solvent and external stimuli. Distribution occurs as adsorbed species move along concentration gradients, moving from areas of higher to lower concentrations. The exchange reactions substitute less tightly bound species with those that have a higher affinity, whereas solvents can modify the interactions involving sawdust/slag and the adsorbed species. Protons compete with binding sites in acidic environments, deteriorating interactions and facilitating the release of adsorbed copper ions, highlighting the significance of solution conditions in desorption phenomena.

Adsorption experiments are being conducted to evaluate the potential for RFM reuse, revealing moderate to high recovery rates of adsorbed copper when using acid regeneration methods. Typically, dilute hydrochloric or nitric acid solutions can desorb 70–90% of the copper from the media, depending on contact time and acid concentration. However, repeated sorption-desorption cycles tend to degrade the structural and chemical integrity of the materials. In sawdust, prolonged acid exposure may hydrolyze cellulose components or leach out functional groups, reducing its adsorption capacity. Iron slag may also undergo surface alterations, including dissolution or passivation of active sites. As a result, the performance of RFM generally diminishes after 3 to 5 cycles, beyond which the cost of regeneration may outweigh the benefits. While RFM can be reused to a certain extent, its service life is finite, and periodic replacement or supplementation with fresh media is necessary to maintain high removal efficiency.

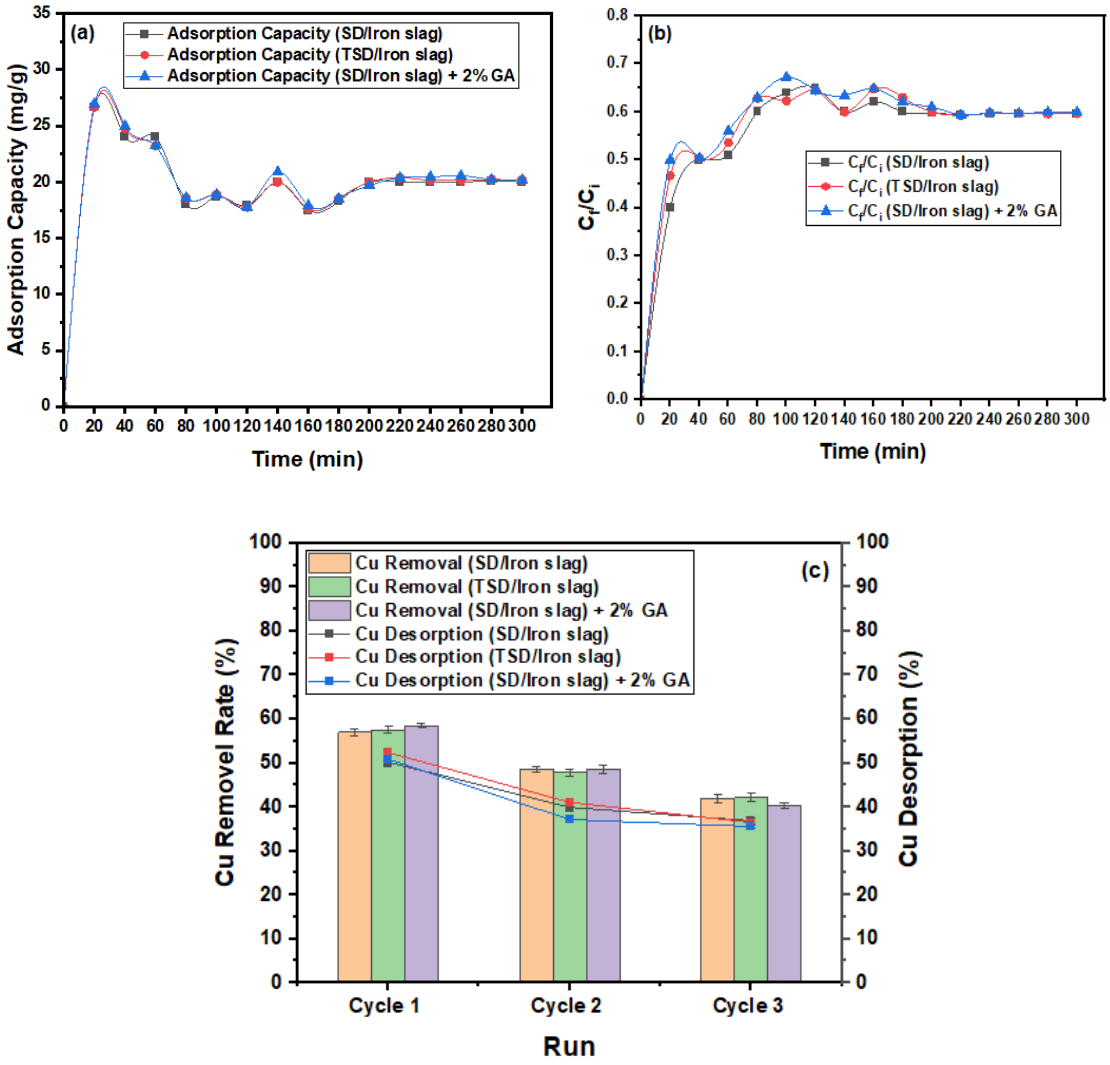

Figure 6.6: Cu^{2+} adsorption tests, (a) The Cu^{2+} adsorption on sawdust/slag, (b) The influence of the duration on the Cu^{2+}adsorption, (c) Adsorption, and desorption of Cu^{2+} across three successive cycles, sawdust (SD), treated sawdust (TSD) with slag, and sawdust/iron slag with 2% GA RFM.

6.4. Implications

EK experiments demonstrated a great potential for using industrial waste materials as an adsorbent in copper removal from the soil. Copper removal from kaolinite soil was 3.21% in the EK process without RFM, then increased to 23.76% when iron slag RFM was coupled with the EK process. Although iron slag is a good adsorbent for heavy metals, it

was unable to prevent the rapid advancement of OH^- in the soil due to its alkaline pH (**Table 6.1**). Therefore, most copper was precipitated in section S6, adjacent to the RFM in Exp2. Using sawdust-iron slag RFM in Exp3 increased copper removal to 71.8%, with 67.7% of the copper captured by the RFM. Sawdust-iron slag RFM of pH 10.19 (**Table 6.1**) was able to suppress the advancement of OH^- in the soil, allowing copper transport toward the RFM. Treated sawdust-iron slag RFM of pH 9.24 (**Table 6.1**) further improved copper removal to 90.3%, with > 84% of the copper captured in the RFM. In Exp7, the total copper removal efficiency increased to 97.92% with the incorporation of a 2% glutaraldehyde. This improvement is likely due to the enhanced properties of the RFM, which consisted of a mixture of sawdust and iron slag. The glutaraldehyde improved copper removal by modifying the cellulose structure in the sawdust and by reducing the pH of the RFM (**Table 6.1**). These modifications likely enhanced the RFM's effectiveness in adsorbing and removing contaminants during the electrokinetic process. The total removal efficiency in Exp8 using natural soil was lower compared to kaolin soil due to the inherent complexity of natural soil. Factors such as its heterogeneity, elevated organic matter content, and stronger metal-binding properties contribute to greater resistance to electrokinetic (EK) treatment, making the remediation process less effective. The results emphasize the potential of applying industrial waste materials as adsorbents in soil treatment, reducing the environmental impact, cost, and waste generation from the remediation process. Although EK requires low energy for operation, coupling the EK-RFM with solar energy will reduce the operation cost of the remediation process. The EK-RFM system will also reduce the human risk associated with conventional ex-situ remediation processes. Combining the EK with RFM will ensure not only better heavy metal removal but also easier heavy metal extraction and control since the relatively high permeability RFM will capture most contaminants at the end of the remediation process.

The RFM-EK hybrid system will facilitate soil decontamination and resource recovery, encouraging more work on recycling waste materials for environmental remediation processes. It is noteworthy that the effectiveness of the RFM decreases at the end of the EK process due to the variation in the soil pH, affecting the functional groups of the FMS and its adsorption capacity. Also, the desorption process is carried out in an acidic environment that alters the surface characteristics and charge of the RFM media (**Figure 6.6c**), rendering it less effective for use in multiple cycles (Ganbat et al., 2023; Hamdi et al., 2024).

6.5. Conclusion

Hybrid RFM consisting of organic and inorganic adsorbents was tested for heavy metals removal from kaolinite and contaminated site soil. Using recyclable and eco-friendly waste materials in the RFM aims to achieve sustainable land-remediation processes. Iron slag, iron slag/sawdust, and treated sawdust/iron slag were investigated for Cu^{2+} removal. Cu^{2+} removal rose from 3.21% in the EK process to 23.76% in the iron slag-EK test. The iron slag's alkaline pH promoted the adsorption and precipitation of copper ions. Still, most Cu^{2+} was found to be precipitated outside the RFM due to the rapid progression of the alkaline front in the soil. Cu^{2+} removal was significantly enhanced by combining the EK method with the sawdust-iron slag RFM, achieving a 71.80% removal. In Exp6, 90.30% copper removal was reached when RFM containing treated sawdust and iron slag was utilized. The glutaraldehyde crosslinked sawdust/iron slag RFM-Ek system attained 97.92% Cu^{2+} removal efficiency from kaolinite soil. Glutaraldehyde crosslinker of pH 4 to pH 5 reduced the pH of the iron slag RFM from pH 11.38 in Exp 2 to pH 9.55 in Exp 7; hence, there is no need for further enhancement. In the natural soil, the removal rates were lower due to the complicated chemistry of natural soils and the interaction between pollutants and the soil's organic matter. Future research should focus on further improving

the conditions of the RMF-EK system by optimizing the experimental conditions, including increasing the amount of RFM in the soil, test duration, and using chemical enhancement agents to prevent alkaline front advancement in soil. RFM-EK pilot plant tests are recommended in future work to confirm the technology's efficiency and cost-effectiveness in the real environment. The environmental impact of the EK process should also be evaluated to develop mitigation systems. For example, the electrokinetic process can cause substantial pH changes in the soil, which may mobilize other harmful metals or disrupt soil ecosystems. There is also a risk of secondary pollution from the improper disposal of spent RFM saturated with heavy metals. A thorough life cycle assessment (LCA) and cost-benefit analysis would be necessary to evaluate the method's sustainability and practical feasibility on an industrial scale.

CHAPTER SEVEN:

CONCLUSIONS AND FUTURE RESEARCH RECOMMENDATIONS

CHAPTER SEVEN: CONCLUSIONS AND FUTURE RESEARCH RECOMMENDATIONS

7.1. Conclusions

This study aimed to enhance the performance of the electrokinetic (EK) process for extracting heavy metals from soil, utilizing custom-designed reactive filter media (RFM). The selected RFMs were a combination of organic and inorganic waste materials of high affinity to heavy metals. Lab-scale experiments revealed that EK remediation alone was ineffective in decontaminating kaolinite clay soil (utilized as typical soil) from copper. The primary limitation was the high pH near the cathode, which led to copper precipitation, restricting removal to areas near the anode. This point was addressed by combining the EK process with an RFM positioned near the cathode, allowing for the capture of contaminants migrating through the soil toward that region. Hybrid RFM consisting of organic and inorganic adsorbents was tested for heavy metals removal from kaolinite and contaminated site soil. Using recyclable and eco-friendly waste materials in the RFM aims to achieve sustainable land-remediation processes.

The EK process was integrated with iron slag or iron slag-activated carbon (AC) RFM to remove single and mixed heavy metals from kaolinite soil. Initially, heavy metal removal increased from 3.11% with EK alone to 23.26% when combined with iron slag. The alkaline pH of iron slag facilitated metal ion adsorption and precipitation. Copper removal was further enhanced by incorporating iron slag-AC RFM, as hydroxyl ion adsorption on AC improved efficiency, resulting in a 70.14% removal rate. Conventional EK processes often rely on enhancement agents to improve heavy metal extraction, but this approach increases remediation costs. The study proposed anolyte recirculation to the cathode compartment to neutralize the alkaline pH front and improve metal removal while

reducing operational costs and minimizing the risks associated with handling acidic or alkaline chemicals. This modification boosted copper removal from 70.14% in the RFM-EK process without anolyte recirculation to 89.21% with recirculation. Extending the RFM-EK process to three weeks further increased copper removal to 93.45%. Additionally, the RFM-EK system with anolyte recirculation was tested for multi-metal removal. After three weeks, the EK process achieved removal efficiencies of 81.1% for copper, 89.04% for nickel, and 92.31% for zinc.

Iron slag from steel manufacturing is an industrial byproduct that was repurposed for contaminated soil remediation, offering a sustainable approach to waste management. Experiments on kaolinite soil showed promising outcomes, with the Slag/BTW RFM-enhanced EK test achieving a heavy metals removal of 98% after three weeks of treatment. Results investigating the impact of iron slag particle size on the remediation process found that PIS (powder iron slag)/BTW significantly outperformed GIS (granular iron slag)/BTW due to its greater surface area and higher reactivity. Copper removal was notably more effective with PIS/BTW, achieving a rate of 98.75%, primarily due to enhanced hydroxyl ion adsorption. Recycling the reactive filter media (RFM) in the electrokinetic (EK) process sustained high pollutant removal efficiency, with copper removal rates of 91.28% for PIS/BTW and 84.90% for GIS/BTW over a three-week treatment period. Energy consumption results showed that specific energy consumption (SEC) increased with longer treatment durations and higher electric currents. In kaolinite soil treatments, SEC ranged from 0.055 kWh/kg to 0.254 kWh/kg, while extending the treatment period to five weeks for natural soil raised it to 0.344 kWh/kg. The PIS/BTW was also tested for multi-heavy metals removal from kaolinite and natural soils to resemble field conditions. For mixed heavy metal removal in kaolinite soil, the EK process removed 97.15% of copper, 98.30% of nickel, and 96.68% of zinc. However, in

natural soil, the removal rates were lower—16.39% for copper, 89.22% for nickel, and 84.38% for zinc. This reduction was attributed to the complex chemistry of natural soils and the interactions between pollutants and organic matter. The alkaline pH of the RFMs played a crucial role in metal ion adsorption and precipitation, enhancing their immobilization.

Iron slag, iron slag/sawdust, and treated sawdust/iron slag were investigated for Cu^{2+} removal. Cu^{2+} removal rose from 3.21% in the EK process to 23.76% in the iron slag-EK test. The iron slag's alkaline pH promoted the adsorption and precipitation of copper ions. Still, most Cu^{2+} was found to be precipitated outside the RFM due to the rapid progression of the alkaline front in the soil. Cu^{2+} removal was significantly enhanced by combining the EK method with the sawdust-iron slag RFM, achieving a 71.80% removal. In Exp6, 90.30% copper removal was reached when RFM containing treated sawdust and iron slag was utilized. A crosslinking agent, glutaraldehyde, was mixed with the sawdust to improve its adsorption capacity and stability. The glutaraldehyde crosslinked sawdust/iron slag RFM-Ek system attained 97.92% Cu^{2+} removal efficiency from kaolinite soil. In the natural soil, the removal rates were lower, with 26.72% for copper, 54.36% for nickel, and 56.44% for zinc due to the complicated chemistry of natural soils and the interaction between pollutants and soil's organic matter.

7.2. The importance of the research and its impact on the field

The study presents a promising approach for sustainable soil remediation by repurposing industrial waste materials like iron slag, sawdust and tea waste. Using waste materials adsorbent will not only improve the efficiency of heavy metal removal but also contribute to waste valorization and environmental sustainability. Also, the relatively high permeability of RFMs facilitates the recovery of heavy metals at the end of the EK process. Hybrid organic-inorganic adsorbents are applied as RFM in the EK process. The

combination of organic and inorganic materials in RFMs provides a more efficient platform for the remediation of soil contaminated with heavy metals due to their unique ion-binding properties. This research also introduces an innovative approach by incorporating anolyte recycling to counteract the alkaline pH at the cathode, promoting the movement of the acid front through the soil. This method offers an alternative to chemical agents traditionally used for alkaline front neutralization, thereby minimizing chemical consumption. This method reduces the environmental risks associated with handling hazardous chemicals, making it a more cost-effective and safer option for large-scale remediation projects.

To the best of the author's knowledge, RFMs such as iron slag and its combination with sawdust or black tea waste have not yet been integrated into the EK system. Previous studies have only explored their applications in soil and water remediation. Among the various RFMs examined in this study, iron slag was selected due to its industrial waste origin, strong adsorption capacity for metal ions, and availability. With an alkaline pH of 11, iron slag facilitates the precipitation of metal ions once the RFM captures them. Additionally, the slightly acidic pH of tea waste (approximately 5.5) helps to slow the rapid advancement of the alkaline front at the cathode. Currently, no studies have investigated the combined use of iron slag and black tea waste in the EK process. Therefore, this research contributes to the effective application of these enhancement strategies in the EK remediation of contaminated soil and supports the optimization of the EK-RFM system design, making it more applicable for field-scale implementation. As an in-situ technique, EK-RFM remediation eliminates the need for soil excavation, reducing human exposure risks, minimizing site disruption, and operating with low energy requirements. Furthermore, it can be integrated with solar energy for enhanced sustainability.

7.3. future studies

The following recommendations are proposed for future research to build on the experimental findings of this research work:

- Future studies should investigate the use of other waste materials, such as rice husk, corncob, fly ash, red mud, eggshell, etc., as RFMs for more sustainable and cost-effective remediation solutions.
- The findings from the lab-scale experiments should be validated in field applications, considering factors like soil heterogeneity, contaminant concentrations, and environmental conditions. Pilot-scale studies will be crucial for assessing the practical viability of the EK process with RFM in real-world scenarios.
- Further research is needed to explore methods for reducing energy consumption while maintaining high removal efficiencies. Strategies like optimizing electric currents, improving anolyte recirculation systems, and integrating renewable energy sources could enhance the cost-effectiveness of the EK process.
- The ability of the EK process with RFM to remove multiple pollutants simultaneously holds promise. Future research could focus on understanding the interactions between different contaminants during the EK process and process optimization.
- Electrokinetic (EK) technology is an effective soil remediation method for removing inorganic contaminants in their charged forms, including anions and cations. However, this study focused solely on the removal of cationic heavy metals in the EK-RFM process from contaminated soil. Future research could explore the mobilization and distribution of negatively charged heavy metals, such as arsenic (As) and chromium (Cr), within the EK-RFM system.

- Anthropogenic activities have led to severe soil contamination with heavy metals and organic compounds. As a result, the efficacy of RFM in conjunction with the EK method should be explored for the simultaneous removal of mixed inorganic and organic pollutants.

References

Aboughalma, H., Bi, R., Schlaak, M., 2008. Electrokinetic enhancement on phytoremediation in Zn, Pb, Cu and Cd contaminated soil using potato plants. Journal of Environmental Science and Health, Part A 43, 926–933. https://doi.org/10.1080/10934520801974459

Acar, Y.B., Alshawabkeh, A.N., 1993. Principles of electrokinetic remediation. Environ Sci Technol 27, 2638–2647. https://doi.org/10.1021/es00049a002

Acosta Hernández, I., Muñoz Morales, M., López-Bellido Garrido, F.J., Rodríguez, L., Villaseñor Camacho, J., 2024. Coupling of bioleaching and electrokinetic soil flushing for the in-situ removal of impurity from Pb-Zn mine tailings. J Environ Chem Eng 12, 112992. https://doi.org/10.1016/j.jece.2024.112992

Adrion, A.C., Nakamura, J., Shea, D., Aitken, M.D., 2016. Screening Nonionic Surfactants for Enhanced Biodegradation of Polycyclic Aromatic Hydrocarbons Remaining in Soil After Conventional Biological Treatment. Environ Sci Technol 50, 3838–3845. https://doi.org/10.1021/acs.est.5b05243

Agnew, K., Cundy, A.B., Hopkinson, L., Croudace, I.W., Warwick, P.E., Purdie, P., 2011. Electrokinetic remediation of plutonium-contaminated nuclear site wastes: Results from a pilot-scale on-site trial. J Hazard Mater 186, 1405–1414. https://doi.org/10.1016/J.JHAZMAT.2010.12.016

Ahmed, M.B., Zhou, J.L., Ngo, H.H., Guo, W., 2015. Adsorptive removal of antibiotics from water and wastewater: Progress and challenges. Science of The Total Environment 532, 112–126. https://doi.org/10.1016/J.SCITOTENV.2015.05.130

Ahmed, S.F., Kumar, P.S., Rozbu, M.R., Chowdhury, A.T., Nuzhat, S., Rafa, N., Mahlia, T.M.I., Ong, H.C., Mofijur, M., 2022. Heavy metal toxicity, sources, and remediation techniques for contaminated water and soil. Environ Technol Innov 25, 102114. https://doi.org/10.1016/j.eti.2021.102114

Ait Ahmed, O., Derriche, Z., Kameche, M., Bahmani, A., Souli, H., Dubujet, P., Fleureau, J.M., 2016. Electro-remediation of lead contaminated kaolinite: An electro-kinetic treatment. Chemical Engineering and Processing: Process Intensification 100, 37–48. https://doi.org/10.1016/j.cep.2015.12.002

Alcántara, M.T., Gómez, J., Pazos, M., Sanromán, M.A., 2008. Combined treatment of PAHs contaminated soils using the sequence extraction with surfactant–electrochemical

degradation. Chemosphere 70, 1438–1444. https://doi.org/10.1016/j.chemosphere.2007.08.070

Alhashimi, H.A., Aktas, C.B., 2017. Life cycle environmental and economic performance of biochar compared with activated carbon: A meta-analysis. Resour Conserv Recycl 118, 13–26. https://doi.org/10.1016/J.RESCONREC.2016.11.016

Almeira O., J., Peng, C.-S., Abou-Shady, A., 2012. Simultaneous removal of cadmium from kaolin and catholyte during soil electrokinetic remediation. Desalination 300, 1–11. https://doi.org/10.1016/j.desal.2012.05.023

Altaee, A., Smith, R., Mikhalovsky, S., 2008. The feasibility of decontamination of reduced saline sediments from copper using the electrokinetic process. J Environ Manage 88, 1611–1618. https://doi.org/10.1016/J.JENVMAN.2007.08.008

Amrate, S., Akretche, D.E., Innocent, C., Seta, P., 2005. Removal of Pb from a calcareous soil during EDTA-enhanced electrokinetic extraction. Science of The Total Environment 349, 56–66. https://doi.org/10.1016/j.scitotenv.2005.01.018

Azhar, U., Ahmad, H., Shafqat, H., Babar, M., Shahzad Munir, H.M., Sagir, M., Arif, M., Hassan, A., Rachmadona, N., Rajendran, S., Mubashir, M., Khoo, K.S., 2022. Remediation techniques for elimination of heavy metal pollutants from soil: A review. Environ Res 214, 113918. https://doi.org/10.1016/j.envres.2022.113918

Bahemmat, M., Farahbakhsh, M., Kianirad, M., 2016. Humic substances-enhanced electroremediation of heavy metals contaminated soil. J Hazard Mater 312, 307–318. https://doi.org/10.1016/j.jhazmat.2016.03.038

Behrouzinia, S., Ahmadi, H., Abbasi, N., Javadi, A.A., 2022. Experimental investigation on a combination of soil electrokinetic consolidation and remediation of drained water using composite nanofiber-based electrodes. Science of The Total Environment 836, 155562. https://doi.org/10.1016/j.scitotenv.2022.155562

Bonnard, M., Devin, S., Leyval, C., Morel, J.-L., Vasseur, P., 2010. The influence of thermal desorption on genotoxicity of multipolluted soil. Ecotoxicol Environ Saf 73, 955–960. https://doi.org/10.1016/j.ecoenv.2010.02.023

Božić, D., Stanković, V., Gorgievski, M., Bogdanović, G., Kovačević, R., 2009. Adsorption of heavy metal ions by sawdust of deciduous trees. J Hazard Mater 171, 684–692. https://doi.org/10.1016/j.jhazmat.2009.06.055

Brillas, E., 2021. Recent development of electrochemical advanced oxidation of herbicides. A review on its application to wastewater treatment and soil remediation. J Clean Prod 290, 125841. https://doi.org/10.1016/j.jclepro.2021.125841

Cang, L., Wang, Q., Zhou, D., Xu, H., 2011. Effects of electrokinetic-assisted phytoremediation of a multiple-metal contaminated soil on soil metal bioavailability and uptake by Indian mustard. Sep Purif Technol 79, 246–253. https://doi.org/10.1016/j.seppur.2011.02.016

Cang, L., Zhou, D.M., Wu, D.Y., Alshawabkeh, A.N., 2009a. Coupling electrokinetics with permeable reactive barriers of zero-valent iron for treating a chromium contaminated soil. Sep Sci Technol 44, 2188–2202. https://doi.org/10.1080/01496390902976699

Cang, L., Zhou, D.-M., Wu, D.-Y., Alshawabkeh, A.N., 2009b. Coupling Electrokinetics with Permeable Reactive Barriers of Zero-Valent Iron for Treating a Chromium Contaminated Soil. Sep Sci Technol 44, 2188–2202. https://doi.org/10.1080/01496390902976699

Castro, L., Blázquez, M.L., González, F., Muñoz, J.A., Ballester, A., 2018. Heavy metal adsorption using biogenic iron compounds. Hydrometallurgy 179, 44–51. https://doi.org/10.1016/j.hydromet.2018.05.029

Çelebi, H., Gök, G., Gök, O., 2020. Adsorption capability of brewed tea waste in waters containing toxic lead(II), cadmium (II), nickel (II), and zinc(II) heavy metal ions. Sci Rep 10, 17570. https://doi.org/10.1038/s41598-020-74553-4

Chatterjee, A., Schiewer, S., 2014. Effect of Competing Cations (Pb, Cd, Zn, and Ca) in Fixed-Bed Column Biosorption and Desorption from Citrus Peels. Water Air Soil Pollut 225, 1854. https://doi.org/10.1007/s11270-013-1854-0

Chen, F., Zhang, Q., Ma, J., Zhu, Q., Wang, Y., Liang, H., 2021. Effective remediation of organic-metal co-contaminated soil by enhanced electrokinetic-bioremediation process. Front Environ Sci Eng 15, 113. https://doi.org/10.1007/s11783-021-1401-y

Chen, J.-L., Yang, S.-F., Wu, C.-C., Ton, S., 2011. Effect of ammonia as a complexing agent on electrokinetic remediation of copper-contaminated soil. Sep Purif Technol 79, 157–163. https://doi.org/10.1016/j.seppur.2011.02.029

Chu, L., Cang, L., Sun, Z., Wang, X., Fang, G., Gao, J., 2022. Reagent-free electrokinetic remediation coupled with anode oxidation for the treatment of phenanthrene polluted soil. J Hazard Mater 433, 128724. https://doi.org/10.1016/j.jhazmat.2022.128724

Cui, H., Wang, Y., Lin, Z., Lv, H., Cui, C., 2024. Unique role of sulfonic acid exchange resin on preventing copper and zinc precipitation and enhancing metal removal in electrokinetic remediation. Chemical Engineering Journal 485, 149994. https://doi.org/10.1016/j.cej.2024.149994

De Gioannis, G., Muntoni, A., Ruggeri, R., Zijlstra, J.J.P., 2008. Chromate adsorption in a transformed red mud permeable reactive barrier using electrokinesis. Journal of Environmental Science and Health, Part A 43, 969–974. https://doi.org/10.1080/10934520801974582

Díaz-Piloneta, M., Ortega-Fernández, F., Terrados-Cristos, M., Álvarez-Cabal, J.V., 2022. Application of Steel Slag for Degraded Land Remediation. Land (Basel) 11, 224. https://doi.org/10.3390/land11020224

Fagnano, M., Agrelli, D., Pascale, A., Adamo, P., Fiorentino, N., Rocco, C., Pepe, O., Ventorino, V., 2020. Copper accumulation in agricultural soils: Risks for the food chain and soil microbial populations. Science of The Total Environment 734, 139434. https://doi.org/10.1016/J.SCITOTENV.2020.139434

Faisal, A.A.H., Alquzweeni, S.S., Naji, L.A., Naushad, M., 2019. Predominant Mechanisms in the Treatment of Wastewater Due to Interaction of Benzaldehyde and Iron Slag Byproduct. Int J Environ Res Public Health 17, 226. https://doi.org/10.3390/ijerph17010226

Fardin, A.B., Jamshidi-Zanjani, A., Darban, A.K., 2021. Application of enhanced electrokinetic remediation by coupling surfactants for kerosene-contaminated soils: Effect of ionic and

nonionic surfactants. J Environ Manage 277, 111422. https://doi.org/10.1016/j.jenvman.2020.111422

Farhad, M., Noor, M., Yasin, M.Z., Nizamani, M.H., Turan, V., Iqbal, M., 2024. Interactive Suitability of Rice Stubble Biochar and Arbuscular Mycorrhizal Fungi for Improving Wastewater-Polluted Soil Health and Reducing Heavy Metals in Peas. Sustainability 16, 634. https://doi.org/10.3390/su16020634

Fernández-Marchante, C.M., Souza, F.L., Millán, M., Lobato, J., Rodrigo, M.A., 2022. Can the green energies improve the sustainability of electrochemically-assisted soil remediation processes? Science of The Total Environment 803, 149991. https://doi.org/10.1016/j.scitotenv.2021.149991

Frick, H., Tardif, S., Kandeler, E., Holm, P.E., Brandt, K.K., 2019. Assessment of biochar and zero-valent iron for in-situ remediation of chromated copper arsenate contaminated soil. Science of The Total Environment 655, 414–422. https://doi.org/10.1016/J.SCITOTENV.2018.11.193

Fu, R., Wen, D., Xia, X., Zhang, W., Gu, Y., 2017. Electrokinetic remediation of chromium (Cr)-contaminated soil with citric acid (CA) and polyaspartic acid (PASP) as electrolytes. Chemical Engineering Journal 316, 601–608. https://doi.org/10.1016/j.cej.2017.01.092

Ganbat, N., Altaee, A., Zhou, J.L., Lockwood, T., Al-Juboori, R.A., Hamdi, F.M., Karbassiyazdi, E., Samal, A.K., Hawari, A., Khabbaz, H., 2022. Investigation of the effect of surfactant on the electrokinetic treatment of PFOA contaminated soil. Environ Technol Innov 28, 102938. https://doi.org/10.1016/J.ETI.2022.102938

Ganbat, N., Hamdi, F.M., Ibrar, I., Altaee, A., Alsaka, L., Samal, A.K., Zhou, J., Hawari, A.H., 2023. Iron slag permeable reactive barrier for PFOA removal by the electrokinetic process. J Hazard Mater 460, 132360. https://doi.org/10.1016/j.jhazmat.2023.132360

Ghobadi, R., Altaee, A., Zhou, J.L., Karbassiyazdi, E., Ganbat, N., 2021a. Effective remediation of heavy metals in contaminated soil by electrokinetic technology incorporating reactive filter media. Science of The Total Environment 794, 148668. https://doi.org/10.1016/j.scitotenv.2021.148668

Ghobadi, R., Altaee, A., Zhou, J.L., McLean, P., Ganbat, N., Li, D., 2021b. Enhanced copper removal from contaminated kaolinite soil by electrokinetic process using compost reactive filter media. J Hazard Mater 402, 123891. https://doi.org/10.1016/J.JHAZMAT.2020.123891

Ghobadi, R., Altaee, A., Zhou, J.L., McLean, P., Yadav, S., 2020. Copper removal from contaminated soil through electrokinetic process with reactive filter media. Chemosphere 252, 126607. https://doi.org/10.1016/J.CHEMOSPHERE.2020.126607

Gholizadeh, M., Hu, X., 2021a. Removal of heavy metals from soil with biochar composite: A critical review of the mechanism. J Environ Chem Eng 9, 105830. https://doi.org/10.1016/j.jece.2021.105830

Gholizadeh, M., Hu, X., 2021b. Removal of heavy metals from soil with biochar composite: A critical review of the mechanism. J Environ Chem Eng 9, 105830. https://doi.org/10.1016/J.JECE.2021.105830

Ghosh, Singh, 2005. A Review on Phytoremediation of Heavy Metals and Utilization of It's by Products . Asian Journal on Energy and Environment 6 (04).

Gill, R.T., Harbottle, M.J., Smith, J.W.N., Thornton, S.F., 2014. Electrokinetic-enhanced bioremediation of organic contaminants: A review of processes and environmental applications. Chemosphere 107, 31–42. https://doi.org/10.1016/j.chemosphere.2014.03.019

Gnanasundar, V.M., Akshai Raj, R., 2021. Remediation of inorganic contaminants in soil using electrokinetics, phytoremediation techniques. Mater Today Proc 45, 950–956. https://doi.org/10.1016/j.matpr.2020.03.038

Gong, Y., Zhao, D., Wang, Q., 2018. An overview of field-scale studies on remediation of soil contaminated with heavy metals and metalloids: Technical progress over the last decade. Water Res 147, 440–460. https://doi.org/10.1016/j.watres.2018.10.024

Groenenberg, J.E., Römkens, P.F.A.M., Zomeren, A. Van, Rodrigues, S.M., Comans, R.N.J., 2017. Evaluation of the Single Dilute (0.43 M) Nitric Acid Extraction to Determine Geochemically Reactive Elements in Soil. Environ Sci Technol 51, 2246–2253. https://doi.org/10.1021/acs.est.6b05151

Guo, H., Wang, Y., Liao, L., Li, Z., Pan, S., Puyang, C., Su, Y., Zhang, Y., Wang, T., Ren, J., Li, J., 2022. Review on remediation of organic-contaminated soil by discharge plasma: Plasma types, impact factors, plasma-assisted catalysis, and indexes for remediation. Chemical Engineering Journal 436, 135239. https://doi.org/10.1016/j.cej.2022.135239

Gupta, V.K., Suhas, 2009. Application of low-cost adsorbents for dye removal – A review. J Environ Manage 90, 2313–2342. https://doi.org/10.1016/j.jenvman.2008.11.017

Hamdi, F.M., Altaee, A., Alsaka, L., Ibrar, I., AL-Ejji, M., Zhou, J., Samal, A.K., Hawari, A.H., 2024. Iron slag/activated carbon-electrokinetic system with anolyte recycling for single and mixture heavy metals remediation. Science of The Total Environment 930, 172516. https://doi.org/10.1016/j.scitotenv.2024.172516

Hamdi, F.M., Ganbat, N., Altaee, A., Samal, A.K., Ibrar, I., Zhou, J.L., Sharif, A.O., 2025. Hybrid and enhanced electrokinetic system for soil remediation from heavy metals and organic matter. Journal of Environmental Sciences 147, 424–450. https://doi.org/10.1016/j.jes.2023.11.005

Han, J.-G., Hong, K.-K., Kim, Y.-W., Lee, J.-Y., 2010. Enhanced electrokinetic (E/K) remediation on copper contaminated soil by CFW (carbonized foods waste). J Hazard Mater 177, 530–538. https://doi.org/10.1016/j.jhazmat.2009.12.065

Hansen, H.K., Rojo, A., Ottosen, L.M., 2007. Electrokinetic remediation of copper mine tailings. Electrochim Acta 52, 3355–3359. https://doi.org/10.1016/j.electacta.2006.02.069

Hassan, I., Mohamedelhassan, E., 2012. Electrokinetic Remediation with Solar Power for a Homogeneous Soft Clay Contaminated with Copper. International Journal of Environmental Pollution and Remediation. https://doi.org/10.11159/ijepr.2012.010

Hawal, L.H., saeed, K. abdulhussein, Al-Sulttani, A.O., 2023. Copper metal elimination from polluted soil by electro-kinetic technique. Environ Monit Assess 195, 443. https://doi.org/10.1007/s10661-023-11057-4

He, J., He, C., Chen, X., Liang, X., Huang, T., Yang, X., Shang, H., 2018. Comparative study of remediation of Cr(VI)-contaminated soil using electrokinetics combined with bioremediation. Environmental Science and Pollution Research 25, 17682–17689. https://doi.org/10.1007/s11356-018-1741-8

Hu, S., Lu, Y., Peng, L., Wang, P., Zhu, M., Dohnalkova, A.C., Chen, H., Lin, Z., Dang, Z., Shi, Z., 2018. Coupled Kinetics of Ferrihydrite Transformation and As(V) Sequestration under the Effect of Humic Acids: A Mechanistic and Quantitative Study. Environ Sci Technol acs.est.8b03492. https://doi.org/10.1021/acs.est.8b03492

Huweg, A.F.S., 2013. Modelling of Electrokinetic Phenomena in Soils. Diss. Uni. South. Queensland 185.

Isidro, J., López-Vizcaíno, R., Yustres, A., Sáez, C., Navarro, V., Rodrigo, M.A., 2022. Recent progress in physical and mathematical modelling of electrochemically assisted soil remediation processes. Curr Opin Electrochem 36, 101115. https://doi.org/10.1016/j.coelec.2022.101115

Jain, M., Yadav, M., Kohout, T., Lahtinen, M., Garg, V.K., Sillanpää, M., 2018. Development of iron oxide/activated carbon nanoparticle composite for the removal of Cr(VI), Cu(II) and Cd(II) ions from aqueous solution. Water Resour Ind 20, 54–74. https://doi.org/10.1016/j.wri.2018.10.001

Jamshidi-Zanjani, Khodadadi, 2016. A review on enhancement techniques of electrokinetic soil remediation. Pollution, 3(1): 157-166, Winter 2017.

Jeon, E.-K., Ryu, S.-R., Baek, K., 2015. Application of solar-cells in the electrokinetic remediation of As-contaminated soil. Electrochim Acta 181, 160–166. https://doi.org/10.1016/j.electacta.2015.03.065

Kabdaşlı, I., Arslan-Alaton, I., Ölmez-Hancı, T., Tünay, O., 2012. Electrocoagulation applications for industrial wastewaters: a critical review. Environmental Technology Reviews 1, 2–45. https://doi.org/10.1080/21622515.2012.715390

Kim, B.-K., Baek, K., Ko, S.-H., Yang, J.-W., 2011. Research and field experiences on electrokinetic remediation in South Korea. Sep Purif Technol 79, 116–123. https://doi.org/10.1016/j.seppur.2011.03.002

Kim, C., Hung, Y.-C., Brackett, R.E., 2000. Efficacy of electrolyzed oxidizing (EO) and chemically modified water on different types of foodborne pathogens. Int J Food Microbiol 61, 199–207. https://doi.org/10.1016/S0168-1605(00)00405-0

Kim, D.-H., Jo, S.-U., Yoo, J.-C., Baek, K., 2013. Ex situ pilot scale electrokinetic restoration of saline soil using pulsed current. Sep Purif Technol 120, 282–288. https://doi.org/10.1016/j.seppur.2013.10.007

Kim, H.-A., Lee, K.-Y., Lee, B.-T., Kim, S.-O., Kim, K.-W., 2012. Comparative study of simultaneous removal of As, Cu, and Pb using different combinations of electrokinetics with bioleaching by Acidithiobacillus ferrooxidans. Water Res 46, 5591–5599. https://doi.org/10.1016/j.watres.2012.07.044

Kim, S.-O., Jeong, J.Y., Lee, W.-C., Yun, S.-T., Jo, H.Y., 2021. Electrokinetic remediation of heavy metal-contaminated soils: performance comparison between one- and two-dimensional

electrode configurations. J Soils Sediments 21, 2755–2769. https://doi.org/10.1007/s11368-020-02803-z

Kim, S.-S., Han, S.-J., Cho, Y.-S., 2002. Electrokinetic remediation strategy considering ground strate: A review. Geosciences Journal 6, 57–75. https://doi.org/10.1007/BF02911336

Kim, W.-S., Kim, S.-O., Kim, K.-W., 2005. Enhanced electrokinetic extraction of heavy metals from soils assisted by ion exchange membranes. J Hazard Mater 118, 93–102. https://doi.org/10.1016/j.jhazmat.2004.10.001

Ko, S.-O., Schlautman, M.A., Carraway, E.R., 2000. Cyclodextrin-Enhanced Electrokinetic Removal of Phenanthrene from a Model Clay Soil. Environ Sci Technol 34, 1535–1541. https://doi.org/10.1021/es990223t

Kulal, P., Badalamoole, V., 2020. Hybrid nanocomposite of kappa-carrageenan and magnetite as adsorbent material for water purification. Int J Biol Macromol 165, 542–553. https://doi.org/10.1016/j.ijbiomac.2020.09.202

Kumar, M., Bolan, N., Jasemizad, T., Padhye, L.P., Sridharan, S., Singh, L., Bolan, S., O'Connor, J., Zhao, H., Shaheen, S.M., Song, H., Siddique, K.H.M., Wang, H., Kirkham, M.B., Rinklebe, J., 2022. Mobilization of contaminants: Potential for soil remediation and unintended consequences. Science of The Total Environment 839, 156373. https://doi.org/10.1016/j.scitotenv.2022.156373

Kuppusamy, S., Palanisami, T., Megharaj, M., Venkateswarlu, K., Naidu, R., 2016. In-Situ Remediation Approaches for the Management of Contaminated Sites: A Comprehensive Overview. pp. 1–115. https://doi.org/10.1007/978-3-319-20013-2_1

Lee, K.-Y., Kim, K.-W., 2010. Heavy Metal Removal from Shooting Range Soil by Hybrid Electrokinetics with Bacteria and Enhancing Agents. Environ Sci Technol 44, 9482–9487. https://doi.org/10.1021/es102615a

Li, B., Li, M., Zhang, P., Pan, Y., Huang, Z., Xiao, H., 2022a. Remediation of Cd (II) ions in aqueous and soil phases using novel porous cellulose/chitosan composite spheres loaded with zero-valent iron nanoparticles. React Funct Polym 173, 105210. https://doi.org/10.1016/j.reactfunctpolym.2022.105210

Li, B., Li, M., Zhang, P., Pan, Y., Huang, Z., Xiao, H., 2022b. Remediation of Cd (II) ions in aqueous and soil phases using novel porous cellulose/chitosan composite spheres loaded with zero-valent iron nanoparticles. React Funct Polym 173, 105210. https://doi.org/10.1016/j.reactfunctpolym.2022.105210

Li, J., Ding, Y., Wang, K., Li, N., Qian, G., Xu, Y., Zhang, J., 2020. Comparison of humic and fulvic acid on remediation of arsenic contaminated soil by electrokinetic technology. Chemosphere 241, 125038. https://doi.org/10.1016/J.CHEMOSPHERE.2019.125038

Lim, J.-M., Salido, A.L., J. Butcher, D., 2004. Phytoremediation of lead using Indian mustard (Brassica juncea) with EDTA and electrodics. Microchemical Journal 76, 3–9. https://doi.org/10.1016/j.microc.2003.10.002

Lim, M.W., Lau, E. Von, Poh, P.E., 2016a. A comprehensive guide of remediation technologies for oil contaminated soil — Present works and future directions. Mar Pollut Bull 109, 14–45. https://doi.org/10.1016/j.marpolbul.2016.04.023

Lim, M.W., Lau, E. Von, Poh, P.E., 2016b. A comprehensive guide of remediation technologies for oil contaminated soil — Present works and future directions. Mar Pollut Bull 109, 14–45. https://doi.org/10.1016/J.MARPOLBUL.2016.04.023

Liu, Y., Zhang, R., Sun, Z., Shen, Q., Li, Y., Wang, Y., Xia, S., Zhao, J., Wang, X., 2021. Remediation of artificially contaminated soil and groundwater with copper using hydroxyapatite/calcium silicate hydrate recovered from phosphorus-rich wastewater. Environmental Pollution 272, 115978. https://doi.org/10.1016/j.envpol.2020.115978

Luthy, R.G., Aiken, G.R., Brusseau, M.L., Cunningham, S.D., Gschwend, P.M., Pignatello, J.J., Reinhard, M., Traina, S.J., Weber, W.J., Westall, J.C., 1997. Sequestration of Hydrophobic Organic Contaminants by Geosorbents. Environ Sci Technol 31, 3341–3347. https://doi.org/10.1021/es970512m

Mao, X., Jiang, R., Xiao, W., Yu, J., 2015. Use of surfactants for the remediation of contaminated soils: A review. J Hazard Mater 285, 419–435. https://doi.org/10.1016/j.jhazmat.2014.12.009

Mao, X., Shao, X., Zhang, Z., Han, F., 2018. Mechanism and optimization of enhanced electro-kinetic remediation on 137Cs contaminated kaolin soils: A semi-pilot study based on experimental and modeling methodology. Electrochim Acta 284, 38–51. https://doi.org/10.1016/j.electacta.2018.07.136

Mao, X., Wang, J., Ciblak, A., Cox, E.E., Riis, C., Terkelsen, M., Gent, D.B., Alshawabkeh, A.N., 2012. Electrokinetic-enhanced bioaugmentation for remediation of chlorinated solvents contaminated clay. J Hazard Mater 213–214, 311–317. https://doi.org/10.1016/j.jhazmat.2012.02.001

Maturi, K., Reddy, K.R., 2008. Cosolvent-enhanced Desorption and Transport of Heavy Metals and Organic Contaminants in Soils during Electrokinetic Remediation. Water Air Soil Pollut 189, 199–211. https://doi.org/10.1007/s11270-007-9568-9

Medina-Díaz, H.L., López-Bellido, F.J., Alonso-Azcárate, J., Fernández-Morales, F.J., Rodríguez, L., 2023. Comprehensive study of electrokinetic-assisted phytoextraction of metals from mine tailings by applying direct and alternate current. Electrochim Acta 445, 142051. https://doi.org/10.1016/j.electacta.2023.142051

Meez, E., Rahdar, A., Kyzas, G.Z., 2021. Sawdust for the Removal of Heavy Metals from Water: A Review. Molecules 26, 4318. https://doi.org/10.3390/molecules26144318

Meng, F., Xue, H., Wang, Y., Zheng, B., Wang, J., 2018. Citric-acid preacidification enhanced electrokinetic remediation for removal of chromium from chromium-residue-contaminated soil. Environ Technol 39, 356–362. https://doi.org/10.1080/09593330.2017.1301565

Millán, M., Bucio-Rodríguez, P.Y., Lobato, J., Fernández-Marchante, C.M., Roa-Morales, G., Barrera-Díaz, C., Rodrigo, M.A., 2020. Strategies for powering electrokinetic soil remediation: A way to optimize performance of the environmental technology. J Environ Manage 267, 110665. https://doi.org/10.1016/j.jenvman.2020.110665

Miller de Melo Henrique, J., Cañizares, P., Saez, C., Vieira dos Santos, E., Rodrigo, M.A., 2021. Relevance of gaseous flows in electrochemically assisted soil thermal remediation. Curr Opin Electrochem 27, 100698. https://doi.org/10.1016/j.coelec.2021.100698

Mohamadi, S., Saeedi, M., Mollahosseini, A., 2019. Enhanced electrokinetic remediation of mixed contaminants from a high buffering soil by focusing on mobility risk. J Environ Chem Eng 7, 103470. https://doi.org/10.1016/j.jece.2019.103470

O'Brien, P.L., DeSutter, T.M., Casey, F.X.M., Khan, E., Wick, A.F., 2018. Thermal remediation alters soil properties – a review. J Environ Manage 206, 826–835. https://doi.org/10.1016/j.jenvman.2017.11.052

O'Connor, C.S., Lepp, N.W., Edwards, R., Sunderland, G., 2003. The Combined Use of Electrokinetic Remediation and Phytoremediation to Decontaminate Metal-Polluted Soils: A Laboratory-Scale Feasibility Study. Environ Monit Assess 84, 141–158. https://doi.org/10.1023/A:1022851501118

Page, M.M., Page, C.L., 2002. Electroremediation of Contaminated Soils. Journal of Environmental Engineering 128, 208–219. https://doi.org/10.1061/(ASCE)0733-9372(2002)128:3(208)

Parameswarappa Jayalakshmamma, M., Ji, W., Khalil, C.A., Marhaba, T.F., Abrams, S., Lee, K., Zhang, H., Boufadel, M., 2021. Removal of hydrocarbons from heterogenous soil using electrokinetics and surfactants. Environmental Challenges 4, 100071. https://doi.org/10.1016/j.envc.2021.100071

Paramkusam, B.R., Srivastava, R.K., Mohan, D., 2015. Electrokinetic removal of mixed heavy metals from a contaminated low permeable soil by surfactant and chelants. Environ Earth Sci 73, 1191–1204. https://doi.org/10.1007/s12665-014-3474-4

Park, J.-Y., Chen, Y., Chen, J., Yang, J.-W., 2002. Removal of phenanthrene from soil by additive-enhanced electrokinetics. Geosciences Journal 6, 1–5. https://doi.org/10.1007/BF02911329

Park, J.-Y., Lee, H.-H., Kim, S.-J., Lee, Y.-J., Yang, J.-W., 2007. Surfactant-enhanced electrokinetic removal of phenanthrene from kaolinite. J Hazard Mater 140, 230–236. https://doi.org/10.1016/j.jhazmat.2006.06.140

Peppicelli, C., Cleall, P., Sapsford, D., Harbottle, M., 2018. Changes in metal speciation and mobility during electrokinetic treatment of industrial wastes: Implications for remediation and resource recovery. Science of The Total Environment 624, 1488–1503. https://doi.org/10.1016/J.SCITOTENV.2017.12.132

Putra, R.S., Ohkawa, Y., Tanaka, S., 2013. Application of EAPR system on the removal of lead from sandy soil and uptake by Kentucky bluegrass (Poa pratensis L.). Sep Purif Technol 102, 34–42. https://doi.org/10.1016/j.seppur.2012.09.025

Rahchamani, J., Mousavi, H.Z., Behzad, M., 2011. Adsorption of methyl violet from aqueous solution by polyacrylamide as an adsorbent: Isotherm and kinetic studies. Desalination 267, 256–260. https://doi.org/10.1016/j.desal.2010.09.036

Rahman, Z., Jagadheeswari, Mohan, A., Tharini, Selvendran, Priya, S., 2021. Electrokinetic remediation: An innovation for heavy metal contamination in the soil environment. Mater Today Proc 37, 2730–2734. https://doi.org/10.1016/j.matpr.2020.08.541

Rebello, S., Sivaprasad, M.S., Anoopkumar, A.N., Jayakrishnan, L., Aneesh, E.M., Narisetty, V., Sindhu, R., Binod, P., Pugazhendhi, A., Pandey, A., 2021. Cleaner technologies to combat heavy metal toxicity. J Environ Manage 296, 113231. https://doi.org/10.1016/j.jenvman.2021.113231

Rehman, Z. ur, Junaid, M.F., Ijaz, N., Khalid, U., Ijaz, Z., 2023. Remediation methods of heavy metal contaminated soils from environmental and geotechnical standpoints. Science of The Total Environment 867, 161468. https://doi.org/10.1016/j.scitotenv.2023.161468

Reinout Lageman, 2011. Electrokinetic Remediation in Practice Experiences with Field Applications. Reinout Lageman, Lambda Consult Wiebe Pool, Holland Environment.

Ren, L., Lu, H., He, L., Zhang, Y., 2014. Enhanced electrokinetic technologies with oxidization–reduction for organically-contaminated soil remediation. Chemical Engineering Journal 247, 111–124. https://doi.org/10.1016/J.CEJ.2014.02.107

Rezaee, M., Asadollahfardi, G., Gomez-Lahoz, C., Villen-Guzman, M., Paz-Garcia, J.M., 2019. Modeling of electrokinetic remediation of Cd- and Pb-contaminated kaolinite. J Hazard Mater 366, 630–635. https://doi.org/10.1016/j.jhazmat.2018.12.034

Robles, I., Lozano, M.J., Solís, S., Hernández, G., Paz, M.V., Olvera, M.G., Bustos, E., 2015. Electrokinetic Treatment Of Mercury-Polluted Soil Facilitated By Ethylenediaminetetraacetic Acid Coupled With A Reactor With A Permeable Reactive Barrier Of Iron To Recover Mercury (II) From Water. Electrochim Acta 181, 68–72. https://doi.org/10.1016/j.electacta.2015.04.099

Rocha, I.M.V., Silva, K.N.O., Silva, D.R., Martínez-Huitle, C.A., Santos, E.V., 2019. Coupling electrokinetic remediation with phytoremediation for depolluting soil with petroleum and the use of electrochemical technologies for treating the effluent generated. Sep Purif Technol 208, 194–200. https://doi.org/10.1016/j.seppur.2018.03.012

Sarankumar, R.K., Selvi, A., Murugan, K., Rajasekar, A., 2020. Electrokinetic (EK) and Bio-electrokinetic (BEK) Remediation of Hexavalent Chromium in Contaminated Soil Using Alkalophilic Bio-anolyte. Indian Geotechnical Journal 50, 330–338. https://doi.org/10.1007/s40098-019-00366-6

Siyar, R., Doulati Ardejani, F., Farahbakhsh, M., Norouzi, P., Yavarzadeh, M., Maghsoudy, S., 2020. Potential of Vetiver grass for the phytoremediation of a real multi-contaminated soil, assisted by electrokinetic. Chemosphere 246, 125802. https://doi.org/10.1016/j.chemosphere.2019.125802

Song, B., Zeng, G., Gong, J., Liang, J., Xu, P., Liu, Z., Zhang, Y., Zhang, C., Cheng, M., Liu, Y., Ye, S., Yi, H., Ren, X., 2017. Evaluation methods for assessing effectiveness of in situ remediation of soil and sediment contaminated with organic pollutants and heavy metals. Environ Int 105, 43–55. https://doi.org/10.1016/J.ENVINT.2017.05.001

Song, P., Xu, D., Yue, J., Ma, Y., Dong, S., Feng, J., 2022. Recent advances in soil remediation technology for heavy metal contaminated sites: A critical review. Science of The Total Environment 838, 156417. https://doi.org/10.1016/j.scitotenv.2022.156417

Song, Y., Cang, L., Zuo, Y., Yang, J., Zhou, D., Duan, T., Wang, R., 2020. EDTA-enhanced electrokinetic remediation of aged electroplating contaminated soil assisted by combining dual cation-exchange membranes and circulation methods. Chemosphere 243, 125439. https://doi.org/10.1016/j.chemosphere.2019.125439

Sörengård, M., Niarchos, G., Jensen, P.E., Ahrens, L., 2019. Electrodialytic per- and polyfluoroalkyl substances (PFASs) removal mechanism for contaminated soil. Chemosphere 232, 224–231. https://doi.org/10.1016/j.chemosphere.2019.05.088

Souza, F.L., Saéz, C., Llanos, J., Lanza, M.R.V., Cañizares, P., Rodrigo, M.A., 2016. Solar-powered electrokinetic remediation for the treatment of soil polluted with the herbicide 2,4-D. Electrochim Acta 190, 371–377. https://doi.org/10.1016/j.electacta.2015.12.134

Stavropoulos, G.G., Samaras, P., Sakellaropoulos, G.P., 2008. Effect of activated carbons modification on porosity, surface structure and phenol adsorption. J Hazard Mater 151, 414–421. https://doi.org/10.1016/j.jhazmat.2007.06.005

Stumpe, B., Engel, T., Steinweg, B., Marschner, B., 2012. Application of PCA and SIMCA Statistical Analysis of FT-IR Spectra for the Classification and Identification of Different Slag Types with Environmental Origin. Environ Sci Technol 46, 3964–3972. https://doi.org/10.1021/es204187r

Suanon, F., Tang, L., Sheng, H., Fu, Y., Xiang, L., Wang, Z., Shao, X., Mama, D., Jiang, X., Wang, F., 2020. Organochlorine pesticides contaminated soil decontamination using TritonX-100-enhanced advanced oxidation under electrokinetic remediation. J Hazard Mater 393, 122388. https://doi.org/10.1016/j.jhazmat.2020.122388

Suzuki, T., Kawai, K., Moribe, M., Niinae, M., 2014a. Recovery of Cr as Cr(III) from Cr(VI)-contaminated kaolinite clay by electrokinetics coupled with a permeable reactive barrier. J Hazard Mater 278, 297–303. https://doi.org/10.1016/j.jhazmat.2014.05.086

Suzuki, T., Niinae, M., Koga, T., Akita, T., Ohta, M., Choso, T., 2014b. EDDS-enhanced electrokinetic remediation of heavy metal-contaminated clay soils under neutral pH conditions. Colloids Surf A Physicochem Eng Asp 440, 145–150. https://doi.org/10.1016/j.colsurfa.2012.09.050

Sweetman, M., May, S., Mebberson, N., Pendleton, P., Vasilev, K., Plush, S., Hayball, J., 2017. Activated Carbon, Carbon Nanotubes and Graphene: Materials and Composites for Advanced Water Purification. C (Basel) 3, 18. https://doi.org/10.3390/c3020018

Tang, X., Li, Q., Wu, M., Lin, L., Scholz, M., 2016. Review of remediation practices regarding cadmium-enriched farmland soil with particular reference to China. J Environ Manage 181, 646–662. https://doi.org/10.1016/j.jenvman.2016.08.043

Tian, Y., Boulangé-Lecomte, C., Benamar, A., Giusti-Petrucciani, N., Duflot, A., Olivier, S., Frederick, C., Forget-Leray, J., Portet-Koltalo, F., 2017. Application of a crustacean bioassay to evaluate a multi-contaminated (metal, PAH, PCB) harbor sediment before and

after electrokinetic remediation using eco-friendly enhancing agents. Science of The Total Environment 607–608, 944–953. https://doi.org/10.1016/j.scitotenv.2017.07.094

Turan, V., 2024. Bioremediation of Lithium and Nickel from Soil and Water, in: Lithium and Nickel Contamination in Plants and the Environment. WORLD SCIENTIFIC, pp. 219–230. https://doi.org/10.1142/9789811283123_0009

USAEC, 2000. In-Situ Electrokinetic Remediation of Metal Contaminated Soils Technology Status Report. US Army Environmental Center Report Number ADA608289.

Usman, M., Jellali, S., Anastopoulos, I., Charabi, Y., Hameed, B.H., Hanna, K., 2022. Fenton oxidation for soil remediation: A critical review of observations in historically contaminated soils. J Hazard Mater 424, 127670. https://doi.org/10.1016/j.jhazmat.2021.127670

Utchimuthu, K., Saravanakumar, D., Joshua Amarnath, 2012. Removal Or Reducing Heavy Metal (Lead) From Soil By Electrokinetic Process. Int. J. Eng. Res. Appl. (IJERA) 2 (3) 2367–2373.

Vidal, J., Báez, M.E., Calzadilla, W., Aranda, M., Salazar, R., 2022. Removal of chloridazon and its metabolites from soil and soil washing water by electrochemical processes. Electrochim Acta 425, 140682. https://doi.org/10.1016/j.electacta.2022.140682

Vidal, J., Báez, M.E., Salazar, R., 2021. Electro-kinetic washing of a soil contaminated with quinclorac and subsequent electro-oxidation of wash water. Science of The Total Environment 761, 143204. https://doi.org/10.1016/j.scitotenv.2020.143204

Vocciante, M., Bagatin, R., Ferro, S., 2017. Enhancements in ElectroKinetic Remediation Technology: Focus on water management and wastewater recovery. Chemical Engineering Journal 309, 708–716. https://doi.org/10.1016/j.cej.2016.10.091

WANG, X., LI, X., YAN, X., TU, C., YU, Z., 2021. Environmental risks for application of iron and steel slags in soils in China: A review. Pedosphere 31, 28–42. https://doi.org/10.1016/S1002-0160(20)60058-3

Wang, Y., Li, A., Cui, C., 2021. Remediation of heavy metal-contaminated soils by electrokinetic technology: Mechanisms and applicability. Chemosphere 265, 129071. https://doi.org/10.1016/j.chemosphere.2020.129071

Wei, K.-H., Ma, J., Xi, B.-D., Yu, M.-D., Cui, J., Chen, B.-L., Li, Y., Gu, Q.-B., He, X.-S., 2022. Recent progress on in-situ chemical oxidation for the remediation of petroleum contaminated soil and groundwater. J Hazard Mater 432, 128738. https://doi.org/10.1016/j.jhazmat.2022.128738

Wen, D., Fu, R., Li, Q., 2021. Removal of inorganic contaminants in soil by electrokinetic remediation technologies: A review. J Hazard Mater 401, 123345. https://doi.org/10.1016/j.jhazmat.2020.123345

Wu, J., Zhang, J., Xiao, C., 2016. Focus on factors affecting pH, flow of Cr and transformation between Cr(VI) and Cr(III) in the soil with different electrolytes. Electrochim Acta 211, 652–662. https://doi.org/10.1016/j.electacta.2016.06.048

Xie, N., Chen, Z., Wang, H., You, C., 2021. Activated carbon coupled with citric acid in enhancing the remediation of Pb-Contaminated soil by electrokinetic method. J Clean Prod 308, 127433. https://doi.org/10.1016/j.jclepro.2021.127433

Xu, D.-M., Fu, R.-B., Wang, J.-X., Shi, Y.-X., Guo, X.-P., 2021. Chemical stabilization remediation for heavy metals in contaminated soils on the latest decade: Available stabilizing materials and associated evaluation methods—A critical review. J Clean Prod 321, 128730. https://doi.org/10.1016/j.jclepro.2021.128730

Xu, H., Song, Y., Cang, L., Zhou, D., 2020. Ion exchange membranes enhance the electrokinetic in situ chemical oxidation of PAH-contaminated soil. J Hazard Mater 382, 121042. https://doi.org/10.1016/j.jhazmat.2019.121042

Xu, W., Wang, C., Liu, H., Zhang, Z., Sun, H., 2010. A laboratory feasibility study on a new electrokinetic nutrient injection pattern and bioremediation of phenanthrene in a clayey soil. J Hazard Mater 184, 798–804. https://doi.org/10.1016/j.jhazmat.2010.08.111

Xue, F., Yan, Y., Xia, M., Muhammad, F., Yu, L., Xu, F., Shiau, Y., Li, D., Jiao, B., 2017. Electro-kinetic remediation of chromium-contaminated soil by a three-dimensional electrode coupled with a permeable reactive barrier. RSC Adv 7, 54797–54805. https://doi.org/10.1039/C7RA10913J

Yang, H., Zhang, G., Fu, P., Li, Z., Ma, W., 2020. The evaluation of in-site remediation feasibility of Cd-contaminated soils with the addition of typical silicate wastes. Environmental Pollution 265, 114865. https://doi.org/10.1016/j.envpol.2020.114865

Yao, Y., Huang, G.H., An, C.J., Cheng, G.H., Wei, J., 2017. Effects of freeze–thawing cycles on desorption behaviors of PAH-contaminated soil in the presence of a biosurfactant: a case study in western Canada. Environ. Sci.: Processes Impacts 19, 874–882. https://doi.org/10.1039/C7EM00084G

Yeongkyoo, K., 2018. Effects of different oxyanions in solution on the precipitation of jarosite at room temperature. J Hazard Mater 353, 118–126. https://doi.org/10.1016/j.jhazmat.2018.04.016

Yeung, A.T., 2011. Milestone developments, myths, and future directions of electrokinetic remediation. Sep Purif Technol 79, 124–132. https://doi.org/10.1016/J.SEPPUR.2011.01.022

Yeung, A.T., Gu, Y.Y., 2011. A review on techniques to enhance electrochemical remediation of contaminated soils. J Hazard Mater 195, 11–29. https://doi.org/10.1016/J.JHAZMAT.2011.08.047

Yi, Y.M., Sung, K., 2015. Influence of washing treatment on the qualities of heavy metal–contaminated soil. Ecol Eng 81, 89–92. https://doi.org/10.1016/j.ecoleng.2015.04.034

Yu, X., Muhammad, F., Yan, Y., Yu, L., Li, H., Huang, X., Jiao, B., Lu, N., Li, D., 2019a. Effect of chemical additives on electrokinetic remediation of Cr-contaminated soil coupled with a permeable reactive barrier. R Soc Open Sci 6, 182138. https://doi.org/10.1098/rsos.182138

Yu, X., Muhammad, F., Yan, Y., Yu, L., Li, H., Huang, X., Jiao, B., Lu, N., Li, D., 2019b. Effect of chemical additives on electrokinetic remediation of Cr-contaminated soil coupled with a

permeable reactive barrier. R Soc Open Sci 6, 182138. https://doi.org/10.1098/rsos.182138

Yuan, C., Chiang, T.S., 2007a. The mechanisms of arsenic removal from soil by electrokinetic process coupled with iron permeable reaction barrier. Chemosphere 67, 1533–1542. https://doi.org/10.1016/J.CHEMOSPHERE.2006.12.008

Yuan, C., Chiang, T.-S., 2007b. The mechanisms of arsenic removal from soil by electrokinetic process coupled with iron permeable reaction barrier. Chemosphere 67, 1533–1542. https://doi.org/10.1016/j.chemosphere.2006.12.008

Yuan, C., Hung, C.-H., Chen, K.-C., 2009. Electrokinetic remediation of arsenate spiked soil assisted by CNT-Co barrier—The effect of barrier position and processing fluid. J Hazard Mater 171, 563–570. https://doi.org/10.1016/j.jhazmat.2009.06.059

Yuan, C., Weng, C.-H., 2006. Electrokinetic enhancement removal of heavy metals from industrial wastewater sludge. Chemosphere 65, 88–96. https://doi.org/10.1016/j.chemosphere.2006.02.050

Yuan, L., Li, H., Xu, X., Zhang, J., Wang, N., Yu, H., 2016a. Electrokinetic remediation of heavy metals contaminated kaolin by a CNT-covered polyethylene terephthalate yarn cathode. Electrochim Acta 213, 140–147. https://doi.org/10.1016/j.electacta.2016.07.081

Yuan, L., Xu, X., Li, H., Wang, N., Guo, N., Yu, H., 2016b. Development of novel assisting agents for the electrokinetic remediation of heavy metal-contaminated kaolin. Electrochim Acta 218, 140–148. https://doi.org/10.1016/J.ELECTACTA.2016.09.121

Yuan, L., Xu, X., Li, H., Wang, Q., Wang, N., Yu, H., 2017. The influence of macroelements on energy consumption during periodic power electrokinetic remediation of heavy metals contaminated black soil. Electrochim Acta 235, 604–612. https://doi.org/10.1016/j.electacta.2017.03.142

Yuan, S., Zheng, Z., Chen, J., Lu, X., 2009. Use of solar cell in electrokinetic remediation of cadmium-contaminated soil. J Hazard Mater 162, 1583–1587. https://doi.org/10.1016/j.jhazmat.2008.06.038

Yusni, E.M., Tanaka, S., 2015. Removal behaviour of a thiazine, an azo and a triarylmethane dyes from polluted kaolinitic soil using electrokinetic remediation technology. Electrochim Acta 181, 130–138. https://doi.org/10.1016/j.electacta.2015.06.153

Zhang, M., Feng, M., Bai, X., Liu, L., Lin, K., Li, J., 2022. Chelating surfactant N-lauroyl ethylenediamine triacetate enhanced electrokinetic remediation of copper and decabromodiphenyl ether co-contaminated low permeability soil: Applicability analysis. J Environ Manage 301, 113888. https://doi.org/10.1016/j.jenvman.2021.113888

ZHANG, S., HE, Y., WU, L., WAN, J., YE, M., LONG, T., YAN, Z., JIANG, X., LIN, Y., LU, X., 2019. Remediation of Organochlorine Pesticide-Contaminated Soils by Surfactant-Enhanced Washing Combined with Activated Carbon Selective Adsorption. Pedosphere 29, 400–408. https://doi.org/10.1016/S1002-0160(17)60328-X

Zhang, Z., Ren, W., Zhang, J., Zhu, F., 2021. Electrokinetic remediation of Pb near the e-waste dismantle site with $Fe(NO_3)_3$ as cathode electrolyte. Environ Technol 42, 884–893. https://doi.org/10.1080/09593330.2019.1648559

Zhao, C., Dong, Yan, Feng, Y., Li, Y., Dong, Yong, 2019. Thermal desorption for remediation of contaminated soil: A review. Chemosphere 221, 841–855. https://doi.org/10.1016/j.chemosphere.2019.01.079

Zhao, S., Fan, L., Zhou, M., Zhu, X., Li, X., 2016a. Remediation of Copper Contaminated Kaolin by Electrokinetics Coupled with Permeable Reactive Barrier. Procedia Environ Sci 31, 274–279. https://doi.org/10.1016/j.proenv.2016.02.036

Zhao, S., Fan, L., Zhou, M., Zhu, X., Li, X., 2016b. Remediation of Copper Contaminated Kaolin by Electrokinetics Coupled with Permeable Reactive Barrier. Procedia Environ Sci 31, 274–279. https://doi.org/10.1016/J.PROENV.2016.02.036

Zheng, X., Li, Q., Wang, Z., Chen, M., 2024. Remediation of heavy metals contaminated soil by enhanced electrokinetic technology: A review. Arabian Journal of Chemistry 17, 105773. https://doi.org/10.1016/j.arabjc.2024.105773

Zhou, D.-M., Chen, H.-F., Cang, L., Wang, Y.-J., 2007. Ryegrass uptake of soil Cu/Zn induced by EDTA/EDDS together with a vertical direct-current electrical field. Chemosphere 67, 1671–1676. https://doi.org/10.1016/j.chemosphere.2006.11.042

Zhou, D.-M., Deng, C.-F., Cang, L., Alshawabkeh, A.N., 2005. Electrokinetic remediation of a Cu–Zn contaminated red soil by controlling the voltage and conditioning catholyte pH. Chemosphere 61, 519–527. https://doi.org/10.1016/j.chemosphere.2005.02.055

Zhou, M., Xu, J., Zhu, S., Wang, Y., Gao, H., 2018. Exchange electrode-electrokinetic remediation of Cr-contaminated soil using solar energy. Sep Purif Technol 190, 297–306. https://doi.org/10.1016/j.seppur.2017.09.006

Zhou, Z., Liu, X., Sun, K., Lin, C., Ma, J., He, M., Ouyang, W., 2019. Persulfate-based advanced oxidation processes (AOPs) for organic-contaminated soil remediation: A review. Chemical Engineering Journal 372, 836–851. https://doi.org/10.1016/j.cej.2019.04.213

Zhuang, Y., 2021. Large scale soft ground consolidation using electrokinetic geosynthetics. Geotextiles and Geomembranes 49, 757–770. https://doi.org/10.1016/j.geotexmem.2020.12.006

Zhuang, Y., Yu, F., Chen, J., Ma, J., 2016. Batch and column adsorption of methylene blue by graphene/alginate nanocomposite: Comparison of single-network and double-network hydrogels. J Environ Chem Eng 4, 147–156. https://doi.org/10.1016/j.jece.2015.11.014